The Hong Kong Polytechnic University

Department of Civil and Structural Engineering

Endocrine Disruptors Elimination by UV Aided Oxidation Processes in Water via Kinetics Study and Reaction Mechanisms

Lau Tim Kwan

A thesis submitted in partial fulfillment of the requirements for

the degree of Doctor of Philosophy

March 2007

CERTIFICATE OF ORIGINALITY

I hereby declare that this thesis is my own work and that, to the best of my knowledge and belief, it reproduces no material previously published or written, nor material that has been accepted for the award of any other degree or diploma, except where due acknowledgement has been made in the text.

Lau Tim Kwan

ABSTRACT

Endocrine disruptor compounds (EDC) are agents that interfere with the production, transport, binding or elimination of natural hormones in vertebrate organisms, such as fishes and further to human body. It can be naturally occurring or anthropogenic. Numerous studies have shown that EDCs are environmentally persistent and significant amounts of which exist in sewage effluents, rivers receiving municipal and industrial effluents, and even groundwater sources infiltrated by sewage effluents. At present, little is known about the degradability and reaction products of three selected EDCs by various chemical treatment processes. Therefore, the aqueous degradation of the important EDCs (i.e. Di-n-butyl phthalate (DBP), Carbofuran (CBF), and Butylated Hydroxyanisole (BHA)) has been investigated under ultraviolet (UV) irradiation treatment, ozonation and other advance oxidation processes.

The investigation was carried out under idealized conditions and has considered both reaction kinetics and degradation mechanisms. In the UV photolysis study, DBP is being irradiated under monochromatic UV at 254 nm over a wide pH range (3–11). It was found that more than 90% of 4 μM DBP can be degraded

within an hour of irradiation in water. A simple model has been developed and used to predict the initial DBP photolysis rate constant at different pH values and initial DBP concentrations. The use of 254 nm UV to photodegrade DBP was found to be a relatively fast and clean process, especially in neutral to basic conditions.

For the second probed EDC compound, CBF, has shown the efficiency of advanced oxidation process (UV/O_3) is higher than those of the direct UV photolysis and ozonation processes. The pH-dependency of CBF has also been shown in both ozonation and UV/O_3 processes. Linear relationship could be found for the latter process in all pH, while for the former process, two stages of reactions (steady and accelerating) were found in the acidic and alkaline pH conditions, respectively.

Other than pesticide pollutants, industrial wastewater containing BHA, a suspected EDC, was also investigated by different treatment processes including UV-irradiation, ozonation, UV/O_3, and $UV/S_2O_8^{2-}$. O-demethylation, dimerization, and oxidation have been found to be the main degradation mechanisms. A

systematic decay pathway was proposed based on ten identified intermediates in the studied processes, including a unique pathway leading to the formation of precipitates in the ozonation process. An unconventional minimum-type variation of BHA decay rate constants from acidic to caustic range has been found for both ozonation and UV/O_3 processes.

Furthermore, the degradation of BHA in water has been studied, with and without the aid of a green oxidant – potassium peroxydisulfate ($S_2O_8^{2-}$) in the presence of UV. Three distinctive phases of BHA reactivity towards UV/$S_2O_8^{2-}$ at acidic, neutral and basic pH range were examined, where 80-100% mineralization has been observed within an hour of irradiation under 254 nm. A reduction in solution pH during the reaction was observed mainly due to the complete conversion of $S_2O_8^{2-}$ to sulfate ions together with proton generation. Seven measurable intermediates were found via an oxidation and dimerization process at all tested pH levels. The BHA decay mechanisms are quite different in acid condition and at other pH levels. There are three unique intermediates that are only detectable at pH 3 via two additional pathways. This is due to the generation of weaker oxidants and/or radicals, which results in a slower degradation of the BHA and

therefore the accumulation of these intermediates to detectable levels. The rate of BHA decay generally increases from low to high pH levels; however, the corresponding mineralization at higher pH is retarded due to the futile process of recombining radicals and involvement of intermediates. Therefore, neutral pH was suggested to be the optimum condition in terms of mineralization and moderate efficiency in removing BHA.

Additionally, three major process variables have been selected for detailed investigation: (i) UV wavelength effects; (ii) pH effects; and (iii) $S_2O_8^{2-}$ dosage effects. It was found that UV at 254 nm demonstrated the best removal efficiency in both direct photolysis and photo-oxidation (UV/$S_2O_8^{2-}$) processes. The reaction rate constant can be improved by increasing either the initial pH levels and/or the $S_2O_8^{2-}$ dosage. When the $S_2O_8^{2-}$ dosage is sufficiently provided in the UV system, the reaction kinetics can be simply characterized by pseudo first-order decay. However, when $S_2O_8^{2-}$ dosage is deficient, though the decay of BHA is fast initially but the process will be retarded at a later stage, and a two-stage pattern is observed. An atypical model has been used to describe such a condition, this is specially useful for predicting the process performance if a shock loading during

wastewater treatment is present.

Since the UV/$S_2O_8^{2-}$ process at acidic pH condition cannot effectively mineralize BHA, therefore metal-mediated oxidation processes were investigated in this study as alternatives. The removal and mineralization of BHA using UV/$S_2O_8^{2-}$ with the assist of silver in both homogeneous and heterogeneous systems were investigated. Three different silver sources including two silver salts (Ag_2SO_4 and $AgNO_3$) and silver oxide (Ag_2O) were compared. In a homogeneous system, silver nitrate is selected for detail study due to lesser interference from its counter anion. The degradation rates of five different treatment processes (UV only, UV/Ag^+, Ag^+/$S_2O_8^{2-}$, UV/$S_2O_8^{2-}$, and UV/Ag^+/$S_2O_8^{2-}$) were studied in order to fully comprehend the details of the UV/Ag^+/$S_2O_8^{2-}$ process. This process by generating the robust sulphate radicals showed the best performance over BHA degradation and mineralization by removing 100% of 0.1 mM BHA and more than 99% of TOC in 3 and 20 min, respectively (at its optimal condition with a silver to peroxydisulfate ratio of 7.5:1). For a heterogeneous system the solid form of silver oxide (Ag_2O) was used to replace the Ag^+ for better recycling. The same dosages of silver in both homogeneous and heterogeneous systems give similar

performance in BHA removal. However, it is interesting to find that the heterogeneous system induces faster mineralization likely due to the selective and non-selective properties of $SO_4^{\bullet-}$ and $^{\bullet}OH$ to the BHA and resulted intermediates, respectively.

Publications arising from the thesis

International journal paper

1. **Lau T. K.**, Chu, W., Graham, N., The Aqueous Degradation of Butylated Hydroxyanisole by UV/$S_2O_8^{2-}$ – Study of Reaction Mechanisms via Dimerization and Mineralization, *Environmental Science and Technology*, 41(2), 613 – 619, 2007.

2. **Lau T. K.**, Chu, W., Graham, N., Reaction Pathways and Kinetics of Butylated Hydroxyanisole with UV, Ozonation and UV/O_3 Processes, *Water Research*, 41, 765-774, 2007.

3. **Lau T. K.**, Chu, W., Graham, N., The Degradation of Endocrine Disruptor Di-n-Butyl Phthalate by UV Irradiation: A Photolysis and Product Study, *Chemosphere*, 60(8), 1045-1053, 2005.

4. **Lau T. K.**, Chu, W., Graham, N., Degradation of the Endocrine Disruptor Carbofuran by UV, O_3 and O_3/UV, *Water Science and Technology*, 55 (12), 275–280, 2007.

5. Chu, W, **Lau T. K.**, Ozonation of Endocrine Disrupting Chemical BHA under the Suppression Effect by Salt Additive – With and Without H_2O_2, *Journal of Hazardous Materials*, 144 (1-2), 249-254, 2007.

6. **Lau T. K.**, Chu, W., Graham, N., Endocrine Disruptor Butylated Hydroxyanisole Elimination by UV/$S_2O_8^{2-}$ in Water – quantification and modelling via kinetic study, *Water Research*, (under submission).

7. **Lau T. K.**, Chu, W., Silver-aided Photodegradation (UV/Ag^+/$S_2O_8^{2-}$ process) of Endocrine Disruptor Contaminated Wastewater with Different Silver Sources – Homogenous and Heterogeneous, *Applied Catalysis B: Environmental*, (under submission).

Conference paper

1. **Lau T. K.**, Chu, W., Graham, N., Degradation of the Endocrine Disruptor Carbofuran by UV, O_3 and O_3/UV, *The Proceeding of the 4th IWA Specialist International Conference on Oxidation Technologies for Water and Wastewater Treatment*, 15-17 May, Goslar, Germany, 735-740, 2006.

2. **Lau T. K.**, Chu, W., Graham, N., Photodegradation of Endocrine Disrupting Chemical by Different Oxidants – H_2O_2, $K_2S_2O_8$, O_3, *The Postgraduate Research Conference*, 4 November, The Hong Kong Polytechnic University, 53-57, 2006.

ACKNOWLEDGEMENTS

I wish to express my deepest gratitude to my supervisor, Dr. Wei Chu, for his invaluable support and supervision throughout the project. Without his guidance and advice, the completion of this thesis is unachievable. Special thank is given to Prof. Nigel Graham for his valuable comments and suggestions.

The support from my former colleagues Dr. Ada K.H. Chan, Dr. Joanna C.Y. Kwan, and Dr. Esther W.K. Choy are gratefully acknowledged for their moral support and precious suggestions. Thanks also go to my family, my husband Dr. Crispin Chio Hang Ao, my Church, and Opus Dei for their encouragement and inspiration.

I would like to thank the technicians in the Waste and Wastewater Laboratory, especially Mr. Wai Shung Lam for his greatest assistance and also Mr. Chi Wai Lau and Mr. Kin Hung Ng for their technical support. Last but not least, I would like to acknowledge the support of the Research Grants Council of the Hong Kong Special Administrative Region, China. (PolyU 5038/02E)

TABLE OF CONTENTS

CHAPTER 1 INTRODUCTION

CHAPTER 2 LITERATURE REVIEW

CHAPTER 3 METHODOLOGY

List of Figures

List of Tables

CHAPTER 1 INTRODUCTION

1.1 Background

At present, more than 80% of Hong Kong's fresh water is imported from the East River in Guangdong, China and the quality of this imported raw water has deteriorated in the last decade from Grade 2 surface water (China's standard) down to Grades 3 or 4 (Lee et al., 2005). This has been caused by continuing, rapid industrialisation in Guangdong, and among the main pollutants found in the imported water are synthetic organic compounds, such as pesticides and industrial chemicals; some of these are likely to have endocrine disrupting potential (Lee et al., 2005). The removal of such micro-pollutants is likely to become an environmental issue in the near future since endocrine disruptor compounds (EDCs) may adversely affect public health via their interference with the synthesis, secretion, transport, binding, action or elimination of hormones in the human body, arising from exposure to inadequately treated drinking water or contaminated food (ENDS, 1999). Unfortunately, conventional treatment processes (coagulation-sedimentation-filtration) cannot adequately remove EDC, and the chlorination process that is employed extensively in Hong Kong (and in other countries) for disinfection may result in more toxic chlorinated byproducts

in the presence of EDCs. In addition, the Hong Kong Government is continuing to seek higher discharge qualities for wastewater effluents, which may include the removal of EDCs, in order to achieve better environmental protection of local marine waters.

1.2 Aims and Objectives

In this study, the use of the well-established treatment processes, ozonation and UV photolysis, and a newly explored green oxidant (peroxydisulfate) and UV-aid system is studied to evaluate their potential to degrade selected EDCs in the context of both potable water treatment (to complement, reduce or replace the use of chlorination), and in wastewater treatment as a source control where additives may be used. Since little detailed information is available at present concerning the treatability of the selected EDCs by these methods, and the respective process design.

Therefore, the aim of this study is to investigate the use of different treatment processes for removal of endocrine disrupting chemicals before discharging to the publics. To truly and effectively benefit the humanities, it is necessary to understand the various treatment processes before it can be used practically in

real treatment plant system, the specific objectives of this study are therefore as follow:

i) To investigate the feasibility of removing wastewater pollutants, five different types of wastewater treatments are focused throughout this study, such as (i) UV photolysis, (ii) Ozonation, (iii) UV-aid Ozonation, (iv) UV-aid peroxydisulfate, and (v) UV-aid silver-peroxydisulfate processes. Additives (i.e. sodium peroxydisulfate or potassium peroxydisulfate) are used in the oxidation process in order to enhance the treatment for applications. Such information is not only important in itself, but will contribute substantially to the bioassay of the degraded EDC in future toxicological studies.

ii) Conduct series of experiments by using the above mentioned chemical wastewater treatments in treating three different endocrine disrupting chemicals (EDCs) at their greatest water solubility (or maximum concentration). The selected pollutants are *dibutylphthalate* (industrial pollutant), *carbofuran* (pesticide), and *butylated hydroxyanisole* (industrial-use antioxidant).

iii) The kinetics and mechanisms of reactions of specific EDC by

UV-irradiation, ozone, and advanced oxidation processes (such as UV/O_3, $UV/S_2O_8^{2-}$ and $UV/Ag^+/S_2O_8^{2-}$ processes) are studied in great details.

iv) Identify which factors that affect the performance of degradation for wastewater treatment processes at different parameters, such as variations of (i) initial pH levels, (ii) pollutant concentrations, (iii) oxidant dosage, (iv) light intensities, and (v) wavelengths;

v) Establish a treatment model for each process and for each EDC by the application of a quantum yield model for the UV process, a direct-radical oxidation model for the ozonation or UV/O_3 process, and establish models for application of $UV/S_2O_8^{2-}$ process at the critical oxidant dosages.

vi) Conduct thorough investigation of mechanistic pathways of each treatment systems using LC/MS-APCI and LC/MS-ESI.

vii) Evaluate the efficiency of ultimate pollutant removal by investigating the mineralization efficiency (or Total Organic Carbon removal) of each process.

It is believed that this study is of general importance in terms of assessing feasible methods of minimizing the potential threat to public health and the

environment posed by the presence of synthetic EDCs in potable water or wastewater effluents, respectively. The study contributes to international work being carried out on the fate and removal of EDCs in water/wastewater treatment, for example work in the UK and USA (UKWIR NEWS, Sept 2001). Whilst the majority of the population in Hong Kong (and in many other countries) is unaware of the EDC issue at present, there is growing concern that environmental contamination is posing a threat to human health, and to the aquatic environment. Locally, it is believed that the results of this study will be of considerable interest and value to the Hong Kong Government Departments responsible for water supplies, wastewater disposal and environmental protection, as well as of general significance to the wider academic community.

CHAPTER 2 LITERATURE REVIEW

2.1 Endocrine disruptor compounds (EDC)

2.1.1 Background

Endocrine disruptor compounds (EDCs) are defined by the USEPA as, "exogenous agents that interfere with the synthesis, secretion, transport, binding, action or elimination of natural hormones in the body, which are responsible for the maintenance of homeostasis, reproduction, development and/or behavior" (USEPA, 2001). Endocrine disruptors are natural or synthetic chemicals that may mimic natural hormones and bind with endocrine receptors, producing unnatural outcomes, or interfere with hormonal processes by blocking hormones from binding with endocrine receptors (USEPA, 2001).

While much concern about EDCs has focused on effects on the environment and wildlife, the potential adverse health effects on humans is now receiving growing attention. For example, human exposure to EDCs is being linked to increased testicular cancer, falling sperm counts, increased breast cancer, and early puberty in female (Hopert et al., 1998). A study in English shows that more than 30% of the male fish have been feminised (growing female reproductive tissues or

organs) (Hopkins, 2004). Similar phenomena have also found in birds, otters, seals and frogs. This has been claimed by the presence of EDCs (Hopkins, 2004). Synthetic compounds with endocrine disrupting potential include pesticides, such as carbofuran, DDT, lindane, trichlorfon, and vinclozolin, and industrial chemicals such as phthalates, butylated hydroxyanisole (BHA), bisphenol A and alkylphenols (Table 2.1). The pesticides and BHA can be found in food and water, phthalates are in many PVC plastics, and bisphenol A is present in the linings of many food cans. The EDC (i.e. phthalates) can also be found in a wide range of industrial products such as plastics, detergents, pai

nts, and pharmaceutical products such as steroids and contraceptive pills (Hopkins, 2004).

Table 2.1: Examples of sources of some typical EDC

(Quoted from The Green Lane, 2002)

Examples of Sources	Category (Example of Uses)	Examples of Substances
Incineration, landfill	Polychlorinated Compounds (from industrial production or by-products of mostly banned substances)	Polychlorinated dioxins, polychlorinated biphenyls
Agricultural runoff / Atmospheric transport	Organochlorine Pesticides (found in insecticides, many now phased out)	DDT, dieldrin , lindane
Agricultural runoff	Pesticides currently in use	Atrazine, trifluralin, permethrin
Harbours	Organotins (found in antifoulants used to paint the hulls of ships)	Tributyltin
Industrial and municipal effluents	Alkylphenolics (Surfactants – certain kinds of detergents used for removing oil – and their metabolites)	Nonylphenol
Industrial effluent	Phthalates (found in placticisers)	**Dibutyl phthalate**, butylbenzyl phthalate
Municipal effluent and agricultural runoff	Natural Hormones (produced naturally by animals); synthetic steroids (found in contraceptives)	17-b-estradiol, estrone, Testosterone; ethynyl estradiol
Pulp mill effluents	Phytoestrogens (found in plant material)	Isoflavones, ligans, coumestans

Aqueous sources of these compounds are sewage effluent discharges and industrial effluents discharged in general. In addition, an official UK study concluded that phthalates, bisphenol and alkyl phenol compounds may leach into drinking water supplies from sealants, cements and pipe linings (ENDS, 1999). Conventional biological treatment can remove or degrade these substances to a limited extent. However, studies in the UK and elsewhere (Montagnani et al., 1996) have shown that endocrine disrupting substances are environmentally persistent and significant amounts exist in sewage effluents, in rivers receiving municipal and industrial effluents, and even in groundwater sources infiltrated by sewage effluents. Although the concentrations of such substances vary substantially from one location to another, in England and Wales the concentration of total nonyl phenol has been found to vary from a few micrograms per litre to 180 μg/l in rivers, and up to 330 μg/l in sewage effluents (Blackburn and Waldock, 1995).

Regarding phthalates, concentrations of up to 32 μg/l have been measured in rivers in England (Fatoki and Vernon, 1990), whereas for sewage effluents in Scotland, total phthalate concentrations as high as 360 μg/l have been found. Environmental Quality Standards for these compounds are still under

development internationally and, at present, it is difficult to assess the importance of such levels of these compounds in the environment.

2.1.2 Previous degradation studies of EDC

As described subsequently, three specific organic compounds have been selected for detailed study in this project on the basis that these are from prominent classes of synthetic EDCs, and are of known or suspected concern. These are: phthalates (dibutyl phthalate, DBP), phenols (butylated hydroxyanisole, BHA), and carbamates (carbofuran ,CBF). While there have been only a few number of previous studies that have referred to the general degradability of DBF, CBF (Kuo, 1999), a review of the scientific literature indicates that there have been no previous studies concerning the treatability of BHA.

2.1.3 Dibutyl Phthalate (DBP)

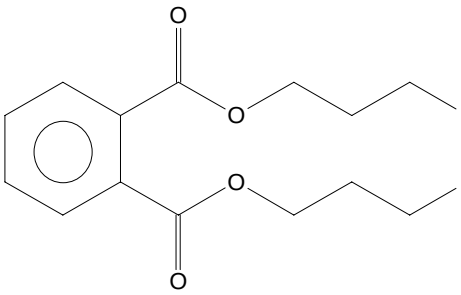

Fig. 2.1: Chemical Structure of DBP

Phthalate esters (PE), the esters of phthalic acid ($C_6H_4(COOH)_2$), have widely been reported to be mutagenic, carcinogenic, and active as endocrine disruptor compounds (EDCs) in experiments with animals (Khaliq et al., 1992). They have been the most abundant man-made industrial chemicals produced in large quantities for nearly 40 years (Fromme et al., 2002) and are mainly used as plasticizers in the manufacture of various plastics. The existence of PE in the environment and their tendency to bioconcentrate in animal fat is of concern (Jobling et al., 1995).

PE have been reported to be etiological agents in several human diseases, including disorders of the male reproductive tract, breast and testicular cancers, disruptors of the neuroendocrine system, and skeletal effects (Spelsberg and Riggs, 1987; Sharpe and Skakkebaek, 1993). Thousands of tons of plastics are

disposed of annually in landfills, thus enabling PE to migrate into groundwater (Jobling et al., 1995), while the general public is potentially exposed to these compounds either from food or drinks directly contaminated by plastic wraps containing PE, or from polluted drinking water (Staples et al., 1995).

One of the most common PE is Dibutyl Phthalate (DBP) (Staples et al., 1995) with an annual production of over 454 x 10^3 kg in the U.S. DBP (Fig. 2.1) initially attracted attention as a potential EDC because it was found to be a weak estrogen receptor agonist in some cell-based assays (Mylchreest et al., 1999). DBP also produces an antiandrogenic effect which alters androgen-dependent processes in the male during development, while its major metabolite, mono butylphthalate (MBP), does not induce estrogen-receptor-mediated transcriptional activity in vitro (Mylchreest et al., 1999). DBP is reported to be estrogenic in vitro at concentrations between 10^{-6} and 10^{-4} M (Jobling et al., 1995).

In general there is little information available on PE concentrations in wastewaters, but one study has reported the presence of DBP in the effluent from a wastewater treatment plant at 6 µg L^{-1} (Fatoki and Vernon, 1990). In contrast, a

concentration of approximately 1 mg L^{-1} DBP in leachates from municipal waste landfill sites was found in Guelph, Ontario (CEPA, 1994), some of which may eventually reach aquatic ecosystems. DBP residues have been detected in fish, water, and sediments (Johnson et al., 1977), and a study in the UK has estimated that the average intake of DBP through food packaged in cellulose film was 230 μg d^{-1} in 1987 (Jobling et al., 1995).

The transformation and volatilization of DBP in different aquatic systems with sunlight irradiation are insignificant (Wolfe et al., 1980). The aqueous hydrolysis half-life of DBP at pH 7 is estimated at 22 years, and the atmospheric photo-oxidation half-life is reported to be between 0.6 to 6 d (Staples et al., 1995). In addition, DBP is considered to be one of the main refractory organic compounds in municipal wastewater that is difficult to be degraded in conventional activated sludge plants (Wang et al., 1997).

2.1.4 Carbofuran (CBF)

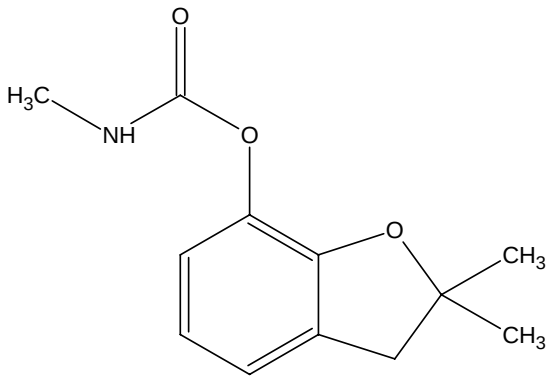

Fig. 2.2: Chemical Structure of CBF

Carbofuran (CBF), one of the carbamates, is found in polluted surface waters and wastewaters as a result of the widespread application of insecticides (trade name – Furadan). Formulations of CBF (Fig. 2.2) are used in agricultural applications worldwide, an estimated 5 million pounds of CBF is used annually in the United States, and 45% of urban African-American women have detectable levels of CBF in their plasma (Bonner et al, 2005). The compound has been classified as a potential endocrine disruptor chemical (EDC) by WWF (ENDS, 1999). Direct photolysis and photo-oxidation (via hydroxyl radicals) are speculated as being the principal mechanisms leading to CBF degradation and removal (ENDS, 1999). According to published study (USEPA, 2001), the approximate hydrolysis half-life of CBF degradation is 0.625 day (900 min) at pH 9.

Some treatment techniques of CBF have been proposed by using ultrasonic irradiation, direct photolysis, UV/O_3 or Fenton reagent, anodic Fenton treatment, and TiO_2 as a photocatalyst (Bachman and Patterson, 1999; Hua and Pfalzer-Thompson, 2001; Huston and Pignatello, 1999; Wang and Lemley, 2003). They have shown that advanced oxidation processes are useful in treating CBF and give a more effective performance than using a single oxidant. They concluded that hydroxyl radical is effective in degrading CBF by using the above AOP processes.

2.1.5 Butylated Hydroxyanisole (BHA)

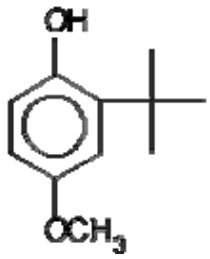

Fig. 2.3: Chemical Structure of BHA

Butylated hydroxyanisole (BHA – Fig. 2.3) is recognised as an endocrine disruptor chemical in experiments with animals (Sarafian et al., 2002; Nagai et al., 1996; Wang and Liu, 2004) and it has been suggested to be an animal carcinogen by the International Agency for Research on Cancer (Verhagen et al., 1991). It is a powerful synthetic phenolic antioxidant, which has been used widely to prevent oxidative rancidity of fats so as to prolong the shelf life of many food commodities (Madsen and Bertelsen, 1995; Wang and Liu, 2004).

However the carcinogenic potential of BHA is currently controversial, it has been referred as an antioxidant, a pro-oxidant, an anticarcinogen, a carcinogen, a co-carcinogen and a tumour initiating or promoting compound (Verhagen et al., 1991). It has been used widely for many years as an effective food antioxidant (Iverson, 1999). BHA may bioconcentrate in humans and it is reported to be present in some sewage effluent (Jobling et al., 1995). However, its use is not

permitted in some countries such as Japan, because BHA could be a tumour promoter (Verhagen et al., 1991).

Studies have shown that BHA expresses its noxious properties when applied at high dosages for long-term periods (Armstrong and Wattenberg, 1985) and mitogenic effects on cell growth has been found at BHA concentrations of 0.01 mM or above (Jobling et al., 1995). In Italy, BHA (at 0.25 μM) is found to be the most abundant phenolic compounds present in river water via the discharge of domestic wastes and industrial wastes (Davì and Gnudi, 1999) and found in an industrial wastewater at a concentration about 39 μM in the U.S. (Bursey and Pellizzari, 1982). Recently, numerous studies have shown the carcinogenicity of BHA in rat and hamster fore stomach, disturbance in mitochondrial electron transport, slightly oestrogenic to breast cancer cells, binds rainbow trout oestrogen receptor and claimed to stimulate transcriptional activity of the human oestrogen receptor (Jobling et al., 1995; Jos et al., 2005).

2.2 Wastewater Treatment Processes

2.2.1 UV photolysis

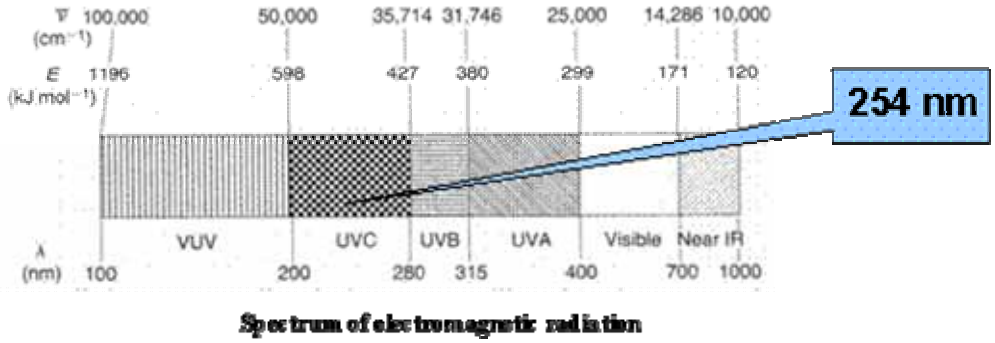

Spectrum of electromagnetic radiation

Fig. 2.4: Spectrum of electromagnetic radiation (Parsons and Williams, 2004)

The photodegradation of organic chemicals by using UV or UV-induced photosensitization is a process that has become increasingly important recently (Cheung et al., 1998; Chu and Tsui, 1999), where the addition of photosensitizer or hydrogen sources in the process has significant advantages over the standard photolysis process at 254 nm (Fig. 2.4) (Chu et al, 1998); rate enhancement is an obvious, and the foremost, benefit to the photodegration process.

Because the use of photosensitizer or hydrogen sources along with UV degradation is a cost-effective and less time-consuming process, it has become an important alternative in wastewater treatment. For example, the photolysis of Arochlor 1254 under solar radiation degraded 25% in 20 hours, while the

photodechlorination was completed in four hours in the presence of the sensitizer phenothiazine (Hawari, 1991). Acetone has also been used as a sensitizer in promoting the UV degradation of trichloroethene due to the high triplet state energy of acetone (Choy and Chu, 2001). In addition, since acetone returns to its original state after the completion of the energy transfer, the recovery of acetone is possible in practice, if an appropriate extraction or purging process is applied (Chu and Tsui, 1999).

The use of additional hydrogen sources (or electron donors) in the photochemical reactions has also been shown to be useful in improving the reaction rates. For example, the increase of hydrogen source triethylamine concentration induced a higher level of methylmethacrylate (MMA) polymer conversion (Rodrigues et al., 1999). Apart from the rate improvement, Freeman and Lee (1992) have demonstrated that the addition of hydrogen sources in the photochemical process prevent the formation of more toxic dimers (Freeman and Lee, 1992). It was also demonstrated that a faster photodegradation rate of trichloroethene was observed in the presence of a hydrogen source, such as non-ionic surfactant Brij 35, than in water (Chu and Choy, 2000).

To determine the quantities of EDC being decomposed, the decay rates and the quantum yield of photodegradation reactions of the EDC should be obtained. A pseudo first-order decay is expected at constant temperature, light intensity, and illumination wavelength (Chu and Tsui, 1999). The quantum yield for pollutant decay using a monochromic light source, therefore, can be calculated from the experimental first order decay rate constant as described by Choudhry and Webster (1987):

$$\Phi_P = \frac{k_p}{2.303\, I_{\lambda,0}\, \varepsilon_{p,\lambda}\, l} = \frac{\{\text{number of pollutant molecules transform}\}}{\{\text{number of quanta absorbed by solution}\}}$$

where ϕ_P = quantum yield for the disappearance of EDC

$I_{\lambda,0}$ = intensity of the incident light at wavelength λ, Einstein / L-s

$\varepsilon_{p,\lambda}$ = molar absorptivity of EDC at wavelength λ, L / mole-cm

l = cell path length within the reactor, cm

k_p = the first order decay rate constant, s^{-1}

In view of this, it is theoretically possible to further improve the photodegradation rates of EDC by introducing a pre-selected sensitizer into the system. Therefore, the reaction kinetics, mechanisms and performance prediction of such processes will be investigated.

2.2.2 Ozonation systems

The treatment of municipal and industrial wastewaters by ozone has been widely used (Chu, 2001; Graham et al., 2003; Hoigné and Bader, 1976). The ozonation alone is often insufficient to meet wastewater treatment objectives because of the selectivity of molecular ozone, however in basic conditions non-selective hydroxyl radicals •OH can then be generated (Kos et al., 2004). The radical •OH can also be generated by combining ozone with other oxidizing agents (e.g. H_2O_2) or irradiation sources (e.g. UV, Vacuum-UV or microwave) (Kos et al., 2004). In this study the photolysis of ozone by UV at 254 nm is used, where the optimal absorption of ozone at this wavelength has been well established (Oppenlander, 2003).

The treatment of water or wastewater containing industrial chemicals or pesticides with ozone has been practiced in the U.S. and Europe over the last 20 years (Anderson, 1997). One of the main reasons is that ozone is a stronger oxidizing agent, and safer to use, than chlorine. Ozone reacts with organic compounds dissolved in water through a combination of direct ozone attack and indirect free radical attack. Molecular ozone is highly selective and reacts slowly with the majority of organic species, while the hydroxyl radical, formed naturally

as ozone decays, is non-selective and reacts extremely fast, so it is sufficient to rupture saturated bonds and ring systems not amenable to attack by molecular ozone (Lambert et al., 1996). Measurement of reaction rate constants and the prediction of the ozonation performance, for the cases of direct oxidation by ozone molecules and indirect oxidation by hydroxyl radicals, have been reported by Xiong and Graham (1992), and Chu and Ma (2000), respectively. Recent work has been investigating the degradation of a problematic pesticide by hydroxide radicals generated from manganese-catalysed ozonation (Ma and Graham, 1999 and 2000).

2.2.3 Advanced Oxidation Processes (AOPs)

A technology in water and wastewater treatment using advanced oxidation processes (AOPs) was considered to be fast and effective, it have shown great potential in the treatment of pollutants and its wide range of applications in groundwater treatment and municipal wastewater sludge destruction (Benitez, 1994; Parsons and Williams, 2004). It is also considered very effective for the mineralization of a great variety of organic compounds, including refractory organics like herbicides (Paterlini and Nogueira, 2005), which AOP could

effectively convert the constituents of an organic pollutants into simple, relatively harmless and inorganic molecules (i.e. CO_2, H_2O).

The use of AOPs involves the combinations of a high oxidation-potential source (H_2O_2 or O_3), UV irradiation and/or catalyst (Fe^{2+}, Fe^{3+} or TiO_2). Karimi et al. (1997) and Ruppert and Rupert (1994) have defined the AOP as processes which involved the generation of hydroxyl radicals in sufficient quantity, such as O_3/OH^-, O_3/H_2O_2, Fe^{2+}/H_2O_2, UVC/H_2O_2, UVC/O_3 and UVA/TiO_2. The aim of these processes is to generate a highly reactive hydroxyl radical ($^{\bullet}OH$), the most powerful oxidizing species after fluorine (Table 2.2). It reacts unselectively with most of organic and inorganic substances present in water.

Table 2.2 Relative power of common oxidants		
Compound	**Oxidation potential (volts)**	**Relative power of chlorine**
Fluorine	3.06	2.25
Sulfate radical ($SO_4^{\bullet -}$)	2.50-3.10	1.84-2.28
Hydroxyl radical ($OH^{\bullet}$)	2.00-2.80	1.47-2.05
Atomic oxygen ($O^{\bullet}$)	2.42	1.78
Ozone	2.08	1.52
Perhydroxyl radical	1.70	1.25
Permanganate	1.67	1.23
Chlorine dioxide	1.50	1.10
Hypochlorous acid	1.49	1.10
Chlorine	1.36	1.00
Bromine	1.09	0.80
Hydrogen peroxide	0.87	0.64
Iodine	0.54	0.40
Oxygen	0.40	0.29

(Ref.: Lin; 1993; Malato et al., 1998; Anipsitakis and Dionysiou, 2003, 2004a, 2004b)

2.2.4 UV/O_3 process

In the case of wastewater effluent treatment, however, higher concentrations of EDCs are expected, and standard ozonation and UV photolysis may not be able to achieve the degree of treatment required. In this case, advanced oxidation process, such as O_3/UV (Fig. 2.1), UV/hydrogen source or UV/sensitization, may be more effective and practically feasible (Chu and Jafvert, 1994).

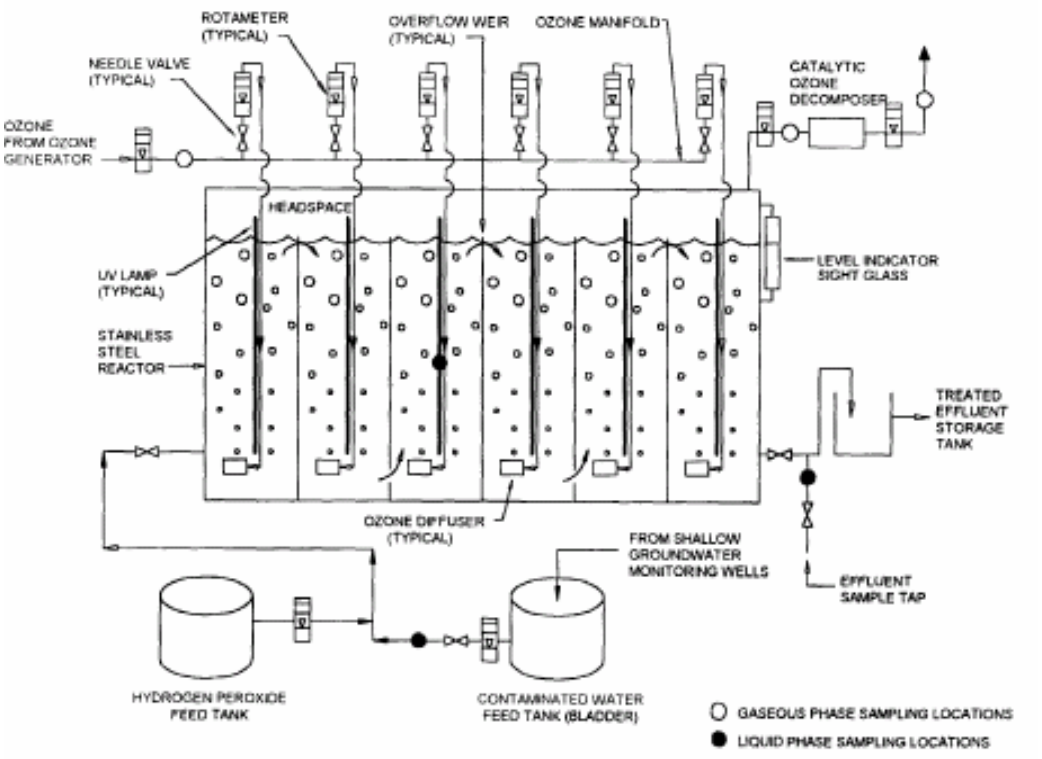

Fig. 2.5: UV/Ozone Reactor – Ultrox® (Jones, 1996)

The combined UV/O_3 system has been widely studied (Beltran, 2004; Jones, 1996), and its overall oxidation reaction has been shown to be due to a synergistic effect of several individual reactions, such as direct (molecular) ozonation, direct photolysis, and $^{\bullet}$OH radical oxidation. According to Canton et al. (2003), UV irradiation at a wavelength of 255 nm and at a pH of 2.5 led to all the ozone being photolyzed into hydrogen peroxide. This primary oxidizing product can then be further photolyzed into the $^{\bullet}$OH and then react with aqueous ozone to produce $^{\bullet}$OH, singlet oxygen, and peroxyl radical (Winarno and Getoff, 2002). It is believed that the UV/O_3 process could provide an effective treatment of EDCs and/or its toxic intermediates, when present in contaminated effluents.

Extended photolysis and thermal decomposition studies of TBHQ, a major metabolite of BHA, have been carried out by other authors (Kurechi et al, 1983), while the study of its parent compound BHA under direct photolysis, O_3 and UV/O_3 processes in aqueous phase is still very limited. Therefore, investigation of the kinetics and mechanisms of BHA degradation by ozonation, with and without UV irradiation will be conducted.

2.2.5 UV/$S_2O_8^{2-}$ process

In other study, extended studies of TBHQ by direct photolysis, a major metabolite of BHA, have been carried out by other authors (Beltran, 2004), and advanced oxidation processes (AOPs) have shown good performance in degrading organic compounds using UV/O_3 or UV/H_2O_2. However, the potential of alternative AOPs to improve the removal performance is always of interest and the photochemical oxidant, peroxydisulfate, could be a good candidate for such a purpose.

Peroxydisulfate ($S_2O_8^{2-}$ ion) is a strong oxidant (E° = 2.05 V) which has been used widely in the petroleum industry for the treatment of hydraulic fluids or as a reaction initiator (McCallum et al., 2000). The peroxydisulfate is normally available as a salt associated with ammonium, sodium or potassium. Potassium peroxydisulfate (KPS) recently was shown to be an effective disinfectant and/or oxidant for the Norwalk virus, foot-and-mouth disease and Coronaviridae (causing severe acute respiratory syndrome - SARS) (Thayer, 2003). It has also been reported to be effective for degrading organics in hazardous wastewaters in acidic or basic media through direct chemical oxidation (DCO) (McCallum et al., 2000), where peroxydisulfate is used as a sacrificial reagent (Romero et al.,

1999). However, since the reactions of peroxydisulfate are generally slow at normal temperatures, the thermal or photochemical activated decomposition of $S_2O_8^{2-}$ ion to $SO_4^{-\bullet}$ radical has been proposed as a method of accelerating the process (House, 1962; Waldemer et al., 2007), as summarised in the following reactions (Eqns. 2.1-2.5):

$$S_2O_8^{2-} + \text{photons or heat} \rightarrow 2SO_4^{\cdot -} \quad (2.1)$$

$$SO_4^{\cdot -} + RH_2 \rightarrow SO_4^{2-} + H^+ + RH^{\cdot} \quad (2.2)$$

$$RH^{\cdot} + S_2O_8^{2-} \rightarrow R + SO_4^{2-} + H^+ + SO_4^{\cdot -} \quad (2.3)$$

$$SO_4^{\cdot -} + RH \rightarrow R^{\cdot} + SO_4^{2-} + H^+ \quad (2.4)$$

$$2\ R^{\cdot} \rightarrow RR \text{ (dimer)} \quad (2.5)$$

In the oxidation process, sulfate ions will be generated as the end-product (Maurino et al., 1997), which leads to an increase in salt content in the effluent. The SO_4^{2-} is practically inert and is not considered to be a pollutant; the USEPA has listed it under the secondary drinking water standards with a maximum concentration of 250 mg/L (1.43 mM), based on aesthetic reasons (Weiner, 2000). Theoretically, sulfate ions can be regenerated electrolytically to peroxydisulfate for reuse in water as shown by Blazas et al. (Balazs et al., 1999). Alternatively,

potassium peroxydisulfate costs US$0.74 per kg (He Bei Ji Heng, 2006), which is much cheaper than other oxidants like hydrogen peroxide and Oxone (Anipsitakis and Dionysiou, 2003). Since peroxydisulfate will start reacting exothermally only at 100°C (Kronholm et al., 2000), it is not recommended for use in conventional water purification processes, other factors such as different light intensity, water pH and temperature might also affect its decomposition rate. However, the potential use of photo-activated peroxydisulfate at ambient temperature is of interest and has been investigated at 254 nm UV wavelength at wide pH ranges in this study.

2.2.6 UV/Ag^{+}/$S_2O_8^{2-}$ process

In order to remove EDCs and carcinogen, various studies have been carried out by using UV, ozone, UV/ozone, UV/peroxydisulfate processes (Anipsitakis and Dionysiou, 2004b, Kuo, 1999). The latter process shows a better mineralization efficiency due to the generation of sulfate radicals ($SO_4^{\bullet -}$) as shown in Eq. (2.6). According to Anipsitakis and Dionysiou (2004a) and Steenken (1998), $SO_4^{\bullet -}$ radical is recognized to be a better oxidant relative to hydroxyl radicals ($OH^{\bullet}$), since $SO_4^{\bullet -}$ demonstrates higher standard reduction potential than $OH^{\bullet}$ at neutral pH, while they are similar at acidic pH. However a faster mineralization process

is often a great interest for ultimate disposal of organics. Therefore, a metal-activated UV/$S_2O_8^{2-}$ system has drawn into consideration.

$$S_2O_8^{2-} + \text{photons} \rightarrow 2SO_4^{\bullet-} \qquad (2.6)$$

According to Cheves et al. (1978), peroxydisulfate may be decomposed to $SO_4^{\bullet-}$, not only by the redox reaction, but also by catalytic quantities of silver ion (Ag^+) as in Eq. (2.7). Silver is a valuable but most widely distributed elements on earth. It can be found in soil at 0.3 mg/kg concentration (Weiner, 2000); and around 1.8 to 2.8 x 10^{-3} mM (or 0.2-0.3 mg/L) in surface waters and particularly higher nearby industrial areas (0.37 mM). Silver is dispersed through the aquatic environment as dissolved and colloidal species. USEPA gives no primary drinking water standard for silver, but its secondary drinking water standard is set at 9.3 x 10^{-4} mM (or 0.10 mg/L) (Weiner, 2000).

In the $Ag^+/S_2O_8^{2-}$ reaction, Ag^+ shows the ability in activating $S_2O_8^{2-}$, where silver can be caged or bound to the metal sulfate radicals as indicated in Eq. (2.8) (Anipsitakis and Dionysiou, 2004a). Peroxydisulfate reactions with transition-metal complexes are not simply due to one electron-transfer reactions but rather involve the cleavage of the peroxydisulfate O-O bond to generate

sulfate radical as in Eqns. (2.9 to 2.13) (Nickel et al., 1994). In some other studies (House, 1962), copper (II) ion has also been studied with addition of $S_2O_8^{2-}$, but the silver ion is mostly investigated due to its best performance over reactivity.

$$Ag^+ + S_2O_8^{2-} \rightarrow Ag^{2+} + SO_4^{\bullet-} + SO_4^{2-} \quad (2.7)$$

$$Ag^+ + S_2O_8^{2-} \rightarrow Ag^{II}(SO_4^{\bullet})^+ + SO_4^{2-} \quad (2.8)$$

$$Ag^+ + SO_4^{\bullet-} \Leftrightarrow Ag^{2+} + SO_4^{2-} \quad (2.9)$$

$$Ag^+ + SO_4^{\bullet-} \rightarrow Ag^{3+} + 2SO_4^{2-} \quad (2.10)$$

$$Ag^+ + S_2O_8^{2-} \rightarrow AgS_2O_8^- \quad \text{(slow)} \quad (2.11)$$

$$AgS_2O_8^- \rightarrow Ag^{3+} + 2SO_4^{2-} \quad (2.12)$$

$$2Ag^+ + S_2O_8^{2-} \rightarrow 2Ag^{2+} + 2SO_4^{2-} \quad (2.13)$$

Silver nitrate is an oxidant as well, according to Butkus et al. (2005) with the aid of UV irradiation it possesses disinfection ability in a biological treatment system in removing *E. coli*. However, very limited studies could be found in discussing the treatability of such a process for organics removal. According to Zhang et al. (2007), in a dye degradation study, UV/$S_2O_8^{2-}$ process exhibits faster removal rate of total organic compounds, TOC or mineralization, than to that of

$Ag^{+}/S_2O_8^{2-}$ process, but vice versa to the case of decolourization. Some other studies also show that 1.2 mM of $Ag_2SO_4/S_2O_8^{2-}$ could transform 50% of 0.3 mM dichlorophenol in 120 min, while the target compound can be removed effectively with the aid of UV photolysis ($UV/Ag^{+}/S_2O_8^{2-}$ process) (Anipsitakis and Dionysiou, 2004a and 2004b).

Since there is no direct comparison study has been conducted so far for all the above processes. In this study, investigation of UV/Ag^{+}, $Ag^{+}/S_2O_8^{2-}$, UV only, $UV/S_2O_8^{2-}$ and $UV/Ag^{+}/S_2O_8^{2-}$ processes will be conducted, where preliminary screening tests of selection of UV wavelength and silver ion sources will also be investigated. The optimization of the $UV/Ag^{+}/S_2O_8^{2-}$ process will be illustrated by varying the dosage of silver ions.

2.2.7 Mineralization

In this study, mineralization refers to the result of the degradation of organic compounds or residuals, where complete conversion of organic compounds to CO_2, H_2O, NO_3, or other oxides, halides, phosphates, etc. will be taken place (Alfano et al., 1997; Wong and Chu, 2003, Zazo et al., 2005). As shown below in Fig. 2.6, a well-known degradation pathway of phenol to simple acids (i.e. Malonic acid, oxalic acid, etc.) and further to inorganic and environmental harmless products is explained schematically how the benzene ring gone ruptures.

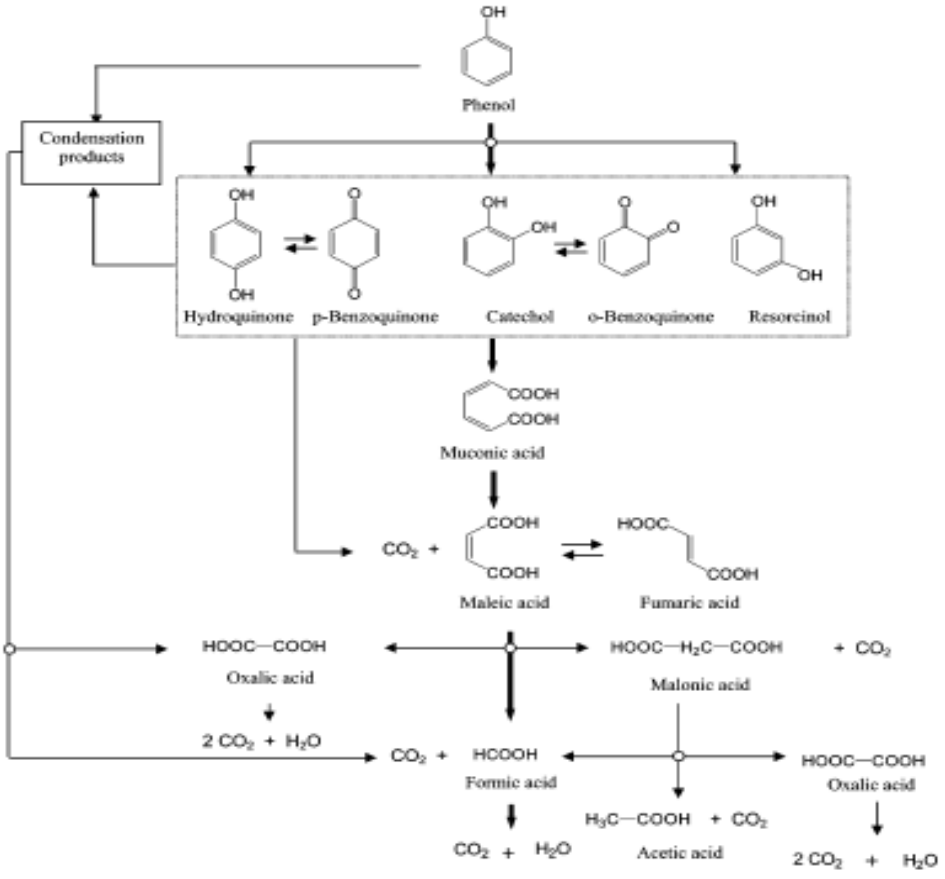

Fig. 2.6: Mineralization pathway of Phenol (Zazo et al., 2005)

CHAPTER 3 METHODOLOGY

3.1 Introduction

This chapter describes the methodology of the experimental setup for the wastewater treatment processes and reactor (or photo-reactor). The sampling and analytical methods of target compounds can be found in this chapter, and also how their intermediates are determined qualitatively and quantitatively are elucidated in detail. The procedure of EDC removal efficiency by different reaction processes in various parameters is also provided. Details of the analytical instruments can be found in Appendix I.

3.2 Target compounds

3.2.1 Dibutyl Phthalate (DBP) concentration and analytical methods

Three different concentrations of DBP were used ranging from 2 to 10 μM for the kinetic studies, while the photolysis-product identification was carried out at 4 μM of DBP (with a TOC of 0.6 mg L^{-1}). Since the maximum solubility of DBP was found to be ranging from 5.4 to 46.7 μM in different environment (Staples et al., 1997), therefore the targeted concentration of 4 μM was chosen to ensure the accuracy of the concentration.

3.2.1.1 Chemical reagents

Phthalic Acid (for Chromatography, 99.5% purity, CAS: 88-99-3), butyl benzoate (99% purity, CAS:136-60-7) and benzoic acid (99.9% purity, CAS: 65-85-0) were obtained from Riedel-De Haën, Aldrich and BDH limited Poole England, respectively. Di-n-butyl phthalate Pestanal® (DBP) (98.7% purity, CAS: 84-74-2) was obtained from Sigma-Aldrich. All solutions were prepared using 18 MΩ deionized distilled water from a Bamstead NANO pure water treatment system. All chemicals and solvents were HPLC grade, and they were used without further purification. For pH adjustment, 0.1 M sulphuric acid or 0.1 M sodium hydroxide was used. All experiments were carried out at room temperature (23±2℃) in duplicates. Dark control tests at different pH without UV-radiation indicated no volatilization of DBP in the laboratory setup.

3.2.1.2 Reactor setup

All experiments were carried out in a 1 L (95 mm ID × 191 mm H) quartz beaker with magnetic stirring, where 750 mL of the DBP sample was placed in the centric of the UV photoreactor, Rayonet™ RPR-200 (Southern New England Ultraviolet Co.). The reactor was equipped with eight phosphor-coated low-pressure mercury lamps (approximately 35 W each), emitting 254 nm

monochromatic UV at a light intensity of 1.5×10^{-6} Einstein L^{-1} s^{-1} (Chu and Tsui, 1999). The quantum yields for photolysis of DBP was calculated according to the well-defined equation from Chu and Jafvert (1994).

3.2.1.3 Target compound analysis and identification of intermediates

Compound analysis was carried out with a Thermo Quest Finnigan LCQ Duo Mass Spectrometer system controlled by XCalibur (software) equipped with a Restek® Pinnacle II column: C8, 250 x 4.6 mm, 5 μm particle size, at room temperature proceeded with a guard column of the same packing material (10×4 mm). The LC detection system consisted of a photodiode array UV-visible detector (PDA-UV), coupled with a electrospray ionization (ESI) or atmospheric pressure chemical ionization (APCI) interface with a quadrupole ion-trap mass spectrometer. The mobile phase consisted of 85% acetonitrile at 0.5 mL min^{-1}. Standards were prepared monthly and stored in the dark at 4°C for validation.

A Thermo AS3000 narrow-bore variable-loop auto-sampler with an injection volume of 20 μL was used for the DBP analysis, while a Thermo P4000 narrow-bore gradient pump was used to identify reaction intermediates (Coldham et al., 1998) and end-products at mobile phases with acetonitrile increased from

10 to 100% in 30 min. Ionization of the HPLC eluate was performed with the following settings: vaporizer temperature 270°C, spray voltage 4.0 kV, current 5 μA, sheath gas and auxiliary gas (N_2) flow rates (arbitrary units) 80 and 20, capillary temperature and voltage 150°C and 3V, respectively, and data collected from m/z 50-300. The DBP was quantified by using LC-APCI-MS operating in the positive ion mode of ionization at m/z 279, while other photolysis products were identified by using LC-ESI-MS operating in the negative ion condition at a capillary temperature of 225°C.

A total of six major intermediates/end products were identified from the DBP photo-degradation at 254 nm and these included: mono butyl phthalate (MBP, 221 m/z), MBP derived ketone (or aldehyde) (MBPK, 212 m/z) and alcohol (MBPA, 213 m/z), butyl benzoate (BB, 177 m/z), benzoic acid (BA, 121 m/z), and phthalic acid (PA, 165 m/z). The quantification of photoproducts or intermediates was mostly established by using standard solutions, such as PA, BB, and BA. For the intermediates that are not commercially available (MBP, MBPA and MBPK), their relative abundance were estimated by comparing their corresponding protonated ion intensity to that of the initial DBP in solution from the MS analysis.

3.2.2 Carbofuran (CBF) concentration and analytical method

0.2 mM CBF was used to investigate in all three different treatment processes, in which at this concentration is of its maximum. Hence the longest reaction time required to fully degrade this recalcitrant chemicals can be found.

3.2.2.1 Chemical reagent

Carbofuran (98%), 2,3-dihydro-2,2-dimethyl-7-benzofuranol (CBF), was obtained from Sigma-Aldrich, and was prepared in 18MΩ deionized distilled water. For pH adjustment, 0.1 M sulphuric acid or 0.1 M sodium hydroxide was used. All chemicals and solvents were of HPLC grade, and they were used without further purification.

3.2.2.2 Reactor setup

For tests involving UV photolysis, 750 mL sample were irradiated in a 1 L quartz beaker with magnetic stirring, which was placed in the centre of a Rayonet™ RPR-200 photoreactor. The reactor was equipped with eight phosphor-coated low-pressure mercury lamps, emitting 253.7 nm monochromatic UV at a light intensity of 1.5×10^{-6} Einstein$L^{-1}s^{-1}$. For those tests involving ozonation, before the introduction of CBF, deionized water was pre-ozonated for 10 minutes

(producing a saturated ozone solution) and thereafter ozone gas was fed continuously into the reactor through a glass sparger located just above the bottom of the reactor. The OZAT® ozone generator (CFS-1A from Ozonia Ltd.) with oxygen feed gas at 1 L min^{-1} produced 0.018 mM saturated ozone which was determined by the Indigo spectrometric method (Chu and Ma, 2000). For the UV/O_3 experiments, simultaneous UV-irradiation was provided during the preozonation period. The remaining ozone in the collected sample was quenched by sodium thiosulphate before quantification of the organic substrates. Comparative experiments were undertaken with O_3 and UV irradiation separately.

3.2.2.3 Target compound analysis

A high-performance liquid chromatograph (HPLC) equipped with a 250-mm, 5-μm, ID 4.6mm Hypersil ODS C18 column (Agilent) was used for the CBF quantification. The mobile phase was a mixture of 0.15% acetic acid and 65% acetonitrile at a flow rate of 1.0 mL/min.

3.2.3 Butylated Hydroxyanisole (BHA) concentration and analytical method

3.2.3.1 Chemical reagent

Butylated Hydroxyanisole, BHA, (98.1% Purity) and 2-*tert*-butyl-1,4-benzoquinone (TBQ, 98%) were obtained from Sigma-Aldrich, and 2,2'-Dihydroxy-5,5'-dimethozy-3,3'-di-t-butylbiphenyl (di-BHA) was synthesized from BHA (Hewgill and Hewitt, 1967). All chemicals including, *tert*-butylhydroquinone (TBHQ, 97%), p-Benzoquinone (PBQ, 97%) and Hydroquinone (HQ**,** 99.5%) purchased from Acros Organics, ammonium peroxydisulfate, ($(NH_4)_2S_2O_8$, APS, Riedel-de-Haen, 98%), potassium peroxydisulfate, ($K_2S_2O_8$, KPS, Sigma-Aldrich, 99+%); silver nitrate ($AgNO_3$, 99.8%, CAS: 7761-88-8, Riedel-de Haën) and silver sulfate (Ag_2SO_4, 99.7%, CAS: 10294-26-5, Uni-Chem Chemical Reagent) were prepared by 18 MΩ deionized distilled water from a Bamstead NANOpure water treatment system, while solid silver oxide (Ag_2O, 99.6%, CAS: 20667-12-3) obtained from International Laboratory USA was applied directly into the reactor without further purification. Unless otherwise stated, the concentrations of KPS used were 2 mM throughout the study.

A preliminary study of choosing an appropriate peroxydisulfate salts was carried out, since many thermal- or photo-decomposition studies (McCallum et al., 2000; Maurino et al., 1997) with various oxidant sources are reported. In this study two of the most common oxidants, ammonium peroxydisulfate (APS) and potassium peroxydisulfate (KPS) were chosen for examination, as they have similar quantum yields: 0.0112 (APS) and 0.0107 (KPS) (Cass et al., 1972).

Structural details of BHA and its degradation derivatives are given in Table 3.1. All chemicals and solvents were of HPLC grade, and they were used without further purification. For pH adjustment, 0.1 M sulphuric acid or 0.1 M sodium hydroxide was used. All experiments were carried out at room temperature (23±2 ℃) in triplicate.

Table 3.1 General structure of butylated hydroxyanisole and its degradation derivatives

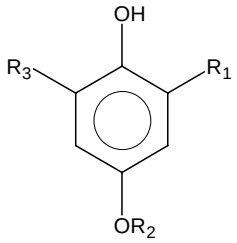

Abbreviations	Compounds	R_1	R_2	R_3	
BHA	Butylated Hydroxyanisole	$C(CH_3)_3$	CH_3	H	
Di-BHA	2,2'-Dihydroxy-5,5'-dimethozy-3,3'-di-t-butylbiphenyl	$C(CH_3)_3$	CH_3	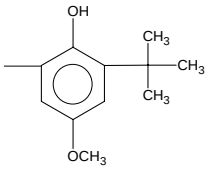	
TBHQ	*tert*-butyl-1,4-hydroquinone	$C(CH_3)_3$	H	H	
BHA-OH	3-tert-butyl-4,5-dihydroxyanisole	$C(CH_3)_3$	CH_3	OH	
HQ	Hydroquinone	H	H	H	

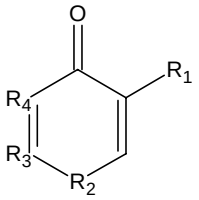

Abbreviations	Compounds	R_1	R_2	R_3	R_4
BBDQ	3,3'-di-*tert*-butyl-biphenyl diquinone-(2,5,2',5')	$C(CH_3)_3$	C=O	H	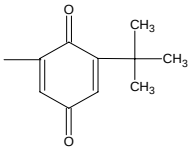
Oxi-di-BHA		$C(CH_3)_3$	OCH_3	H	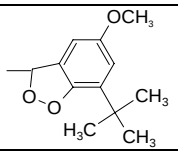
BHA-OQ	3-tert-butyl-5-methoxy-1,2,-benzoquinone	$C(CH_3)_3$	OCH_3	H	C=O
TBQ	*tert*-butyl-1,4-benzoquinone	$C(CH_3)_3$	C=O	H	H
PBQ	1,4-Benzoquinone	H	C=O	H	H
BHDQ	2,6-di-tert-butyl-8-hydroxy-dibenzofuran-1,4-quinone	$C(CH_3)_3$	C=O	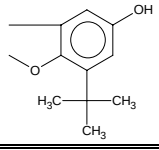	

While in the UV/Ag^{+}/$S_2O_8^{2-}$ study, the initial pH of the solution was at 3, this is to avoid precipitation of silver colloids at elevated pH levels as suggested by Anipsitakis and Dionysiou (2004b), where silver ion will undergo speciation and precipitation at alkaline condition.

3.2.3.2 Reactor setup

For tests involving UV photolysis, and ozonation or UV/ozonation process, 750 mL sample were irradiated in the centre of Rayonet™ photoreactor as described in section 3.2.2.1and 3.2.2.2, respectively.

3.2.3.3 Target compound analysis and identification of intermediates

During ozonation it was noticed that an orange brown crystalline solid was produced, the reaction mixture was filtered using a 0.2 μm nylon filter at the end of the reaction, prior to compound analysis using LC-ESI-MS/MS. All other samples taken during reaction were dissolved with acetonitrile at a 1:1 ratio for LC-ESI-MS/MS analysis, so that the sample matrix of those hydrophobic and hydrophilic intermediates can all be detected throughout the experiment. As the sample filtrates only show the distribution of soluble intermediates (TBHQ, HQ, PBQ, BHA-OH), it is believed that the insoluble intermediates also play an

important role or contribute significantly to the whole mechanism; that is, to the formation of TBQ, di-BHA, BBHQ, BHDQ, oxi-di-BHA, BHA-OQ, etc. Therefore, the precipitates are dissolved in 100% acetonitrile for verification. Those intermediate compounds with available standards were quantified in this study, while for other, minor substances that could not be purchased commercially they are presented in terms of ion intensity relative to the initial BHA concentration for comparison.

A Thermo Quest Finnigan LCQ Duo Mass Spectrometer system controlled by XCalibur (software) was used with an Agilent Hypersil ODS column (250 x 4.6 mm, 5 μm particle size) at room temperature, which consisted of a PDA-UV detector, and an electrospray ionization with a quadrupole ion-trap mass spectrometer. The mobile phase consisted of 70% acetonitrile at 1 ml/min with a detection limit of 0.003 mM BHA. A Thermo AS3000 narrow-bore variable-loop auto-sampler with a gradient pump was used to identify reaction intermediates and end-products at mobile phases with acetonitrile increased from 10 to 100% in 40 min. The photoproducts were identified by using LC-ESI-MS/MS operating in the positive or negative ion condition at a capillary temperature of 225 °C with different voltage applied (Table 3.2), the tuning method is

predetermined by using direct infusion of BHA standard solution into the LCMS/MS in order to magnify the sensitivity of quadrupole ion-trap detector. Ionization of the HPLC eluate was performed with the following settings: vaporizer temperature 270 °C, spray voltage 4.0 kV, current 5 μA, sheath gas and auxiliary gas (N_2) flow rates (arbitrary units) 80 and 20, capillary temperature and voltage 150 °C and 3 V, respectively, and data collected from m/z 50–500.

For those samples collected from the UV/$S_2O_8^{2-}$ and UV/Ag^+/$S_2O_8^{2-}$ process, they were mixed with an excess of sodium nitride (Anipsitakis and Dionysiou, 2003) to quench the radicals before the quantification of the probe compound, intermediates and TOC.

Control tests without UV-irradiation and with $K_2S_2O_8$ alone in the dark did not induce any transformation of BHA (data are not given here). For the UV/$S_2O_8^{2-}$ tests, those intermediate compounds for which standards were available, were quantified in this study, while for other, minor substances that could not be purchased commercially they were calculated in terms of ion intensity relative to the initial BHA concentration for comparison.

Table 3.2: The detection mode and its corresponding ESI-MS/MS spectrum for each intermediates (selected MS spectra indicated with asteroid - *)

Compounds	Retention time (min)	UV (λ_{max})	Detection Mode	Characteristic *m/z* ions	ESI-MS/MS spectrum ions (m/z)	Collision Energy (V)
BHA	27.1	226	-ve	179 [M – H]	165, 121	
BBDQ	36.5		+ve	327 [M + H]	311, 179, 164	
di-BHA*	35.75	299	-ve	357 [M – H]	342	29 (10)
Oxi-di-BHA	33.78		-ve	373 [M – H]	357, 342, 179, 165	
BHDQ	30.26		-ve	327 [M + 2 - H]	312, 299, 179, 165, 120	
TBQ	25.2	248	-ve	164 [M + 1 – H]	149, 120	29 (5)
BHA-OQ	23.55	257;	-ve	193 [M – H]	179, 165, 163, 120	
BHA-OH	20.33	268;	-ve	195 [M – H]	179, 165, 121,	
TBHQ*	17.38	226, 291	-ve	165 [M – H]	150, 121, 108	
PBQ	7.95	237, 292	-ve	108 [M + 1 – H]	-	20 (5)
HQ	5.5	221, 290	-ve	108 [M – 1 – H]	-	20 (5)

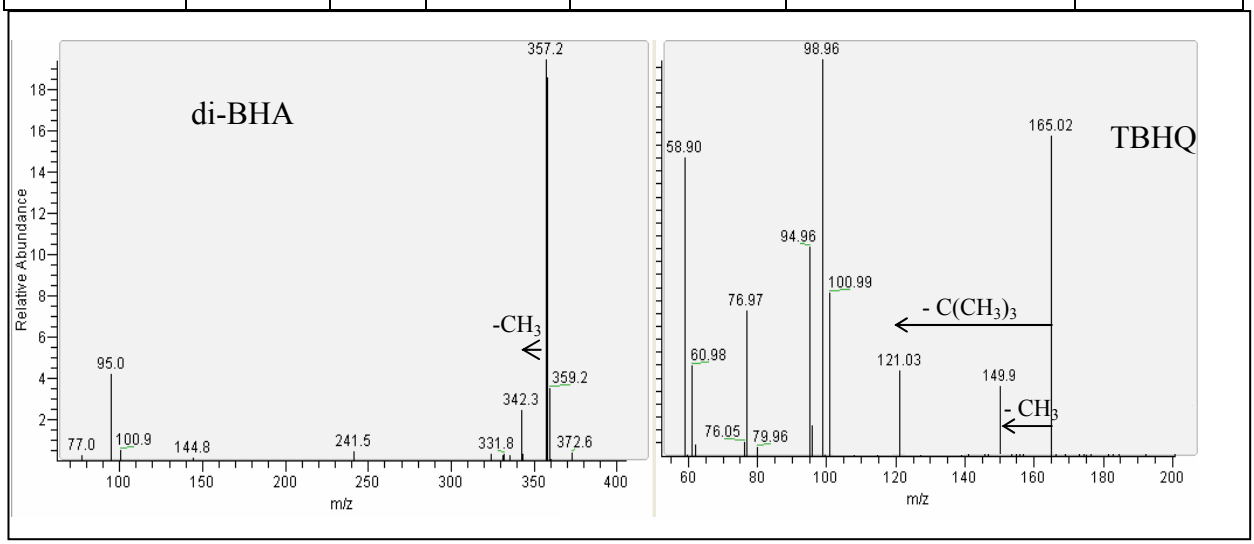

3.2.3.4 Determination of peroxydisulfate and its reaction product (sulphate ion)

The $S_2O_8^{2-}$ residual was measured by the iodometric method (Buck et al., 1954) with a correlation coefficient of $r^2 = 0.999$. 30 mL of the preserved sample was mixed with potassium iodide (4 g) and stopped until dissolved for 15 min. 1 mL of 6 N acetic acid and starch indicator were also added prior to titration with 0.01 N sodium thiosulfate. Since two mole of iodide will react with 1 mole of peroxydisulfate as indicate in the equation (3.1). The amount of sulfate released in the solution was determined by ion chromatography, using a Metrosep A Supp5 column (Metrohm Ion Analysis, 250 x 4 mm), an Alltech ERIS^{TM} 1000HP autosuppressor, and a BIO-RAD HPCM conductivity monitor. The mobile phase consisted of 1.8 mM Na_2CO_3 and 1.8 mM $NaHCO_3$ buffer solution and the flow rate was 1.3 ml/min with a detection limit of 0.125 mM [SO_4^{2-}].

$$S_2O_8^{2-} + 2\ I^- \rightarrow 2\ SO_4^{2-} + I_2 \qquad (3.1)$$

3.2.4 Mineralization (TOC analyzer)

Total organic carbon (TOC) analyzer is used to measure the TOC of samples. The principle of it is to break down the single carbon units and convert to single carbon molecular form (i.e. carbon dioxide) that can be measured quantitatively. The inorganic carbon is first removed by acidification and sparging. Each sample is acidified to pH 3 prior to TOC analysis. The analyzer is calibrated bi-monthly. The sample is loaded into the analyzer by automatic sampler and the carrier gas, O_2, will carry the sample right into the reactor. A high temperature catalytic combustion is used to convert organic carbons to carbon dioxide (CO_2). The resulting CO_2 is then measured directly by an infrared analyzer. The TOC content is calculated and displayed in mg/L by the computer.

3.2.5 List of Experiments

Here below shown a list of experiments that have been conducted throughout this study, including different EDC compounds at various conditions, i.e. pH, oxidant dosages, and light intensity, etc. Their corresponding raw data can be found in Appendix II.

Experiment No.	Compound	Initial Concentration	Parameters				
			pH	***O_3 (mM)***	***UV (nm)***	***Intensity (Einsten L^{-1} min^{-1})***	***$S_2O_8^{2-}$ (mM)***
DBP1	DBP	4 μM	3.0		254	7.20×10^{-4}	
DBP2	DBP	4 μM	5.0		254	7.20×10^{-4}	
DBP3	DBP	4 μM	7.0		254	7.20×10^{-4}	
DBP4	DBP	4 μM	9.0		254	7.20×10^{-4}	
DBP5	DBP	4 μM	11.0		254	7.20×10^{-4}	
DBP6	DBP	2 μM	3.0		254	7.20×10^{-4}	
DBP7	DBP	2 μM	5.0		254	7.20×10^{-4}	
DBP8	DBP	2 μM	7.0		254	7.20×10^{-4}	
DBP9	DBP	2 μM	11.0		254	7.20×10^{-4}	
DBP10	DBP	10 μM	2.7		254	7.20×10^{-4}	
DBP11	DBP	10 μM	3.3		254	7.20×10^{-4}	
DBP12	DBP	10 μM	4.3		254	7.20×10^{-4}	
DBP13	DBP	10 μM	7.4		254	7.20×10^{-4}	
DBP14	DBP	10 μM	8.9		254	7.20×10^{-4}	
DBP15	DBP	10 μM	10.7		254	7.20×10^{-4}	

Experiment No.	Compound	Initial Concentration	Parameters				
			pH	***O_3 (mM)***	***UV (nm)***	***Intensity (Einsten L^{-1} min^{-1})***	***$S_2O_8^{2-}$ (mM)***
CBF1	CBF	0.2 mM	3.0		254	7.20×10^{-4}	
CBF2	CBF	0.2 mM	5.0		254	7.20×10^{-4}	
CBF3	CBF	0.2 mM	7.0		254	7.20×10^{-4}	
CBF4	CBF	0.2 mM	9.0		254	7.20×10^{-4}	
CBF5	CBF	0.2 mM	11.0		254	7.20×10^{-4}	
CBF6	CBF	0.2 mM	3.0	0.018			
CBF7	CBF	0.2 mM	5.0	0.018			
CBF8	CBF	0.2 mM	7.0	0.018			
CBF9	CBF	0.2 mM	9.0	0.018			
CBF10	CBF	0.2 mM	11.0	0.018			
CBF11	CBF	0.2 mM	3.0	0.018	254	7.20×10^{-4}	
CBF12	CBF	0.2 mM	5.0	0.018	254	7.20×10^{-4}	
CBF13	CBF	0.2 mM	7.0	0.018	254	7.20×10^{-4}	
CBF14	CBF	0.2 mM	9.0	0.018	254	7.20×10^{-4}	
CBF15	CBF	0.2 mM	11.0	0.018	254	7.20×10^{-4}	

Experiment No.	Compound	Initial Concentration	Parameters				
			pH	*O_3 (mM)*	*UV (nm)*	*Intensity (Einsten L^{-1} min^{-1})*	*$S_2O_8^{2-}$ (mM)*
BHA1	BHA	0.1	3		254	7.20×10^{-4}	
BHA2	BHA	0.1	5		254	7.20×10^{-4}	
BHA3	BHA	0.1	7		254	7.20×10^{-4}	
BHA4	BHA	0.1	9		254	7.20×10^{-4}	
BHA5	BHA	0.1	11		254	7.20×10^{-4}	
BHA6	BHA	0.2	3		254	7.20×10^{-4}	
BHA7	BHA	0.2	5		254	7.20×10^{-4}	
BHA8	BHA	0.2	7		254	7.20×10^{-4}	
BHA9	BHA	0.2	9		254	7.20×10^{-4}	
BHA10	BHA	0.2	11		254	7.20×10^{-4}	
BHA11	BHA	0.3	3		254	7.20×10^{-4}	
BHA12	BHA	0.3	5		254	7.20×10^{-4}	
BHA13	BHA	0.3	7		254	7.20×10^{-4}	
BHA14	BHA	0.3	9		254	7.20×10^{-4}	
BHA15	BHA	0.3	11		254	7.20×10^{-4}	

Experiment No.	Compound	Initial Concentration	Parameters				
			pH	*O_3 (mM)*	*UV (nm)*	*Intensity (Einsten L^{-1} min^{-1})*	*$S_2O_8^{2-}$ (mM)*
BHA16	BHA	0.1	3	0.018			
BHA17	BHA	0.1	5	0.018			
BHA18	BHA	0.1	7	0.018			
BHA19	BHA	0.1	9	0.018			
BHA20	BHA	0.1	11	0.018			
BHA21	BHA	0.2	3	0.018			
BHA22	BHA	0.2	5	0.018			
BHA23	BHA	0.2	7	0.018			
BHA24	BHA	0.2	9	0.018			
BHA25	BHA	0.2	11	0.018			
BHA26	BHA	0.3	3	0.018			
BHA27	BHA	0.3	5	0.018			
BHA28	BHA	0.3	7	0.018			
BHA29	BHA	0.3	9	0.018			
BHA30	BHA	0.3	11	0.018			

Experiment No.	Compound	Initial Concentration	Parameters				
			pH	*O_3 (mM)*	*UV (nm)*	*Intensity (Einsten L^{-1} min^{-1})*	*$S_2O_8^{2-}$ (mM)*
BHA31	BHA	0.1	3	0.018	254	7.20×10^{-4}	
BHA32	BHA	0.1	5	0.018	254	7.20×10^{-4}	
BHA33	BHA	0.1	7	0.018	254	7.20×10^{-4}	
BHA34	BHA	0.1	9	0.018	254	7.20×10^{-4}	
BHA35	BHA	0.1	11	0.018	254	7.20×10^{-4}	
BHA36	BHA	0.2	3	0.018	254	7.20×10^{-4}	
BHA37	BHA	0.2	5	0.018	254	7.20×10^{-4}	
BHA38	BHA	0.2	7	0.018	254	7.20×10^{-4}	
BHA39	BHA	0.2	9	0.018	254	7.20×10^{-4}	
BHA40	BHA	0.2	11	0.018	254	7.20×10^{-4}	
BHA41	BHA	0.3	3	0.018	254	7.20×10^{-4}	
BHA42	BHA	0.3	5	0.018	254	7.20×10^{-4}	
BHA43	BHA	0.3	7	0.018	254	7.20×10^{-4}	
BHA44	BHA	0.3	9	0.018	254	7.20×10^{-4}	
BHA45	BHA	0.3	11	0.018	254	7.20×10^{-4}	

Experiment No.	Compound	Initial Concentration	Parameters				
			pH	***O_3 (mM)***	***UV (nm)***	***Intensity (Einsten L^{-1} min^{-1})***	***$S_2O_8^{2-}$ (mM)***
BHAS1	BHA	0.1 mM	3.0		254	7.20×10^{-4}	
BHAS2	BHA	0.3 mM	3.0		254	7.20×10^{-4}	
BHAS3	BHA	0.5 mM	3.0		254	7.20×10^{-4}	
BHAS4	BHA	0.1 mM	3.0		254	7.20×10^{-4}	2.0
BHAS5	BHA	0.2 mM	3.0		254	7.20×10^{-4}	2.0
BHAS6	BHA	0.3 mM	3.0		254	7.20×10^{-4}	2.0
BHAS7	BHA	0.5 mM	3.0		254	7.20×10^{-4}	2.0
BHAS8	BHA	0.3 mM	3.0		254	7.20×10^{-4}	0.1
BHAS9	BHA	0.3 mM	3.0		254	7.20×10^{-4}	0.5
BHAS10	BHA	0.3 mM	3.0		254	7.20×10^{-4}	1.0
BHAS11	BHA	0.3 mM	3.0		254	7.20×10^{-4}	5.0
BHAS12	BHA	0.3 mM	3.0		254	7.20×10^{-4}	10
BHAS13	BHA	0.5 mM	3.0		254	7.20×10^{-4}	1.0
BHAS14	BHA	0.5 mM	3.0		254	7.20×10^{-4}	5.0
BHAS15	BHA	0.5 mM	3.0		254	7.20×10^{-4}	10

Experiment No.	Compound	Initial Concentration	Parameters				
			pH	***O_3 (mM)***	***UV (nm)***	***Intensity (Einsten L^{-1} min^{-1})***	***$S_2O_8^{2-}$ (mM)***
BHAS16	BHA	0.1 mM	3.0		254	7.20×10^{-4}	0.10
BHAS17	BHA	0.1 mM	3.0		254	7.20×10^{-4}	0.25
BHAS18	BHA	0.1 mM	3.0		254	7.20×10^{-4}	0.50
BHAS19	BHA	0.1 mM	3.0		254	7.20×10^{-4}	1.00
BHAS20	BHA	0.1 mM	3.0		254	7.20×10^{-4}	5.00
BHAS21	BHA	0.1 mM	3.0		254	7.20×10^{-4}	10.00
BHAS22	BHA	0.1 mM	3.0		254	7.20×10^{-4}	15.00
BHAS23	BHA	0.1 mM	3.0		254	7.20×10^{-4}	20.00
BHAS24	BHA	0.1 mM	3.0		254	7.20×10^{-4}	40.00
BHAS25	BHA	0.1 mM	7.0		254	7.20×10^{-4}	0.10
BHAS26	BHA	0.1 mM	7.0		254	7.20×10^{-4}	0.25
BHAS27	BHA	0.1 mM	7.0		254	7.20×10^{-4}	0.50
BHAS28	BHA	0.1 mM	7.0		254	7.20×10^{-4}	2.00
BHAS29	BHA	0.1 mM	7.0		254	7.20×10^{-4}	1.00
BHAS30	BHA	0.1 mM	7.0		254	7.20×10^{-4}	5.00

Experiment No.	Compound	Initial Concentration	Parameters				
			pH	*O_3 (mM)*	*UV (nm)*	*Intensity (Einsten L^{-1} min^{-1})*	*$S_2O_8^{2-}$ (mM)*
BHAS31	BHA	0.1 mM	7.0		254	7.20×10^{-4}	10.00
BHAS32	BHA	0.1 mM	7.0		254	7.20×10^{-4}	15.00
BHAS33	BHA	0.1 mM	11.0		254	7.20×10^{-4}	0.10
BHAS34	BHA	0.1 mM	11.0		254	7.20×10^{-4}	0.25
BHAS35	BHA	0.1 mM	11.0		254	7.20×10^{-4}	0.50
BHAS36	BHA	0.1 mM	11.0		254	7.20×10^{-4}	1.00
BHAS37	BHA	0.1 mM	11.0		254	7.20×10^{-4}	2.00
BHAS38	BHA	0.1 mM	11.0		254	7.20×10^{-4}	5.00
BHAS39	BHA	0.1 mM	11.0		254	7.20×10^{-4}	10.00
BHAS40	BHA	0.1 mM	11.0		254	7.20×10^{-4}	15.00
BHAS41	BHA	0.1 mM	7.0		254	7.20×10^{-4}	$(NH_3)_2S_2O_8$ 2.00
BHAS42	BHA	0.1 mM	3.0		300	6.72×10^{-4}	2.00
BHAS43	BHA	0.1 mM	3.0		350	7.46×10^{-4}	2.00
BHAS44	BHA	0.1 mM	3.0		300	3.36×10^{-4}	2.00

Experiment No.	Compound	Initial Concentration	Parameters				
			pH	*Ag^+ (mM)*	*UV (nm)*	*Intensity (Einsten L^{-1} min^{-1})*	*$S_2O_8^{2-}$(mM)*
BHAS45	BHA	0.1 mM	3.0		350	14.9×10^{-4}	2.00
BHAS46	BHA	0.1 mM	3.0		300	6.72×10^{-4}	
BHAS47	BHA	0.1 mM	3.0		350	7.46×10^{-4}	
BHAS48	BHA	0.1 mM	3.0		300	3.36×10^{-4}	
BHAS49	BHA	0.1 mM	3.0		350	14.9×10^{-4}	
BHAAS1	BHA	0.1 mM	3.0	Ag_2SO_4 1.0	254	7.20×10^{-4}	
BHAAS2	BHA	0.1 mM	3.0	Ag_2SO_4 1.0			2.0
BHAAS3	BHA	0.1 mM	3.0	Ag_2SO_4 1.0	254	7.20×10^{-4}	2.0
BHAAS4	BHA	0.1 mM	3.0	2.0	254	7.20×10^{-4}	2.0
BHAAS5	BHA	0.1 mM	3.0		350	7.46×10^{-4}	
BHAAS6	BHA	0.1 mM	3.0		350	7.46×10^{-4}	2.0
BHAAS7	BHA	0.1 mM	3.0	2.0	350	7.46×10^{-4}	
BHAAS8	BHA	0.1 mM	3.0	2.0	350	7.46×10^{-4}	2.0

Experiment No.	Compound	Initial Concentration	Parameters				
			pH	*Ag^+ (mM)*	*UV (nm)*	*Intensity (Einsten L^{-1} min^{-1})*	*$S_2O_8^{2-}$(mM)*
BHAAS9	BHA	0.1 mM	3.0	0.1	254	7.20×10^{-4}	2.0
BHAAS10	BHA	0.1 mM	3.0	1.0	254	7.20×10^{-4}	2.0
BHAAS11	BHA	0.1 mM	3.0	1.5	254	7.20×10^{-4}	2.0
BHAAS12	BHA	0.1 mM	3.0	2.5	254	7.20×10^{-4}	2.0
BHAAS13	BHA	0.1 mM	3.0	5.0	254	7.20×10^{-4}	2.0
BHAAS14	BHA	0.1 mM	3.0	15.0	254	7.20×10^{-4}	2.0
BHAAS15	BHA	0.1 mM	3.0	20.0	254	7.20×10^{-4}	2.0
BHAAS16	BHA	0.1 mM	3.0	30.0	254	7.20×10^{-4}	2.0
BHAAS17	BHA	0.1 mM	3.0	Ag_2O 1.0	254	7.20×10^{-4}	2.0
BHAAS18	BHA	0.1 mM	3.0	Ag_2O 7.5	254	7.20×10^{-4}	2.0

CHAPTER 4 REMOVAL OF DIBUTYLPTHHALTE BY UV PHOTOLYSIS

4.1 Introduction

This chapter depicts the applicability of using UV direct photolysis as a mean of transforming DBP into simple organic compounds. In view of this situation there is growing interest in the capability and performance of additional treatment processes that may be applied to remove EDCs, including DBP, from raw waters, wastewaters and leachates. Given that UV-irradiation at 254 nm is used for disinfecting wastewater effluents, it is of interest to know whether this process can also achieve a simultaneous degradation of EDCs. Currently, there is limited information concerning the UV photolysis of DBP and in this study the results of an investigation of the kinetics and mechanisms of DBP degradation by UV-irradiation at a wavelength of 254 nm is reported. It is believed that the results of this study will be of considerable interest and value to the authorities responsible for water supply, wastewater disposal and environmental protection, as well as of general significance to the academic community.

4.2 Photodegradation of DBP

4.2.1 Rate constants for the degradation of DBP and the associated effects of pH

A nearly complete removal (≈100%) of 4 μM DBP in water can be achieved by a irradiation period of 90 min. The photolysis of DBP was then found to follow pseudo-first-order kinetics ($C_T = C_0e^{-kt}$) initially (1st stage); however, after an extended period of irradiation (20 to 30 min) the decay rate reduced (2nd stage), as shown in Fig. 4.1. In general, the initial rate of compound decay increased with increasing pH, which is believed to be due to the involvement of basic-catalytic hydrolysis (to be discussed subsequently). However, it was found that the highest rate of compound decay (1st stage) was at the lowest initial pH level (i.e. 3). This is believed to arise because of the involvement of an additional decay pathway which will also be discussed later. In stage 1, the pseudo-first order rate constants were in the range from 0.07 to 0.09 min^{-1}, corresponding with a 73 to 91% of DBP removal, respectively.

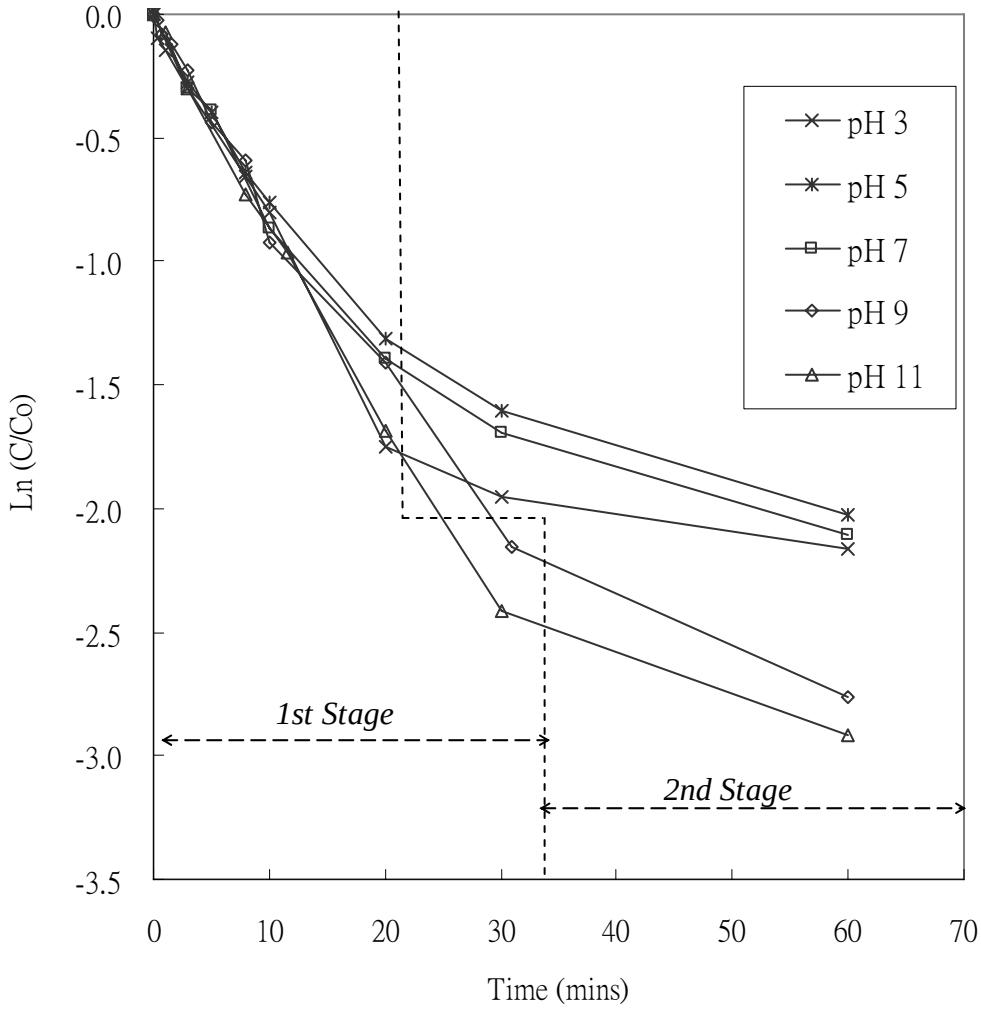

Fig. 4.1: Photodegradation of DBP (DBP0: 4 μM, UV: 254 nm, 1.5 x 10^{-5} Einstein $L^{-1}s^{-1}$.)

The direct photolysis induced by UV (Grossmann et al., 2001) should be one of the major reaction pathways responsible for the DBP decay. Upon the absorption of UV irradiation at 254 nm DBP is transferred to its corresponding excited states (singlet or triplet), which is then followed by either chemical degradation (of

DBP) or futile energy decays (e.g. fluorescence, phosphorescence, and heat release). It was noted that the rates of DBP degradation were higher at both the highest and lowest pH levels tested. This is believed to be due to the involvement of indirect photolysis via the acid and based catalyzed photo-hydrolysis analogue to the traditional hydrolysis processes that can be catalyzed in acidic and basic solutions (Loudon, 1988). To verify the influence of pH on the process, the rate constants of DBP decay at different initial concentrations (i.e. 2, 4, and 10 μM) were determined and the values are summarized in Fig. 4.2 with their corresponding quantum yields. The minima in the measured rate constant appeared to occur at a pH between around 4.5 to 5.0, regardless of the initial DBP concentration.

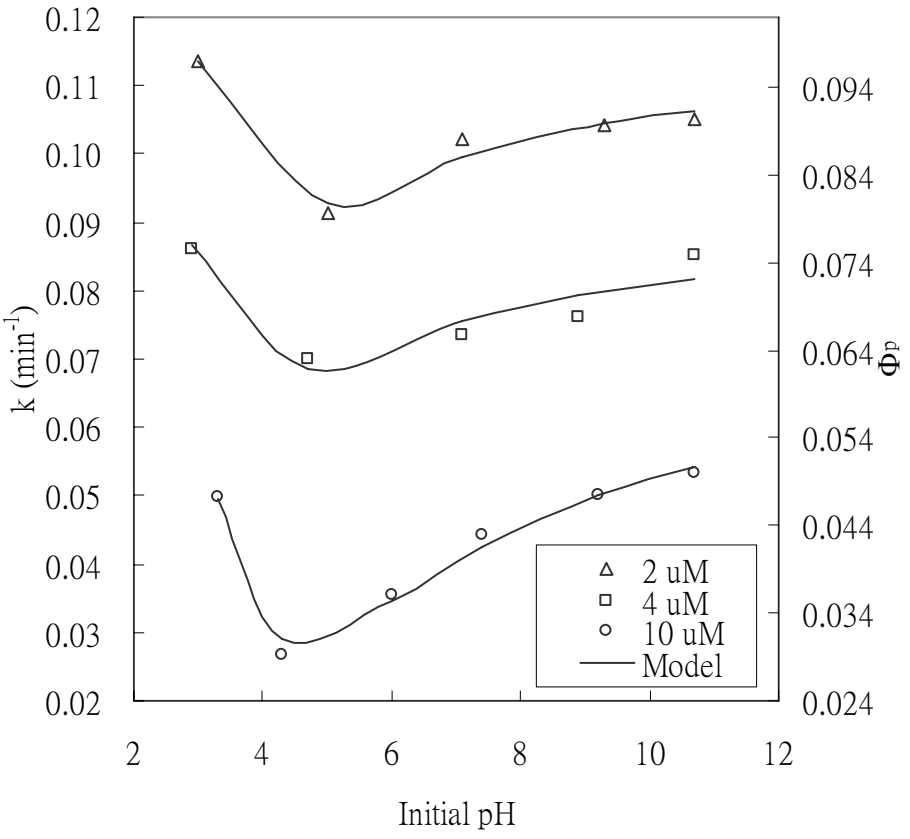

Fig. 4.2: Pseudo-first order rate constants of different initial [DBP] at 2, 4 and 10 μM within the first stage irradiation (the lines indicate modelled values)

Since the fast first-stage decay is more critical for a reactor or process design, a nonlinear empirical model was developed to predict the decay rate of DBP for different initial pH conditions, as shown in Eq. 4.1.

$$\mathrm{Ln}\, k_{DBP} = a + \frac{b}{\ln pH_0} + \frac{c}{pH_0} \qquad (4.1)$$

where the k_{DBP} is the pseudo first-order rate constant of DBP decay for the first-stage; a, b, and c are the coefficients which depending on the initial DBP concentration ($[DBP]_0$). These coefficients were determined from the measured rate constants at different pH_0 and $[DBP]_0$ with good correlations (minimum r^2 of 0.96); the coefficients are summarized in Table 4.1.

Table 4.1: Variation of Model Coefficients (Equation 4.1) with initial DBP Concentration

Model Factor	**10 μM**	**4 μM**	**2 μM**
a	-13.79	-4.74	-4.45
b	46.15	9.63	9.42
c	-91.95	-19.58	-18.90

As the photolysis reaction progressed with continuing irradiation (second-stage), it was evident that the DBP degradation rate gradually reduced. The retardation in rate is believed to be due to the combination of the following:

(i) The generation of intermediates in the solution will compete for the photons which retards the further degradation of DBP. In theory, such an effect will become more and more dominant as the intermediates

accumulate to higher levels.

(ii) Some of the intermediates and/or photolysis end products may absorb light, thereby attenuating the incident UV intensity available for photodegradation (Kagan, 1993; Chu and Jafvert, 1994). Such an effect is believed to be applicable to all the degradable components in the solution and not only limits to the DBP.

(iii) During the photolysis process, it is interesting to note that the solution pH will gradually increase or decrease as the initial pH level is in acidic or basic conditions, respectively (see Fig. 4.3). Since the trends of pH variation are all toward to the neutral zone, which lessen the acid and based catalyzed photo-hydrolysis mechanisms as discussed before.

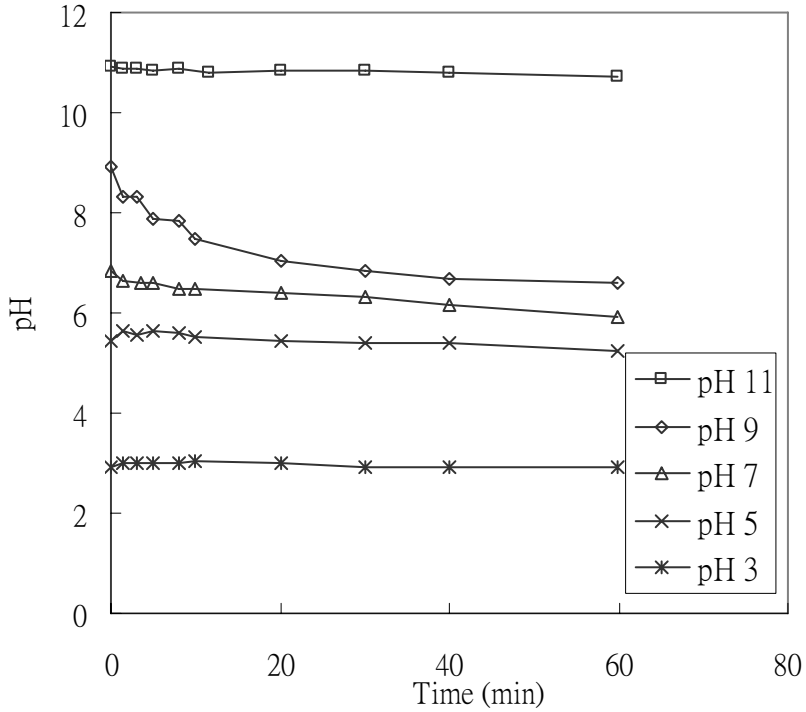

Fig. 4.3: The overall changes of pH levels during the irradiation of DBP

In view of the variation of degradation rates and solution pH with the initial pH value, it is believed that the reaction mechanisms were different at each pH condition and these mechanisms are considered in the following sections.

4.2.2 Reaction Mechanisms and Photoproduct of DBP Photodegradation

To investigate the intermediates and products of DBP photolysis, the previously described procedure involving LC-MS-ESI was used to determine and quantify (depending on the availability of the chemicals) these compounds without using a solvent extraction and/or sample derivatization step that conventional GC-MS

analysis usually requires; thereby minimizing the loss of some polar intermediates and analytical errors (due to the extraction efficiency). From previous studies, it was known that the photodecomposition of aromatic esters is mainly through a nucleophilic reaction (ring opening) and/or bond-scission (or H-abstraction) (Hizal et al., 1992, 1993; Balabanovich and Schnabel, 1998; Bajt et al., 2001). In addition, the photolysis of simple alkyl phthalate involving absorption of a photon by the carbonyl group has also been reported, which was believed to be responsible for the decay of phthalates with longer alkyl groups (Balabanovich and Schnabel, 1998).

In this study, it was found that the photolytic degradation of DBP mainly occurred via the aliphatic chain rather than the aromatic ring. As mentioned previously in methodology, a total of six major intermediates/end products were identified from the DBP photo-degradation at 254 nm and these included: MBP, MBP derived ketone (or aldehyde) (MBPK) and alcohol (MBPA), BB, BA, and PA. It is noted that the presence of PA was also reported to be found in the effluent of a wastewater treatment process receiving effluent containing phthalate esters, and it was suggested that the hydrolysis of the PE was responsible for the formation of PA (Paxéus, 1996).

The appearance of these daughter compounds depends on the initial pH conditions as expected, and the proposed pathways (after eliminating other feasible hypotheses) are shown in Fig. 4.4. The pathways were resolved by interpreting and organizing the possible degradation mechanisms from the evolution profiles of different degradation products, and assisted by comparison with analogous studies of photodegradation processes in the medium to near UV region (290-400 nm) (Hizal et al., 1992, 1993; Bajt et al., 2001).

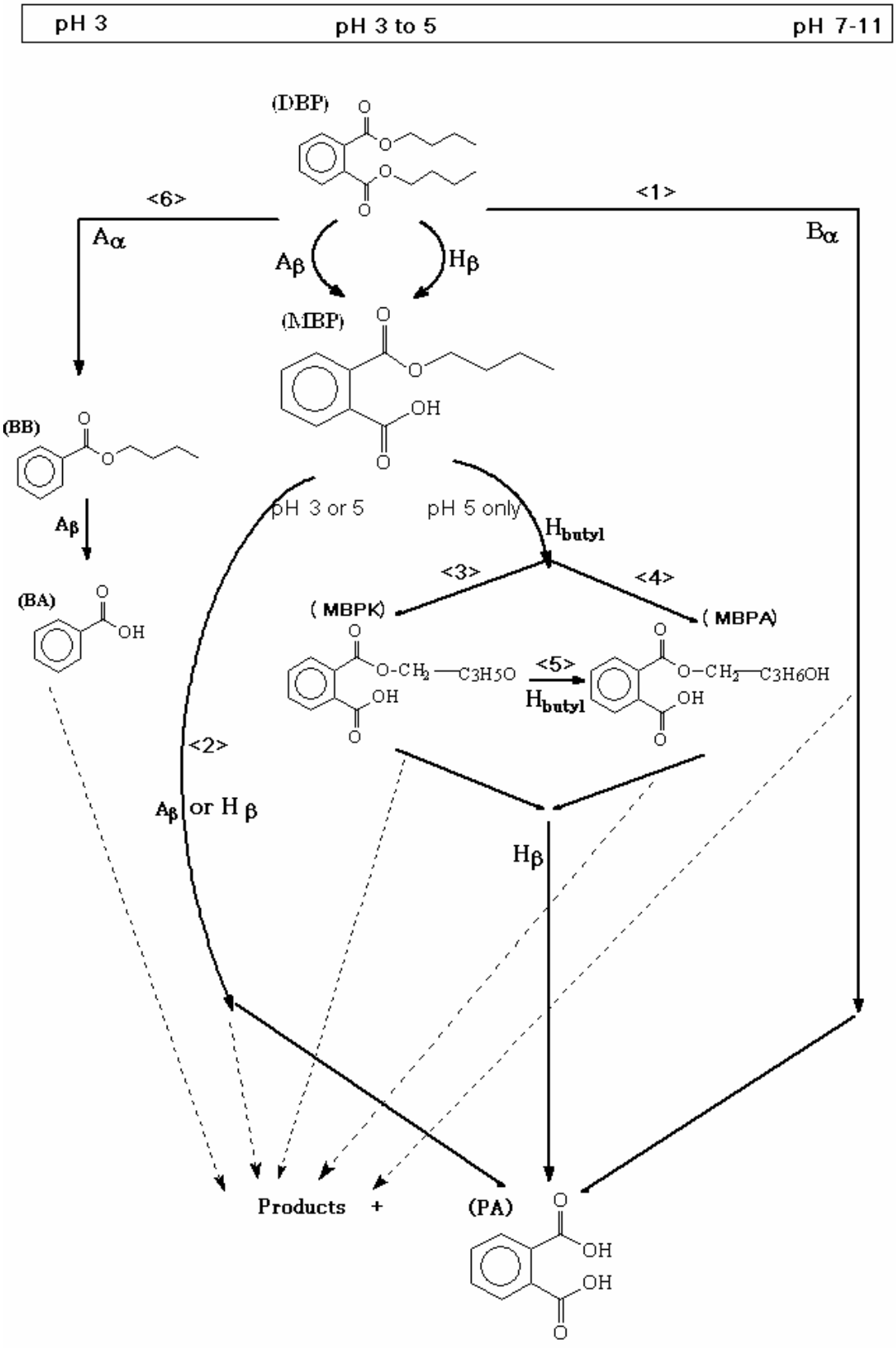

Fig. 4.4: Proposed degradation mechanism of DBP photolysis at different pH

(The six different pathways are numbered in brackets, <1>)

The photodegradation of DBP at 254 nm involves photo-induced decarboxylation, hydroxylation, dealkylation, and scission of C-O, C-C, and O-Butyl bonds. Judging from the major intermediates identified in the photolysis, it is believed that either α, β, or butyl- scissions of the aliphatic part (ester chain) of DBP is the dominant mechanism of the process, with the aromatic ring remaining intact. This observation is consistent with the results from other studies (Hizal et al., 1992, 1993; Balabanovich and Schnabel, 1998).

To analyze the individual reaction pathways for different pH conditions, associated with different cleavage positions in the ester chains of the DBP, the various reaction mechanisms were divided into three major routes depending on the pH level: (i) acidic catalysis (A_α and A_β) at pH 3, (ii) hydrolysis (H_β) and oxidation/reduction of the butyl chain (H_{butyl}) at a pH of approximately 5, and (iii) basic catalysis (B_α) at pH ≥ 7, see Table 4.2. The term $\mathbf{A_\alpha}$ is the α-cleavage of the C-C bond connecting a carbonyl group (C-C=O) with the aromatic ring; $\mathbf{B_\alpha}$ (α-cleavage) is a fast decomposition of both ester groups (to PA) simultaneously without noticeable intermediates in between; $\mathbf{A_\beta}$ or $\mathbf{H_\beta}$ is a single β-cleavage of one ester group, leaving the dicarbonic acid (COOH) structure intact; and $\mathbf{H_{butyl}}$ is the reaction on all other possible sites along the butyl group

Table 4.2: Various hydrolytic-photolysis degradation pathways of DBP and intermediates at different cleavage positions over their ester chain

Reaction Pathway	Cleavage Position: α or β	Photoproducts
B	α	DBP $(O=C)-O$ $\xrightarrow[OH^-, NaOH]{}$ PA $(O=C)-OH$
H	β	DBP MBP $(O=C)O-R$ $\xrightarrow[H^+, H_2O]{}$ MBP PA $(O=C)O-H$
H	-Butyl	MBP $COO-CH_2C_3H_7$ $\xrightarrow[OH^-, H_2O]{}$ MBPK, MBPA $COO-CH_2C_3H_5O$ or $COO-CH_2C_3H_6OH$
A	α	DBP $C-(C=O)$ $\xrightarrow[H^+, H_2SO_4]{}$ BB $C-H$
A	β	MBP BB $(O=C)O-R$ $\xrightarrow[H^+, H_2SO_4]{}$ PA BA $(O=C)O-H$

4.2.3 Sub Mechanisms and Their Corresponding Bond-Cleavage

At a pH of 3 (denoted as sub-mechanism **A**), the pathways 2 and 6 are believed to dominate. They initially involve protonation of the carbonyl oxygen, then the polarized carbonyl group becomes more susceptible to nucleophilic reactions due

to its increased electrophilicity through the withdrawal of electron density from the carbon atom (Larson, 1994). The A_α is responsible for the BB and BA through a stepwise dealkylation, while $\mathbf{A_\beta}$ process is responsible for producing the subsequent MBP and PA. The curves of DBP decay and the formation (and decomposition) of MBP, PA, BB, and BA are shown in Fig. 4.5. The acidic-catalyzed photohydrolysis is faster than the reactions at neutral pH (Fig. 4.2), and the faster reaction is likely to be the result of the two parallel decay pathways.

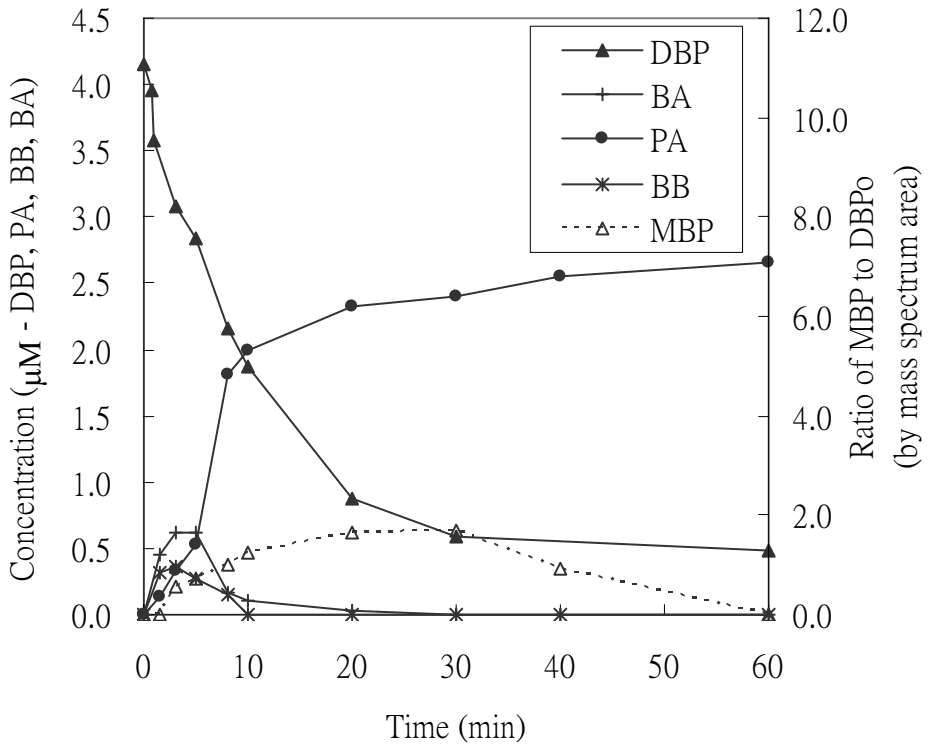

Fig. 4.5: Concentration and relative ratio of intermediates in respect to the irradiation time at pH 3

At the higher pH level of 5 (sub-mechanism H), another pathway that is also capable of generating MBP is a β-cleavage of a O-C bond (**H_β** pathway). The reason to specify this as an individual pathway is because two additional intermediates (MBPK and MBPA) were identified as pathways 3 and 4 in between the decay of MBP and the formation of PA, which is not detected in the **A_β** pathway at a lower pH. The overall curves of DBP decay and the formation (and decomposition) of MBP, PA, MBPK, and MBPA are shown in Fig. 4.6.

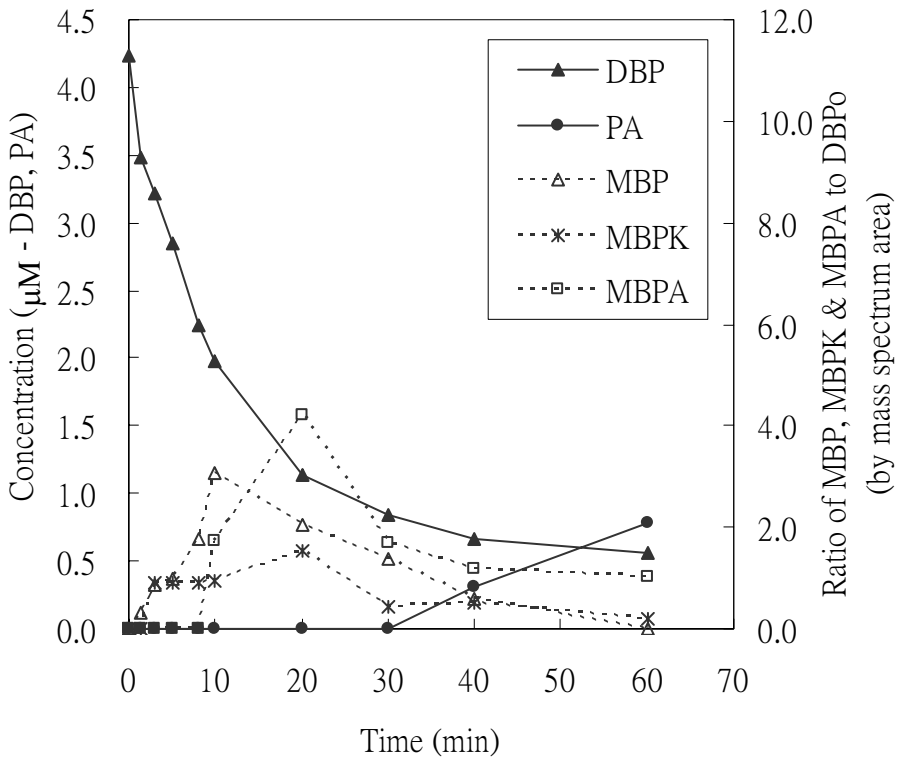

Fig. 4.6: Concentration and relative ratio of intermediates in respect to the irradiation time at pH 5

The transformation of MBP to MBPK (pathway 3) or MBPA (pathway 4) are basically oxidative processes, while MBPK to MBPA (pathway 5) is a reductive process. A similar observation on the generation of MBPK was also reported for the Fenton-photocatalysis of DBP in the medium to near UV region (Bajt et al., 2001), where in this case an oxidant is present. However, there is no primary oxidant present in a pure UV photolysis process but a secondary oxidant is likely to be generated after the reaction begins. The possible precursor of a secondary oxidant that may be responsible for implementing the oxidative transformation is likely to be the radical groups, ·OR or ·R, that could be formed through direct photolysis induced by high energy UV (Grossmann et al., 2001).

On the other hand, the precursor for the reductive reaction (MBPK to MBPA) should be the electron donors available in the solution after the initiation of the reaction, including the hydrogen in the butyl chain fractions or the intermediates carrying aliphatic groups. These aliphatic chains have a similar structure to the hydrophobic chains in a surfactant, which has been suggested to be a good electron donor and is capable of promoting photo-reduction under 254 nm UV light (Chu and Jafvert, 1994).

Another interesting observation concerns the non-linear 2^{nd} stage photo-degradation of DBP at pH 5, which was the pH that gave the lowest overall DBP reduction compared to the other pH conditions (see Fig. 4.1). One of the reasons for this is possibly the existence of photo-isomerization reactions in which structural isomers (ketone and aldehyde forms of MBPK) absorb the UV radiation and waste the photon energy in changing the structure of isomers without contributing to the forward reaction (Chu et al., 2002).

As the initial pH is elevated to the basic range (7-11), a simple α-cleavage (sub-mechanism **B**, B_α) dominates the process through a photochemical homolytic decarboxylation (pathway 1). In this pathway, only the end-product PA was identified and no intermediate species were long-lived enough to be observed. This evidence was consistent with a fast photohydrolysis in the alkali range as shown in Fig. 4.1. It is known that OH^- is a stronger nucleophile than water alone, and hence the B_α pathway via the direct nucleophilic addition of OH^- to the carbonyl group is possible (Larson, 1994). In addition, since the concentration of hydroxyl ions is about the same or one-to-two orders of magnitude greater than that of [DBP] in the solution, this makes a double nucleophilic addition (dihydroxylated) on the two ester chains possible, which

significantly accelerates the hydrolysis process and leads to the apparent absence of the theoretical middle intermediate (i.e. MBP).

4.2.4 Verification of the Proposed Mechanism through the Examination of Product Yields

PA was determined to be one of the dominant end products of the DBP photolysis and this was the case for each of the initial pH conditions studied. The ratio of [PA] accumulation to the initial DBP concentration ($[PA]/[DBP]_0$) during the process was determined and the results are shown in Fig. 4.7. A time lag in the formation of PA (i.e. $[PA]/[DBP]_0 = 0$) was observed for the pH range of 5 to 9, with the longest lag occurring at pH 5, and this is in agreement with our previous observation that the lowest 1^{st} stage DBP degradation rates corresponded to the weak acid-to-base range (Fig. 4.2). This observation can be used to support the proposed mechanisms summarised in Fig. 4.4. At pH 5, the MBP needs to go through the intermediate formation of MBPK and/or MBPA before the PA can be formed, which is either one or two more steps than that at pH 3 and 11, respectively.

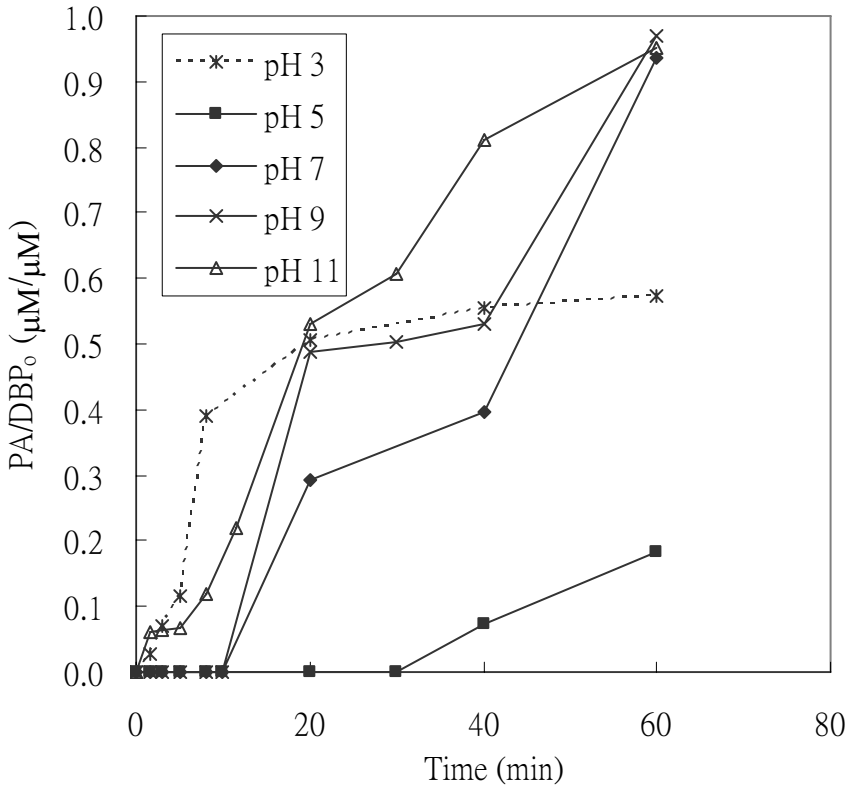

Fig. 4.7: Ratio of Phthalic Acid Formation Per Unit of initial DBP throughout the irradiation

At an initial pH equal to, or greater than, 7, the $[PA]/[DBP]_0$ molar ratio approached unity by the end of the reaction period (60 min). Since DBP can be completely converted to PA in neutral to basic conditions, this suggests that UV irradiation at 254 nm is a feasible solution in principle for removing DBP; however, the practical suitability of this approach would need separate and detailed consideration. In addition, the TOC concentration was monitored throughout the photolysis reactions and there was no detectable TOC degradation

observed. The absence of any significant change in TOC in various UV processes has also been reported previously (Canonica and Hoigné, 1995; Alborzfar et al., 2000). Therefore, it can be assumed that no mineralization (arising from ring cleavage and major molecular decomposition) took place during the 60 min of irradiation. In view of this it is likely that minor photolysis products, such as alcohols, ketones, aldehydes, and acids, are formed in the solution, but in this study their concentration was too low to be detected. Although no TOC degradation was exhibited, the toxicity causing endocrine disruption associated with DBP was believed to be removed or lowered successfully by degrading it to MBP and PA in the UV process. It was reported that MBP does not induce estrogen-receptor-mediated transcriptional activity in vitro (Mylchreest et al., 1999), while PA did not induce any toxicity in a bacteria test (Jonsson and Baun, 2003).

A final observation that can be made from the proposed mechanisms concerns the reduced PA production (~60%) at pH 3 compared to that at pH 7, 9 and 11 (Fig. 4.7). This is believed to be because the photodegradation of DBP at pH 3 involves two separate and parallel pathways (A_α and A_β to form BA and PA, respectively), only one of which results in PA formation (pathway A_β). Thus, the

total conversion of DBP to PA is significantly reduced compared to that at pH ≥ 7 where there is a direct pathway (B_α) to PA. However, because of the involvement of two parallel reaction pathways, the greatest 1st stage DBP photodegradation rate was observed at pH 3.

4.3 Summary

An investigation of DBP degradation by UV photolysis at 254 nm wavelength was conducted over a wide range of pH conditions. Different reaction pathways were thoroughly examined and a theoretical mechanism was proposed and found to be consistent with experimental observations. In the pH range of 5-11 the initial DBP degradation rate increased with pH due to the domination of base-catalyzed hydrolysis. However, the greatest initial DBP degradation rate occurred at pH 3 because an additional reaction pathway involving the formation of benzoic acid. Multi-degradation pathways have been proposed for acid-catalyzed hydrolytic photolysis in the pH range of 3 to 5, leading to the formation of intermediate products such as the ketone-, aldehyde- or alcohol-forms of mono butyl phthalate. An end product of the acid-hydrolyzed photolysis, and particularly of base-catalyzed photolysis (pH ≥ 7), is phthalic acid (PA). In the latter case (pH ≥ 7) there was a complete conversion of DBP to

PA over 60 min. The results of this study suggest that the use of UV irradiation in water or wastewater treatment (eg. as commonly applied for disinfection) will have a beneficial effect in reducing DBP concentrations.

CHAPTER 5 REMOVAL OF CARBOFURAN

5.1 Introduction

In this section, the results of an extensive laboratory investigation of CBF degradation by the separate processes of UV photolysis, ozonation and combined UV/O_3 as an advanced oxidation system will be reported. Currently, the detailed information on pH variation of photolytic degradation of CBF is very limited. The results will describe the dependence of the degradation rate constants on different pH levels at a range of 3.0 to 11.3. The preliminary findings of this investigation suggest that the treatment process of UV/O_3 could provide an effective remediation method for this substance of concern.

5.2 Reaction Rate Constants

The study of CBF degradation by different wastewater treatments has been carried out, and its decay ratios (C/C_0) at pH 7 are shown in Fig. 5.1. Their ascending reactivities distribute as the following order: UV-alone, O_3–alone and UV/O_3 process, where UV-alone could merely provide a 36% removal of 0.2 mM CBF within 30 min irradiation time. While O_3 and UV/O_3 processes may

lead to an enhancement of 2.3 and 2.7 times (83.2 and 100%) removal efficiency of CBF, respectively.

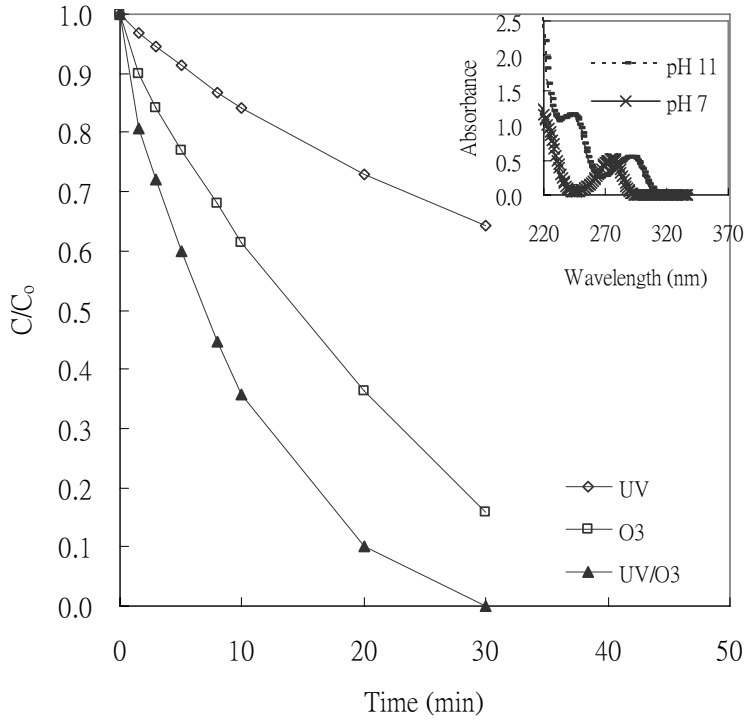

Fig. 5.1: Different treatment process of removing 0.2 mM CBF at pH 7

(Sub-graph: UV spectrum of pH 7 and 11 under dark control)

The ozonation of CBF alone gave an increasing pseudo first-order rate constant (k) ranging from 0.05 to 0.14 min^{-1} by increasing the solution pH. This shares a similar behaviour as the other phenolic pesticide towards ozonation (Boncz et al., 1997). By summarizing the reaction rate constants, two different phases of reaction were surprisingly found as shown in Fig. 5.2a: (1) a steady stage at pH

3 – 7; and (2) an accelerating stage at pH > 7. This uprising second stage of ozonation at alkaline pH is possibly due to alkaline hydrolysis. The hydrolysis rate of CBF at alkaline pH (i.e. 11.3) has been determined to be 0.01 min^{-1} under dark control.

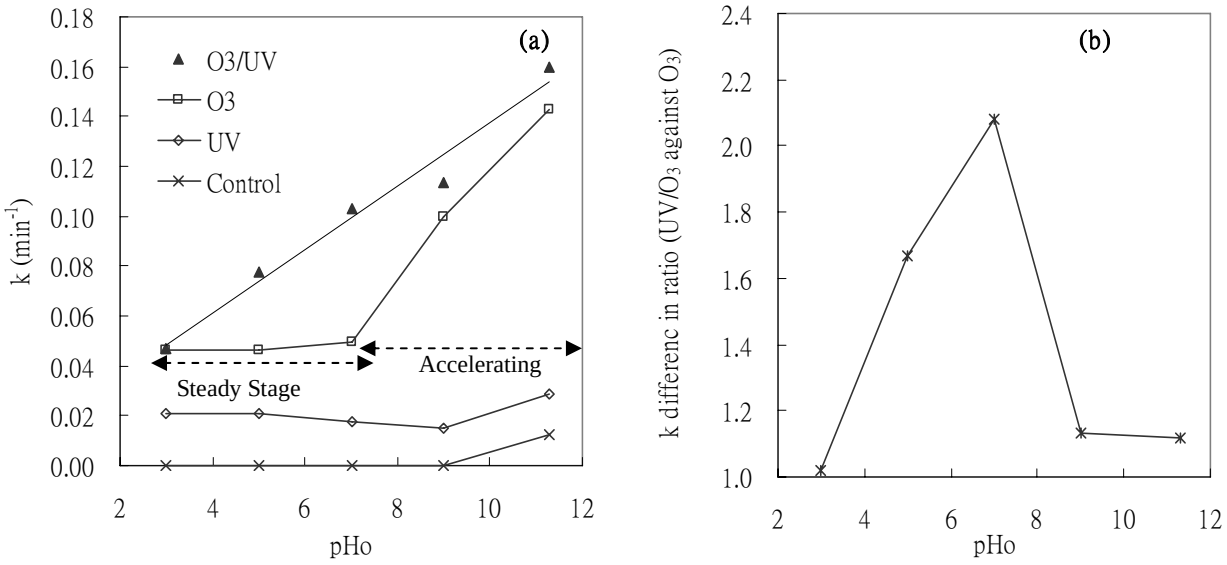

Fig. 5.2: (a) Pseduo first-order rate constant of different initial pH with different degradation process: Ozone plus UV; Ozone only; UV only; and dark control; (b) the ratio of kinetic rate constant of the former two processes.

5.3 *Effect of initial pH*

The alkaline-hydrolysis is also believed to be taken place in all treatment processes at pH ≥ 9. Based on the visual verification, the sample solution turned to brown colour once the reaction starts (including dark control in a slower extent), then lightened gradually to yellow. Coincidentally, the more effective the treatment process in transforming CBF, sooner the colour development especially in the cases of alkaline pH level (≥ 9). Furthermore, additional mechanistic pathways of CBF intermediates are validated by the earlier disappearance of these coloured intermediates, for instance in UV/O_3 and O_3 processes, clearing of sample solutions took place at 10 min and 20 min of reaction time, respectively. According to various studies on CBF degradation (Samanidou et al., 1988; USEPA 2001; Miltner et al., 1989), it is suspected that some of the common hydroxylation phenolic degradation products might be produced at highly alkaline conditions (i.e. 3-hydroxycarbofuran, carbofuran-7-phenol, 3-ketocarbofuran and 3-ketocarbofuran phenol).

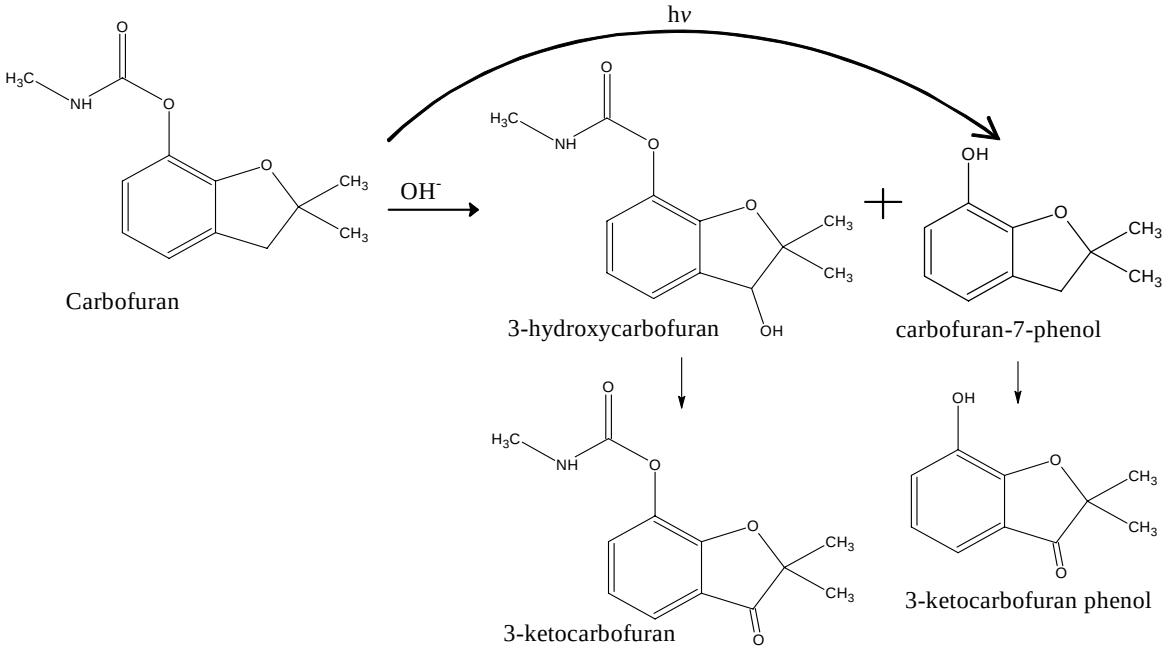

Fig. 5.3: Proposed Pathway of CBF degradation

The different pattern of UV spectrums at pH 11 at Fig. 5.1 can primitively validate this hypothesise, where two new peaks were found at 250 and 290 nm comparing with the pH 7 (273 nm only). The speeding up of the mechanism by the treatment processes can be due to bond scission, H-abstraction (for UV-alone process), oxidation (for O_3), and combination of the above reactions (for UV/O_3). Therefore, the preceding mechanism pathways are proposed as shown in Fig. 5.3.

In reviewing the pH measurement, the photolysis process (Fig. 5.4a), unlike those in ozonation and UV/O_3 (Fig. 5.4 b and c), its solution pH will gradually increase or decrease as the initial pH level is in acidic or basic condition, respectively. Since the trends of pH variation are all toward to the neutral zone, which lessen the acid and based catalyzed photo-hydrolysis mechanisms. Therefore, the reaction rate constants of direct photolysis are more or less the same (Fig. 5.2a).

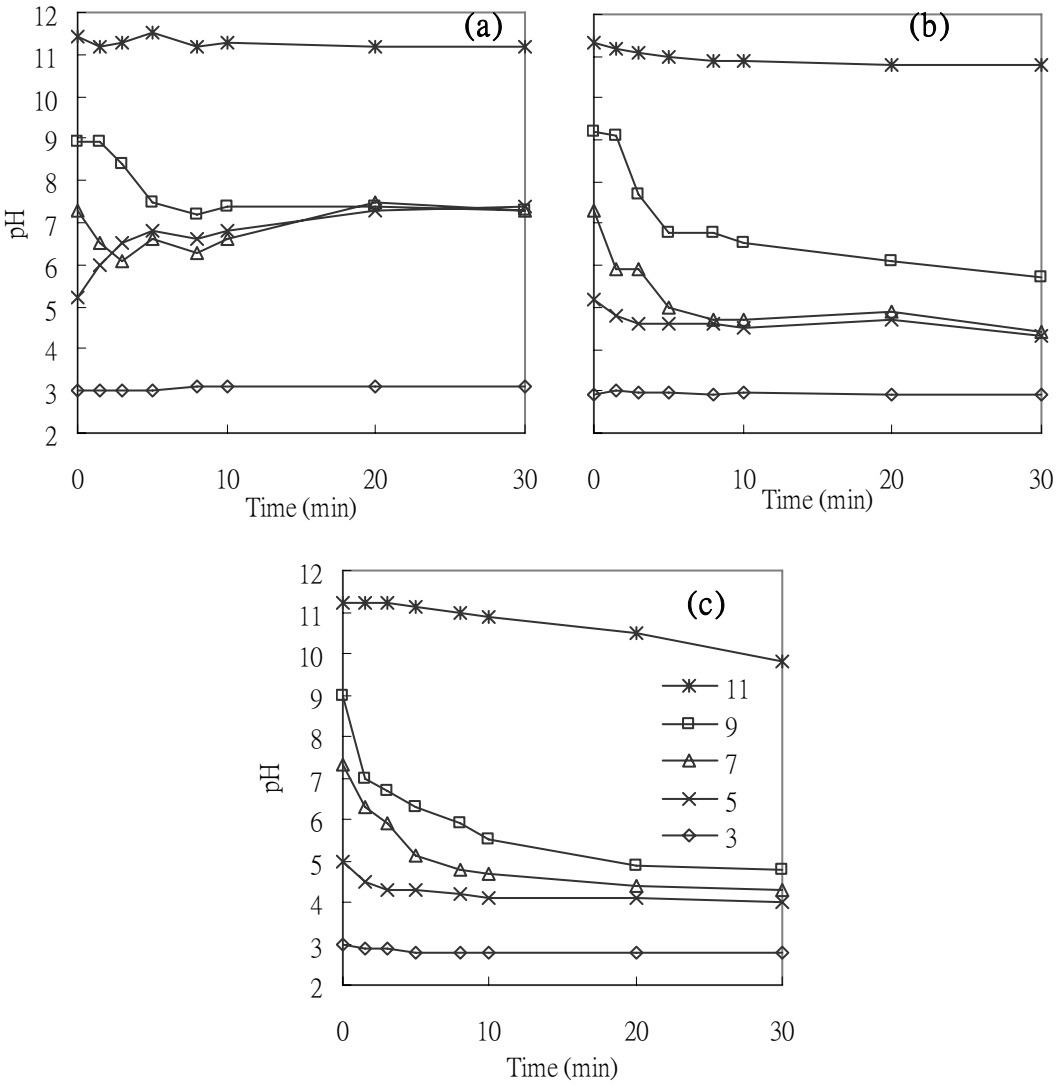

Fig. 5.4: pH trend of 3 different processes: (a) UV only; (b) O3 only; and (c) UV/O_3.

5.4 Advanced oxidation process, AOP (UV/O_3)

In this study, the photolysis of ozone by UV at 254 nm is used, where the optimal absorption of ozone at this wavelength has been well established (Oppenlander, 2003). The combined UV/O_3 system providing a synergistic effect of individual reactions: direct molecular ozonation, direct photolysis, and •OH radical oxidation (Beltran, 2004). In this study, the UV/O_3 process has proven that it is an effective treatment of CBF at all pH levels (Fig. 5.2a) and a preliminary 24% total organic carbon (TOC) removal or mineralization (nil for the UV or O_3 processes) could be achieved within 30 min reaction. The degradation rates increase as the initial pH levels increase, in which the pseudo-first-order rate constant lying in the range of 0.05 to 0.16 min^{-1}. Moreover, a well-fitted linear relationship of reactivity (k in terms of min^{-1}) by increasing initial pH has been found and it could be expressed in the following equation with a correlation coefficient (r^2) of 0.9718:

$$k = 0.0127 \quad [pH_0] + 0.0103 \qquad (5.1)$$

In order to illustrate or identify the best efficiency of advanced oxidation process (UV/O_3) among the ozonation process at different pH levels, the ratio of reaction rate constants enhanced by UV/O_3 against the O_3 process has been presented at

Fig. 5.2b. The enhancement is gradually increased from acidic to neutral and reaches the maxima at pH 7, where a boost up of more than a double of faster degradation could be achieved by the synergistic effect of O_3 and UV. On the other hand, at pH 3, the CBF decay rates are about the same in the UV/O_3 and O_3 processes (ratio = 1.02). This similar performance is possibly due to the generation of weaker oxidant (hydrogen peroxide, H_2O_2) rather than hydroxyl radicals. Generally H_2O_2 will undergo homolytic photolysis to generate hydroxyl radicals (Chu, 2001):

$$H_2O_2 + hv \rightarrow 2\ OH^{\bullet} \qquad (5.2)$$

However, H_2O_2 is comparatively stable to undergo photolytic-decomposition at acidic pH than alkaline (Chu, 2001), therefore it is believable that this intermediate pathway will interfere (or at lower potential) of direct generation of OH• at acidic pH (i.e. 3). As indicated by Canton et al. (2003), UV irradiation at a wavelength of 255 nm and at a pH of 2.5 will lead to all the ozone being photolyzed into hydrogen peroxide. Last but not least, the little enhancement by AOP at alkaline pH (9 and 11) seemed to be the result of solely individual reactions (UV-alone, O_3-alone and hydrolysis) rather than synergistic. This assumption can be rationalized by simple summation of the k-values (from Fig.

5.2a) of each individual reaction at the following self-explanatory equation:

$$AOP = (O_3 - Hydrolysis) + (UV- Hydrolysis) + Hydrolysis \qquad (5.3)$$

In this high pH condition, little (or no) extra generation of radicals (i.e. $OH^{\bullet}$) is believed to be taking place in the AOP, its preceding reaction of $OH^{\bullet}$ generation via the basic O_3-alone process is highly possible by the evidence of similar protonation in solution (i.e. pH 9) for both O_3-alone and AOP process (Fig. 5.4b and c). O_3 molecule is directly hydrolyzed to $OH^{\bullet}$ due to the abundant [OH-] in solution, as the prevailing mechanism, rather than formation of other oxidants or radicals (i.e. H_2O_2, $O_3^{-\cdot}$, or $O^{-\cdot}$)

5.5 Summary

An investigation of CBF degradation by UV photolysis at 254 nm wavelength, ozonation and a combined UV/O_3 system, was conducted over a wide range of pH conditions. The UV/O_3 system has shown a promising transformation treatment process of the pesticide and a linear ascending pH-dependent relationship has also been established. It is believable that CBF itself/or its toxic intermediates could be easily cleanup, when present in contaminated effluents. By O_3 alone, CBF could also be degraded but in a lesser extent, and two stages of reactions have been found at acidic pH ($\leq$ 7) and alkaline pH ($>$ 7), where an accelerating stage of reactivity has been exhibited for the latter case.

CHAPTER 6 REMOVAL OF BUTYLATED HYDROXYANISOLE

6.1 Introduction

In this chapter, the four different remediation processes of BHA are studied and investigated in details which each optimal condition can be found for future studies. It shows not only the degradation of the probe compounds, but also its reaction products (or intermediates), and further to the ultimate removal of all organic micro-compounds leading to mineralization. First of all, the ozone related processes (i.e. UV, O_3, UV/O_3) are firstly investigated and compared.

In the ozone related processes, o-demethylation, dimerization, and oxidation have been found to be the main degradation mechanisms. A systematic decay pathway was proposed based on ten identified intermediates in the studied processes, including a unique pathway leading to the formation of precipitates in the ozonation process. An unconventional minimum-type variation of BHA decay rate constants from acidic to caustic range has been found for both ozonation and UV/O_3 processes. The precipitates formed during ozonation can be removed during the process to optimize the treatment, while the UV/O_3 process

can offer a relatively fast and clean process to degrade BHA and its associated intermediates.

Furthermore, in the UV/$S_2O_8^{2-}$ process, three distinctive phases of BHA reactivity towards UV/$S_2O_8^{2-}$ at acidic, neutral and basic pH range were examined, where 80-100% mineralization has been observed within an hour of irradiation under 254 nm. A reduction in solution pH during the reaction was observed mainly due to the complete conversion of $S_2O_8^{2-}$ to sulfate ion together with proton generation. Seven measurable intermediates were found via an oxidation and dimerization process at all tested pH levels. The BHA decay mechanisms are quite different in acid condition and at other pH levels. There are three unique intermediates that are only detectable at pH 3 via two additional pathways. This is due to the generation of weaker oxidants or radicals which results in a slower degradation of the BHA and therefore the accumulation of these intermediates to detectable levels. The rate of BHA decay generally increases from low to high pH levels; however, the corresponding mineralization at higher pH is retarded due to the futile process of recombining radicals and involvement of intermediates. Therefore, neutral pH was suggested to be the

optimum condition in terms of mineralization and moderate efficiency in removing BHA.

Finally, to establish a practical modelling for the UV/$S_2O_8^{2-}$ process, three major process variables have been selected for detailed investigation: (i) UV wavelength effect; (ii) pH effect; and (iii) $S_2O_8^{2-}$ dosage effect. It was found that UV at 254 nm demonstrated the best removal efficiency in both direct photolysis and photo-oxidation (UV/$S_2O_8^{2-}$) processes. The reaction rate constant can be improved by increasing either the initial pH levels and/or the $S_2O_8^{2-}$ dosage. When the $S_2O_8^{2-}$ dosage is sufficiently provided in the UV system, the reaction kinetics can be simply characterized by pseudo first-order decay. However, when $S_2O_8^{2-}$ dosage is deficient, though the decay of BHA is fast initially but the process will be retarded at a later stage, and a two-stage pattern was observed. An atypical modelling has been used to describe such a condition, this is specially useful for predicting the process performance if a shock loading during wastewater treatment was present.

6.2 UV, O_3, and UV/O_3 processes

6.2.1 Rate constants for the degradation of BHA and the pH effect

Different concentrations of BHA (0.1 – 0.29 mM) were tested at various pH levels (from 3 to 11) by different treatment processes: (1) UV photolysis, (2) Ozone, and (3) combined UV/Ozone system. Fig. 6.1 shows the decomposition of BHA (C/C_0) at pH 7 and the corresponding changes in total organic carbon, TOC (TOC/TOC_0), where the reduction of TOC indicates the degree of mineralization.

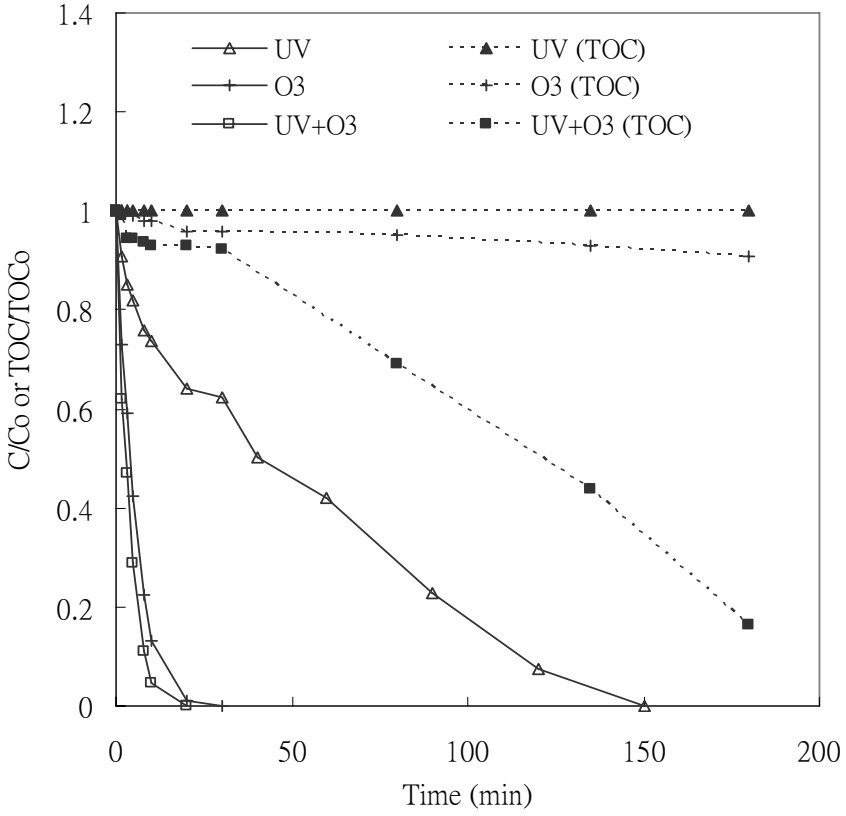

Fig. 6.1: Comparison of BHA decay (C/C_0) and TOC removal by the different treatment processes at pH 7 (Co=0.29 mM).

The accompanying pH variation during the experiments was also monitored and the trend for the three different systems are shown in Fig. 6.2a to 6.2c, indicating the generation of acidic intermediates and/or end products. This is evident by the occurrence of the two acidic final products, HQ and PBQ, which are well known to be further oxidized to carboxylic acid (i.e. maleic, oxalic, acrylic, malonic, or acetic acid) before mineralization takes place (Santos et al, 2002). In general, the degradation of BHA increases in order: UV photolysis, ozone, and UV/O_3 The TOC removal was insignificant in both the UV photolysis and ozonation processes, but 90% mineralization and no precipitation in the solution (to be discussed) were achieved by using the UV/O_3 process (Fig. 6.1) after 180 min.

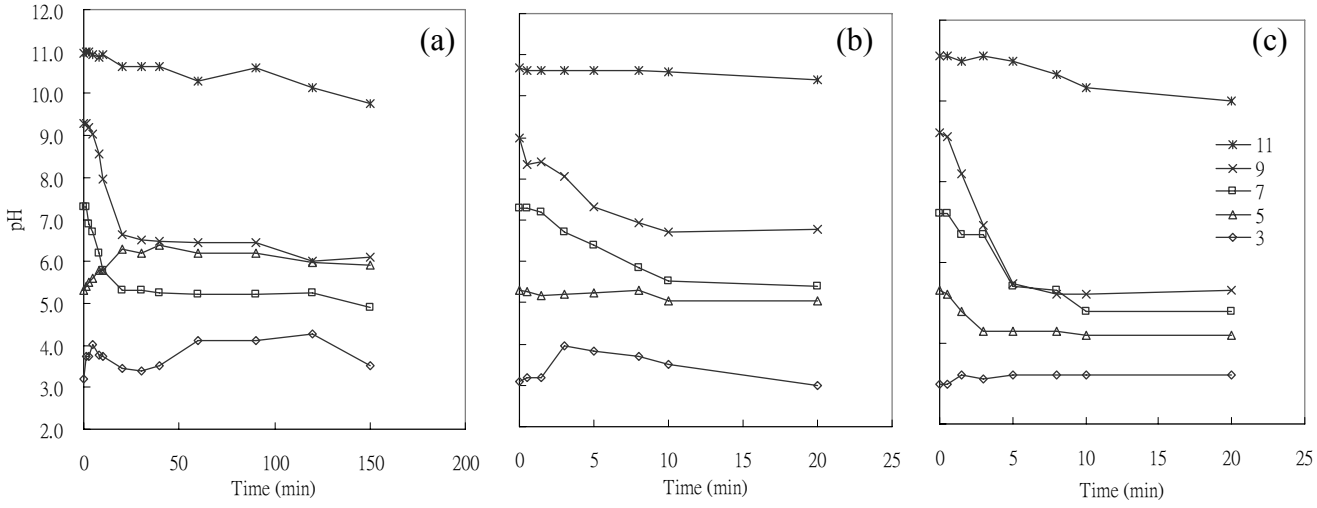

Fig. 6.2: Variation of pH with time for three different processes: (a) UV, (b) O_3, and (c) UV/O_3 ([BHA]= 0.29 mM).

The BHA can be completely (100%) removed by the three proposed processes. It takes 150 min to decompose 0.29 mM BHA in water by UV-irradiation, while only 20 min are required for O_3 and UV/O_3 processes (i.e. five times faster) respectively. The photolysis and oxidation of BHA were found to follow pseudo-first-order kinetics at various initial pH levels and the rates are summarized in Fig. 6.3, which shown its dependency of initial BHA concentration. It was known that, due to the generation of free radicals, an increased ozonation rate is usually expected at elevated pH levels (Winarno and Getoff, 2002).

It is interesting to note that the ozonation of BHA did not exactly follow this expected trend. A minimum-type variation of kinetic rate constants from the acidic to the alkaline range was identified, where the rate generally decreased with the increase of pH from pH 3 to 9, and then the rate constant increased substantially when the solution pH increased to 11, as shown in Fig. 6.3. This phenomenon is partly attributed to the unique antioxidant property of BHA, a well-known radical scavenger with trapping properties (Vargas et al, 1993), which can inhibit the radicals formation in solution. Given that BHA is a weak acid with a reported aqueous pK_a of 8.8 (Kaposi et al, 2001), it is likely that at

pH values greater than 9 the dissociated form of BHA is more reactive (Hoigné and Bader, 1983) and its radical inhibition effect is reduced. In addition, the reactions related to dimeric intermediates that result from the BHA degradation and oxidant competition from intermediates may also contribute to such a pattern (to be discussed in detail later).

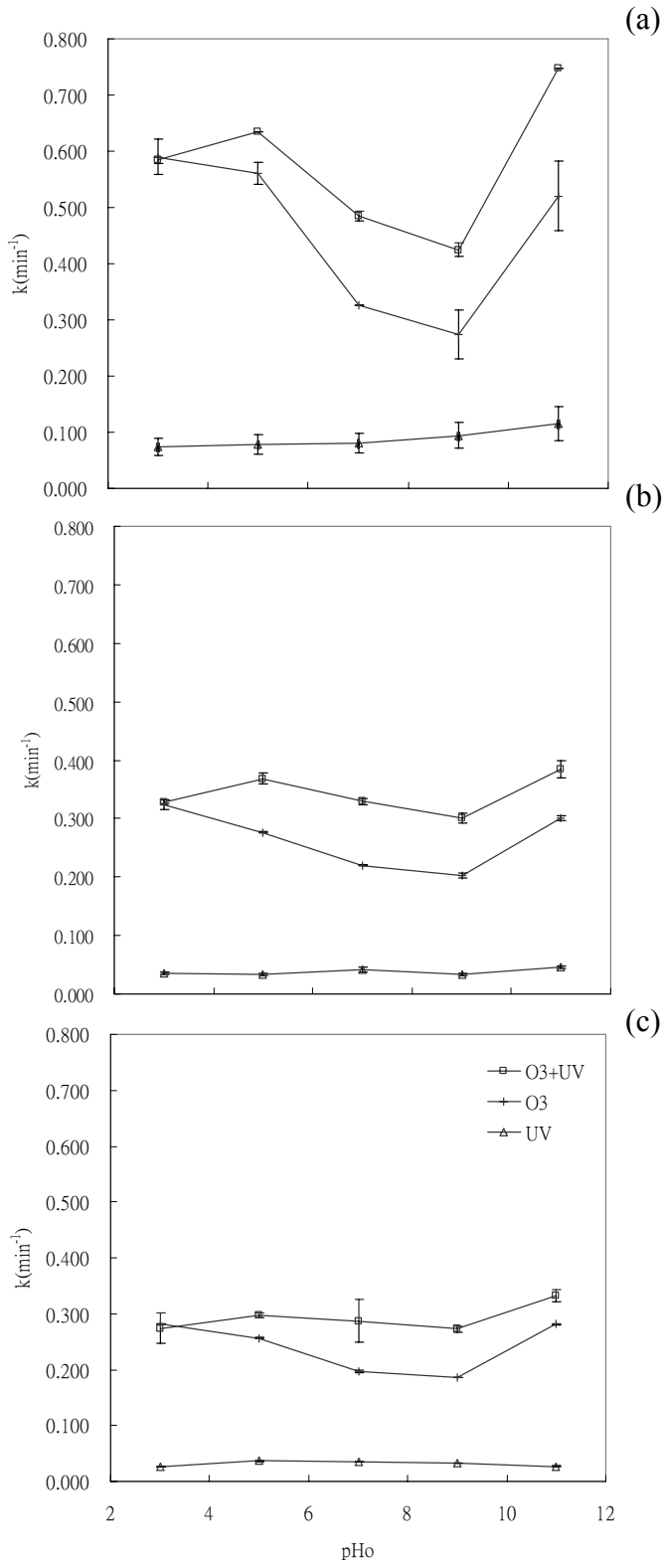

Fig. 6.3: Variation of the kinetic rate constant with initial pH for the three degradation processes at three initial BHA concentrations: (a) 0.1, (b) 0.2, and (c) 0.29 mM.

At high pH levels greater than 9, additional reaction mechanisms such as basic-catalysed oxidation and/or hydrolysis due to the presence of excessive hydroxide ions is feasible and may enhance the overall decay rate of BHA under these conditions. Another interesting observation in this study is that at pH 3 there was no rate improvement with UV/O_3 compared to that with ozone alone, in contrast to the greater kinetic rates observed with UV/O_3 at higher pH levels (~ 5 to 11); the rates with UV/O_3 were greater by 15 to 55% than with O_3 alone (see Fig. 6.3). These phenomena can be explained by a combination of the following reasons:

a) The lowest rates were observed in the UV process because UV-irradiation at 254 nm is not powerful enough to induce the generation of hydroxyl radicals ($^{\bullet}OH$). In the ozonation process, it is expected that fewer $^{\bullet}OH$ were generated compared to the UV/O_3 process, hence the former process always had a lower removal efficiency for BHA at all pH levels. At pH 3, although the BHA decay rates were about the same for the O_3 and UV/O_3 processes, it is interesting to note that a faster overall decay of the associated intermediate compounds is observed for the latter process. The intermediate compound decay is summarized in terms of mole balance, which provides analytical expressions (Chu et al., 2002) of those quantifiable intermediates against the initial molarity of BHA. The mole

balance calculated is about 90%, 50% and 20% within 20 min for the UV/O_3, O_3, and UV processes, respectively (see Fig. 6.6a, 6.4a & 6.5a).

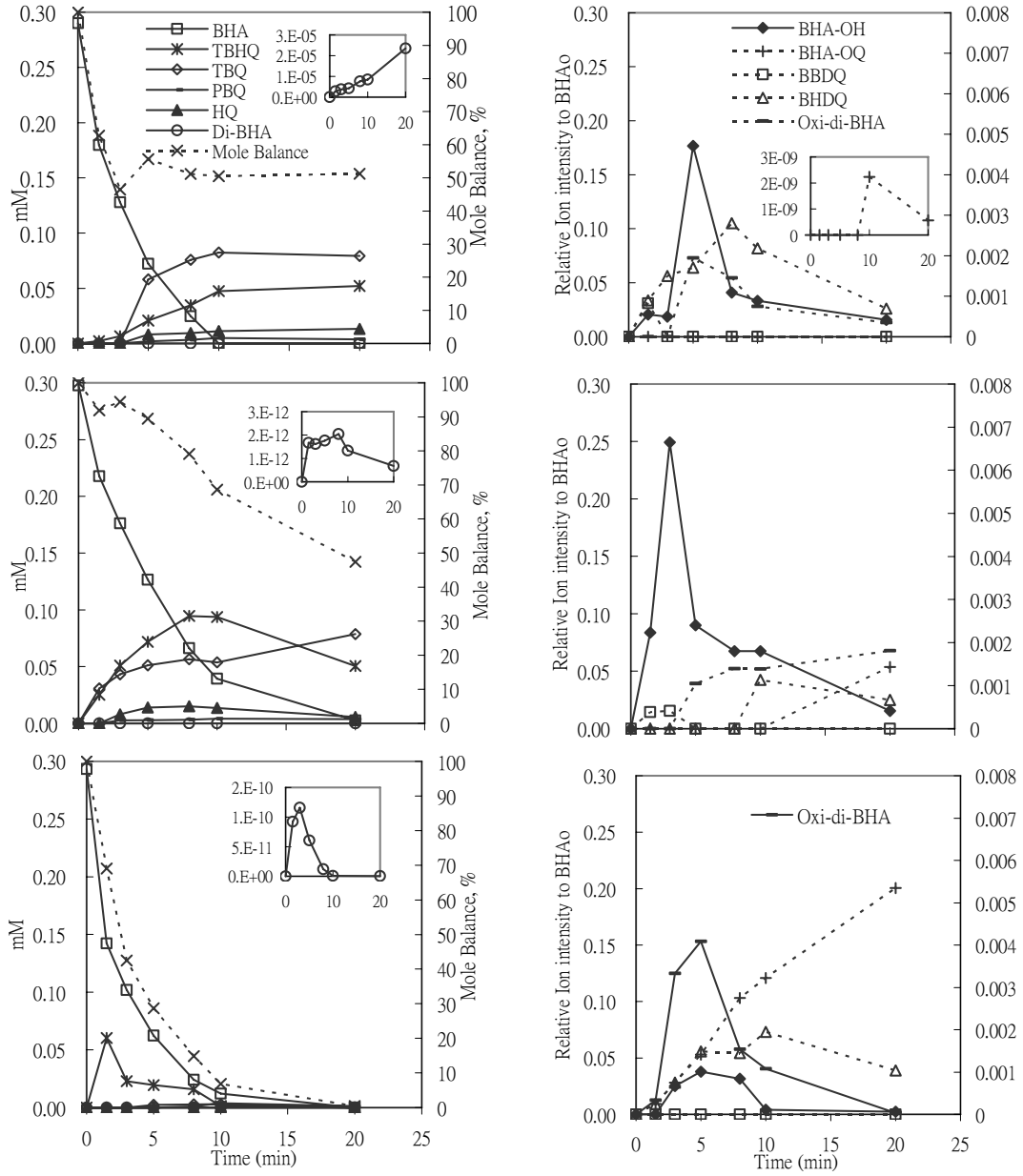

Fig. 6.4: Formation of intermediate compounds during the degradation of 0.29 mM BHA at pH 3 (a, b), pH 7 (c, d) and pH 11 (e, f) by the ozonation process, where solid line (—) and dotted lines (---) were used for primary and secondary y-axis, respectively.

This shows that while the BHA decay is similar for the UV/O_3 and O_3 systems, the greater oxidative capacity with UV/O_3 (i.e. $^{\bullet}OH$ in UV/O_3 versus molecular ozone in ozonation) has been used to oxidize the reactive intermediates.

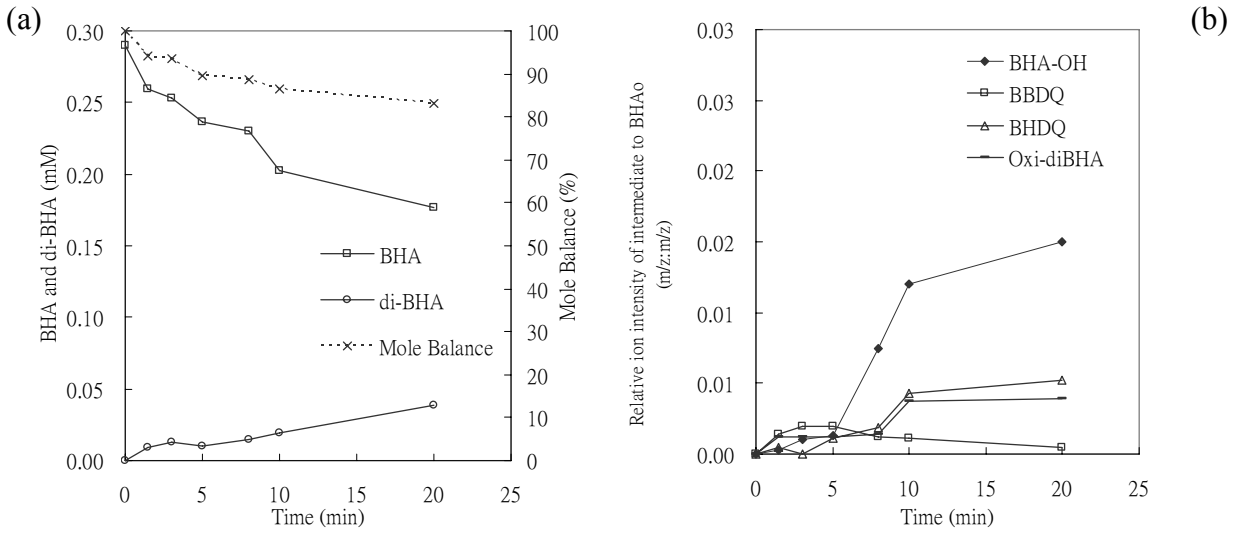

Fig. 6.5: Formation of intermediate compounds during the degradation of 0.29 mM BHA by UV photolysis at pH 3.

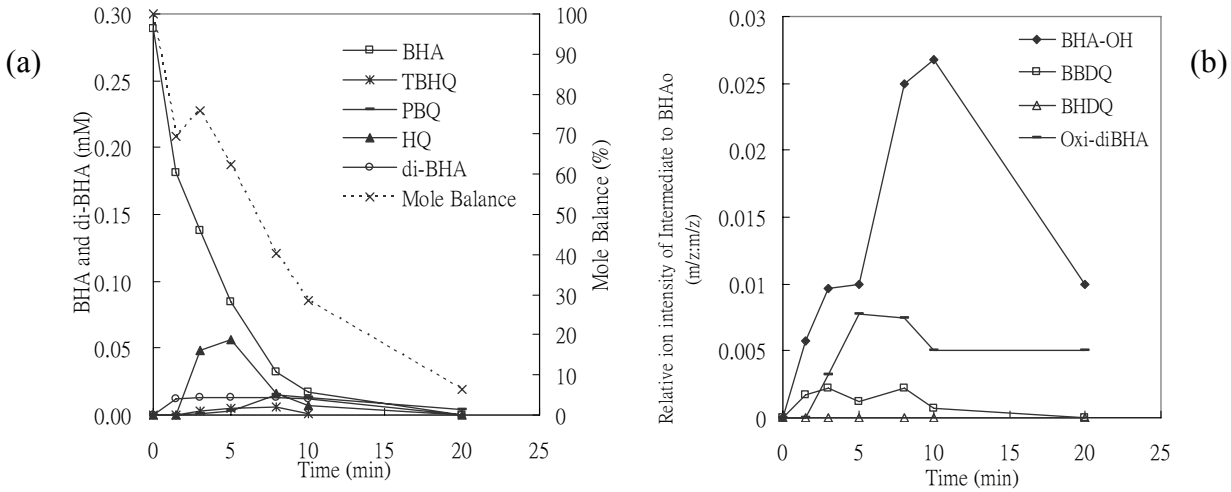

Fig. 6.6: Formation of intermediate compounds during the degradation of 0.29 mM BHA by the UV/O_3 process at pH 3.

b) As well as the difference in $^{\bullet}OH$ generation in the UV/O_3 and ozonation processes, the formation of insoluble intermediates may partly explain the lower kinetic rate with ozonation. The proposed reaction pathways of BHA decay in the three processes are summarized in Fig. 6.7. A pathway, termed 'Precipitation', is exclusively proposed for the ozonation reaction, where two unique insoluble orange-coloured quinonic derivatives (BHA-OQ and TBQ) are found in the process. The change from a homogeneous to a heterogeneous (presence of insoluble products) system hinders the performance of the ozonation reaction.

c) For the UV process, since no $^{\bullet}OH$ are expected to be present in the solution, the decay of BHA is believed to be due to direct photolysis, which is pH independent, as shown in Fig 6.3b and 6.3c. However, at lower initial [BHA] (or higher photon/[BHA] ratio), the additional photons may induce another mechanism known as basic-catalytic photohydrolysis, which is pH dependent and a gradual increase of BHA photolysis with pH is observed, as shown in Fig. 6.3a.

Process	Oxidation	Precipitation	Dimerization
UV/O_3	✓		✓
O_3	✓	✓	✓
UV	BHA-OH only		✓

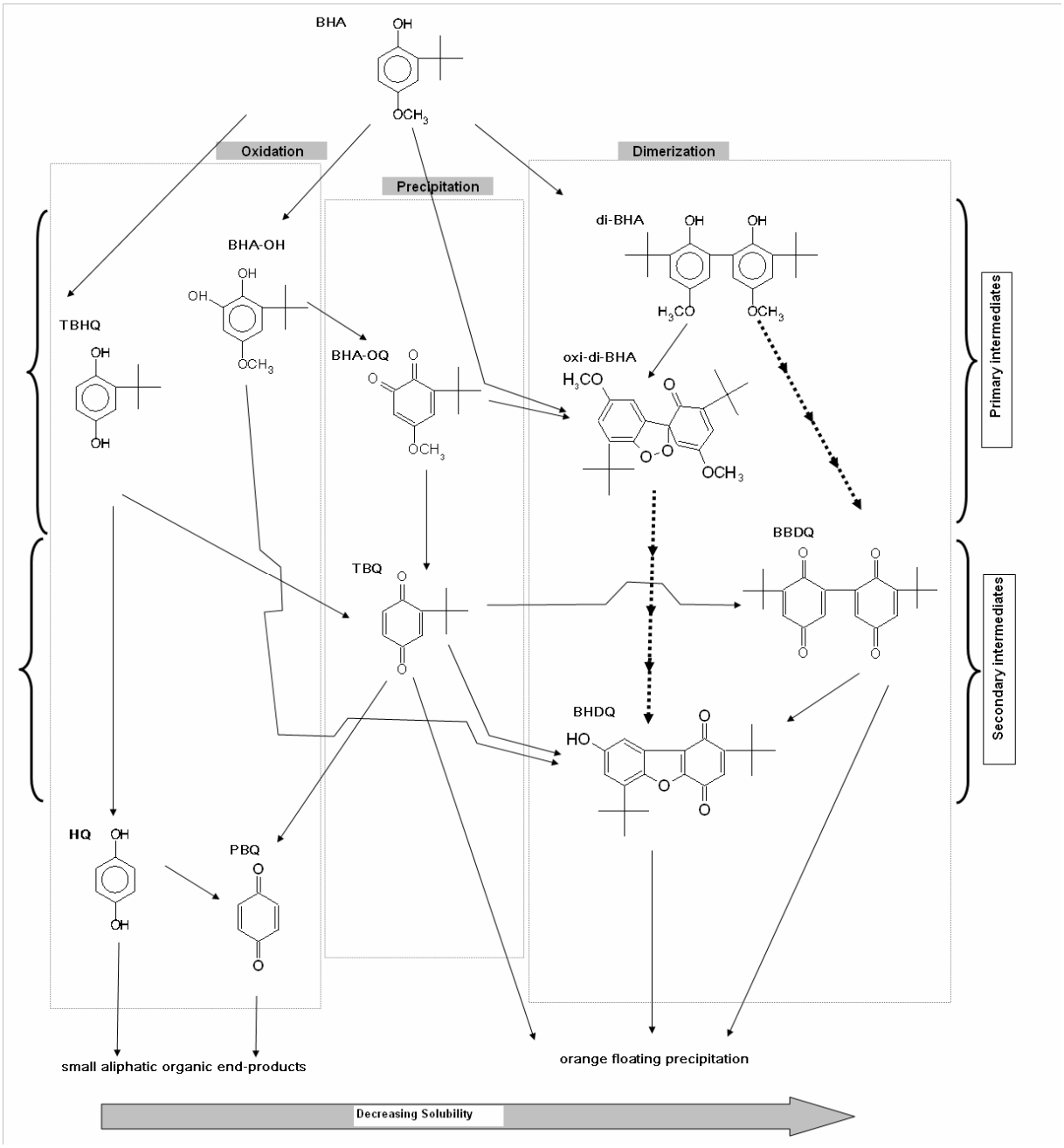

Fig. 6.7: Proposed degradation mechanism of BHA for the different treatment processes (dashed arrows indicate pathway of short-lived and non-detectable intermediates).

6.2.2 UV Photolysis

The direct photolysis of BHA by UV at 254 nm is shown in Fig. 6.5. The LC-MS analysis revealed that the treatment process is less effective than the UV/O_3 and O_3 processes and yields mainly primary intermediates (Fig. 6.7), including macro-dimers (di-BHA, oxi-diBHA, BBDQ and BHDQ) and BHA-OH. The 'Dimerization' pathway is believed to be the principal reaction pathway, starting from the excitation of BHA by UV, followed by the hydroxylation, H-abstraction, heterolytic cleavage, and scission of bonds. The presence of oxygen in water is likely to contribute to the BHA dimerization process (Verhagen et al., 1991). The excited radicals ($BHA^{\bullet}$) could be converted into resonance-stabilized intermediates (i.e. di-BHA) via the following equations:

$$RH + h\nu \longrightarrow R^{\bullet} + H^{\bullet} \quad (6.1)$$

$$R^{\bullet} + O_2 \rightarrow ROO^{\bullet} \quad (6.2)$$

$$ROO^{\bullet} + RH \rightarrow ROOH + R^{\bullet} \quad (6.3)$$

$$ROO^{\bullet} + ROO^{\bullet} \rightarrow ROOR + O_2 \quad (6.4)$$

$$ROO^{\bullet} + R^{\bullet} \rightarrow ROOR \quad (6.5)$$

$$R^{\bullet} + R^{\bullet} \rightarrow RR \rightarrow \text{inert dimers} \quad (6.6)$$

The stable molecules can then interfere with, or terminate, the free radical chain reactions (Eqs. 6.2 and 6.3), thereby making the UV process less effective.

6.2.3 Ozonation

Aromatic compounds are susceptible to electrophilic substitution reactions with an electrophilic agent, such as ozone, in which the ring structure remains mostly intact due to its stability (Beltran, 2004). In the ozonation process, the O-methoxy group and/or the hydroxyl group of BHA are primarily attacked through oxidation (Fig. 6.7), where the BHA is O-demethylated to TBHQ then subsequently oxidized to TBQ via the semiquinone radical as an intermediate. This oxidation pathway alternatively could hydrolyze BHA to yellow-orange BHA-OH (catechol of BHA). Its methoxy group could donate electrons to the ring to increase the receptivity of the catechol and induce a faster oxidation forming an o-quinone, BHA-OQ (Armstrong and Wattenberg, 1985).

In addition, according to Gottschalk and Libra (2000), ozonation can lead to bond splitting by breaking the t-butyl chain of TBHQ and TBQ to HQ and PBQ, respectively. The product of dimerization (di-BHA) was also observed in the ozonation process, so both the “oxidation” and “dimerization” pathways are

effective and result in fast BHA and di-BHA decay and the accumulation of oxi-diBHA, BBDQ and BHDQ.

It should be noted that insoluble intermediates (e.g. BHA-OQ and BBDQ) were formed during ozonation and because most of them can not be quantified by LC/MS, their concentrations are not included in Fig. 6.4. Additional filtration tests were therefore conducted to quantify the total mass production of these compounds, as shown in Fig. 6.8. It is interesting to note that the formation of primary intermediates (TBHQ**,** BHA-OH, di-BHA, Oxi-di-BHA including BHA-OQ) has the opposite trend compared to the decay rate of BHA; it was also observed that the formation of secondary intermediates (BHDQ, BBDQ, including TBQ from the decay of primary intermediates) increased with pH. The results indicate that the higher the mass of primary intermediates, the lower the BHA decay rate, suggesting that the primary intermediates can effectively compete for the O_3 (from low to neutral pH levels) and/or $^{\bullet}OH$ (from neutral to high pH levels) in the solution with BHA, and form secondary intermediates depending mainly on the presence of $^{\bullet}OH$. Therefore, the decay of BHA itself may not be the dominant process in the solution and a minimum-type variation of BHA decay rate with pH rise is overall result, as indicated in Fig 6.3 and 6.8.

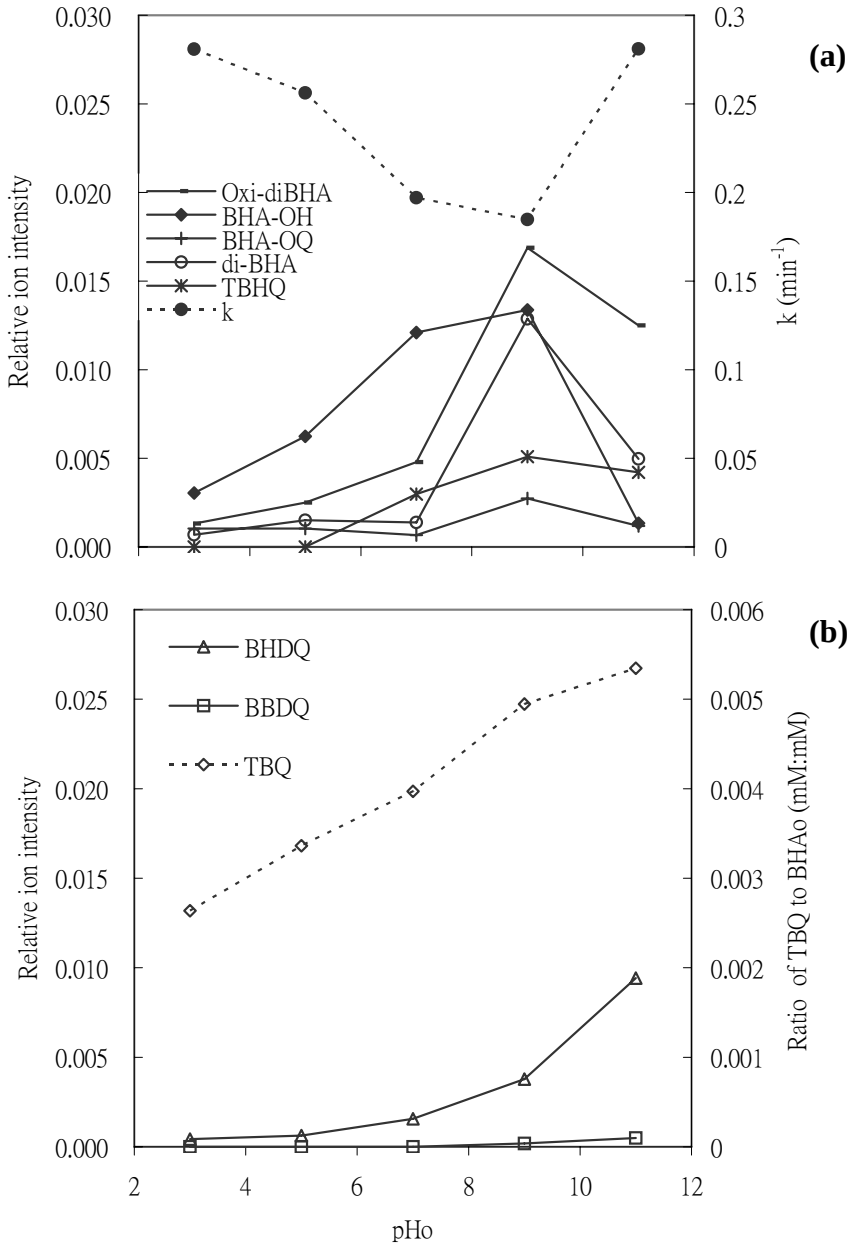

Fig. 6.8: Primary (a) and Secondary (b) intermediate compound formation for the degradation of 0.29 mM BHA at different pH by the ozonation process at 20 min, where solid lines (—) and dotted line (---) were used for primary and secondary y-axis, respectively. (Remark: The intensity of TBHQ curve in Fig. (a) is doubled to give a better resolution)

In highly alkaline conditions (pH 11), the rapid degradation of both BHA and primary intermediates cannot be adequately explained solely by the reaction competition between BHA and the primary intermediates, and other mechanisms are likely to be present. In addition to the increasing reactivity of dissociated BHA and primary intermediate compounds at high pH, the generation of basic-catalyzed $^{\bullet}OH$ is likely to be partly responsible for the higher reaction rates, through indirect chain reactions (Gottschalk and Libra, 2000)

$$O_3 + OH^- \rightarrow HO_2^{\bullet} + O_2^{-\bullet} \rightarrow {}^{\bullet}OH \qquad (6.7)$$

In the ozonation process (Fig. 6.4), the initial pH level governs the mechanism of BHA degradation, with dimerization and oxidation the dominant pathways in acidic and basic condition, respectively. In acidic conditions, TBQ formation is greater in the aqueous phase than TBHQ, whereas in neutral and alkaline conditions TBHQ formation is greater. At pH 3, the dimerization pathway is evident by the highest concentration of the dimer di-BHA in solution (Fig. 6.4a) in conjunction with the lowest precipitate formation (Fig. 6.8). This suggests that the di-BHA can be easily formed from BHA and decays quickly in the solution before the solid state can be produced, so the transformation of BHA to di-BHA is apparently preferable in acidic conditions than in neutral and alkaline pH (7

and 11). In addition, in acidic conditions, the cleavage of the dimer BBDQ into TBQ (single-ringed) was observed, where TBQ appears at 5 min of ozonation soon after the decrease of BBDQ at 3 min of ozonation (Fig. 6.4a-6.4d). The early disappearance of BBDQ was attributed to both oxidation (into BHDQ) and dimer cleavage (into TBQ), which is not the case at higher pH levels. Therefore the extra decay pathway of intermediates in acidic conditions will indirectly promote the decay of the parent compound BHA.

6.2.4 UV/O_3 Process

The observed reaction pathways for the UV/O_3 process were similar to that of the ozonation process but with a faster kinetics presumably induced by non-selective $^{\bullet}$OH radical reactions. The reaction profiles of BHA and its associated intermediates by UV/O_3 were investigated at various pH levels with similar patterns; a typical profile at pH 3 is shown in Fig. 6.6. The decay rate constants of BHA follow a minimum-type variation with pH similar to that with ozonation (Fig. 6.3), but with the rates enhanced by 1.2 – 1.5 times, except at pH 3. The fastest BHA decay by UV/O_3 was obtained at pH 11, where excessive OH^- is present for generating $^{\bullet}$OH from the decomposition of ozone (Eq. 6.7) plus the extra basic-catalytic hydrolysis, UV-induced radical generation (Eqs. 6.8 and 6.9)

and direct photolysis of BHA.

$$O_3 + H_2O + h\nu \longrightarrow H_2O_2 + O_2 \quad (6.8)$$

$$H_2O_2 + h\nu \longrightarrow 2\ ^{\bullet}OH \quad (6.9)$$

It was also found that the difference in BHA decay rate between UV/O_3 and O_3 was not the greatest at this high pH level, but appeared to be greatest in the weak acid to weak base range (Fig. 6.3a-6.3c). This phenomenon is possibly due to the lower reactivity of undissociated BHA with molecular ozone (relative to $^{\bullet}OH$) and the high production of $^{\bullet}OH$ at high pH level which leads to a recombination of the $^{\bullet}OH$ (Eq. 6.10) into hydrogen peroxide (Gottschalk and Libra, 2000).

$$2\ ^{\bullet}OH \rightarrow H_2O_2 \quad (6.10)$$

In general, the UV/O_3 process showed various advantages over ozonation including: (1) 90% mineralization; (2) greater removal in terms of mole balance; (3) the final detectable products (HQ and PBQ) could be fully degraded within 20 min (Fig. 6.6); and (4) no precipitation in the solution.

6.3 UV/$S_2O_8^{2-}$ kinetics and mechanisms

6.3.1 Rate constants for the degradation of BHA and the pH dependency

The comparative performance of using 2 mM $K_2S_2O_8$ (KPS) and $(NH_4)_2S_2O_8$ (APS) as the oxidant in the UV photolysis of 0.3 mM BHA degradation at pH 7 is shown in Fig. 6.9(a). Although Balazs et al. (Balazs et al., 1999) recommended APS due to its exceptional solubility, it was observed in the screening tests that KPS gave a more rapid removal of BHA (1.42 times) than APS at neutral pH, corresponding to a pseudo first-order kinetic rate constant of 0.3461 and 0.2443 min^{-1}, respectively. The difference in the removal efficiency is apparently due to the presence of the ammonium ion. The aqueous ammonium can undergo photo-oxidation (Bonsen et al., 1997) leading to nitrate and/or nitrite by the available oxidants in the solution, such as, $S_2O_8^{2-}$, and its related intermediates H_2O_2 or O_2 (Eqns. 6.11-6.17). Furthermore, the reaction of NH_4^+/NH_3 with UV/ $S_2O_8^{2-}$ process are proved to be able to convert it to nitrate under the 254 nm photolysis at a rate constant of 0.25 mg L^{-1} min^{-1} or 4 x 10^{-3} mM min^{-1} (Roig et al., 1999), thereby making the ammonium a competitor of BHA. In view of this, and the general unsuitability of adding ammonia to waters and wastewaters, APS is not recommended to be used in the UV/$S_2O_8^{2-}$ oxidation process.

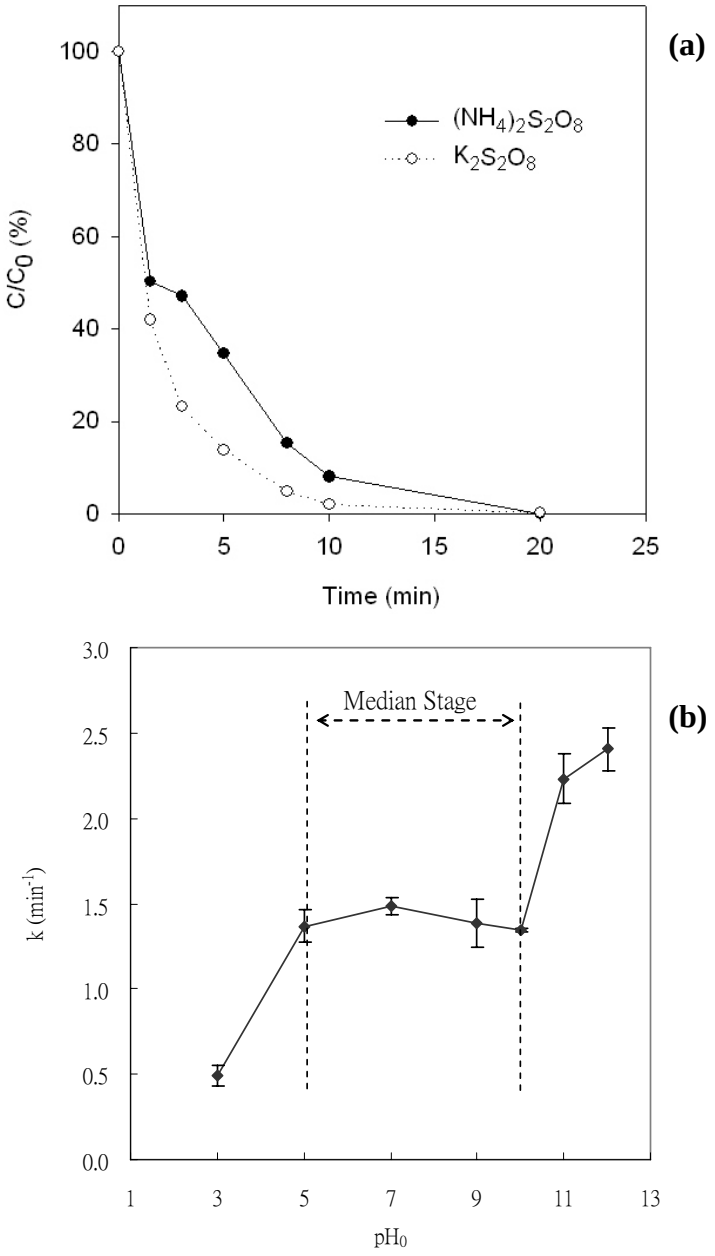

Fig. 6.9: (a) Photodegradation of 0.3 mM BHA with different peroxydisulfate salts (2 mM $S_2O_8^{2-}$) at pH 7 (UV: 254 nm, 1.5×10^{-5} Einstein L^{-1} s^{-1}); (b) pseudo-first-order rate constants for the reaction of 0.1 mM BHA at different initial pH with 2 mM KPS under 254 nm irradiation.

Therefore, the UV/KPS combination was chosen for further investigation throughout this study, where reactions with 0.1 mM BHA were evaluated at pH values ranging from 3 to 11. It was observed that there was a stepwise increase in the kinetic rate constant for the BHA decay, as shown in Fig. 6.9(b). Relatively low and high decay rates were observed under strong acid (pH < 5) and strong base (pH > 10) conditions, respectively, and a relatively constant decay rate evident in the weak acid to weak base region. The increase in BHA decay rate was about three times and five times with increasing pH from acidic to neutral and alkaline levels, respectively. These three distinctive phases reveal the high pH-dependency of KPS under irradiation at 254 nm.

This phenomenon can be explained by both the decreasing trends of pH during the process and the corresponding reaction pathways of radical formation (i.e. $SO_4^{\bullet-}$ or $OH^{\bullet}$). For example, at pH 7, once the irradiation started, the solution pH dropped to about 3.6 – 3.9 depending on the KPS dosage (0.5 – 15 mM), where the higher the KPS dosage the greater the pH reduction. The acidification of the sample partially validates the occurrence of acidic photoproducts of peroxydisulfate, i.e. bisulfate (HSO_4^-) and protons. In water, $SO_4^{\bullet-}$ is known to produce HSO_4^- and $OH^{\bullet}$ (Morgan et al., 1997), and they will further decompose

to give sulphate ion (SO_4^{2-}), as indicated in the following equations (House, 1962; Laat and Le, 2005; Tsao and Wilmart, 1959; McElroy and Waygood, 1990):

$$SO_4^{\bullet-} + H_2O \rightarrow HSO_4^- + OH^{\bullet} \qquad (k = 500 \pm 60\ s^{-1}) \qquad (6.11)$$

$$HSO_4^- \rightarrow H^+ + SO_4^{2-} \qquad (6.12)$$

$$OH^{\bullet} + S_2O_8^{2-} \rightarrow HSO_4^- + SO_4^{\bullet-} + \tfrac{1}{2}\ O_2 \qquad (6.13)$$

$$SO_4^{\bullet-} + OH^{\bullet} \rightarrow SO_4^{2-} + \tfrac{1}{2}\ O_2 \qquad (6.14)$$

$$2\ OH^{\bullet} \rightarrow H_2O_2 \qquad \text{(except in alkaline solution)} \qquad (6.15)$$

$$H_2O_2 \rightarrow H_2O + \tfrac{1}{2}\ O_2 \qquad \text{(mostly in acidic solution)} \qquad (6.16)$$

$$S_2O_8^{2-} + H_2O_2 \rightarrow 2H^+ + 2SO_4^{2-} + O_2 \qquad (6.17)$$

$$SO_4^{\bullet-} + H_2O_2 \rightarrow SO_4^{2-} + H^+ + HO_2^{\bullet} \qquad (6.18)$$

$$SO_4^{\bullet-} + HO_2^{\bullet} \rightarrow SO_4^{2-} + H^+ + O_2 \qquad (6.19)$$

The observed overall result of the above equations was a stoichiometric generation of SO_4^{2-} from $S_2O_8^{2-}$ at 60 min as shown in Fig. 6.10, where complete mineralization of BHA and its associated intermediates took place simultaneously.

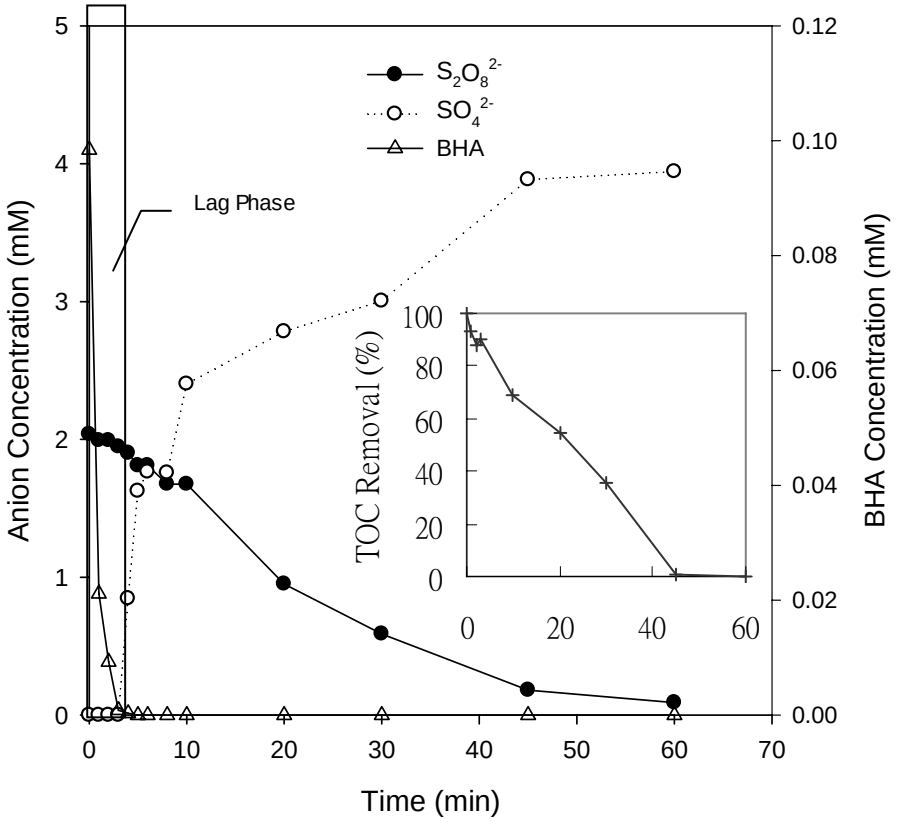

Fig. 6.10: Relationship of $[S_2O_8^{2-}]$ conversion to $[SO_4^{2-}]$, and TOC removal (%) at pH 7.

It can be seen in Fig. 6.10 that after a "lag phase" of no detectable sulphate ion formation at the beginning of the reaction (< 4 min), the subsequent formation of SO_4^{2-} became appreciable once the BHA had been entirely removed (99.8%) from the solution. Since $S_2O_8^{2-}$ was linearly consumed during the lag phase without the formation of SO_4^{2-}, it is believed that the highly reactive radicals (i.e. $SO_4^{\bullet-}$ or $OH^{\bullet}$) are dominant in the solution and responsible for the fast BHA decay.

In general, after the cleavage of the peroxide bond in $S_2O_8^{2-}$ via homolysis to the sulfate radical, the latter will further react with water to produce $OH^{\bullet}$ (Eq. 6.11). According to Tsao and Wilmarth (Laat and Le, 2005), the higher the pH the more quickly will be the dissociation of $S_2O_8^{2-}$ (via photolysis) to the $SO_4^{\bullet-}$ radical, and the further conversion to $OH^{\bullet}$ via the reaction with OH^- (McCallum et al., 2000). This could be one of the reasons to justify the higher kinetic rate constant of BHA decay at pH 11 (Fig. 6.9b), and the continuous increase in rate constant with $[S_2O_8^{2-}]$ (Fig. 6.11), in contrast to the observed independence of the rate constant at higher $[S_2O_8^{2-}]$ doses than 2 mM under acidic and neutral conditions. In addition, in the absence of the recombination effect of hydroxyl radicals to H_2O_2 (Eq. 6.15) in alkaline solution (Tsao and Wilmart, 1959), a faster removal of BHA by hydroxyl radical was believed to be dominant; therefore, the reactions shown by Eqns 6.17 to 6.19 were not thought to be significant.

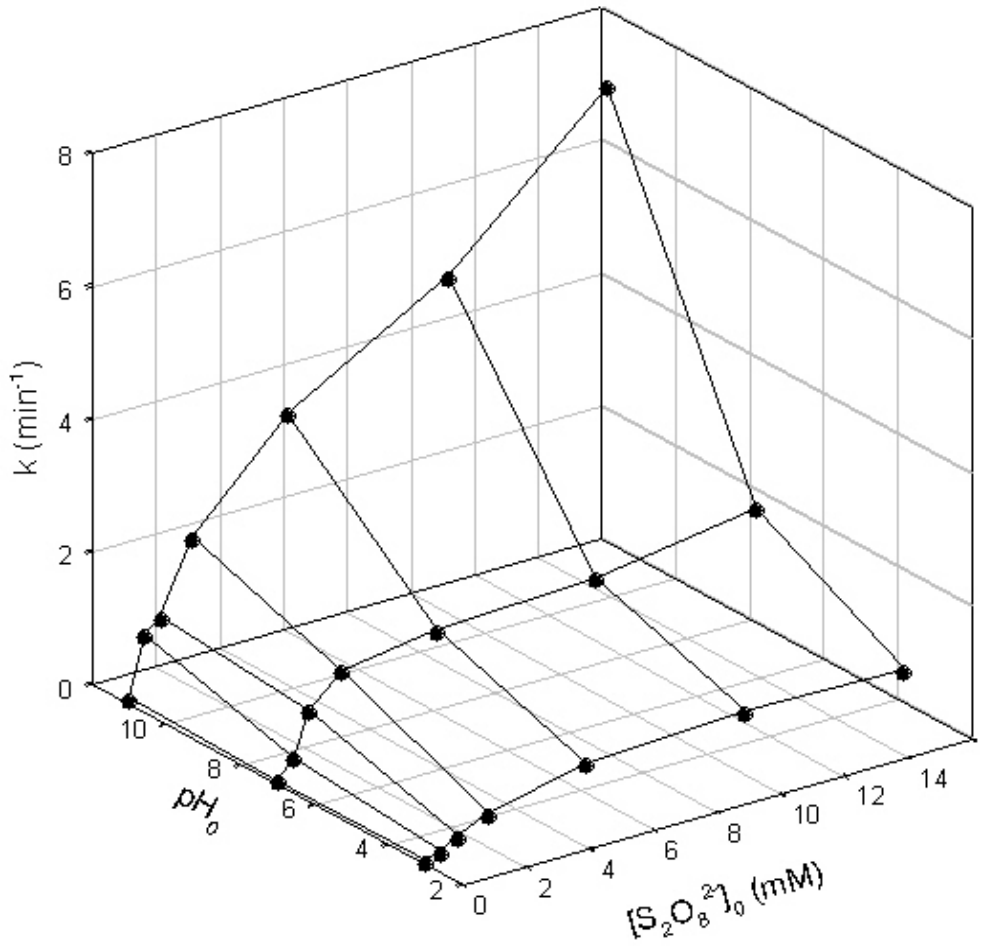

Fig. 6.11: Pseudo-first-order rate constant of 0.1 mM BHA at pH 3, 7 and 11 by different initial $S_2O_8^{2-}$ doses under 254 nm irradiation.

In acidic conditions (pH level of 3), the pH of the reacting solution was further reduced to about pH 2.7. It is believed that this is not only the result of proton formation, as proposed in Eqns 6.17-6.19, but also the formation of additional acidic inorganic products which are favourable at lower pH, such as monopersulfuric acid (H_2SO_5) and sulfuric acid (H_2SO_4), via decomposition of

$S_2O_8^{2-}$ and $SO_4^{\bullet-}$ as summarized in Eqns. 6.20 to 25 (McCallum et al., 2000, McElroy and Waygood, 1990; Lobree and Bell, 2001).

$$SO_4^{\bullet-} + H_2SO_4 \rightarrow HSO_4^{\bullet} + HSO_4^- \quad (6.20)$$

$$SO_4^{\bullet-} + S_2O_8^{2-} \rightarrow S_2O_8^- + SO_4^{2-} \quad (k = 6.1 \pm 0.6 \times 10^8\ M^{-1}\ s^{-1}) \quad (6.21)$$

$$S_2O_8^{2-} + H^+ \rightarrow HS_2O_8^- \quad (6.22)$$

$$HS_2O_8^- \rightarrow SO_4 + HSO_4^- \quad (6.23)$$

$$HS_2O_8^- + H_2O \rightarrow H_2SO_5 + HSO_4^- \quad (6.24)$$

$$H_2SO_5 + H_2O \rightarrow H_2O_2 + H_2SO_4 \quad (6.25)$$

Furthermore, at pH 3, the generation of ineffectual anions or weaker oxidants is prevalent throughout the reaction, such as $HS_2O_8^-$, H_2SO_5, sulfur tetroxide (SO_4), bisulfate (HSO_4^-), and H_2O_2 ($E° = 0.87$ V), instead of stronger radicals, like $OH^{\bullet}$ (2.8 V) and $SO_4^{\bullet-}$ (2.5 – 3.1 V) (Anipsitakis and Dionysiou, 2003; Steenken, 1988). The lowest reactivity of BHA was therefore observed in acidic conditions.

6.3.2 Verification of the Proposed Degradation Pathway and Mineralization

The profiles of intermediate compound formation, as determined by LC-MS analysis, resulting from the degradation of 0.1 mM BHA using 2 mM $S_2O_8^{2-}$ under 254 nm UV-irradiation at pH 3, 7 and 11, are shown in Fig. 6.12 to 6.13, and the proposed reaction pathways of BHA decay are summarized in Fig. 6.14. Ten major oxidized and dimeric intermediates were identified, and their corresponding occurrence is summarized (See Table 6.1). It should be noted that in addition to the oxidation induced by radicals or oxidants as mentioned before, BHA may also be degraded by direct UV-photolysis. After absorbing 254 nm UV-irradiation, BHA undergoes excitation to singlet and/or triplet state where hydroxylation, H-abstraction, heterolytic cleavage, and scission of bonds can be followed (Rustgi and Riesz, 1978; Gilbert et al., 1999). Furthermore, as an antioxidant, BHA can also be dehydrogenated and dimerized with its own probe compound or different radical-species (Kurechi et al., 1983). In this case, the excited antioxidant radicals ($BHA^{\bullet}$) were found to convert to resonance-stabilized intermediates, di-BHA, which could be further oxidized to oxi-di-BHA, BBDQ or BHDQ as shown in Fig. 6.14.

Table 6.1: The occurrence of BHA and intermediates at different pH levels

Compounds	**pH 3**	**pH 7**	**pH 11**	**Retention time (min)**	**Detection Mode**	**Characterization: ESI-MS/MS spectrum ions (m/z)**
BHA				27.1	-ve	1791, 65, 121
BBDQ	✓	✓	✓	36.5	+ve	327, 311, 179, 164
Di-BHA	✓	✓	✓	35.75	-ve	357, 342
Oxi-di-BHA	✓	✓	✓	33.78	-ve	373, 357, 342, 179, 165
BHDQ	✓	✓	✓	30.26	-ve	327, 312, 299, 179, 165, 120
TBQ	✓ trace	-	-	25.2	-ve	164, 149, 120
BHA-OQ	✓	-	-	23.55	-ve	193, 179, 165, 163, 120
BHA-OH	✓	✓	✓	20.33	-ve	195, 179, 165, 121
TBHQ	✓ trace	-	-	17.38	-ve	165, 150, 121, 108
PBQ	✓	✓	✓	7.95	-ve	108
HQ	✓	✓	✓	5.5	-ve	108

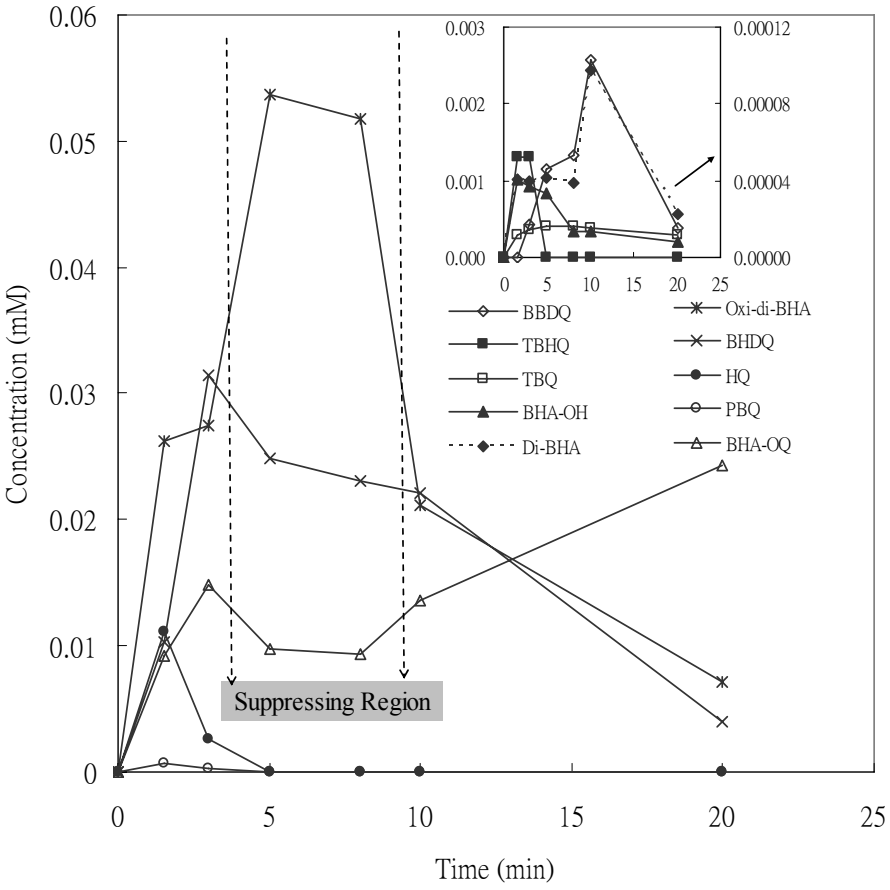

Fig. 6.12: Profile of intermediates of BHA degradation by UV/$S_2O_8^{2-}$ at pH 3

(dotted line6.12 refers to the secondary axis)

In viewing the intermediate profile of BHA at pH 3 (Fig. 6.12), two unique pathways via acid-catalysis were proposed, where three intermediates of BHA-oxidation products (TBHQ, TBQ, and BHA-OQ) were found exclusively at pH 3 (as indicated in the dotted box of Fig. 6.14).

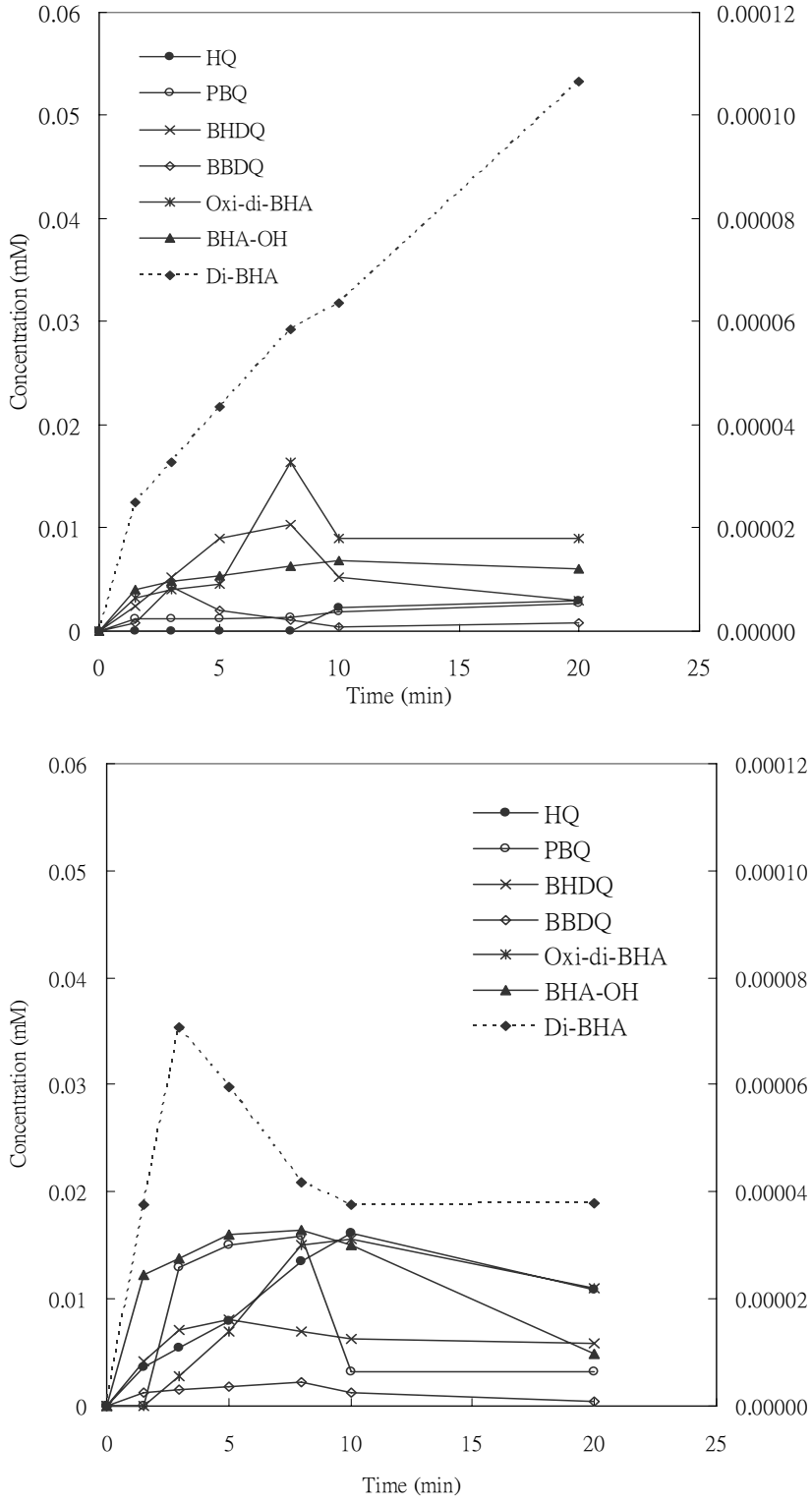

Fig. 6.13: (a) Intermediates profile of BHA degradation by UV/$S_2O_8^{2-}$ at pH 7; (b) Intermediates profile of BHA degradation by UV/$S_2O_8^{2-}$ at pH 11 (dotted line refers to the secondary axis).

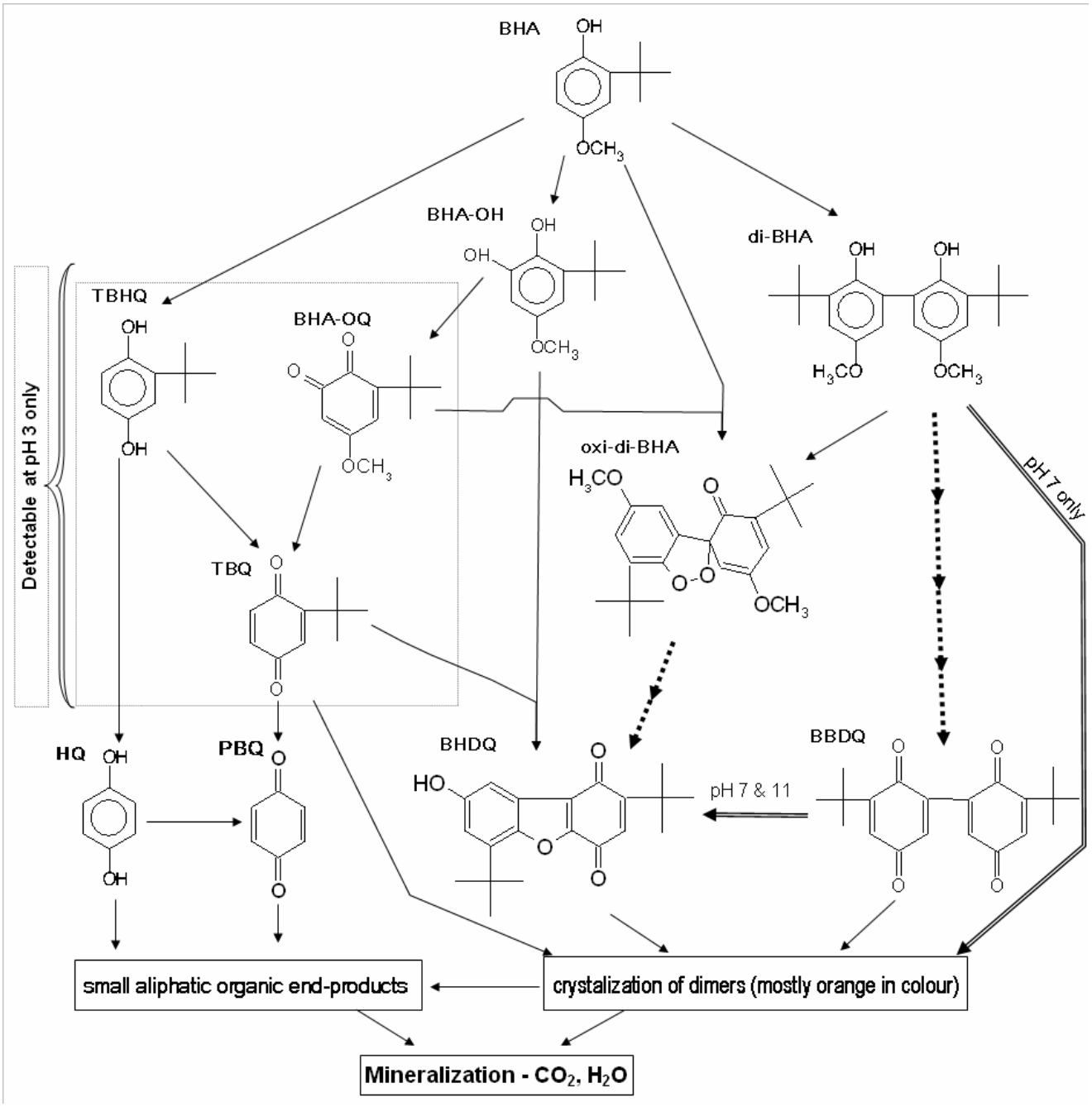

Fig. 6.14: Proposed degradation pathways for UV/ $S_2O_8^{2-}$ process of 0.1 mM BHA at different pH (double arrows indicate pathway of pH 7 or 11; and dotted lines indicate pathway of short-lived and non-detectable intermediates)

The TBHQ-related pathway was based on the observation of the formation and decay profiles of TBHQ and its daughter products HQ and PBQ, which are all diminished within 5 min of reaction, simultaneously (Fig. 6.12). The second pathway is the formation/decay of BHA-OQ. BHA-OQ is a quinonic compound derived directly form BHA-OH (the primary intermediate) through an oxidative mechanism and it can be further degraded to TBQ. Furthermore, the steady accumulation of TBQ on the other hand could be recognized as the oxidized product of TBHQ, as TBQ reaches its peak concentration after the disappearance of TBHQ at 5 min.

Interestingly, at a reaction time of 5 to 10 min (Fig. 6.12), the oxi-di-BHA concentration reaches its peak, while simultaneously discrete "suppressing regions" of BHA-OQ and di-BHA were observed. This suggested that the formation of oxi-di-BHA comes either from the dimerization of precursors BHA-OQ and BHA, or from the oxidization of single dimer di-BHA (Fig. 6.14). Similarly, such a fusion mechanism of precursors (i.e. dimerization) is also responsible for the formation of BHDQ by combining TBQ and BHA-OH in addition to the oxidation of oxi-di-BHA.

For pH ≥ 7, the proposed reaction mechanism is similar to that of pH 3. However, as mentioned previously, neutral and basic-catalytic reactions could behave differently and a variation of reaction mechanism was therefore expected. The observations listed below could be helpful in explaining the improvement in the reaction rate of BHA degradation at pH ≥ 7:

1) At neutral to alkaline pH, lower concentrations of intermediates were generally observed. For instance, the peak of [oxi-di-BHA] at pH ≥ 7 (Fig. 6.13a and b) is only one-third of that at pH 3 (Fig. 6.12) with relative ion intensities of 0.015 and 0.055, respectively. This can be verified by the faster decay of BHA and its associated intermediates as indicated in Fig. 6.9(b) and 6.15(a), respectively. According to the mass balance of mole number and benzene rings for BHA and all detectable intermediates, the reduction of molecule number is faster than the benzene rings at pH 3. In fact, the latter remains constant in the first 5 min. This suggests that the dimerization dominates at the beginning of the reaction and no ring-opening occurs. At pH ≥ 7, however, the reduction of mole number is faster than that in acidic conditions and is synchronized with the benzene ring reduction. This suggests that the degradation of intermediates and

ring-opening are the dominant pathways for neutral to alkaline pH levels at the beginning of the reaction.

2) The HQ and PBQ were also observed in the alkaline-catalytic hydrolysis reaction, however, it is interesting to note that there were no traces of TBHQ, BHA-OQ, and TBQ in the solution. This is likely due to the faster decay of these intermediates at neutral to high pH conditions, so they do not accumulate to detectable levels. For example, according to our measurements, the decay rates of 0.1 mM [TBHQ] with 2 mM $S_2O_8^{2-}$ are 2.68, 3.11 and 4.77 min^{-1} at pH levels of 3, 7 and 11, respectively.

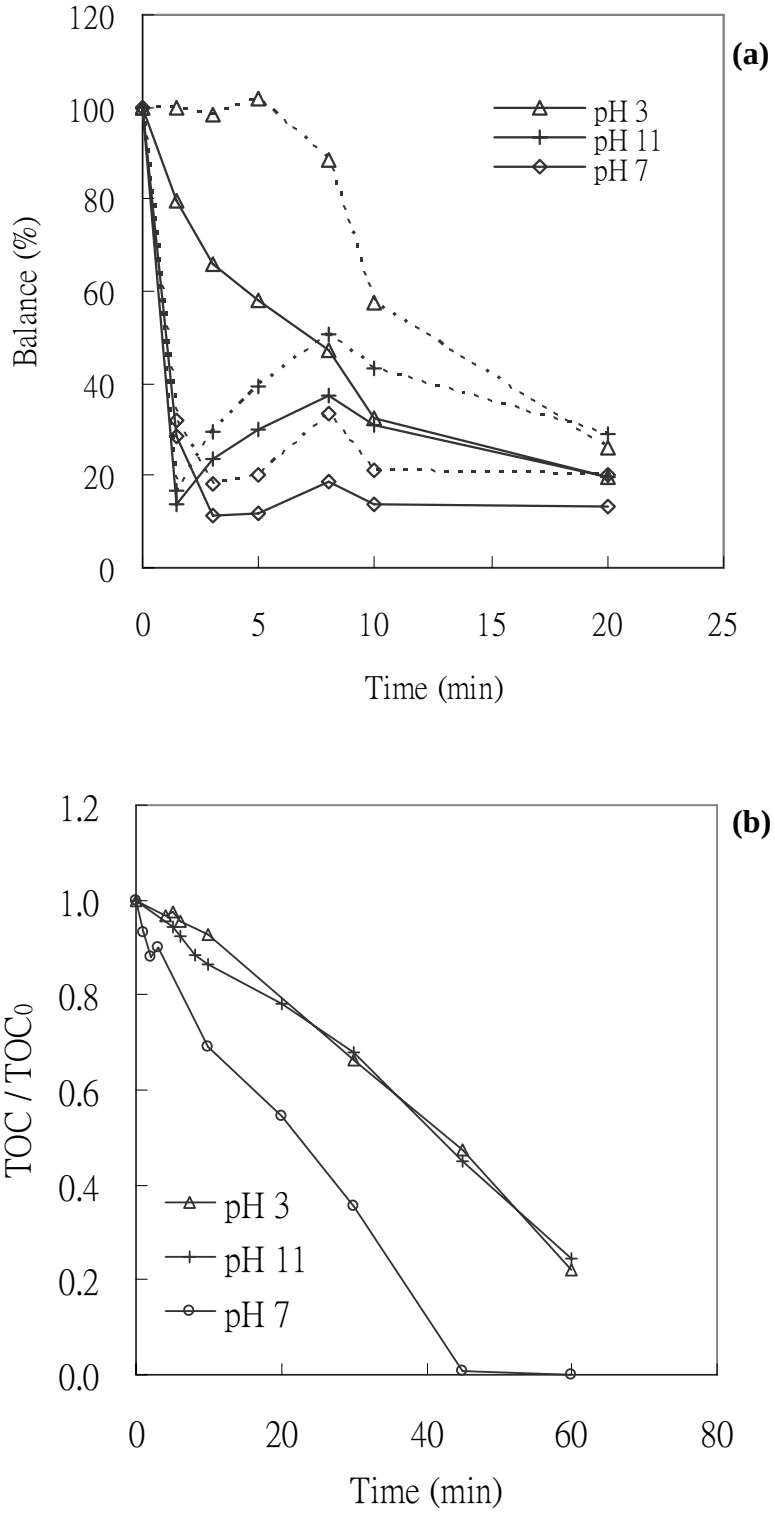

Fig. 6.15: (a) The mole balance (%), where the dotted lines (--) are the benzene ring mole balances, and the solid lines (–) are mole balances only; (b) mineralization of 0.1 mM BHA by 2 mM [$S_2O_8^{2-}$] at different pH.

3) It is known that both $SO_4^{\bullet-}$ and $^{\bullet}OH$ can react with organic compounds by electron transfer and/or addition to a double bond (Pasiuk-Bronikowska et al., 2003). Comparatively intensive generation of robust $SO_4^{\bullet-}$ and/or $OH^{\bullet}$ radicals at pH ≥ 7 without converting to a weaker oxidant (e.g. H_2O_2 at acidic condition) would allow faster oxidation of BBDQ to BHDQ, and likewise to subsequent mineralization. Additionally, it was noticed that the appearance and decay of BBDQ, one of the final dimeric products, is generally synchronized with the degree of mineralization; i.e. the faster the BBDQ degraded, the faster the mineralization of the process. For instance, at pH 7, the peak [BBDQ] appeared at 3 min (Fig. 6.13a), while at pH 3 and 11 the peaks were later at 10 and 8 min (Fig. 6.12 and 6.13b), respectively.

A high degree of mineralization by the UV/$S_2O_8^{2-}$ process was observed, where more than 80% TOC was removed within 60 min at all tested pH levels. The mineralization performance increased from low to neutral pH levels as predicted but decreased under basic conditions as shown in Fig. 6.15(b), which is inconsistent with the higher BHA decay rate at high pH (Fig. 6.9b). This is likely due to the concentration effect of active radicals in the solution. At the beginning

of the reaction, the generated [$OH^{\bullet}$] and [$SO_4^{\bullet-}$] were still low and mostly used for BHA decay because the latter was the sole species with a high initial concentration in the solution, therefore a high BHA decay rate was observed. However, at a later stage, relatively higher [$OH^{\bullet}$] and [$SO_4^{\bullet-}$] were generated catalytically in alkaline conditions, which induced recombination of these two radicals (Eq. 6.14), though this could be minor. This futile reaction consumed the available oxidants in the solution, and the decay rates of primary/secondary intermediates, and therefore the subsequent mineralization, were reduced. Additionally, smaller rate constant at pH 11 is believed to be taken place for the reaction between BHA and intermediates than those at pH<7, this is partly verified by the mass balance at pH 11, as shown in Fig 6.15(a), where the initial reduction in mass (for both mole number and ring number) is rapid but an accumulation of the mass was observed for the intermediates and therefore the overall mineralization was retarded.

To enhance the mineralization, a test of solid/liquid separation has been performed at pH 3 by removing the fine particulates (i.e. intermediates) that were generated in the process. This will minimize the possible attenuation of UV irradiation in the process and accelerate the water purification process. The

particulates were removed periodically by filtration (using a 0.2 μm filter) during the reaction; and it was surprisingly to note that mineralization could be improved from 34% ($k = 0.4937\ min^{-1}$) to 80% ($k = 0.6853\ min^{-1}$) by filtering out the particulates at 30 min of reaction time. Therefore, a solid/liquid separation-aided UV/$S_2O_8^{2-}$ process could be a useful strategy for full scale applications.

6.4 Model development of UV/$S_2O_8^{2-}$ process

In this study, the efficiency of photo-aided peroxydisulfate in removing BHA was investigated. Peroxydisulfate is usually used in TOC analyzers via UV irradiation (254 nm) or heating, and is suggested to be effective against SARS recently (Anipsitakis and Dionysiou, 2004). Other than using against disease or virus (Thayer, 2003), peroxydisulfate is being recognised to be a reliable and a low-cost electron acceptor for contaminants in different media (McCallum et. al, 2000), such as wastewater, soils, sludges, contaminated metal surfaces (Balazs et al., 1999), and caustic nuclear wastes (Anipsitakis and Dionysiou, 2003).

According to previous studies, sulfate radicals demonstrate higher standard redox potential (E^o= 2.5-3.1 eV) than hydroxyl radicals (E^o= 2.0–2.3 eV at neutral and 2.7 eV at pH = 0) (Malato et al., 1998; Anipsitakis and Dionysiou, 2003, 2004a, 2004b) in degrading organic compounds, but sulfate radicals ($SO_4^{-\bullet}$) are more selective than hydroxyl radicals in an oxidation process (Steenken, 1988). The usage of $SO_4^{-\bullet}$ oxidation process over a diverse group of waste matrixes was suggested, which proved an effective and prudent remediation process even under extreme conditions (i.e. acidic or basic media) (Balazs et al., 1999).

UV and heat are the two common ways to effectively generate the $SO_4^{-\bullet}$ from $S_2O_8^{2-}$, however, there are known disadvantages of the pressurized-heating process (Kronholm and Riekkola, 1999). Since some potassium and sulphur compounds can be released at high temperature (195 – 275 °C) which could lead to occurrence of color and corrosion problem due to the oxidation processes. In this study, the UV/$S_2O_8^{2-}$ process exhibits none of these problems in the solution after extended irradiations (1 hr).

According to Bardwell et al. (2001), at UV wavelengths shorter than 310 nm, peroxydisulfate absorbs photons resulting in the generation of the $SO_4^{-\bullet}$ radical. Depending on the different pH of the solution, the $SO_4^{-\bullet}$ radical can either recombines or further convert to the production of hydroxyl radical ($OH^{\bullet}$) especially in an alkaline solution (House, 1962; Laat and Le., 2005; McCallum et al., 2000; and Tsao and Wilmarth, 1959). Therefore, the reaction kinetics of BHA degradation by the UV/$S_2O_8^{2-}$ process was investigated in this study. In addition, a proper model in predicting the BHA decay by the UV/$S_2O_8^{2-}$ process is limited. Therefore, mathematical models were proposed as well via the results of reaction kinetics at different pH levels, UV/$S_2O_8^{2-}$ dosages and UV wavelengths.

6.4.1 UV Wavelength Effects: Degradation of BHA by different UV lamps (with or without $S_2O_8^{2-}$)

The direct photolysis (sole-UV) and photo-oxidation of 0.1 mM BHA using 2 mM $S_2O_8^{2-}$ under three different UV wavelengths were investigated at pH 3. They follow pseudo first-order kinetics, where significant increases of reaction rate were observed by the UV/$S_2O_8^{2-}$ process comparing to that of sole-UV at selected wavelengths (Fig. 6.16a). The BHA decay rate were found linearly correlated with UV wavelengths without or with the addition of $S_2O_8^{2-}$ as shown in the Eqns 6.26 and 6.27, when using our standard condition of eight lamps:

$$k_{UV} = - 0.0077 \lambda + 0.2748 \quad (6.26)$$

$$k_{UV/Oxi} = 6.25 (k_{UV}) \quad (6.27)$$

where λ is the UV wavelength used in the reaction (i.e. 254, 300, and 350 nm). Interestingly, the $k_{UV/Oxi}$, the kinetic rate constant of UV/$S_2O_8^{2-}$ process, is of 6.25 times higher than that of UV direct photolysis, k_{UV}. This is apparently resulted from the generation of robust sulphate radicals by the cleavage of $S_2O_8^{2-}$ under UV photolysis, which can further oxidized BHA and its related intermediates as shown previously.

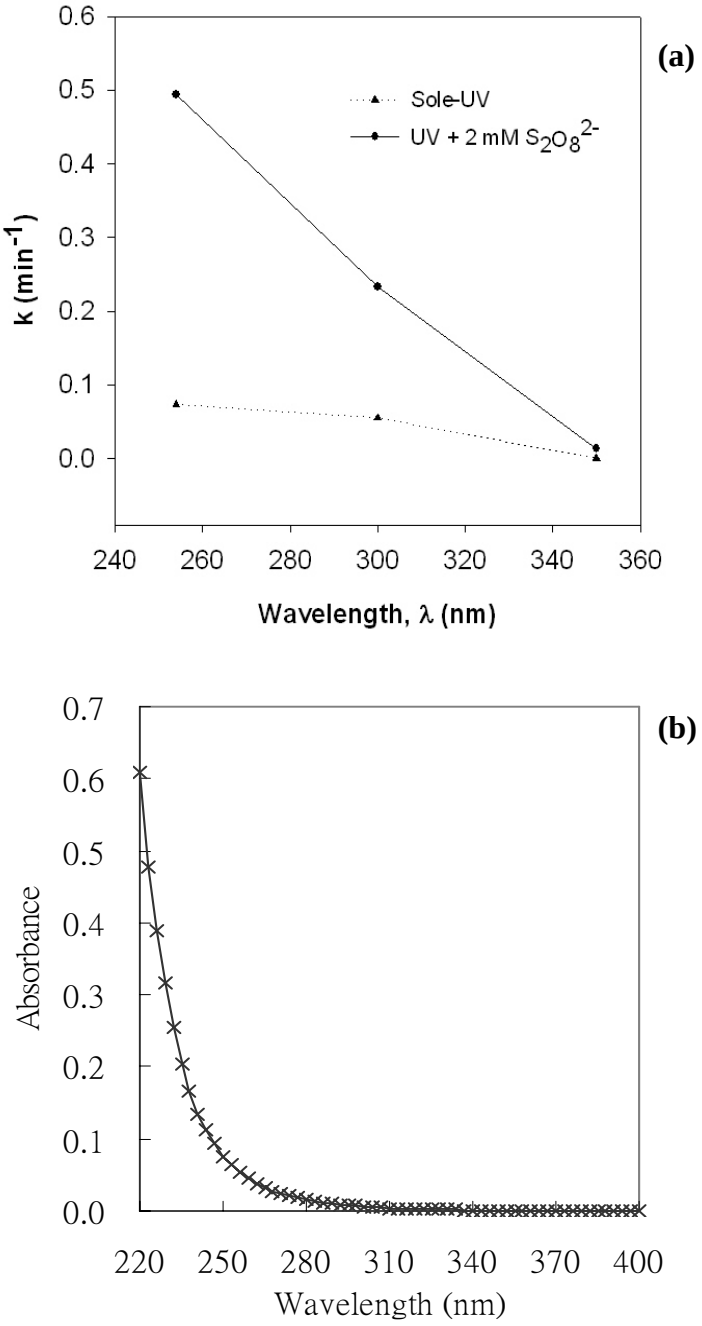

Fig. 6.16: (a) Pseudo-first-order rate constant of 0.1 mM BHA at pH 3 under irradiation of different wavelengths (no. of lamps: 8 in all cases); (b) the UV spectrum of $K_2S_2O_8$.

To further explore the influence of different wavelengths towards BHA degradation, another parallel test using similar light intensity (7.1×10^{-4} Einstein L^{-1} min^{-1}) of the three different wavelengths was carried out.

Table 6.2: The corresponding intensity of different number of lamps and kinetic rate constants at three different wavelengths at pH 3.

Wavelength (λ, nm)	**Total intensity, Einstein $L^{-1}min^{-1}$ (no. of lamps)**	**Kinetic rate constants, k (min^{-1})**
254	7.20×10^{-4} (8)	0.4937
300	3.36×10^{-4} (8)	0.2336
350	14.9×10^{-4} (8)	0.0133
300	6.72×10^{-4} (16)	0.6297
350	7.46×10^{-4} (4)	0.0072

As shown in Table 6.2, 300 nm possessed a higher reactivity among the three wavelengths. This is due to the fact that BHA absorbs about 4 to 67 times more photons at 300 nm (molar absorptivity $\varepsilon = 1.142$, cm^{-1} mol^{-1} L) than that of 254 (0.317 cm^{-1} mol^{-1} L) and 350 nm (0.017 cm^{-1} mol^{-1} L,). The excited BHA can then be easily reacted with sulfate radicals, hence to the degradation process. However, the number of the lamps and therefore power consumption has to be doubled in order to increase a 27% removal rate by using sixteen 300 nm lamps than eight 254 nm lamps, as shown in Table 6.2. This may not be cost-effective

in practice, since most organic compounds have higher absorption at 254 nm, and faster direct-photolysis due to higher energy of 254 nm. As a result, 254 nm is chosen for further investigation in term of different BHA and $S_2O_8^{2-}$ concentrations at various pH levels. In addition, $S_2O_8^{2-}$ has higher absorbance at this wavelength as well (Fig. 6.16b) where $SO_4^{\bullet-}$ radicals can be produced more effectively and a better remediation process is guaranteed.

6.4.2 Effects of Initial BHA or $S_2O_8^{2-}$ Concentration (BHA:$S_2O_8^{2-}$ ratio)

At Fig. 6.17, different $S_2O_8^{2-}$ dosages (0 – 10 mM) were firstly tested under pH 3 with 254 nm irradiation, generally higher the dosage higher the BHA decay efficiency. On the other hand, the higher the initial BHA concentration could reduce the decay efficiency as shown in one typical example using the 2 mM $S_2O_8^{2-}$ dosage at pH 3 (Fig. 6.18). The slow down of reaction is likely due to the deficiency of the oxidants at higher [BHA], as more BHA or intermediates being formed during the photodegradation process, the demand of the oxidant will be increased, so the oxidant could be quickly depleted.

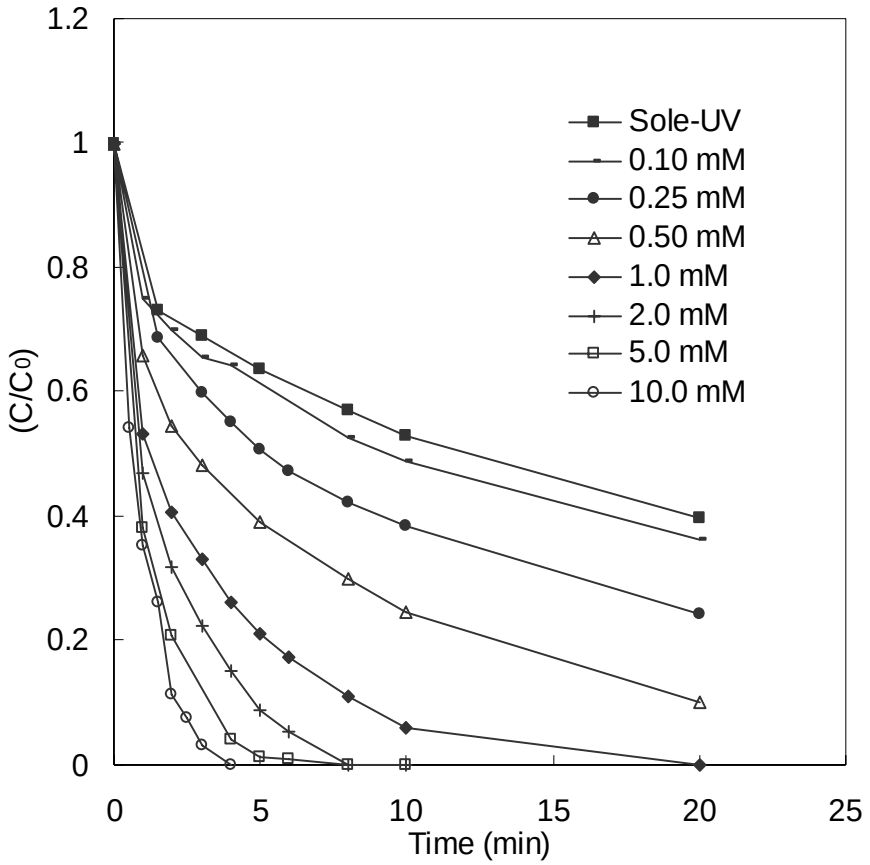

Fig. 6.17: Photodegradation of 0.1 mM BHA with different [$S_2O_8^{2-}$] doses (mM) at pH 3 under 254 nm wavelength.

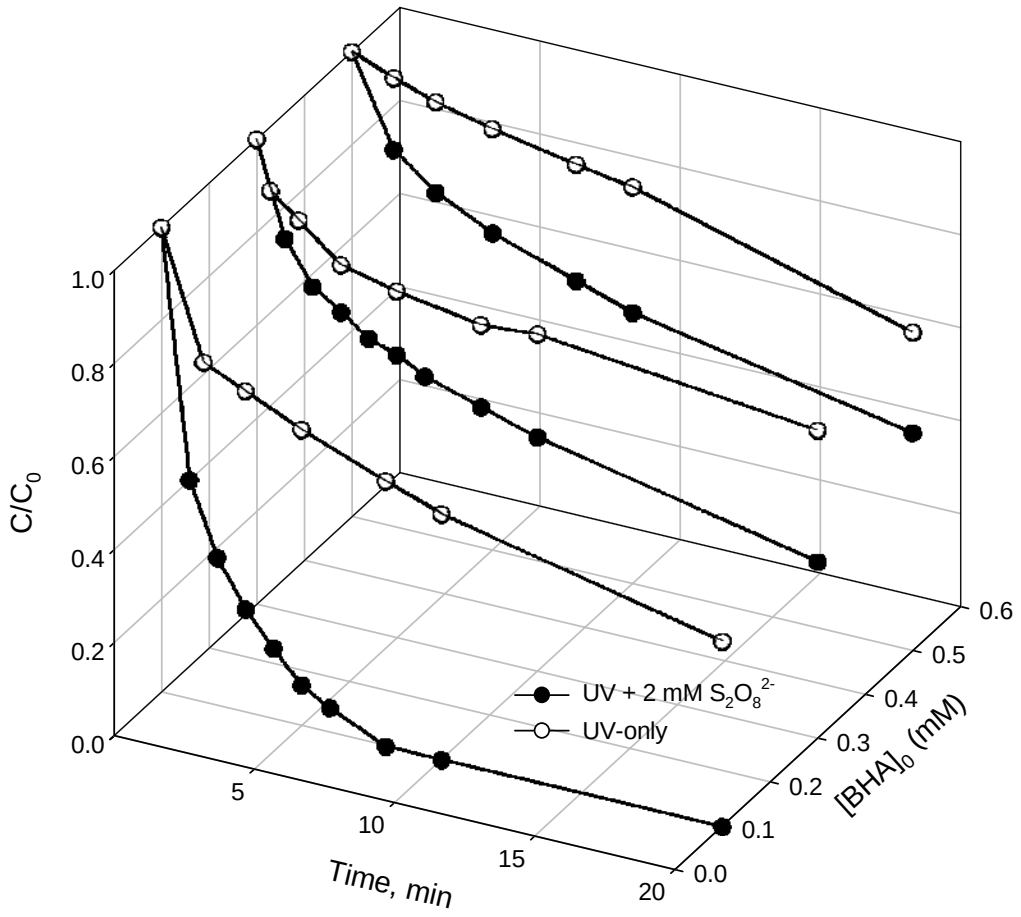

Fig. 6.18: Photodegradation of different initial [BHA] at 0.1 to 0.5 mM with and without addition of 2 mM $K_2S_2O_8$ at pH 3 (UV: 254 nm, 7.2×10^{-4} $EinsteinL^{-1}min^{-1}$).

Therefore, at the highest [BHA] (0.5 mM), completion of BHA decay is not observed (86% removal, data not shown) and the degradation pattern slowed down very quickly (after 10 min reaction) as shown in Fig. 6.18. Interestingly, similar pattern were also observed for sole-UV process, so no matter with or

without the addition of $S_2O_8^{2-}$, the higher the BHA concentration always lower the removal efficiency. This can be explained by the free radical reactions between BHA, intermediates and sulphate radical ($SO_4^{-\bullet}$) when UV is involved. Eqns. 6.28 and 6.29 indicate the prevailing decay mechanism leading to the generation of two $SO_4^{-\bullet}$ radicals from $S_2O_8^{2-}$ via photolysis (House, 1962) and the subsequent decay of BHA. The BHA will consume photon and $SO_4^{-\bullet}$ radicals to generate intermediates, which will also compete for the photon and oxidant (Eqn. 6.30) until mineralization. It is believable at high BHA concentration, excess BHA with its related photo-intermediates could greatly hinder the oxidation efficiency of $S_2O_8^{2-}$, by competition of not only radicals or oxidant but also the consumption of photon energy.

$$S_2O_8^{2-} + h\nu \rightarrow 2SO_4^{\bullet-} \quad (6.28)$$

$$SO_4^{\bullet-} + BHA \rightarrow BHA^{\bullet} \text{ or intermediates} \quad (6.29)$$

$$BHA \text{ or intermediates} + h\nu/SO_4^{\bullet-} \rightarrow \rightarrow CO_2 + H_2O \quad (6.30)$$

The detailed investigation of 0.1 mM BHA at different pH levels were studied previously where no linear relationship can be found, especially at the region when the $S_2O_8^{2-}$ is overdosed. Therefore, further investigations of different

initial BHA or $S_2O_8^{2-}$ concentration were carried out. Additionally as shown at Fig. 6.18, a tailing (or stagnant stage) of BHA degradation pattern was observed in UV/$S_2O_8^{2-}$ process, when $[BHA]_0$ was higher than 0.3 mM (using 2 mM [$S_2O_8^{2-}$]). The relationship between BHA and $S_2O_8^{2-}$ has been recognized to be influential to the overall reaction efficiency. Therefore, the BHA/$S_2O_8^{2-}$ ratio will be used as a parameter throughout the tests unless otherwise stated. The stoichiometric equation (Eqn 6.31) in a chemical reaction is proposed and it can be used to estimate the required minimum $S_2O_8^{2-}$ dosage for complete mineralization theoretically. For the case of 0.1 mM BHA, it requires at least 0.35 mM $S_2O_8^{2-}$ (ratio = 0.286:1) as shown in the following equation:

$$2C_{11}H_{16}O_2 \text{ (i.e. BHA)} + 7K_2S_2O_8 \rightarrow 22CO_2+16H_2O+14K + 14S \quad (6.31)$$

According to the equation, any ratio larger than 0.286 (or oxidant deficient) could lead to an incomplete mineralization of BHA in theory. Practically, the Eqn 6.31 is an over-simplified approach without considering the interferences from intermediates or sub-reactions of UV involved $S_2O_8^{2-}$ photolysis processes. It was found that when concentration of BHA was too high or $S_2O_8^{2-}$ was too low (BHA/$S_2O_8^{2-}$ ratio > 0.286) they do not exactly follow the pseudo first-order

decay. In stead, a two-stage reaction with a faster initial decay followed by a slower one was observed.

For such a particular condition, an atypical model with two stages of decay patterns was used to derive a better and predictable model (Fig. 6.19), where the first stage is the fast initial decay and the second stage is a stagnant phase. After applying this model (detail to be discussed later) in analyzing the data, it was found that the BHA/$S_2O_8^{2-}$ ratio of higher than 0.05 can fit into this model perfectly, where 1 mole of BHA required at least 20 mole of $S_2O_8^{2-}$ for complete degradation of BHA. This evidence supports the previous hypothesis that sub-reaction of photo-intermediates or oxidant itself also played a major role in this molar ratio calculation.

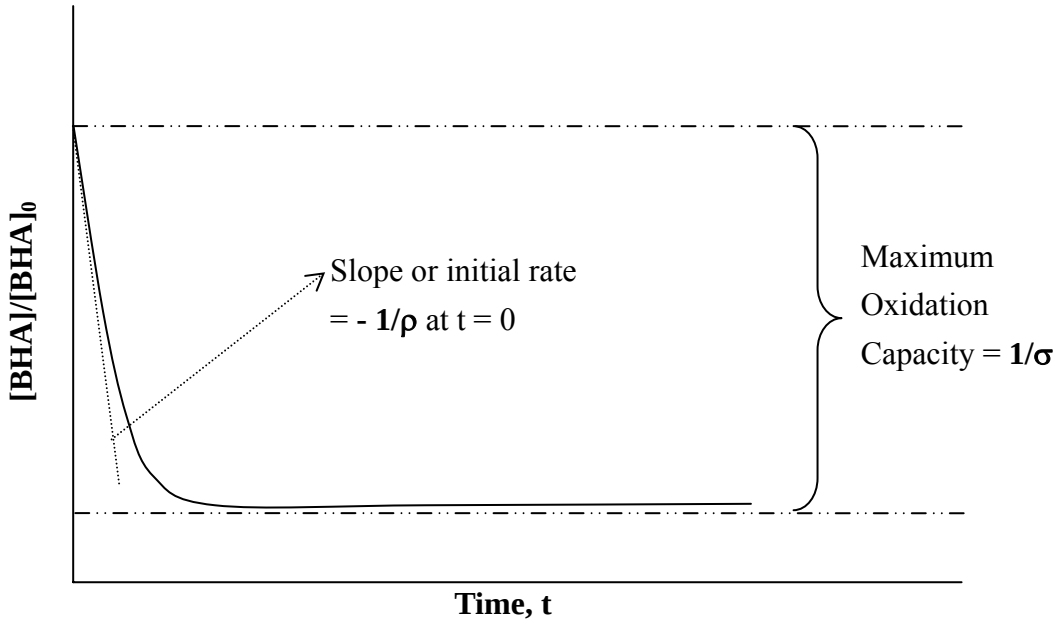

Fig. 6.19: The schematic diagram of the proposed model used to outline the reaction kinetics, with the two parameters: 1/ρ and 1/σ.

6.4.3 Development of Oxidant Deficient Reaction Model

At low concentration of $S_2O_8^{2-}$ or high BHA/$S_2O_8^{2-}$ ratio (> 0.05), fully degrade BHA is not observed due to insufficient radicals. The reaction does not follow the conventional pseudo first-order decay kinetics, because various indirect or parallel reactions are involved in the UV/$S_2O_8^{2-}$ reaction.

For instance, the decay of 0.3 mM $[BHA]_0$ at 2 mM $[S_2O_8^{2-}]$ (ratio = 0.15) in Fig. 6.18 showed a fast initial rate due to the abundant oxidant initially, and then it slowed down gradually due to the depletion of oxidants, and the rate eventually

levelled off after an extended reaction time. It was believed that the sole UV photolysis (or direct photolysis) was the only remaining active mechanism at this latter stage. As mentioned before, the direct photolysis cannot cause a significant BHA transform, so a constant [BHA] concentration is observed and approaching to the maximum oxidative capacity in the stagnant stage of the UV/$S_2O_8^{2-}$.The proposed oxidant deficient reaction model could be useful in simulating a wastewater treatment system when sizing a proper reactor for a pre-determined removal fraction or evaluating a potential shock-loading.

A two stages model incorporating two measurable parameters: a rapid 'initial decay rate' (the tangent line at time zero as denoted by a symbol of $-1/\rho$) and a retarded stagnant stage with a 'maximum oxidative capacity' (the removed BHA fraction denoted by a symbol of $1/\sigma$) which is no greater than 1 (Fig. 6.19) were used to reproduce the reaction kinetics of those oxidant deficient UV/$S_2O_8^{2-}$ processes. To explain how these two parameters are defined, a set of differentiation equations is shown below. The governing equation of this model is expressed in the following equation as reported previously by Chan and Chu (2003) in a UV irradiation process:

$$\frac{[BHA]}{[BHA]_0} = 1 - \frac{t}{\rho + \sigma t} \quad (6.32)$$

where $[BHA]_0$ (mM) is the initial concentration of BHA, and [BHA] is the corresponding concentration at the particular reaction time t (s). The ρ (s^{-1}) and σ (dimensionless) are two constants that correlate the initial decay kinetics and oxidation capacity. By differentiating Eq. (6.32), the term ρ can then be resolved as following when time approaches to zero:

$$\frac{d(\frac{[BHA]}{[BHA]_0})}{dt} = -\frac{1}{\rho t} \quad (6.33)$$

where 1/ρ is slope of initial removal rate of BHA as indicated at Fig. 6.19, higher the value faster the initial BHA decay rate. Furthermore, the physical meaning of σ term as the maximum oxidation capacity in UV/$S_2O_8^{2-}$ process can be revealed from Eq. (6.32), when t approaches infinite, the ρ becomes insignificant and can be ignored, which results in Eq. 6.34. The value of the Eqn 6.34 on its right-hand side is generally between 1 and 0, and the latter case indicates a total removal of

the BHA. Therefore, smaller the value of 1/σ, the higher the total removal efficiency could be achieved.

$$\frac{[\mathrm{BHA}]_{t\to\infty}}{[\mathrm{BHA}]_0} = 1 - \frac{1}{\sigma_{t\to\infty}} \tag{6.34}$$

To solve these two unique constants, Eq. (6.32) can be linearized by plotting $t/(1 - [BHA]/[BHA]_0)$ versus t, where straight lines with an intercept ρ and a slope σ could be obtained (data not shown). The corresponding regression results with very high correlation coefficients of r^2 ranging from 0.980 to 0.999 were achieved, which indicated that the BHA decay kinetics by UV/$S_2O_8^{2-}$ were well-predicted by the proposed model in Eq. (6.35).

$$\frac{t}{1-(\frac{[BHA]}{[BHA]_0})} = \rho + \sigma t \tag{6.35}$$

6.4.4 Analysis of ρ and 1/σ

Based on the Eqn 6.35, the tested data have been analyzed and the resulted ρ and 1/σ were plotted onto Fig. 6.20 and 6.21 in a 3-D format, respectively. Two layers of flat surfaces have been established, which summarise the correlations among [BHA], 1/[$S_2O_8^{2-}$], ρ and 1/σ. In Fig. 6.21, for example, the term 1/σ

indicates the maximum oxidative capacity at stagnant stage. Higher $1/\sigma$ value (i.e. lower the remaining fraction in the solution) can be achieved by either lowering the $[BHA]_0$ or increasing $[S_2O_8^{2-}]$ dosage (i.e. decrease the reciprocal of the oxidant or $1/[S_2O_8^{2-}]$).

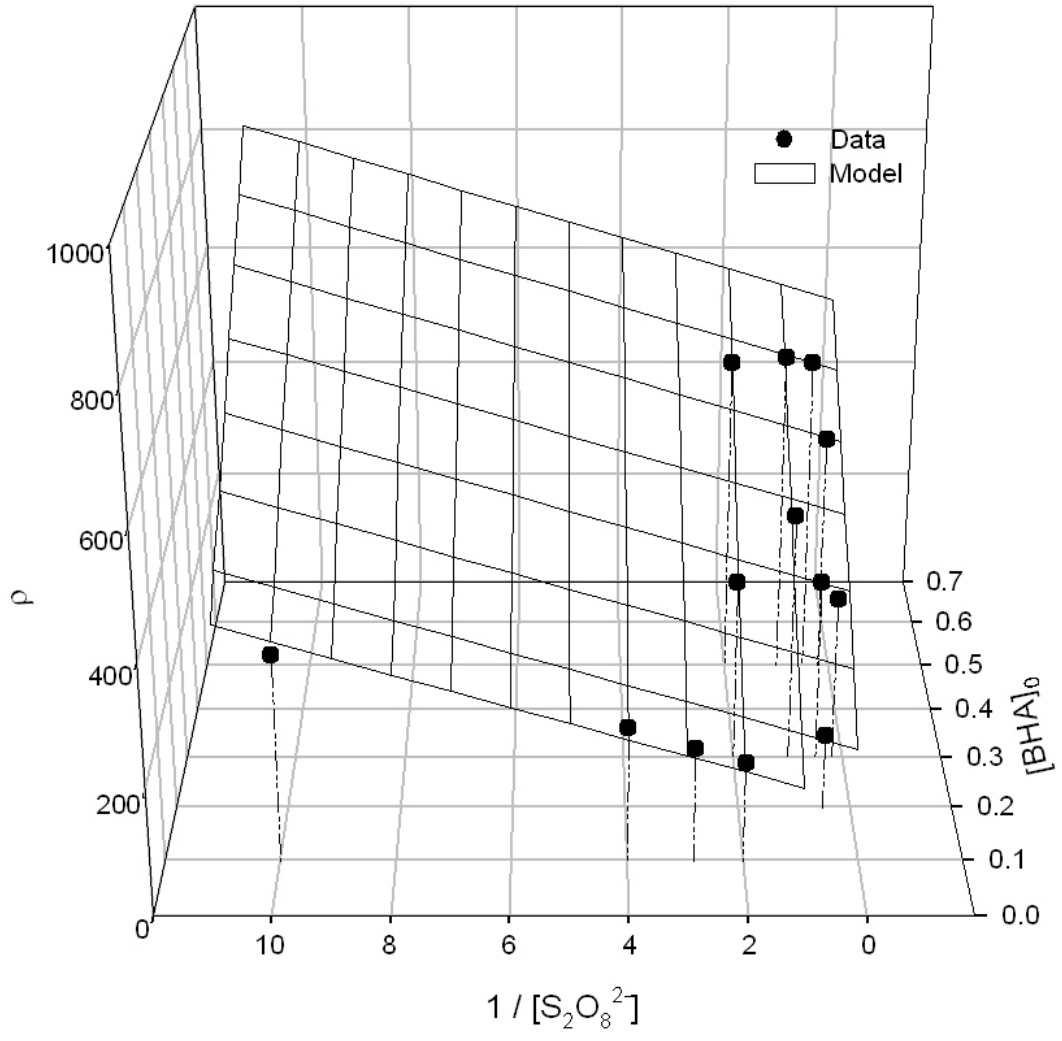

Fig. 6.20: Linear relationships of ρ (the reciprocal of the initial rate) versus the different initial concentration of BHA at pH 3.

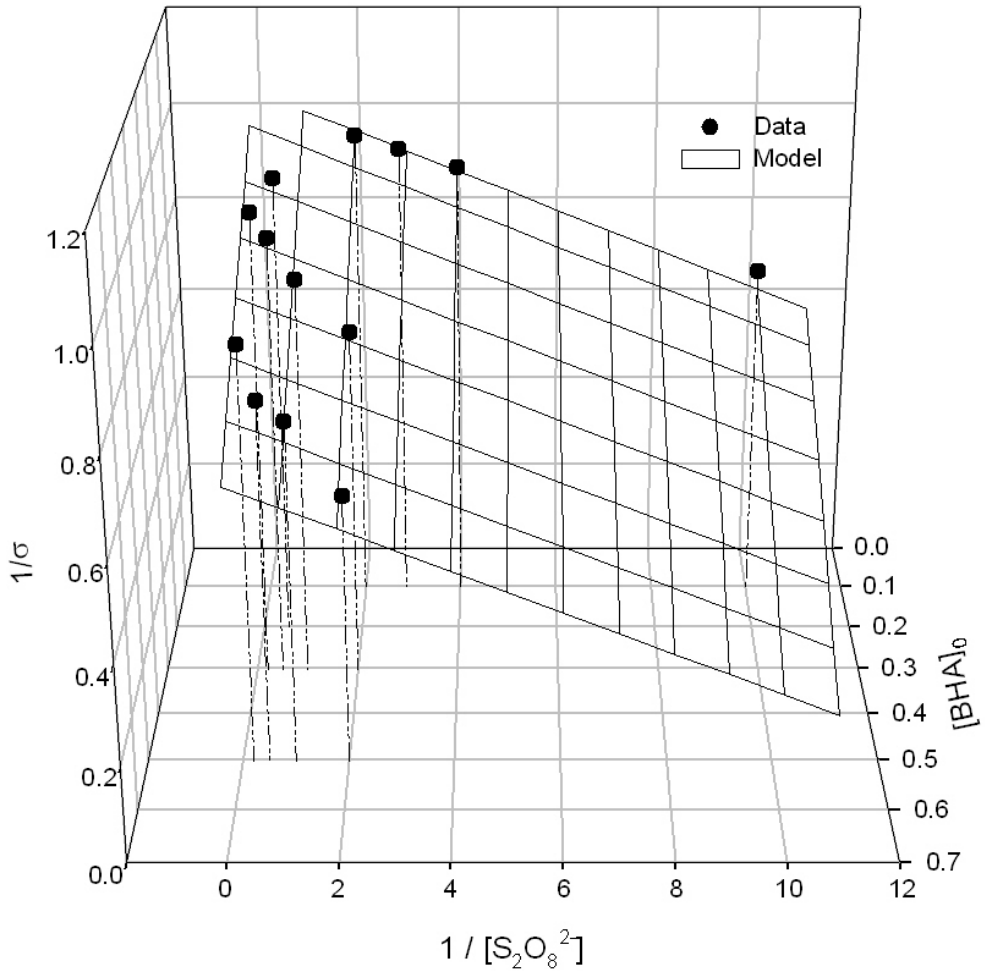

Fig. 6.21: Linear relationships of 1/σ versus the different initial concentration of BHA at pH 3.

The surfaces were then fitted into two equations (6.36 and 6.37) by incorporating individual [BHA] and $1/[S_2O_8^{2-}]$ into $[BHA]/[S_2O_8^{2-}]$ ratio with a good correlation as shown below:

$$\rho = 2618.5\ [BHA]/[S_2O_8^{2-}] - 118.5 \qquad (r^2 = 0.9924) \qquad (6.36)$$

$$1/\sigma = -1.4594\ [BHA]/[S_2O_8^{2-}] + 1.0802 \qquad (r^2 = 0.8439) \qquad (6.37)$$

It is interesting to notice when the 3-D surface is projected beyond the tested range, an extrapolated area can be found. For this particular region, the estimation of $1/\sigma$ is above unity, which is mathematically possible but physically meaningless. Practically, this suggests that the cases using excess supply of oxidant are overdosed and should be avoided in real applications for better cost-effectiveness. However, these cases could be easily described by the conventional pseudo first-order model as discussed below.

6.4.5 pH Effects in predicting reaction rate by sufficient oxidant

As indicated in the previous work , higher BHA decay efficiency was observed at basic condition, this was due to the complicated photolytic sub-reaction of $S_2O_8^{2-}$ and $OH^{\bullet}$, induced by addition of hydroxide ion into the system. Higher the pH the more quickly the dissociation of $S_2O_8^{2-}$ (via photolysis) to the $SO_4^{\bullet-}$ radical is expected. Through the reaction with OH^-, $SO_4^{\bullet-}$ radical will further converted to $OH^{\bullet}$ (Chawla and Fewenden, 1975; McCallum et al., 2000).

$$SO_4^{\bullet-} + OH^- \rightarrow OH^{\bullet} + SO_4^{2-} \qquad (6.38)$$

The application of 10-fold excess amount of [$S_2O_8^{2-}$] at 1.0 mM to treat 0.1 mM [BHA] at pH 11 could completely remove the latter within 2 min (50% removal at 45 s) under 254 nm monochromatic irradiation. In addition, at acidic condition, acidic inorganic product such as bisulfate (HSO_4^-), protons, monopersulfuric acid (H_2SO_5) and sulfuric acid (H_2SO_4) were produced via decomposition of $S_2O_8^{2-}$ and $SO_4^{\bullet-}$ (McCallum et al., 2000; and Lobree and Bell, 2001), which would hinder or interfere the $SO_4^{\bullet-}$ radical production. At alkaline pH, these interferences are insignificant.

Because the reaction rate constant is highly dependent on the initial pH levels. A series of experiment using initial BHA concentration of 0.1 mM at different excess supply of $S_2O_8^{2-}$ dosages were conducted accordingly.

A model is then derived for those critical concentration and both the reaction rate constant (k) and [BHA/$S_2O_8^{2-}$] ratio are correlated under tested pH levels as shown in Fig. 6.22a. In general, as the initial pH level increased, the slope of

each correlation line in Fig. 6.22a increased as well, indicating a positive rate acceleration along the increment of initial pH level. To illustrate the detailed correlation of slopes and intercepts of the three straight lines (of Fig. 6.22a), these information are summarized in Fig. 6.22b. It was found that the resulted slope and intercept constant descending and ascending as the initial pH increase, respectively. By incorporating the two correlations (from Fig. 6.22b) into the linear formula in Fig. 6.22a, the relationship of reaction rate at various initial pH level and BHA/$S_2O_8^{2-}$ ratio become predictable and can be linearized in Eq. (6.39) as following:

$$\text{Ln } k = (-0.0117\ pH_0 - 0.4832)\ \text{Ln}\ (BHA/S_2O_8^{2-}) + (0.1536\ pH_0 - 2.6842) \qquad (6.39)$$

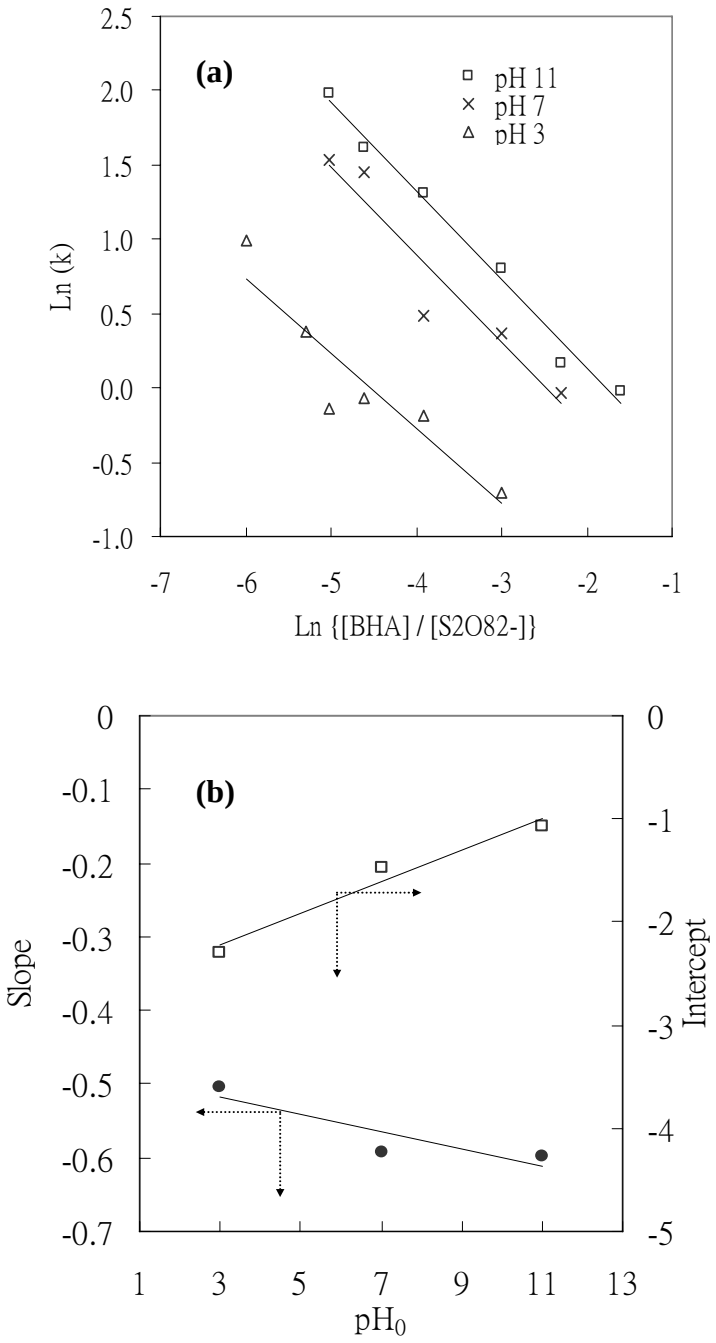

Fig. 6.22: Modeling of 0.1 mM BHA degradation with sufficient oxidant ($S_2O_8^{2-}$) at three different pH levels: (a) linearlized their pseudo-first-order decay (k) and [BHA/$S_2O_8^{2-}$] ratio; and (b) slope and intercept of Fig. 6.23a.

Experimental data have been incorporated into the equation, and the resulted curves fit well to the data (Fig. 6.23), this has validated the Eq. (6.39) in describing the UV/$S_2O_8^{2-}$ process under the case of sufficient oxidant.

Furthermore, as shown previously at pH 3, the effective [$S_2O_8^{2-}$] dosage which follows a pseudo first-order decay of BHA is observed at 2.0 mM, with its corresponding ratio of BHA/$S_2O_8^{2-}$ at 0.05. For the other pH levels, i.e. 7 and 11, the effective [$S_2O_8^{2-}$] dosage decreases, as the pH increases and BHA/$S_2O_8^{2-}$ ratio decreases (Table 6.3). This indicates that the higher the pH, lesser the [$S_2O_8^{2-}$] dosage is required to photodegrade BHA. The trend of the effective working range in application of BHA/$S_2O_8^{2-}$ ratio is found and the test results are summarized in Table 6.3. The linear relationship can then be found at Fig. 6.24, where the shadow region indicates the application of insufficient dosage modelling while those above clear region are for those reactions follow pseudo first-order decay kinetics.

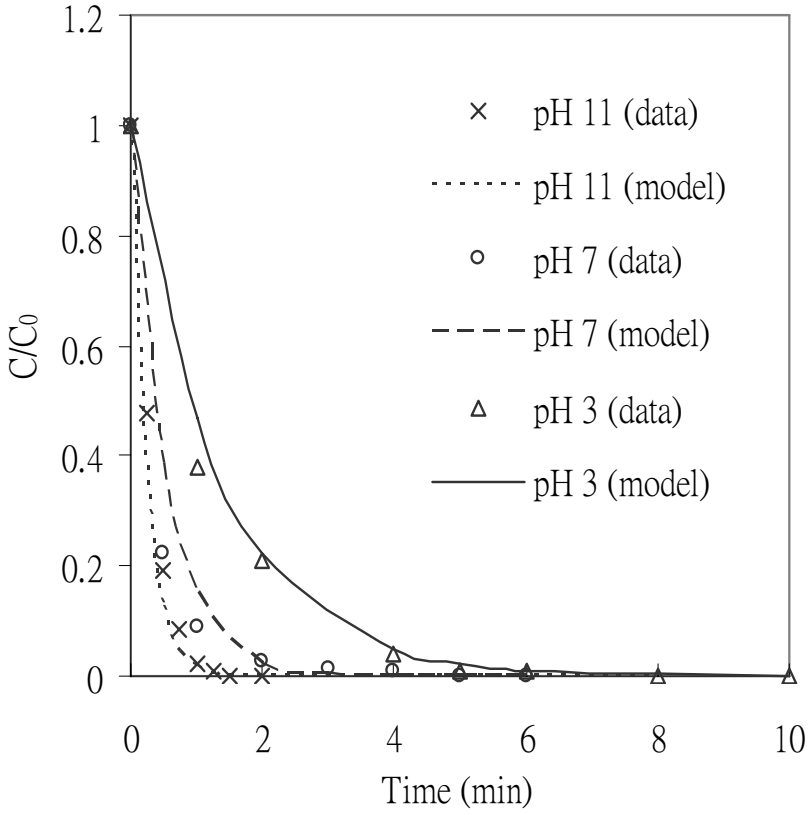

Fig. 6.23: Modeling of 0.1 mM BHA with 2 mM [$S_2O_8^{2-}$] at different pH levels.

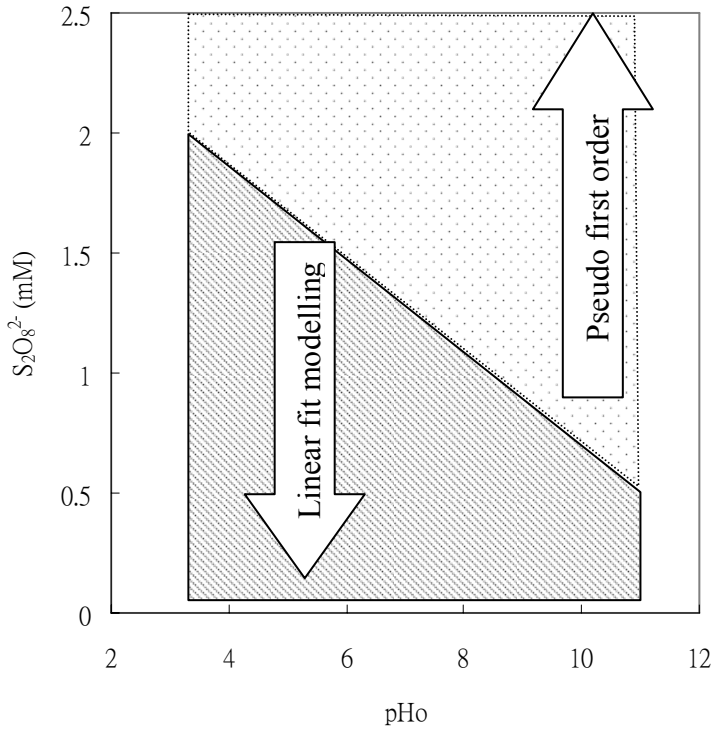

Fig. 6.24: Effective BHA/$S_2O_8^{2-}$ ratio at different initial pH levels

Table 6.3: Effective BHA/$S_2O_8^{2-}$ ratio and its corresponding $S_2O_8^{2-}$ dosage at 0.1 mM BHA

pH	**BHA/$S_2O_8^{2-}$ ratio**	**Effective $S_2O_8^{2-}$ dosage**
3	0.05	2.0
7	0.10	1.0
11	0.20	0.5

6.5 Summary

By ozonation process BHA can be degraded easily through an extra precipitation pathway, and the formation of quinonic compounds (TBQ and BHA-OQ) was identified. Different reaction pathways are found to be pH-dependent, and their reaction mechanisms were therefore proposed via the experimental observations (i.e. LC/MS). Intermediate compounds resulting from dimerization and precipitation pathways (mostly mutagens) are formed at the end of the ozonation process. In real applications, these orange-coloured solids could be easily removed by solid-liquid separation processes in wastewater treatment. Last but not least, among these three treatment processes, UV/O_3 process has exhibited the best overall performance. It shown advantages not only to the elimination of these separable solids, but also capable of achieving 90% mineralization at the end of the process (180 min).

While in the UV/$S_2O_8^{2-}$ process, two additional reaction pathways at pH 3 involving three unique intermediates were found, which supports the hypothesis of a slower BHA decay by weaker oxidants or radicals under acidic conditions. The use of UV/$S_2O_8^{2-}$ at pH 7 is recommended for wastewater treatment where a complete and faster mineralization was observed to occur within 40 min due to

successive simultaneous degradation of intermediate compounds. It is believable that UV/$S_2O_8^{2-}$ is applicable to the existing drinking water or wastewater treatment plants. With the advantages of the high reactivity of the UV/$S_2O_8^{2-}$ process and the high solubility of peroxydisulfate, it is practically possible to dose the chemical solution at the upstream of wastewater to remove recalcitrant organic compounds effectively.

Finally the modelling of UV/$S_2O_8^{2-}$ process, at different UV wavelengths, $S_2O_8^{2-}$ photolysis can behave differently. With the same number of lamps provided in the irradiation process, 254 nm exhibited the best efficiency of removing BHA for both direct photolysis and UV/$S_2O_8^{2-}$ process. However, with the similar light intensity, 300 nm possesses the best instead, as BHA have the highest absorption at this particular wavelength. Due to economic aspects, doubling of lamp usage of 300 nm is not recommended, therefore detailed modelling of $S_2O_8^{2-}$ process at 254 nm were suggested and investigated. The BHA degradation by UV photolysis at 254 nm wavelength using various $S_2O_8^{2-}$ dosages was described with two different models depending on the ratio of BHA and $S_2O_8^{2-}$. The excess supply of the oxidant (lower BHA/$S_2O_8^{2-}$ ratio) results in a conventional pseudo first-order decay and the process is strongly dependent on the initial pH levels.

However, in the deficiency of oxidant (higher BHA/$S_2O_8^{2-}$ ratio), two-stage reaction kinetics is identified and an atypical model using initial decay rate and maximum oxidative capacity can be used to describe the process successfully.

CHAPTER 7 UV/Ag^+/$S_2O_8^{2-}$ PROCESS

7.1 Introduction

In this chapter, the investigation of UV/Ag^+, Ag^+/$S_2O_8^{2-}$, UV only, UV/$S_2O_8^{2-}$ and UV/Ag^+/$S_2O_8^{2-}$ processes are conducted, where preliminary screening tests of selection of UV wavelength and silver ion sources are also investigated. The optimization of the UV/Ag^+/$S_2O_8^{2-}$ process will be studied by varying the dosage of silver ion. The removal and mineralization of BHA using UV/$S_2O_8^{2-}$ process with the assist of silver in both homogeneous and heterogeneous systems are investigated. Three different silver sources including two silver salts (Ag_2SO_4 and $AgNO_3$) and silver oxide (Ag_2O) are being compared.

7.2 UV/Ag^+/$S_2O_8^{2-}$ process

7.2.1 Reaction kinetics of various treatment processes

Treatment processes involving different combinations of UV, Ag_2SO_4, and/or $S_2O_8^{2-}$ have shown varied performances in degrading 0.1 mM BHA at the following ascending reaction rate: UV/Ag_2SO_4, Ag_2SO_4/$S_2O_8^{2-}$, UV only, UV/Ag_2SO_4/$S_2O_8^{2-}$, and UV/$S_2O_8^{2-}$ (Fig. 7.1). The two UV treatment processes (UV/Ag_2SO_4/$S_2O_8^{2-}$ and UV/$S_2O_8^{2-}$) also shown the advantage of advanced

oxidation processes, where 100% removal of 0.1 mM BHA can be easily achieved within 10 min of irradiation time, while the others could only possess 30-50 % removal efficiency. In addition, Ag_2SO_4 or $S_2O_8^{2-}$ alone in the dark (no UV) does not induce any transformation of BHA (data not shown).

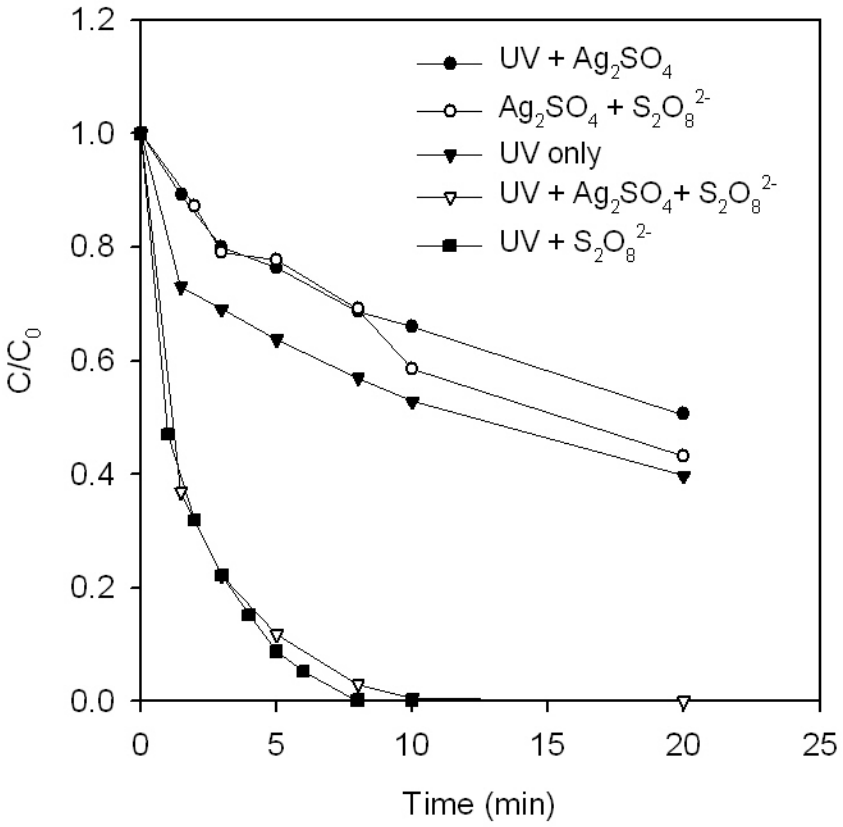

Fig. 7.1: Comparison of different processes: UV, UV/Ag_2SO_4, UV/$S_2O_8^{2-}$, UV/Ag_2SO_4/$S_2O_8^{2-}$, and Ag_2SO_4/$S_2O_8^{2-}$ (UV: 254 nm, 1.5×10^{-5} Einstein l^{-1} s^{-1}; 1 mM Ag_2SO_4; and 2 mM $S_2O_8^{2-}$)

Those processes involved peroxydisulfate with or without the aid of UV irradiation and/or silver-catalyst are basically due to the generation of sulphate radical ($SO_4^{\bullet-}$) as indicated in Eqns. 7.1 to 7.3. According to the previous section,

an extensive investigation of UV/$S_2O_8^{2-}$ process at various pH condition has been conducted, it explains clearly how the sulphate radical could effectively oxidize BHA via production of phenols or dimers as intermediates, and proceeds to the mineralization.

$$S_2O_8^{2-} + \text{photons} \rightarrow 2SO_4^{\bullet-} \quad (7.1)$$

$$Ag^{+} + S_2O_8^{2-} \rightarrow Ag^{2+} + SO_4^{\bullet-} + SO_4^{2-} \quad (7.2)$$

$$Ag^{+} + S_2O_8^{2-} \rightarrow Ag^{II}(SO_4^{\bullet})^{+} + SO_4^{2-} \quad (7.3)$$

However, one weakness of UV/$S_2O_8^{2-}$ is that, at acidic pH condition, BHA cannot be effectively mineralized (even though the decay of BHA itself is fast), therefore metal-mediated oxidation processes were investigated in this study as alternatives if mineralization of BHA and its derivatives is a critical design target. The selection of transition metal is based on the previous studies (Anipsitakis and Dionysiou, 2004a and 2004b), which show that the silver ion, Ag(I), is the best metal activator for the decomposition of $S_2O_8^{2-}$ (in turn to generate the robust oxidizing radicals, $SO_4^{\bullet-}$) among the other transition metals such as cobalt, iron (II or II), etc. In our BHA degradation study at $S_2O_8^{2-}$ and Ag^{+} concentration at 2.0 mM each, $Ag_2SO_4/S_2O_8^{2-}$ process could remove 89% of 0.1 mM BHA in 120

min under dark condition (data not shown). This catalytic reaction has justified its effectiveness in removing BHA. However, as shown in Fig. 7.1, its reactivity was slightly slower than that of UV direct photolysis reaction. The $Ag_2SO_4/S_2O_8^{2-}$ process will also generates yellow disperse precipitation throughout the reaction, where additional filtration or solid/liquid separation systems might be needed for polishing the effluent. In addition, silver cannot be regenerated in the $Ag_2SO_4/S_2O_8^{2-}$ process (Anipsitakis and Dionysiou, 2004b). Therefore the $Ag_2SO_4/S_2O_8^{2-}$ process is not recommended to be used in wastewater treatment, while more attention should be focused on the UV irradiation enhanced treatment processes with various trials for optimization as discussed below.

7.2.2 Selection of Silver Salts

Until now, only limited studies concerning about silver-mediated peroxydisulfate oxidation at 254 nm UV irradiation have been carried out (Anipsitakis and Dionysiou, 2004b). In this study, the removal of BHA by the $UV/Ag^+/S_2O_8^{2-}$ process is extensively investigated. The $UV/Ag^+/S_2O_8^{2-}$ process could eliminate the colour problem that has been found in $Ag_2SO_4/S_2O_8^{2-}$ process as mentioned previously. In the former process, soluble yellowish intermediates were found

during the irradiation process and the colour will be faded out before the end of the experiment. However, at shown in Fig. 7.1, the addition of Ag_2SO_4 in the UV/$S_2O_8^{2-}$ process did not show noticeable enhancement over the UV/$S_2O_8^{2-}$ system. This might due to the "counter ion effect" induced by silver salts. According to Anipsitakis et. al. (2006) in a homologus catalytic study of Co/$KHSO_5$ system, the counter anion sulphate exhibited a slightly poorer performance than nitrate in degrading phenolic compounds. Therefore a test on investigating the different performance of two silver salts was conducted, where a 7 % improvement of BHA degradation rate by using nitrate salt instead of sulfate was identified after a 5 min irradiation (Fig. 7.2).

It is believed that the selection of Ag^+ counter anion is crucial in determining the BHA removal rate. According to Anipsitakis and Dionysiou (2004a), the behaviour of the dissolved aqueous metals is greatly affected by the charge, the ionic radius, and the electronic structure. The reaction rates of BHA removal by two different salts were found in the following ascending order: UV/Ag_2SO_4/$S_2O_8^{2-}$, UV/$S_2O_8^{2-}$, and UV/$AgNO_3$/$S_2O_8^{2-}$. Therefore, $AgNO_3$ is chosen for detail study in the following experiments, as it exhibits an add-on effect to the UV/$S_2O_8^{2-}$ process.

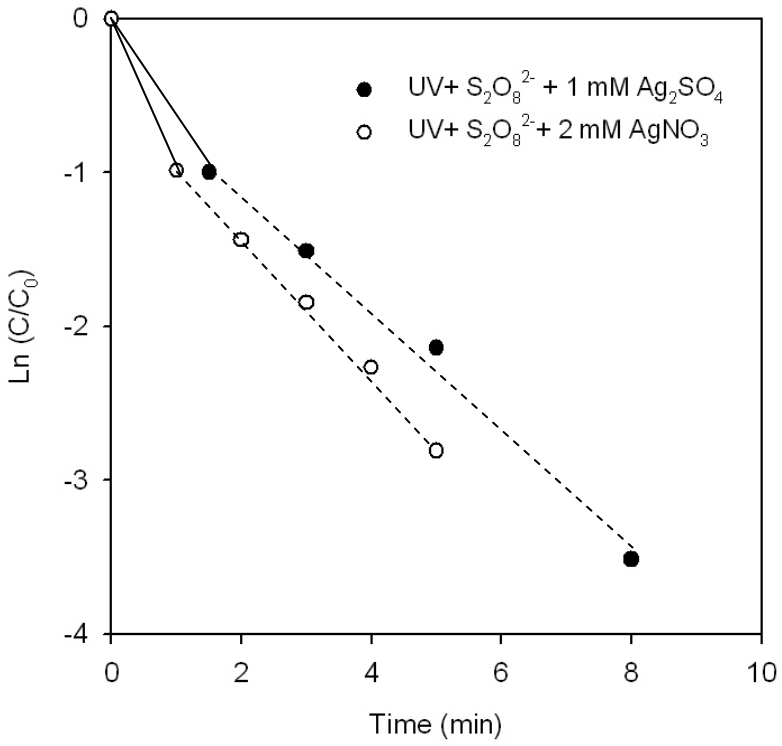

Fig. 7.2: Two separated stages of pseudo first order decays of BHA (solid line: 1st, and dotted line: 2nd) by different silver salts in UV/Ag^+/$S_2O_8^{2-}$. (1 mM Ag_2SO_4 and 2 mM $AgNO_3$, and 2 mM $S_2O_8^{2-}$ at UV 254 nm, pH 3)

7.2.3 Degradation of BHA at near UV

In order to explore the possibility of degrading BHA with lower irradiation energy, near UV wavelength at 350 nm was tried as an alternative irradiation source. Four separated tests were conducted and their reactivity was listed in the ascending order as follow: UV, UV/$S_2O_8^{2-}$, UV/Ag^+, and UV/Ag^+/$S_2O_8^{2-}$. At this wavelength, almost no direct photolysis was observed (Fig. 7.3). This is because

the BHA has extremely low absorbance (close to zero) at this wavelength, which makes the excitation of the BHA by absorbing 350 nm UV inefficiently. Under these circumstance, the involvement of direct photolysis is eliminated, and the degradation of BHA by UV/Ag^{+}/$S_2O_8^{2-}$ process at 350 nm is mainly due to the activation and generation of sulphate radical by silver ion and peroxydisulfate. In Fig. 7.3, UV/Ag^{+}/$S_2O_8^{2-}$ process has shown the best efficiency at this near UV wavelength, where complete degradation of BHA was found at 30 min of reaction time. However, the weaker irradiation energy of 350 nm (comparing to 254 nm) does not demonstrate useful mineralization. Therefore, this approach is suitable for the BHA decay only, it is not recommended for ultimate remediation (or mineralization) purpose.

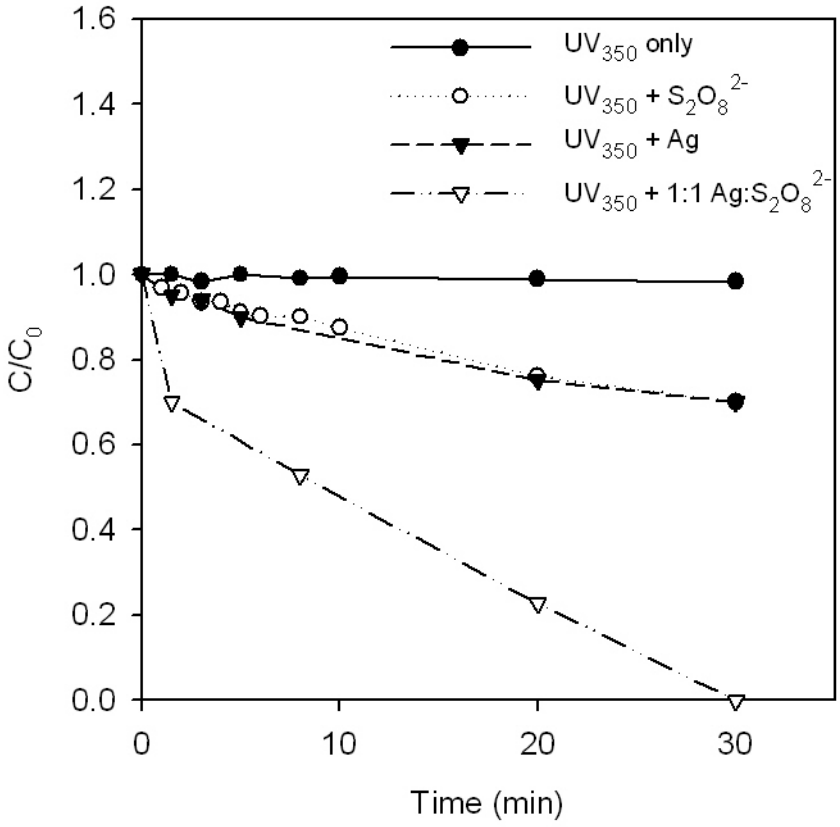

Fig. 7.3: Different treatment processes at 350 nm wavelength in degrading 0.1 mM BHA (2 mM $AgNO_3$ and $S_2O_8^{2-}$).

7.2.4 Dosage Effect of $AgNO_3$

In order to optimize the proposed process, the Ag^+ to $S_2O_8^{2-}$ ratio (denoted as A:S ratio thereafter) in UV/Ag^+/$S_2O_8^{2-}$ process was extensively investigated, where a series dosages of $AgNO_3$ has been tested at a fixed $S_2O_8^{2-}$ concentration of 2 mM. It was interesting to find that at very low [Ag^+] (i.e low A:S ratio), the BHA decay reaction would be retarded, as shown in Fig. 7.4, where a 0.05:1 of A:S ratio exhibited a slower reaction rate compared to the case of 0:1 (i.e. UV/$S_2O_8^{2-}$

only, no Ag^+). In those tests, for those A:S ratio ranging from 0.05:1 to 0.50:1 also exhibited an retardation of degradation rate but in a lesser extent (data not shown). In general, higher the ratio, lower the retardation. Similar observation was also reported by Anipsitakis and Dionysiou (2004b).

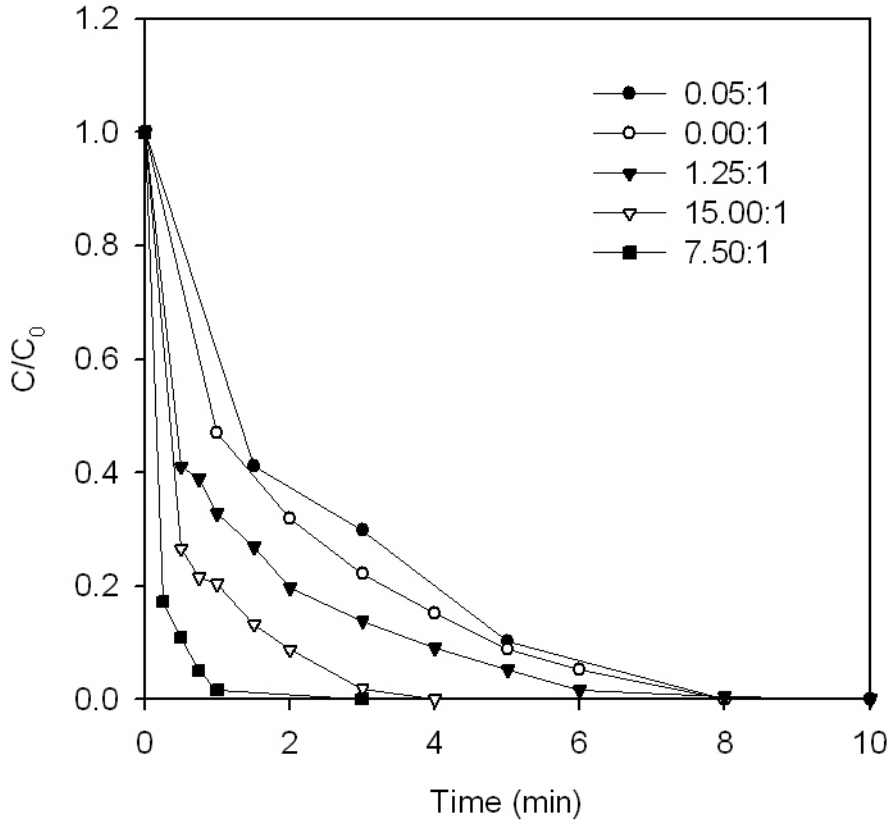

Fig. 7.4: Degradation UV/$AgNO_3$/$S_2O_8^{2-}$ process at different $AgNO_3$ concentration (2 mM $S_2O_8^{2-}$; and 0-30 mM $AgNO_3$)

The retardation at low A:S ratios, is likely due to the consumption of photons (UV) by Ag^+, which gives the formation of dark precipitation, while the UV

intensity available for BHA decay is therefore reduced. Such an effect can be verified by the UV/Ag^+ and UV only processes as indicated in Fig. 7.1, where the latter is faster than the former only because of the involvement of Ag^+. However when the A:S ratio is higher than a critical level, the above reactions become insignificant, where sufficient Ag^+ is capable of activating $S_2O_8^{2-}$ to form useful radical ($SO_4^{\bullet-}$) as shown in Eq. (7.2). Therefore the retardation will only be observed as A:S ratio is below 0.5.

Increased dosage of [Ag^+] ion at higher A:S ratios will alternatively enhance the reaction rate compare to that of UV/$S_2O_8^{2-}$ process. For instance, a 7.5:1 ratio could completely decay the BHA within 3 min of irradiation and also more than 99.95% to mineralization within 20 min (Fig. 7.4 and Table 7.1). At higher A:S ratios, the decay rate constant was analyzed using pseudo first-order kinetics (Fig. 7.2), where two discrete stages are found: (i) a fast initial decay (solid line), and (ii) a slower second stage (dotted line). This pattern was found applicable to all experiment and the analytical result was summarized in Fig. 7.5, where a sub-graph beneath is the indication of whence the separation of the two stages. Interestingly, the higher the A:S ratio the earlier the occurrence of the 2nd stage.

Table 7.1: Mineralization efficiency (TOC, %) by various Ag^+ concentration at 2 mM $S_2O_8^{2-}$ in UV/$AgNO_3$/$S_2O_8^{2-}$ system

Ag^+ (mM)	TOC (%)		
	at 5 min	at 20 min	at 60 min
0.05:1	83.93	83.57	0.39
0.50:1	55.56	17.44	0.10
1.00:1	55.60	17.60	0.07
2.50:1	56.00	8.90	0.06
7.50:1	27.11	0.05	0.04
10.00:1	0.05	0.04	0.04

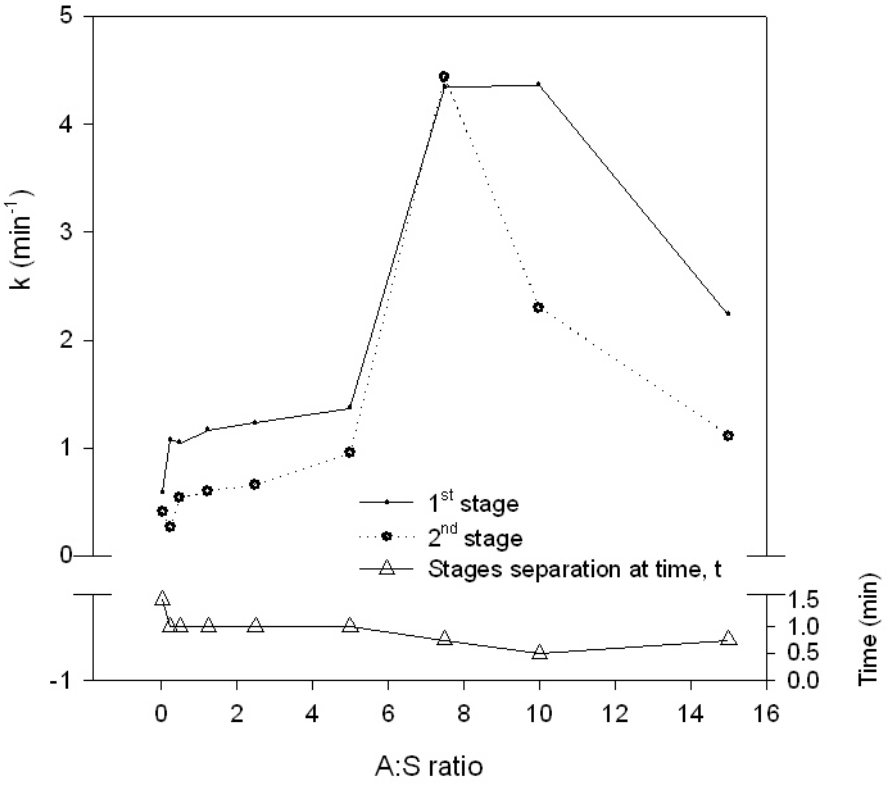

Fig. 7.5: Summary of pseudo first order kinetic rate constant (k) of UV/$AgNO_3$/$S_2O_8^{2-}$ process at 2 mM [$S_2O_8^{2-}$] in two different stages (1st and 2nd); and sub-graph underneath presents the time of two stages separated.

In Fig. 7.5, the initial decay rates (1st stage) are generally greater than the 2nd stage; this implies that $S_2O_8^{2-}$ can quickly be photolyzed into sulphate radical and hence to the removal of BHA at the very beginning of the reaction. However at the 2nd stage, for those A:S ratios less than 0.5, the kinetic rate constants are lower than that of 0:1 ratio (sole UV/$S_2O_8^{2-}$ process), which is due to the UV light attenuation by Ag^+ as mentioned before.

When the A:S ratio approaching its optimum at an A:S ratio of 7.5:1, the boundary to separate the two kinetics stages becomes vague, as shown in Fig. 7.4 and 7.5. This ratio is therefore recommended to be the optimal dosage, which gives an overall pseudo kinetic rate constant of 4.21 min^{-1} with a high correlation coefficient of R^2=0.94. Beyond this point at higher A:S ratios, the reduction of reactivity reappeared. The overdose effect is likely due to excessive Ag^+ ion in solution that can quench the $SO_4^{\bullet-}$ and/or react with $S_2O_8^{2-}$ directly to for the futile SO_4^{2-} anion as indicated in the Eqns. 7.4 to 7.8 (House, 1962; Minisci et al., 1983).

$$Ag^+ + SO_4^{\bullet-} \Leftrightarrow Ag^{2+} + SO_4^{2-} \qquad (7.4)$$

$$Ag^+ + SO_4^{\bullet-} \rightarrow Ag^{3+} + 2SO_4^{2-} \qquad (7.5)$$

$$Ag^{+} + S_2O_8^{2-} \rightarrow AgS_2O_8^{-} \quad \text{(slow)} \quad (7.6)$$

$$AgS_2O_8^{-} \rightarrow Ag^{3+} + 2SO_4^{2-} \quad (7.7)$$

$$2Ag^{+} + S_2O_8^{2-} \rightarrow 2Ag^{2+} + 2SO_4^{2-} \quad (7.8)$$

In addition, since the production of fine precipitation is found as well as the $AgNO_3$ dosage increased, the physical photon energy attenuation was observed as the formation of solid increased. According to our observation, higher the Ag^{+} concentration, earlier the dark precipitate will be formed. This results in an earlier appearance of the 2nd stages and a higher retardation of the corresponding 2nd stage as shown in Fig. 7.5. As the A:S ratio increased from 7.5:1 to 10:1, both cases have the same 1st stage kinetic rate constants, but the 2nd stage rate constant of the latter has been reduced half, while the separation time was shortened from 0.75 min to 0.5 min. This justifies that earlier presence of precipitation by increasing Ag^{+} dosage would induce the earilier occurrence of the retardation stage (i.e. 2nd stage).

Furthermore, as shown in Fig. 7.6, UV/Ag^{+}/$S_2O_8^{2-}$ process shown its advantage over sole UV/$S_2O_8^{2-}$ process regarding the mineralization efficiency. At an A:S ratio of 1:1, TOC could be effectively decreased to 5% with 30 min irradiation

time while only 40% was removed in the sole UV/$S_2O_8^{2-}$ process. This suggesting that UV/Ag^+/$S_2O_8^{2-}$ process is a promising treatment method for fast mineralization, and higher the silver dosage higher the mineralization performance (Table 7.1).

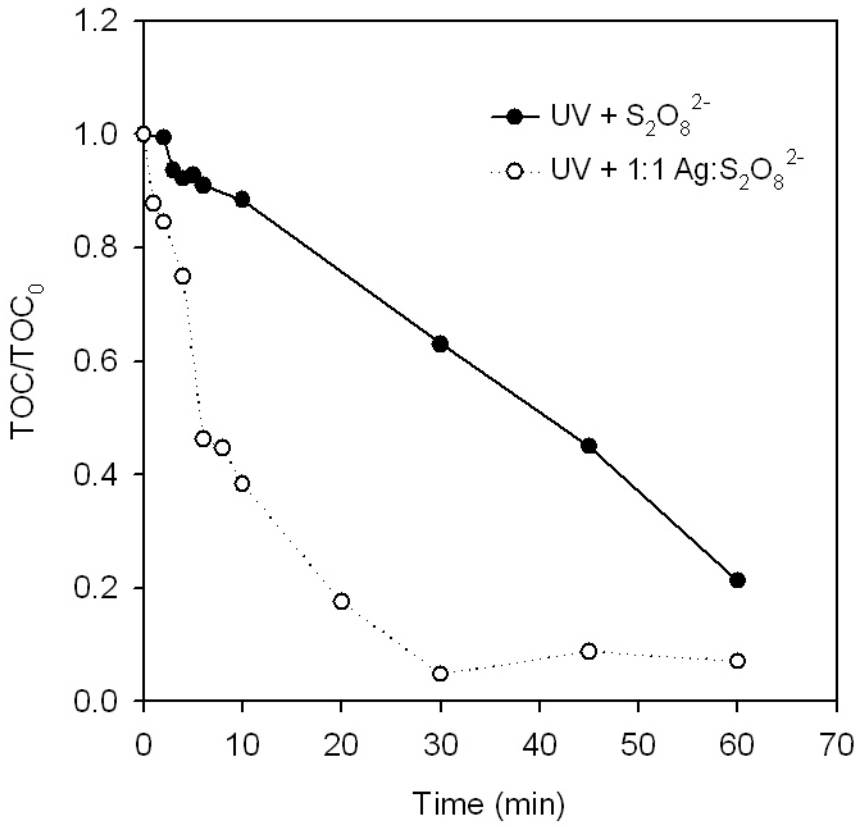

Fig. 7.6: TOC removal by UV/$S_2O_8^{2-}$ and UV/$AgNO_3$/$S_2O_8^{2-}$ systems (2 mM $AgNO_3$ and $S_2O_8^{2-}$).

7.2.5 Heterogeneous Oxidation using Silver-oxide

Since silver is a valuable metal, the reuse or recycle of silver salt is a reasonable strategy in application. Solid state silver oxide (Ag_2O) therefore was used as an alternative in this process to replace the Ag^+ in homogeneous systems. As mentioned previously of those control tests in homogeneous systems, the black precipitation appears immediately after the reaction is started, no matter in the UV/Ag^+ or $UV/Ag^+/S_2O_8^{2-}$ systems. Interestingly, in the heterogeneous $UV/Ag_2O/S_2O_8^{2-}$ process, no precipitation was formed in the aqueous phase during the reaction, and the solid phase silver oxide can be easily separated afterward. Therefore it is necessary to investigate the reactivity in BHA degradation and mineralization under this heterogeneous system in the presence of silver oxide.

As shown in Fig. 7.7, the reaction rate in degrading BHA did not show significant difference between the homogeneous (aqueous $AgNO_3$) and heterogeneous (solid phase of Ag_2O) at A:S ratio of 1:1 or 7.5:1; the stability of the Ag_2O implies an important advantage of recycling this catalyst after the irradiation process.

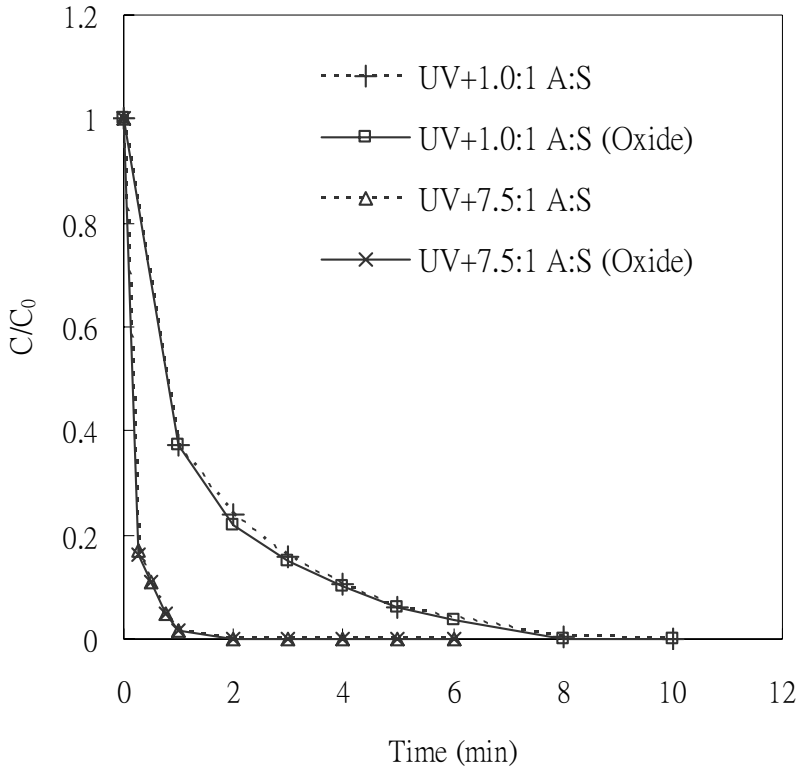

Fig. 7.7: Decay difference of using aqueous $AgNO_3$ and solid Ag_2O (oxide).

Interestingly, at the mineralization test (TOC removal) by heterogeneous system, the UV/Ag_2O/$S_2O_8^{2-}$ can significantly improve the mineralization to 91% at the irradiation time of 5 min comparing to that of 73% in homogeneous system as shown in Fig. 7.8. It is believed that the Ag_2O could directly activate the generation of sulphate radical at the catalyst surface, hence to its product of hydroxyl radical as indicated in Eqn. 7.9 (House, 1962; Laat and Le., 2005; Tsao and Wilmarth, 1959)

$$SO_4^{\bullet-} + H_2O \rightarrow HSO_4^- + OH^{\bullet} \qquad (7.9)$$

Because hydroxyl radicals are known to be a less selective oxidant than sulphate radical (Anipsitakis and Dionysiou, 2004a,). The hydroxyl radicals could oxidize the intermediates (of BHA) much quicker. In addition, there is no additional precipitate formed in the heterogeneous system, which minimize the continuous growing light attenuation effect that we observed in the homogeneous system.

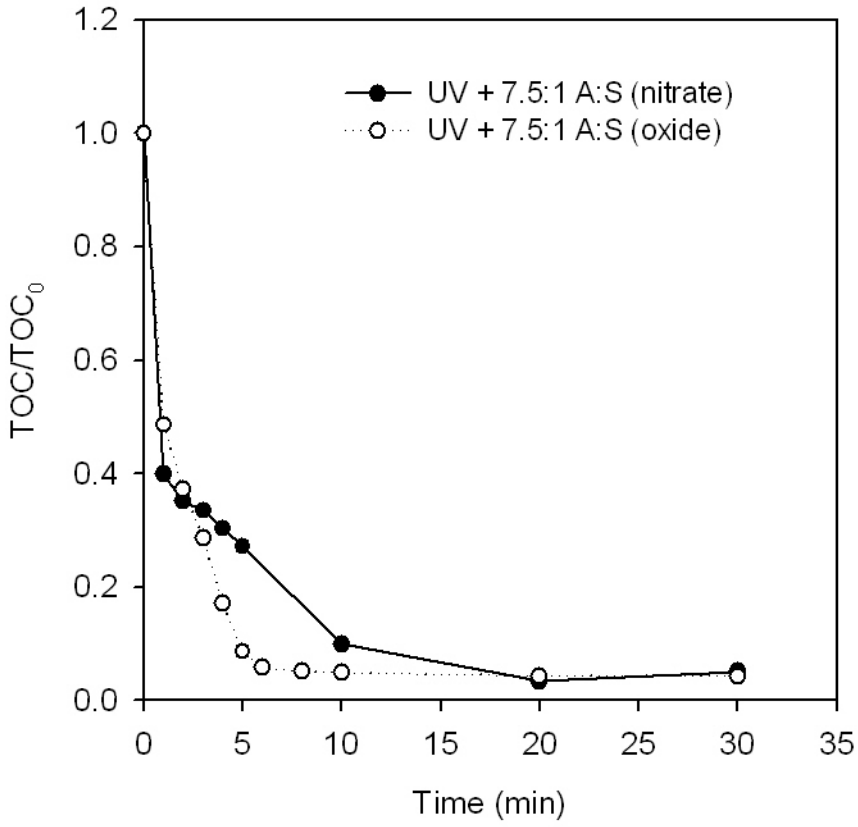

Fig. 7.8: Advantage of using silver oxide than silver nitrate in terms of mineralization efficiency (TOC/TOC_0).

7.3 Summary

The degradation rates of five different treatment processes in removing BHA were studied and compared in homogeneous modes including UV/Ag^+, $Ag^+/S_2O_8^{2-}$, UV only, UV/$Ag^+/S_2O_8^{2-}$, and UV/$S_2O_8^{2-}$. The UV/$Ag^+/S_2O_8^{2-}$ has an optimal condition with an A:S ratio of 7.5:1, where BHA could be degraded and mineralized in 3 and 20 min, respectively. According to other study (Anipsitakis and Dionysiou, 2004a), similar phenolic compound (i.e. dichlorophenol) can be removed by UV/$Ag^+/S_2O_8^{2-}$ process with in a much longer degradation time (30 min). The A:S ratio was found to be a critical factor in determining the BHA decay rate, too high and too low will retard the process as discussed in this study. Since silver is a valuable material, it is reasonable to recycle it in the system for future use, a heterogeneous system is introduced. A solid form of silver oxide (Ag_2O) was used by replacing Ag^+. The UV/$Ag^+/S_2O_8^{2-}$ and UV/$Ag_2O/S_2O_8^{2-}$ have similar performance in removing BHA, but the latter does show an advantage in removing TOC at a much faster rate likely due to the selectivity of $SO_4^{\bullet-}$ and $^{\bullet}OH$ to the intermediates. Additionally, simple solid/liquid separation can be applied to recover Ag_2O, which makes this process more attractive for real application. Furthermore, various treatment processes in degrading BHA are summarized in Table 7.2, their optimum conditions and their abilities of

mineralization are compared. UV/$S_2O_8^{2-}$ process is found to be the fastest treatment process in removing BHA at pH 11, and the easiest process to be handled in real application.

Table 7.2: Comparison of different treatment processes in degrading BHA and their mineralization efficiency

Treatment process	**Degradation rates of BHA (min^{-1})**		**Mineralization**	**Remarks**
	pH 3	**pH 11 (optimal)**		
UV	0.07	0.11	×	Direct Photolysis only
Ozone	0.59	0.52	×	O_3 is dangerous to handle, hazardous at low concentration
UV/O_3	0.59	0.75	Little	Generation of $^{\bullet}OH$ radicals
UV/$S_2O_8^{2-}$	0.49	2.23	✓	Generation of $SO_4^{\bullet-}$ & $^{\bullet}OH$ radicals
UV/Ag^+/$S_2O_8^{2-}$	1.17 (1st stage) 0.59 (2nd stage)	N/A	✓	Generation of $SO_4^{\bullet-}$ radicals

CHAPTER 8 CONCLUSION

The three selected Endocrine Discrupting Chemicals (*dibutylphthalate*, *carbofuran*, and *butylated hydroxyanisole*) were investigated by using different wastewater treatment processes, including continuous UV irradiation, ozonation, UV/ozonation, UV/peroxydisulfate, and UV/silver/peroxydisulfate. These lab-scale treatment data provide critical information for the engineer to design the reactor, not only limited to those crucial variables (i.e. wavelength, oxidant dosages, pH, reaction time, etc.), but also the interference of their intermediates and final products in the chemical reactions.

8.1 Dibutylphthalate

Dibutylphthalate (DBP) degradation by UV photolysis at 254 nm wavelength was conducted over a wide range of pH conditions. Different reaction pathways were thoroughly examined and a proposed mechanism was found to be consistent with experimental observations. In the pH range of 5-11 the initial DBP degradation rate increased with pH due to the domination of base-catalyzed hydrolysis. However, the greatest initial DBP degradation rate occurred at pH 3 because an additional reaction pathway involving the formation of benzoic acid.

Multi-degradation pathways have been proposed for acid-catalyzed hydrolytic photolysis in the pH range of 3 to 5, leading to the formation of intermediate products such as ketone-, aldehyde- or alcohol-forms of mono butyl phthalate. An end product of the acid-hydrolyzed photolysis, and particularly of base-catalyzed photolysis (pH ≥ 7), is phthalic acid (PA). In the latter case (pH ≥ 7) there was a complete conversion of DBP to PA over 60 min. The results suggest that the use of UV irradiation in water or industrial wastewater treatment will have a beneficial effect in reducing DBP concentrations.

The major decomposition mechanism of DBP is believed to involve the hydrolytic photolysis of the carbon in the α and/or β-position of the ester chain with the production of aromatic carboxylic derivatives. Additionally, multi-degradation pathways are proposed for acid-catalyzed hydrolytic photolysis (pH 3-5), which was found to be useful in explaining the photo-degradation of DBP under acidic conditions.

8.2 Carbofuran

Degradation of another type of EDC compound, CBF, was also investigated by using UV photolysis at 254 nm wavelength, ozonation and a combined UV/O_3 system, over a wide range of pH conditions. The UV/O_3 system showed a promising transformation treatment process of the pesticide and a liner ascending pH-dependent relationship has also been established. It is believed that CBF itself/or its toxic intermediates could be easily cleanup, when present in contaminated effluents. Using O_3 alone, CBF could also be degraded but in a lesser extent, and two stages of reactions have been found at acidic pH (≤ 7) and alkaline pH (> 7), where an accelerating stage of reactivity has been exhibited for the latter case.

8.3 Butylated hydroxyanisole

For the third EDC compound, BHA, an industrial pollutant, it can be degraded easily by using ozonation process through an extra precipitation pathway, with the formation of quinonic compounds (TBQ and BHA-OQ) was identified. Different reaction pathways are found to be pH-dependent, and their reaction mechanisms were therefore proposed via the experimental observations (i.e.

LC/MS). Intermediate compounds resulting from dimerization and precipitation pathways (mostly mutagens) are formed at the end of the ozonation process. In real applications, these orange-coloured solids could be easily removed by solid-liquid separation processes in industrial wastewater treatment. Last but not least, among these three treatment processes, UV/O_3 process has exhibited the best overall performance. It shown advantages not only to the elimination of these separable solids but also achieving 90% mineralization at the end of the treatment process (180 min).

However, in studying a newly explored area of green chemical application (peroxydisulfate), the $UV/S_2O_8^{2-}$ process is believed to be the best treatment processes among, no matter in the aspects of easy application, its harmlessness of the chemical itself or its final product sulphate ion, but also the flexibility of dosage application (either continuous or discrete dosage). Unlike ozonation, the ozone itself have to be handle with great care, and the cost of electricity and provision of oxygen (the optimal condition in producing pure ozone and hydroxyl radical) will be the greatest drawback from the engineering point of view.

Wastewater at neutral pH would be recommended to use UV/$S_2O_8^{2-}$ process as the best remediation process, according to this study a complete and faster mineralization was observed to occur within 40 min due to successive simultaneous degradation of intermediate compounds. On the other hand, two additional reaction pathways at pH 3 involving three unique intermediates were found, which supports the hypothesis of a slower BHA decay by weaker oxidants or radicals under acidic conditions. It is believed that UV/$S_2O_8^{2-}$ is applicable to the existing drinking water or industrial wastewater treatment plants. With the advantages of the high reactivity of UV/$S_2O_8^{2-}$ process and the high solubility of peroxydisulfate, it is practically possible to dose the chemical solution at the upstream of wastewater to remove recalcitrant organic compounds effectively.

Additionally, the BHA degradation by UV photolysis at 254 nm wavelength using various $S_2O_8^{2-}$ dosages was described with two different models depending on the ratio of BHA and $S_2O_8^{2-}$. The excess supply of the oxidant (lower BHA/$S_2O_8^{2-}$ ratio) results in a conventional pseudo first-order decay and the process is strongly dependent on the initial pH levels. However, in the deficiency of oxidant (higher BHA/$S_2O_8^{2-}$ ratio), two-stage reaction kinetics is identified and an atypical model using initial decay rate and maximum oxidative capacity

can be used to describe the process successfully.

Last but not least, the degradation rates of five different treatment processes in removing BHA were studied and compared in homogeneous modes including UV/Ag^{+}, $Ag^{+}/S_2O_8^{2-}$, UV only, $UV/Ag^{+}/S_2O_8^{2-}$, and $UV/S_2O_8^{2-}$. The $UV/Ag^{+}/S_2O_8^{2-}$ has an optimal condition with an A:S ratio of 7.5:1, where BHA could be degraded and mineralized in 3 and 20 min, respectively. The A:S ratio was found to be a critical factor in determining the BHA decay rate, too high and too low will retard the process as discussed in the paper. Since silver is a valuable material, it is reasonable to recycle it in the system for future use, a heterogeneous system is introduced. A solid form of silver oxide (Ag_2O) was used by replacing Ag^{+}. The $UV/Ag^{+}/S_2O_8^{2-}$ and $UV/Ag_2O/S_2O_8^{2-}$ have similar performance in removing BHA, but the latter does show an advantage in removing TOC at a much faster rate likely due to the selectivity of $SO_4^{\bullet-}$ and $^{\bullet}OH$ to the intermediates. Additionally, simple solid/liquid separation can be applied to recover Ag_2O, which makes this process more attractive for real application.

References:

Acero, J.L., Benitez, F.J., Gonzalez, M., Benitez, R. Kinetics of Fenuron Decomposition by Single-Chemical Oxidants and Combined Systems. *Industrial and Engineering Chemistry Research* 2002, 41, 4225-4232.

Alborzfar, M., Escande, K., Allen, S.J. Removal of 3,4-dichlorobut-1-ene using ozone oxidation. *Water Research* 2000, 34, 2963-2970.

Alfano, O.M., Cabrera, M.I., Cassano, A.E. Photocatalytic Reactions Involving Hydroxyl Radical Attack. *Journal of Catalysis* 1997, 172, 370-379.

Anderson, R. Treatability of wastewater by ozone, *Proceedings of a seminar held at the Centre for Environmental Control & Waste Management, Imperial College of Science*, Technology & Medicine, Ozotech Ltd, UK, p.14., 1997.

Anipsitakis, G.P., Dionysiou, D.D. Degradation of organic contaminants in water with sulfate radicals generated by the conjunction of peroxymonosulfate with cobalt. *Environmental Science and Technology* 2003, 37, 4790-4797.

Anipsitakis, G.P., Dionysiou, D.D. Radical Generation by the Interaction of Transition Metals with Common Oxidants, *Environmental Science and Technology* 2004a, 38, 3705-3712.

Anipsitakis G.P., Dionysiou, D.D. Transition metal/UV-based advanced oxidation technologies for water decontamination. *Applied Catalysis B-Environment.* 2004b, 54, 155-163.

Anipsitakis, G.P., Dionysiou. D.D., Gonzalez, M.A., Cobalt-mediated activation of peroxymonosulfate and sulfate radical attack on phenolic compounds. Implications of chloride ions. *Environmental Science & Technology.* 2006, 40, 1000-1007.

Armstrong, K.E., Wattenberg, L.W. Metabolism of 3-tert-butyl-4-hydroxyanisole to 3-tert-butyl-4,5-dihydroxyanisole by rat liver microsomes, *Cancer Research* 1985, 45, 1507-1510.

Bachman, J., Patterson, H. H. Photodecomposition of the Carbamate Pesticide Carbofuran: Kinetics and the Influence of Dissolved Organic Matter. *Environmental Science and Technology* 1999**,** 33, 874-881.

Bajt, O., Maihot, G., Bolte, M., Degradation of dibutyl phthalate by homogeneous photocatalysis with Fe III in aqueous solution. *Applied Catalysis B: Environmental* 2001, 33, 239-248.

Balabanovich, A.I., Schnabel, W. On the photolysis of phthalic acid dimethyl and diethyl ester: a product analysis study. *Journal of Photochemistry and Photobiology A: Chemistry* 1998, 113, 145-153.

Balazs, G.B., Cooper, J.F., Shell, T. Effect of trace additives on the efficiency of peroxydisulfate regeneration. *Journal of Applied Electrochemistry* 1999, 29, 285-292.

Bardwell, J.A., Webb, J.B., Tang, H., Fraser, J., Moisa, S. Ultraviolet photoenhanced wet etching of GaN in $K_2S_2O_8$ solution. *Journal of Applied Physics* 2001, 89, 4142-4149.

Beltran, F.J. *Ozone Reaction Kinetics For Water And Wastewater Systems*, Boca Raton, FL : Lewis, 2004.

Benitez, F. J. Degradation by ozone and UV-radiation of the herbicide cyanazine. *Ozone Science and Engineering* 1994, 16,213-234.

Blackburn, M. A., Waldock, M.J. Concentrations of alkylphenols in rivers and estuaries in England and Wales. *Water Research* 1995, 29, 1623-1629.

Boncz, M.A., Bruning, H., Rulkens, W. H., Sudhölter, E. J. R., Harmsen G. H. and Bijsterbosch, J. W. Kinetic and mechanistic aspects of the oxidation of chlorophenols by ozone. *Water Science and Techology* 1997, 35, 65-72.

Bonner, M.R., Lee, W.J., Sandler, D.P., Hoppin, J.A., Dosemeci, M., Alavanja, M.C.R. Occupational exposure to carbofuran and the incidence of cancer in the agricultural health study. *Environmental Health Perspectives* 2005, 113, 285-297.

Bonsen, E.M., Schroeter, S., Jacobs, H., Broekaert, J.A.C. Photocatalytic degradation of ammonia with TiO_2 as photocatalyst in the laboratory and under the use of solar radiation. *Chemosphere* 1997, 35, 1431-1445.

Buck, R.P., Singhadeja, S., Rogers, L.B. Ultraviolet absorption spectra of some inorganic ions in aqueous solutions. *Analytical Chemistry* 1954, 26, 1240 – 1242.

Bursey, J.T., Pellizzari, E.D. Analysis of industrial wastewater for organic pollutants in consent decree survey Contract Number 68-03-2867. Athens GA. *USEPA Environmental Research Laboratory*, p.1–34, 1982.

Butkus, M.A., Talbot, M., Labare, M.P. Feasibility of the silver-UV process for drinking water disinfection. *Water Research* 2005, 39, 4925-4932.

Canonica, S., Hoigné, J. Enhanced oxidation of methoxy phenols at micromolar concentration photosensitized by dissolved natural organic material. *Chemosphere* 1995, 30, 2365-2374.

Canton, C., Esplugas, S. and Casado, J. Mineralization of phenol in aqueous solution by ozonation using iron or copper salts and light. *Applied Catalysis B: Environmental* 2003, 43, 139-149.

Cass, M.W., Rapaport, E., White, E.H. Chemiluminescent reaction of 9-carboxy-N-methylacridinium chloride with potassium peroxydisulfate. *Journal of American Chemical Society* 1972, 94, 3168-3175.

CEPA. *Canadian Environmental Protection Act Priority Substances List Assessment Report - Dibutyl Phthalate*. Government of Canada, Beauregard Printers Limited, 1994.

Chan, K.H., Chu, W. Modeling the reaction kinetics of Fenton's process on the removal of atrazine. *Chemosphere* 2003, 51, 305-311.

Chawla O.P., Fewenden R.W. Electron spin resonance and pulse radiolysis studies of some reactions of $SO_4^{\bullet-}$. *Journal of Physical Chemistry* 1975**,** 79, 2693-2699.

Cheung T. C., Fung K. M., Lam H. W. Visible photosensitization of TiO_2-photodegradation of CCl_4 in aqueous medium. *Chemosphere* 1998, 36, 2641-2473.

Cheves, W., Camaioni, D.M., Kim, S.S. Aromatic hydroxylation by peroxydisulfate. *Journal of American Chemical Society* 1978, 100, 4814-4818.

Choudhry, G.G., Webster, G.R.B. Quantum yields of polychlorodibenzo-p-dioxins. *Photochemistry of Environmental Aquatic System ACS* 1987, 61-73.

Choy W. K., Chu, W. The rate improvement and modeling of TCE photodegradation by acetone sensitizer in surfactant solution, *Chemosphere* 2001, 44, 943-947.

Chu W., Jafvert, C. T., Diehl C. A., Marley K., Larson, R. A. Phototransformations of polychlorobiphenyls in Brij 58 micellar solutions. *Environmental Science and Technology* 1998, 32, 1989-1993.

Chu, W. Modeling the quantum yields of herbicide 2,4-D decay in UV/H_2O_2 process. *Chemosphere* 2001, 44, 935-941.

Chu, W., Ching, M. H. Modeling the ozonation of 2,4-dichlorophoxyacetic acid through a kinetic approach. *Water Research* 2003, 37, 39-46.

Chu, W., Choy W. K. The study of lag phase and rate improvement of TCE decay in UV/surfactant systems. *Chemosphere* 2000, 41, 1199-1204.

Chu, W., Hunt, J.R., Jafvert, C.T. Modeling the sequential photodechlorination of hexachlorobenzene in surfactant micelles. *Water Research* 2002, 36, 843-850.

Chu, W., Jafvert, C.T. Photodechlorination of polychlorobenzene congeners in surfactant micelle solutions. *Environmental Science and Technology* 1994, 28, 2415-2422.

Chu, W., Ma, C.W. Quantitative prediction of direct and indirect dye ozonation kinetics. *Water Research* 2000, 34, 3153-3160.

Chu, W., Tsui, S.M. Photo-sensitization of diazo disperse dye in aqueous acetone. *Chemosphere* 1999, 39, 1667-1677.

Coldham, N.G., Dave, M., Sauer, M.J. Analysis of di-n-butylphthalate biotransformation in cattle by liquid chromatography/ion trap mass spectrometry/mass spectrometry. *Journal of Mass Spectrometry* 1998, 33, 803-810.

Davì, M.L., Gnudi, F. Phenolic compounds in surface water. *Water Research* 1999, 33, 3213-3219.

Dogliotti, L., Hayon, E. Flash photolysis of per[oxydi]sulfate ions in aqueous solutions. The sulfate and ozonide radical anions. *Journal of Physical Chemistry* 1967, 71, 2511-2516.

ENDS, Industry glimpses new challenges as endocrine science advances. *ENDS Report* 290, 26-30, 1999.

Fatoki, O.S., Vernon, F. Phthalate esters in rivers of the Greater Manchester area, UK. *Science of Total Environment* 1990, 95, 227-232.

Freeman P. K., Lee Y. S. Photochemistry of polyhaloarenes. 12. The photochemistry of pentachlorobenzene in micellar media. *Journal of Organic Chemistry* 1992, 57, 2846-2850.

Fromme, H., Küchler, T., Otto, T., Pilz, K., Müller, J., Wenzel, A. Occurrence of phthalates and bisphenol A and F in the environment. *Water Research* 2002, 36, 1429-1438.

Gilbert, B.C., Smith, J.R.L., Taylor, P., Ward, S., Whitwood, A.C. The interplay of electronic, steric and stereoelectronic effects in hydrogen-atom abstraction reactions of $SO_4^{\bullet-}$ center dot, revealed by EPR spectroscopy. *Journal of the Chemical Society, Perkin Transactions* 1999, 2, 1631-1637.

Gottschalk, C.J.A., Libra, A.S. Ozonation of Water and Waste Water: A Practical Guide to Understanding Ozone and its Application. Wiley-VCH Verlage GmbH, Germany, 2000.

Graham, N., Chu, W., Lau, C. Observations of 2,4,6-trichlorophenol degradation by ozone. *Chemosphere* 2003, 51, 237-243.

Grossmann, D., Köser, H., Kretschmer, R., Porobin, M. Treatment of diglyme containing wastewater by advanced oxidation - process design and optimization. *Water Science and Technology* 2001, 44, 287-293.

Hawari, J., Demeter, A., Greer, C., Samson, R. Acetone-induced photodechlorination of Aroclor 1254 in alkaline 2-propanol: Probing the

mechanism by thermolysis in the presence of di-t-butyl peroxide. *Chemosphere* 1991, 22, 1161-1174.

He Bei Ji Heng Group Co. Ltd., *www.jihenggroup.com*, 2006.

Hewgill, F.R., Hewitt, D.G. Oxidation of alkoxyphenols. Part X. The reaction of 2,2'-dihydroxy-5.5'-dimethoxy-3,3'-di-butylbiphenyl with lead tetra-acetate. *Journal of Chemical Society Section C Organic Chemistry* 1967, 726-730.

Hizal, G., Zhu, Q.Q., Fischer, Ch.H., Fritz, P.M., Schnabel, W. On the photolysis of phthalic acid dialkyl esters: a product analysis study. *Journal of Photochemistry and Photobiology A: Chemistry* 1993, 72, 147-152.

Hoigné, J., Bader, H. The role of hydroxyl radical reactions in ozonation processes in aqueous solutions, *Water Research* 1976, 10, 377.

Hoigné, J., Bader, H. Rate constants of reactions of ozone with organic and inorganic compounds in water II: dissociating organic compounds. *Water Research* 1983, 17 (2), 185-194.

Hopert, A. C., Beyer, A., Frank, K., Strunck, E., Wünsche, W., Vollmer, G. Characterization of estrogenicity of phytoestrogens in an endometrial-derived experimental model. *Environmental Health Perspectives* 1998, 106, 581-586.

Hopkins K. Study finds large amounts of sex change chemicals in English rivers. *Edie Weekly Summaries* 30 July, 2004.

House, D.A. Kinetics and mechanism of oxidations by peroxydisulfate. *Chemical Review* 1962, 62, 185-203.

Hua, I., Pfalzer-Thompson, U. Ultrasonic irradiation of carbofuran: Decomposition kinetics and reactor characterization. *Water Research* 2001, 35, 1445-1452.

Huston, P.L., Pignatello, J.J. Degradation of selected pesticide active ingredients and commercial formulations in water by the photo-assisted Fenton reaction. *Water Research* 1999, 33, 1238-1246.

Iverson, F. In vivo studies on butylated hydroxyanisole. *Food and Chemical Toxicology* 1999, 37, 993-997.

Jobling, S., Reynolds, T., White, R., Parker, M.G., Sumpter, J.P. A variety of environmentally persistent chemicals, including some phthalate plasticizers, are weakly estrogenic. *Environmental Health Perspectives* 1995, 103, 582-587.

Johnson, B., Stalling, D.L., Hogan, J.W., Schoettger, R.A. Dynamics of phthalate acid esters in aquatic organisms. In: Suffet, I.H. (Eds.), Fate of Pollutants in the Air and Water Environment. *Advances in Environmental Science and Technology*, Part 2, Vol. 8. Wiley, New York, p. 283-300, 1977.

Jones, C., Engineering and Design: Ultraviolet/chemical oxidation. *Technical Letter,* No. 1110-1-161, Department of The Army, U.S. Army Corps of Engineers, Washington, DC, 1996.

Jonsson, S., Baun, A. Toxicity of mono- and diesters of o-phthalic esters to a crustacean, a green alga, and a bacterium. *Enviromental Toxicology Chemistry* 2003, 2, 3037-3043.

Jos A., Repetto G, Ríos J.C., Peso A. del, Salguero M., Hazen M.J., Molero M. L., Fernández-Freire P., Pérez-Martín J.M., Labrador V., Cameán A. Ecotoxicological evaluation of the additive butylated hydroxyanisole using a battery with six model systems and eighteen endpoints. *Aquatic Toxicology* 2005, 71, 183-192.

Kagan, J. *Organic Photochemistry: Principles and Applications.* Academic Press Ltd., London, 1993.

Kaposi, A.D., Wright, W.W., Fidy, J., Stavrov, S.S., Vanderkooi, J.M., Rasnik, I. Carbonmonoxy horseradish peroxidase as a function of pH and substrate: influence of local electric fields on the optical and infrared spectra. *Biochemistry* 2001, 40, 3483-3491.

Karimi A.A., Redman J.A., Glaze W.H., Stolarik G.F. Evaluating an AOP for TCE and PCE removal, *Journal of American Water Works Association* 1997, 89, 41-53.

Khaliq, M.A., Alam, M.S., Srivastava, S.P. Implications of physico-chemcial factors on the migration of phthalate esters from tubing commonly used for oral/nasal feeding. *Bulletin of Environmental Contamination and Toxicology* 1992, 48, 572-578.

Knipe, A.C. Oxidation and Reduction, *Organic Reaction Mechanisms*. Publisher London: Interscience Publishers. 2000, P. 179-208.

Kos, L., Perkowski, J., Ledakowicz, S. Application of ozone, hydrogen peroxide, and UV irradiation in textile wastewater treatment. *AATCC Review* 2004, 4, 30-34.

Kronholm, J., Jyske, P., Riekkola, M.L. Oxidation efficiencies of potassium persulfate and hydrogen peroxide in pressurized hot water with and without preheating. *Industrial and Engineering Chemistry Research* 2000, 39, 2207-2213.

Kronholm, J., Riekkola, M.L. Potassium Persulfate as Oxidant in Pressurized Hot Water. *Environmental Science and Technology* 1999, 33, 2095-2099.

Kuo, W.S. Destruction of Toxic Organics in Water by an Injection-Type Downflow UV/O_3 Oxidation Reactor. *Ozone Science & Engineering* 1999, 21, 539-550.

Kurechi, T., Aizawa, M., Kunugi, A. Studies on the anti-oxidant.18. Oxidation-product of tertiary butyl hydroquinone (TBHQ) 1. *Journal of the American Oil Chemists' Society* 1983, 60, 1878-1882.

Laat, J.D., Le, T.G. Kinetics and modeling of the Fe(III)/H_2O_2 system in the presence of sulfate in acidic aqueous solutions. *Environmental Science and Technology* 2005, 39, 1811-1818.

Lambert, S.D., Graham, N.J.D., Croll, B.T. Degradation of Selected Herbicides in a Lowland Surface Water by Ozone and Ozone-Hydrogen Peroxide. *Ozone Science and Engineering* 1996, 18, 251-269.

Larson, R.A. *Reaction Mechanisms in Environmental Organic Chemistry. B*oca Raton, Lewis Publishers, 1994.

Lee, W., Liang, Z. Y., Sanchez-Torres, A., Zhang, K. Achieving Sustainable Clean Water Supply in South China. Worcester Polytechnic Institute, *Civic Exchange Ltd.* *http://www.civic-exchange.org/publications/Intern/2005%20-%20WPI%20-%20water.pdf*. USA, 2005.

Lin S. H. Looking to treat wastewater? Try ozone. *Chemical Engineering* 1993, 100, 112-116.

Liu E., Yue S. Y., Kwong, W. Water Quality Control Measures In Overseas Places. Report No. RP11/99-00, *Research and Library Services Division*, Legislative Council Secretariat,

http://www.legco.gov.hk/yr99-00/english/sec/library/990rp11.pdf. Hong Kong, 2000.

Lobree, L.J., Bell, A.T. $K_2S_2O_8$-initiated sulfonation of methane to methanesulfonic acid. *Industrial and Engineering Chemistry Research* 2001, 40, 736-742.

Loudon, G.M. *Organic Chemistry*. Boca Raton, Benjamin/Cummings Publishing Co. Inc., p. 427-433, 1988.

Ma, J., Graham, N.J.D. Degradation of Atrazine by Manganese-Catalysed Ozonation: Influence of Humic Substances. *Water Research* 1999, 33, 785-793.

Ma, J.,Graham, N.J.D. Degradation of atrazine by manganese-catalysed ozonation: Influence of radical scavengers'. *Water Research* 2000, 34, 3822-3828.

Madsen, H.L., Bertelsen, G. Spices as antioxidants. *Trends in Food Science and Technology* 1995, 6, 271-277.

Malato, S., Blanco, J., Richter, C., Braun, B., Maldonado, M.I. Enhancement of the rate of solar photocatalytic mineralization of organic pollutants by inorganic oxidizing species. *Applied Catalysis B-Environmental* 1998, 17, 347-356.

Maurino, V., Calza, P., Minero, C., Pelizzetti, E., Vincenti, M. Light-assisted 1,4-dioxane degradation. *Chemosphere* 1997, 35, 2675-2688.

McCallum, J.E.B., Madison, S.A., Alkan, S., Depinto, R.L., Wahl, R.U.R. Analytical studies on the oxidative degradation of the reactive textile dye Uniblue A. *Environmental Science and Technology* 2000, 34, 5157-5164.

McElroy, W. J., Waygood, S. J. Kinetics of the reactions of the SO^{-4} radical with SO^{-4}, $S_2O_2^{-8}$, H_2O and Fe^{2+}. *Journal of the Chemical Society. Faraday Transactions* 1990, 86, 2557 – 2564.

Miltner, R.J., Baker, D.B., Speth, T.F., Fronk, C.A. Treatment of seasonal pesticides in surface waters. *Journal of American Water Works Association* 1989, 81, 43–52.

Minisci, F., Citterio, A., Giordan. C. Electron-transfer processes: peroxydisulfate, a useful and versatile reagent in organic chemistry. *Accounts of Chemical Research.* 1983,16, 27-32

Montagnani, D. B., Puddefoot, J., Davie, T. J. A., Vinson, G. P. Environmentally persistent oestrogen-like substances in UK river systems, *Journal of the Chartered Institution of Water and Environmental Management* 1996, 10, 399-406.

Morgan, J.D., Lusvardi, K.M., Kaler, E.W. Kinetics and mechanism of microemulsion polymerization of hexyl methacrylate. *Macromolecules* 1997, 30, 1897-1905.

Mylchreest, E., Sar, M., Cattley, R.C., Foster, P.M.D. Disruption of androgen-regulated male reproductive development by di(n-butyl)phthalate during late gestation in rats is different from flutamide. *Toxicology and Applied Pharmacology* 1999, 156, 81-95.

Nagai, F., Okubo, T., Ushiyama, K., Satoh, K., Kano, I. Formation of 8-hydroxydeoxyguanosine in calf thymus DNA treated with tert-butylhydroquinone, a major metabolite of butylated hydroxyanisole. *Toxicology Letters* 1996, 89, 163-167.

Nickel, U., Chen, Y.H., Schneider, S., Silva, M.I., Burrows, H.D., Formosinho, S.J. Mechanism and kinetics of the photocatalyzed oxidation of p-phenylenediamines by peroxydisulfate in the presence of tri-2,2'-bipyridylylruthenium(II). *Journal of Physical Chemistry* 1994, 98(11), 2883-2888.

Oppenlander, T. *Photochemical Purification of Water and Air.* Wiley-VCH, Germany, 2003.

Parsons, S.A., Williams, M. Introduction. In: *Advanced Oxidation Processes for Water and Wastewater Treatment*, 1st ed., Parsons, S.A., Eds., IWA Publishing: UK, 2004.

Pasiuk-Bronikowska, W., Bronikowski, T., Ulejczyk, M. Synergy in the autoxidation of S(IV) inhibited by phenolic compounds. *Journal of Physical Chemistry* 2003, 107, 1742-1748.

Paterlini, W.C., Nogueira, R.F.P. Multivariate analysis of photo-Fenton degradation of the herbicides tebuthiuron, diuron and 2,4-D. *Chemosphere* 2005, 58, 1107-1116.

Paxéus, N. Organic pollutants in the effluents in large wastewater treatment plants in Sweden. *Water Research* 1996, 30, 1115–1122.

Rodrigues M. R., Catalina F., Neumann M. G. Photoinitiaion of MMA polymerization by thionine/amine systems in the presence of SDS micelles. *Journal of Photochemistry and Photobiology A: Chemistry* 1999, 124, 29-34.

Roig, B., Gonzalez, C., Thomas, O. Measurement of dissolved total nitrogen in wastewater by UV photooxidation with peroxodisulphate. *Analytica Chimica Acta* 1999, 389, 267-274.

Romero, M., Blanco, J., Sanchez, B., Vidal, A., Malato, S., Cardona, A.I., Garcia, E. Solar photocatalytic degradation of water and air pollutants: challenges and perspectives. *Solar Energy* 1999, 66, 169-182.

Ruppert G., Rupert B.G.H. UV-O_3, UV-H_2O_2, UV-TiO_2 and the photo-Fenton reaction comparison of advanced oxidation processes for wastewater treatment. *Chemosphere* 1994, 28, 1447-1454.

Rustgi, S.N., Riesz, P. An E.S.R. and spin-trapping study of the reactions of the SO_4^- radical with protein and nucleic acid constituents. *International Jouranl of Radiation Biology and Related Study in Physics Chemistry and Medicine* 1978, 34, 301-16.

Samanidou, V., Fytianos, K., Pfister, G., Bahadir M. Photochemical decomposition of carbamate pesticides in natural-waters of northern Greece. *Science of Total Environment* 1988, 76, 85-92.

Santos, A., Yustos, P., Quintanilla, A., Rodríguez, S., García-Ochoa, F. Route of the catalytic oxidation of phenol in aqueous phase. *Applied Catalysis B: Environmental* 2002, 39, 97–113.

Sarafian, T.A., Kouyoumjian, S., Tashkin, D., Roth, M.D. Synergistic cytotoxicity of D 9-tetrahydrocannabinol and butylated hydroxyanisole. *Toxicology Letters* 2002, 133, 171-179.

Sharpe, R.M., Skakkebaek, N.E. Are oestrogens involved in falling sperm counts and disorder of the male reproductive tract?. *Lancet* 1993, 341, 1392-1395

Spelsberg, T.C., Riggs, B.L. Evidence of estrogen receptors in normal human osteoblast-like cells. *Science* 1987, 241, 84-86

Staples, C.A., Peterson, D.R., Parkerton, T.F., Adams, W.J. The environmental fate of phthalate esters: a literature review. *Chemosphere* 1997, 35, 667-749.

Steenken, S. Electron Transfer Between Radicals And Organic Molecules Via Addition/Elimination. An Inner-Sphere Path. In *Free Radicals: Chemistry, Pathology and Medicine*, Rice-Evans, C., Dormandy, T., Eds., Richelieu Press: London, p.51-73,1988.

Thayer, A. Fighting SARS – Common disinfectants may slow SARS. *Chemical Engineering News* 2003, 81, 9.

The Green Lane. Endocrine Disrupting Substances in the Environment. *Environment Canada's World Wide Web site* http://www.ec.gc.ca/eds/fact/broch_e.htm. *Oct*., Canada, 2002.

Tsao M.S., Wilmarth, W.K. The aqueous chemistry of inorganic free radicals. i. the mechanism of the photolytic decomposition of aqueous persulfate ion and evidence regarding the sulfate–hydroxyl radical interconversion equilibrium. *Journal of Physical Chemistry* 1959, 63, 346 – 353.

UKWIR NEWS. QSAR Studies on Fate and Behaviour of Steroid Endocrines in Sewage Treatment, UK Water Industry Research Limited, London, 2001.

USEPA. The Incorporation of Water Treatment Effects on Pesticide Removal and Transformations in Food Quality Protection Act (FQPA) Drinking Water Assessments, *United States Environmental Protection Agency*, United States, 2001.

Vargas, F., Canudas, N., Miranda, M.A., Boscá, F. In vitro phototoxicity of clofibrate. Photochemical and photohemolytic studies on its metabolite clofibric acid. *Journal of Photochemistry and Photobiology B: Biology* 1993, 21, 61-67.

Verhagen, H., Schilderman, P.A.E.L., Kleinjans, J.C.S. Butylated hydroxyanisole in perspective. *Chemico-Biology Interactions* 1991, 80, 109-134.

Waldemer, R.H., Tratnyek, P.G., Johnson, R.L., Nurmi J.T. Oxidation of chlorinated ethenes by heat-activated persulfate: kinetics and products. *Environmental Science and Technology* 2007, 41,1010-1015.

Wang, H., Liu, W. Optimization of a high-performance liquid chromatography system by artificial neural networks for separation and determination of antioxidants. *The Journal of Separation Science* 2004, 27, 1189-1194.

Wang, J., Liu, P., Shi, H., Qian, Y. Kinetics of phthalic acid ester degradation by acclimated activated sludge. *Process Biochemistry* 1997, 32, 567-571.

Wang, Q.Q., Lemley, A.T. Oxidative degradation and detoxification of aqueous carbofuran by membrane anodic Fenton treatment. *Journal of Hazardous Material* 2003, 98, 241-255.

Weiner, E.R. A Dictionary of Inorganic Water Quality Parameters and Pollutants. In *Applications of Environmental Chemistry, A Practical Guide for Environmental Professionals.* Lewis Publishers, CRC Press LLC, N.W. Corporate Blvd., Boca Raton: Florida, Ch.7, pp 27, 2000.

Winarno, E.K., Getoff, N. Comparative studies on the degradation of aqueous 2-chloroaniline by O_3 as well as by UV-light and γ-rays in the presence of ozone. *Radiation Physics and Chemistry* 2002, 65, 387 –395.

Wolfe, N.L., Burns, L.A., Steen, W.C. Use of linear free-energy relationships and an evaluative model to assess the fate and transport of phthalate-esters in the aquatic environment. *Chemosphere* 1980, 9, 393-402.

Wong, C.C., Chu, W. The hydrogen peroxide-assisted photocatalytic degradation of alachlor in TiO_2 suspensions. *Environmental Science and Technology* 2003, 37, 2310-2316

Xiong, F., Graham, N.J.D. Rate constants for herbicide degradation by ozone. *Ozone Science and Engineering* 1992, 14, 283-302.

Zazo, J.A., Casas, J.A., Mohedano, A.F., Gilarranz, M.A., Rodriguez, J. J. Chemical pathway and kinetics of phenol oxidation by fenton's reagent. *Environmental Science and Technology* 2005, 39, 9295-9302.

Zhang, N.D., Kong, X.P., Zhang, M.X., Liu, Y, Zhu, Y.M. Study on treatment of methyl-orange in water by derivable oxidation of peroxydisulfate. *Journal of Advanced Oxidation Technologies* 2007, 10, 193-195.

APPENDIX I ANALYTICAL EQUIPMENTS & PROCEDURES

1. Rayonet^{TM} RPR-200 photoreactor

2. Schematic diagram of photoreactor with ozone inlet

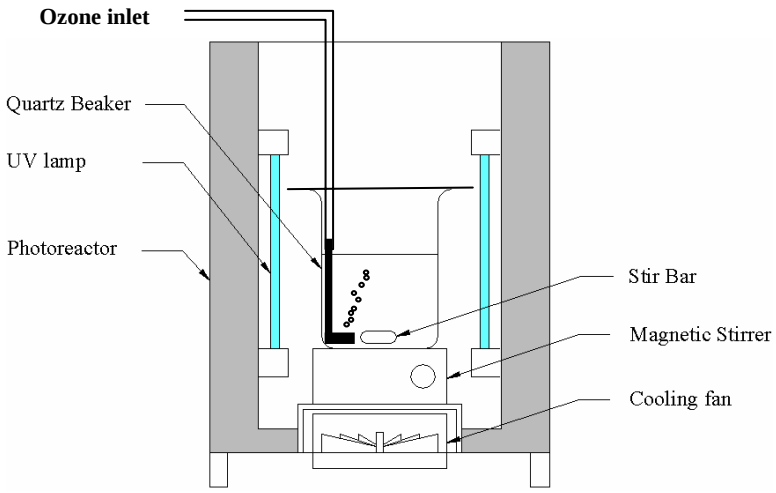

3. OZAT® ozone generator (CFS-1A from Ozonia Ltd.)

Telfon tubing for the ozone gas and cooling pipe

Internal of Ozonia

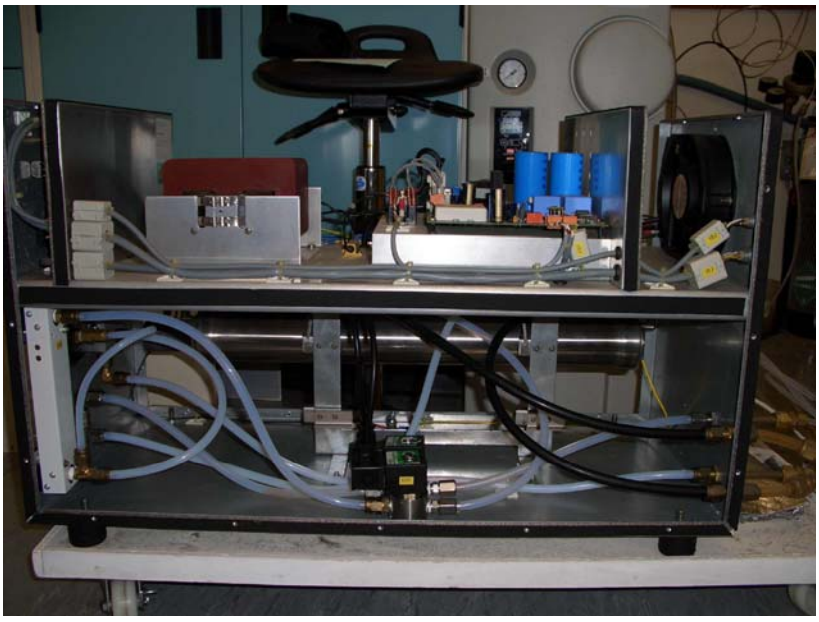

The ozonia is purged with pure oxygen before switching on the electricity which will subsequently generate ozone. Also, the cooling system has to be ready before the high voltage is involved, where the ozonia might be over-heated and damaged. The ozonia has two separate setting to control the output of ozone concentration. For example: the pressure to control the oxygen input, and the flow rate. As shown in the figure below, with different Power supply (%) at Flow: 1.5 and pH 4.3, the saturated ozone concentration increase. In this preliminary test, it is found that the minimum pre-ozonation period is 10 min.

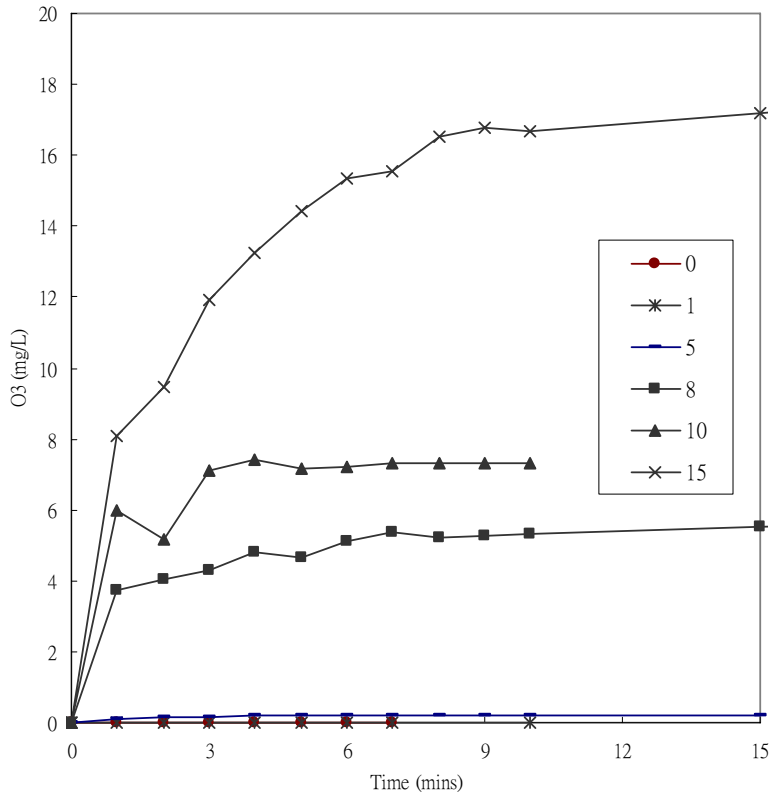

The ozonia is consistently clean and purged every time after usage, in order to remove the residual ozone inside the system, and the cooling water is shut off to make sure no water will be back feed to the system.

4. Ozone analyzer (Orbisphere)

4.1 Use

Ozone analyzer is used to determine the concentration of saturated ozone before the start of the experiment make sure it reaches the maximum and consistence supply of ozone gas.

4.2 Membrane Service

Precaution: Keep the LEMO-10 connector away from moisture.

The membrane has to be replaced monthly to ensure the proper protection of the probe, here below is the procedures:

1. Firstly, unscrew the LEMO connector and close it with O-ring protected black base (away from liquid/electrolyte spill)
2. Unscrew sensor protector by hand (anticlockwise) or with metal wrench

3. Pry the membrane holding ring with the metal plate provided in recharge kit (28116)
4. AVOID CONTACT WITH ELECTROLYTE (STAIN CLOTHING PERMANENTLY)
5. Dispose the membrane and membrane mask,
6. Keep the holding ring, and shake out any electrolyte.
7. Use the membrane support tool, match up the prongs of the tool to 2 of the holes in the membrane support, turn anticlockwise to remove the support.
8. Rinse the membrane support with WATER. (if discoloured clean it with <70% HNO_3 for 30 seconds, then rinsed again with water).
9. Rinse the electrolyte reservoir with water
10. Further cleaning: Ammonium hydroxide (for clean electrodes refer to manual) or Nitric acid (discoloured electrodes)
    - Fill up the ANODE only (not cathode – inner part) with <70% HNO_3 for no longer than 5 seconds.
    - Then empty out the acid and rinse thoroughly with water.
    - If still unclean, use alternative nitric acid and ammonium hydroxide cleaning
11. Polishing sensor face

- Use the mounting tool to screw back the membrane support ‘finger tight’, (install the smooth side with a groove faces out)
- Place the polish cloth in the dish on a flat surface and shake a little pol powder onto the cloth, add clean water to make a loose watery mixture, and hold the sensor vertically and use a circular motion to polish the sensor face for 30 seconds until the gold cathode is clean and shiny.

12. Remove the membrane support.
13. Rinse the membrane support and sensor with strong jet of DI water.
14. ELECTRODE CLEANING – fill the anode with water but do not cover the cathode, and then add just a few drops of HNO3 to cover the cathode for 15 mins (NEVER SPILL onto the anode), and then rinse with water
15. Replace the membrane support with tool (fight tight)
16. Tilt the sensor slightly, use syringe to fill the sensor head with electrolyte,
17. Fill the head form the lowest of the four holes, try to force air out via the top hole, and continue filling and return the sensor to vertical until overflow of electrolyte
18. Rest the cylindrical guide with the narrow side down onto the sensor place the membrane angularly (avoid air bubble), and then place the sensor

mask on top

19. To mount the membrane, insert the plunger with holding ring, and push down to a stop. If the membrane is not smooth enough, push it down with fingers, or otherwise replace membrane
20. Replace if the holding ring turns easily.
21. Wash excess electrolyte off the sensor and wipe dry. Unscrew the plastic base, MAKE SURE NOT to WET the LEMO.
22. Replace the protection cap finger tight and an extra of 1/8-1/4 turn with the metal wrench.
23. After 30 minutes, calibrate the system with the LEMO connected. Ready for measurement.
24. Place a drop or two of water in the calibration storage and screw it onto the sensor to prevent dry out during weekends.
25. If inactive more than a months clean and dry the sensor without electrolyte with calibration cap in place.

5. HIGH PERFORMANCE LIQUID CHROMATOGRAPHY MASS SPECTROMETERS

Finnigan SpectraSYSTEM® LC and Finnigan ThermoQuest LCQ Duo

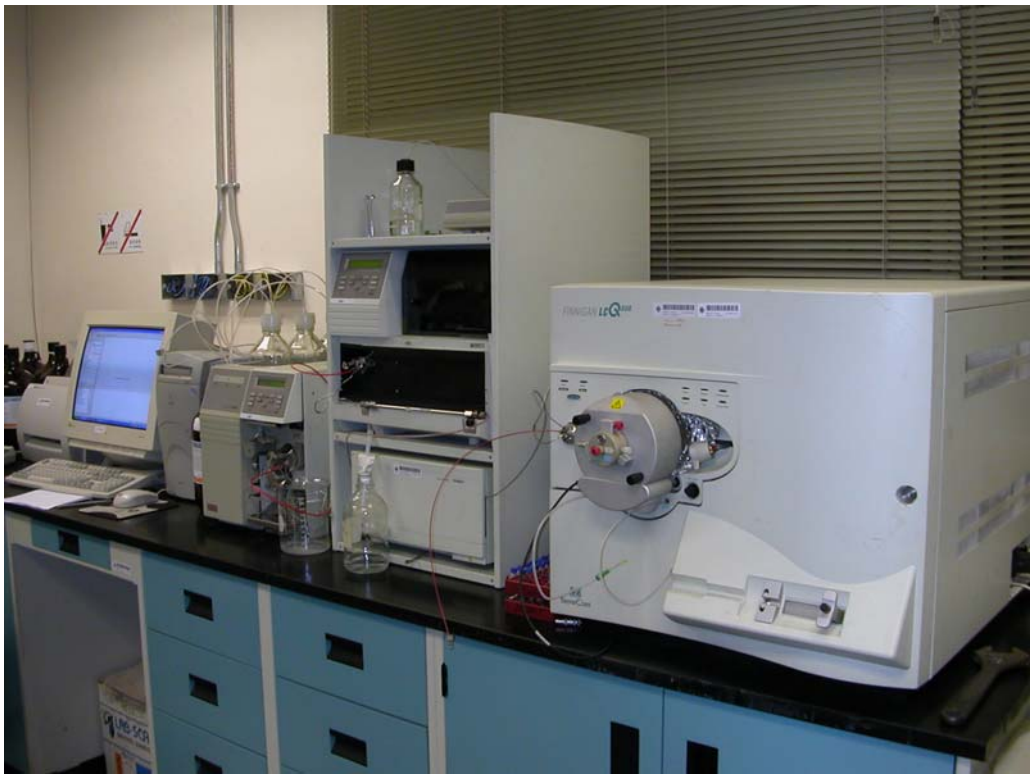

Calibration of LCMS (APCI and ESI)

Two different types of Liquid Chromatography Mass Spectrometers are used in this study:

(i) Electrospray Ionization (LC/MS-ESI) and

(ii) Atmospheric pressure chemical ionization (APCI)

The former one is mainly used to detect polar compounds (i.e BHA, TBHQ, etc.), and APCI is used for non-polar compounds (i.e. DBP). The negative ion mode is usually use for acidic molecule at high pH, or basic molecule in low pH. The LCMS was calibrated periodically with the calibration solution indicated at Table 3.3.

Table 3: Calibration solution

Chemicals	Stock solution	m/z	Volume
Caffenie	1 mg/mL in 100% Methanol	195	100 μL
MRFA	1 mL 5 nmole/μL in 50% Methanol	524	5 μL
Ultramark 1621	10 mL of 0.1% in acetonitrile	1022, 1122, 1222, 1322, 1422, 1522, 1622, 1722, 1822	2.5 mL
Acetic Acid			50 μL
50% Methanol			2.34 mL

Prior to tuning of the MS, the syringe, transfer line and ESI probe is clean with 5% acetic acid, 50% methanol and acetone. Then the instrument is ready for calibration. For the tuning method, the mode of detection was selected to be positive, and purge speed is at a rate of 5 times faster than the auxiliary unit. The programme will automatically infuse the calibration solution into the MS system. These calibration procedures were being performed twice a year, or after the system have been shut down for maintenance of the suction pump.

6. Total Organic Carbon Analyzer (TOC-5000A)

APPENDIX II EXPERIMENTAL RESULTS

DBP

Expt. No.:	DBP1	
Initial pH:	3	
Probe cpd:	DBP	4 μM
time (min)	Conc. (μM)	C/Co
0.00	4.15	1.00
0.33	3.76	0.90
0.75	3.95	0.95
1.00	3.58	0.86
3.00	3.08	0.74
5.00	2.84	0.69
8.00	2.16	0.52
10.00	1.86	0.45
20.00	0.72	0.17
30.00	0.59	0.14
60.00	0.48	0.12

Expt. No.:	DBP2	
Initial pH:	5	
Probe cpd:	DBP	4 μM
time (min)	Conc. (μM)	C/Co
0.00	4.23	1.00
1.50	3.48	0.82
3.00	3.21	0.76
5.00	2.84	0.67
8.00	2.24	0.53
10.00	1.98	0.47
20.00	1.14	0.27
30.00	0.85	0.20
40.00	0.67	0.16
60.00	0.56	0.13

Expt. No.:	DBP3	
Initial pH:	7	
Probe cpd:	DBP	4 μM
time (min)	Conc. (μM)	C/Co
0.00	4.23	1.00
1.50	3.48	0.82
3.00	3.21	0.76
5.00	2.84	0.67
8.00	2.24	0.53
10.00	1.98	0.47
20.00	1.14	0.27
30.00	0.85	0.20
40.00	0.67	0.16
60.00	0.56	0.13

Expt. No.:	DBP4	
Initial pH:	9	
Probe cpd:	DBP	4 μM
time (min)	Conc. (μM)	C/Co
0.33	4.04	1.00
0.75	3.82	0.94
1.50	3.67	0.91
3.00	3.29	0.81
5.00	2.67	0.66
8.00	2.28	0.56
10.00	1.64	0.41
20.00	1.01	0.25
30.00	0.48	0.12
60.00	0.26	0.06

Expt. No.:	DBP5	
Initial pH:	11	
Probe cpd:	DBP	4 μM
time (min)	Conc. (μM)	C/Co
0.00	4.23	1.00
1.00	3.93	0.93
3.00	3.14	0.74
8.00	2.05	0.48
11.50	1.62	0.38
20.00	0.78	0.19
30.00	0.38	0.09
60.00	0.23	0.05

Expt. No.:	DBP6	
Initial pH:	3	
Probe cpd:	DBP	2 μM
time (min)	Conc. (μM)	C/Co
0.00	1.94	1.00
0.33	1.66	0.86
0.75	1.54	0.80
3.00	1.30	0.67
5.00	1.05	0.54
8.00	0.76	0.39
10.00	0.67	0.35
20.00	0.37	0.19
30.00	0.15	0.08
60.00	0.09	0.04

Expt. No.:	DBP7	
Initial pH:	5	
Probe cpd:	DBP	2 μM
time (min)	Conc. (μM)	C/Co
0.00	1.89	1.00
1.50	1.57	0.83
5.00	1.09	0.58
8.00	0.91	0.48
20.00	0.29	0.15
30.00	0.09	0.05
40.00	0.00	0.00
60.00	0.00	0.00

Expt. No.:	DBP8	
Initial pH:	7	
Probe cpd:	DBP	2 μM
time (min)	Conc. (μM)	C/Co
0.00	2.26	1.00
0.33	1.92	0.85
3.50	1.42	0.63
5.00	1.39	0.61
8.00	0.97	0.43
10.00	0.86	0.38
20.00	0.23	0.10
30.00	0.00	0.00
60.00	0.00	0.00

Expt. No.:	DBP9	
Initial pH:	11	
Probe cpd:	DBP	2 μM
time (min)	Conc. (μM)	C/Co
0.00	1.96	1.00
0.33	1.89	0.96
0.75	1.72	0.88
3.00	1.35	0.69
5.00	1.20	0.61
8.00	0.83	0.42
10.00	0.72	0.37
20.00	0.24	0.12
30.00	0.08	0.04
60.00	0.00	0.00

Expt. No.:	DBP10	
Initial pH:	2.7	
Probe cpd:	DBP	10 μM
time (min)	Conc. (μM)	C/Co
0.00	10.46	1.00
2.00	4.81	0.46
6.00	2.51	0.24
10.00	1.31	0.12
20.00	0.22	0.02
30.00	0.05	0.00
60.00	0.00	0.00

Expt. No.:	DBP11	
Initial pH:	3.3	
Probe cpd:	DBP	10 μM
time (min)	Conc. (μM)	C/Co
0.00	10.38	1.00
2.00	7.42	0.72
6.00	4.60	0.44
10.00	2.95	0.28
20.00	1.39	0.13
30.00	0.65	0.06

Expt. No.:	DBP12	
Initial pH:	4.3	
Probe cpd:	DBP	10 μM
time (min)	Conc. (μM)	C/Co
0.00	9.99	1.00
2.00	9.00	0.90
5.00	6.63	0.66
8.00	5.30	0.53
10.00	6.42	0.64
15.00	5.65	0.57
20.00	5.03	0.50
30.00	4.25	0.43
35.00	3.71	0.37
40.00	3.71	0.37
50.00	3.29	0.33
55.00	2.84	0.28
60.00	2.16	0.22

Expt. No.:	DBP13	
Initial pH:	7.4	
Probe cpd:	DBP	10 μM
time (min)	Conc. (μM)	C/Co
0.00	9.77	1.00
2.00	6.95	0.71
6.00	4.68	0.48
10.00	3.82	0.39
20.00	1.79	0.18
30.00	0.75	0.08

Expt. No.:	DBP14	
Initial pH:	8.9	
Probe cpd:	DBP	10 μM
time (min)	Conc. (μM)	C/Co
0.00	10.46	1.00
3.00	10.34	0.99
6.00	5.83	0.56
10.00	4.15	0.40
20.00	1.59	0.15
30.00	0.61	0.06
60.00	0.11	0.01

Expt. No.:	DBP15	
Initial pH:	10.7	
Probe cpd:	DBP	10 μM
time (min)	Conc. (μM)	C/Co
0.00	9.52	1.00
2.00	6.60	0.69
6.00	3.73	0.39
10.00	3.08	0.32
20.00	0.84	0.09
32.00	0.27	0.03
60.00	0.11	0.01

Expt. No.: DBP1
Initial pH: 3
Probe cpd: DBP 4 μM

time (min)	μM BA	μM PA	Area MBP	Ratio =area/DBPo	Area BB	Ratio =area/DBPo
0.00	0.00	0.00	0	0.000	0	0.000
1.50	0.45	0.13	0	0.000	1038833	0.337
3.00	0.63	0.33	92000	0.058	1202005	0.390
5.00	0.61	0.53	116000	0.073	913593	0.297
8.00	0.17	1.81	156000	0.098	518302	0.168
10.00	0.10	2.00	215000	0.135	0	0.000
20.00	0.03	2.33	204000	0.128	0	0.000
30.00	0.00	2.40	183000	0.115	0	0.000
40.00	0.00	2.56	118000	0.074	0	0.000
60.00	0.00	2.65	50000	0.031	0	0.000

Expt. No.: DBP2
Initial pH: 5
Probe cpd: DBP 4 μM

time (min)	μM PA	Area MBP	Ratio =area/DBPo	Area MBPK	Ratio =area/DBPo	Area MBPA	Ratio =area/DBPo
0.00	0.00	0	0.000	0	0.000	0	0.000
1.50	0.00	443920	0.302	0	0.000	0	0.000
3.00	0.00	1281117	0.870	0	0.000	0	0.000
5.00	0.00	1473490	1.001	0	0.000	0	0.000
8.00	0.00	2609462	1.772	0	0.000	0	0.000
10.00	0.00	4505406	3.060	2562500	1.741	2562500	1.741
20.00	0.00	3000000	2.038	6203743	4.214	6203743	4.214
30.00	0.00	2000000	1.358	2482569	1.686	2482569	1.686
40.00	0.31	846308	0.575	1740901	1.183	1740901	1.183
60.00	0.78	0	0.000	1484290	1.008	1484290	1.008

PA (μM)	pH 3		pH 5		pH 7		pH 9		pH 11
time (min)	C	time (min)	C	time (min)	C	time (min)	C	time (min)	C
0.00	0.00	0.00	0.00	0.00	0.00	0.00	0.00	0.00	0.00
1.50	0.13	1.50	0.00	1.50	0.00	1.50	0.00	1.50	0.24
3.00	0.33	3.00	0.00	3.00	0.00	3.00	0.00	3.00	0.26
5.00	0.53	5.00	0.00	5.00	0.00	5.00	0.00	5.00	0.27
8.00	1.81	8.00	0.00	8.00	0.00	8.00	0.00	8.00	0.47
10.00	2.59	10.00	0.00	10.00	0.00	10.00	0.00	11.50	0.87
20.00	2.33	20.00	0.00	20.00	1.22	20.00	2.01	20.00	2.09
30.00	2.67	30.00	0.00	30.00	1.22	30.00	2.07	30.00	2.39
40.00	2.56	40.00	0.31	40.00	1.63	40.00	2.19	40.00	3.19
60.00	2.65	60.00	0.78	60.00	3.87	60.00	4.01	60.00	3.75

CBF

Expt. No.: CBF1
Initial pH: 3
Probe cpd: CBF 0.2 mM
Rx: UV only

time (min)	Conc. (mM)	C/Co
0.00	0.19	1.00
5.00	0.17	0.89
8.00	0.17	0.85
10.00	0.16	0.82
20.00	0.14	0.73
30.00	0.13	0.65
40.00	0.11	0.59

Expt. No.: CBF2
Initial pH: 5
Probe cpd: CBF 0.2 mM
Rx: UV only

time (min)	Conc. (mM)	C/Co
0.00	0.21	1.00
5.00	0.18	0.89
8.00	0.18	0.85
10.00	0.17	0.82
20.00	0.14	0.69
30.00	0.12	0.59
40.00	0.11	0.51

Expt. No.: CBF3
Initial pH: 7
Probe cpd: CBF 0.2 mM
Rx: UV only

time (min)	Conc. (mM)	C/Co
0.00	0.20	1.00
5.00	0.19	0.91
8.00	0.18	0.87
10.00	0.17	0.84
20.00	0.15	0.73
30.00	0.13	0.64
40.00	0.11	0.56

Expt. No.: CBF4
Initial pH: 9
Probe cpd: CBF 0.2 mM
Rx: UV only

time (min)	Conc. (mM)	C/Co
0.00	0.22	1.00
5.00	0.21	0.95
8.00	0.20	0.92
10.00	0.19	0.89
20.00	0.19	0.87
30.00	0.17	0.78
40.00	0.16	0.71

Expt. No.: CBF5
Initial pH: 11
Probe cpd: CBF 0.2 mM
Rx: UV only

time (min)	Conc. (mM)	C/Co
0.00	0.19	1.00
5.00	0.16	0.84
8.00	0.15	0.80
10.00	0.14	0.77
20.00	0.13	0.71
30.00	0.12	0.64
40.00	0.11	0.58

Expt. No.: CBF6
Initial pH: 3
Probe cpd: CBF 0.2 mM
Rx: ozone only

time (min)	Conc. (mM)	C/Co
0.00	0.19	1.00
1.50	0.17	0.85
3.00	0.15	0.80
5.00	0.14	0.72
8.00	0.12	0.61
10.00	0.11	0.55
20.00	0.05	0.26
30.00	0.01	0.07
40.00	0.00	0.01

Expt. No.: CBF7
Initial pH: 5
Probe cpd: CBF 0.2 mM
Rx: ozone only

time (min)	Conc. (mM)	C/Co
0.00	0.21	1.00
1.50	0.17	0.82
3.00	0.17	0.79
5.00	0.16	0.77
8.00	0.15	0.70
10.00	0.14	0.66
20.00	0.10	0.47
30.00	0.06	0.31

Expt. No.: CBF8
Initial pH: 7
Probe cpd: CBF 0.2 mM
Rx: ozone only

time (min)	Conc. (mM)	C/Co
0.00	0.20	1.00
1.50	0.18	0.90
3.00	0.17	0.84
5.00	0.15	0.77
8.00	0.13	0.68
10.00	0.12	0.62
20.00	0.07	0.36
30.00	0.03	0.16
40.00	0.01	0.04

Expt. No.: CBF9
Initial pH: 9
Probe cpd: CBF 0.2 mM
Rx: ozone only

time (min)	Conc. (mM)	C/Co
0.00	0.18	1.00
1.50	0.13	0.71
3.00	0.11	0.63
5.00	0.10	0.55
8.00	0.09	0.49
10.00	0.07	0.38
20.00	0.04	0.21
30.00	0.01	0.07

Expt. No.: CBF10
Initial pH: 11
Probe cpd: CBF 0.2 mM
Rx: ozone only

time (min)	Conc. (mM)	C/Co
0.00	0.20	1.00
1.50	0.13	0.65
3.00	0.11	0.57
5.00	0.09	0.45
8.00	0.07	0.35
10.00	0.05	0.25
20.00	0.04	0.20
30.00	0.00	0.00

Expt. No.: CBF11
Initial pH: 3
Probe cpd: CBF 0.2 mM
Rx: UV/O_3

time (min)	Conc. (mM)	C/Co
0.00	0.20	1.00
1.50	0.17	0.87
3.00	0.17	0.83
5.00	0.15	0.78
8.00	0.14	0.69
10.00	0.13	0.64
20.00	0.08	0.40
30.00	0.03	0.17

Expt. No.: CBF12
Initial pH: 5
Probe cpd: CBF 0.2 mM
Rx: UV/O_3

time (min)	Conc. (mM)	C/Co
0.00	0.20	1.00
1.50	0.16	0.82
3.00	0.15	0.75
5.00	0.13	0.66
8.00	0.11	0.54
10.00	0.09	0.48
20.00	0.04	0.21
30.00	0.01	0.06

Expt. No.: CBF13
Initial pH: 7
Probe cpd: CBF 0.2 mM
Rx: UV/O_3

time (min)	Conc. (mM)	C/Co
0.00	0.20	1.00
1.50	0.16	0.81
3.00	0.15	0.72
5.00	0.12	0.60
8.00	0.09	0.45
10.00	0.07	0.36
20.00	0.02	0.10
30.00	0.00	0.00

Expt. No.: CBF14
Initial pH: 9
Probe cpd: CBF 0.2 mM
Rx: UV/O_3

time (min)	Conc. (mM)	C/Co
0.00	0.19	1.00
1.50	0.16	0.84
3.00	0.13	0.67
5.00	0.12	0.59
8.00	0.10	0.50
10.00	0.07	0.37
20.00	0.06	0.30
30.00	0.01	0.06

Expt. No.: CBF15
Initial pH: 11
Probe cpd: CBF 0.2 mM
Rx: UV/O_3

time (min)	Conc. (mM)	C/Co
0.00	0.20	1.00
1.50	0.12	0.63
3.00	0.11	0.56
5.00	0.09	0.44
8.00	0.06	0.32
10.00	0.04	0.20
20.00	0.03	0.15
30.00	0.01	0.03

BHA

Expt. No.: BHA1
Initial pH: 3
Probe cpd: BHA 0.1 mM
Rx: UV only

time (min)	Conc. (mM)	C/Co
0.00	0.11	1.00
1.50	0.08	0.73
3.00	0.07	0.69
5.00	0.07	0.64
8.00	0.06	0.57
10.00	0.06	0.53
20.00	0.04	0.40

Expt. No.: BHA2
Initial pH: 5
Probe cpd: BHA 0.1 mM
Rx: UV only

time (min)	Conc. (mM)	C/Co
0.00	0.10	1.00
1.50	0.07	0.72
3.00	0.07	0.66
5.00	0.06	0.61
8.00	0.06	0.55
10.00	0.05	0.51
20.00	0.04	0.38

Expt. No.: BHA3
Initial pH: 7
Probe cpd: BHA 0.1 mM
Rx: UV only

time (min)	Conc. (mM)	C/Co
0.00	0.11	1.00
1.50	0.08	0.69
3.00	0.07	0.65
5.00	0.06	0.59
8.00	0.06	0.54
10.00	0.05	0.51
20.00	0.04	0.37

Expt. No.: BHA4
Initial pH: 9
Probe cpd: BHA 0.1 mM
Rx: UV only

time (min)	Conc. (mM)	C/Co
0.00	0.11	1.00
1.50	0.08	0.68
3.00	0.07	0.63
5.00	0.06	0.57
8.00	0.05	0.48
10.00	0.05	0.44
20.00	0.03	0.31

Expt. No.: BHA5
Initial pH: 11
Probe cpd: BHA 0.1 mM
Rx: UV only

time (min)	Conc. (mM)	C/Co
0.00	0.11	1.00
1.50	0.07	0.62
3.00	0.06	0.56
5.00	0.05	0.50
8.00	0.04	0.41
10.00	0.04	0.37
20.00	0.03	0.25

Expt. No.: BHA6
Initial pH: 3
Probe cpd: BHA 0.2 mM
Rx: UV only

time (min)	Conc. (mM)	C/Co
0.00	0.20	1.00
1.50	0.18	0.92
3.00	0.17	0.86
5.00	0.16	0.82
8.00	0.15	0.76
10.00	0.14	0.72
20.00	0.12	0.60

Expt. No.: BHA7
Initial pH: 5
Probe cpd: BHA 0.2 mM
Rx: UV only

time (min)	Conc. (mM)	C/Co
0.00	0.20	1.00
1.50	0.18	0.92
3.00	0.17	0.86
5.00	0.16	0.82
8.00	0.15	0.77
10.00	0.15	0.74
20.00	0.12	0.63

Expt. No.: BHA8
Initial pH: 7
Probe cpd: BHA 0.2 mM
Rx: UV only

time (min)	Conc. (mM)	C/Co
0.00	0.20	1.00
1.50	0.17	0.88
3.00	0.16	0.82
5.00	0.15	0.77
8.00	0.14	0.72
10.00	0.14	0.70
20.00	0.12	0.60

Expt. No.: BHA9
Initial pH: 9
Probe cpd: BHA 0.2 mM
Rx: UV only

time (min)	Conc. (mM)	C/Co
0.00	0.20	1.00
1.50	0.18	0.92
3.00	0.17	0.87
5.00	0.17	0.84
8.00	0.15	0.76
10.00	0.15	0.74
20.00	0.12	0.62

Expt. No.: BHA10
Initial pH: 11
Probe cpd: BHA 0.2 mM
Rx: UV only

time (min)	Conc. (mM)	C/Co
0.00	0.19	1.00
1.50	0.17	0.86
3.00	0.16	0.80
5.00	0.15	0.76
8.00	0.14	0.71
10.00	0.13	0.66
20.00	0.10	0.50

Expt. No.: BHA11
Initial pH: 3
Probe cpd: BHA 0.3 mM
Rx: UV only

time (min)	Conc. (mM)	C/Co
0.00	0.29	1.00
1.50	0.26	0.91
3.00	0.26	0.90
5.00	0.25	0.87
8.00	0.24	0.82
10.00	0.23	0.79
20.00	0.20	0.70
30.00	0.18	0.61
40.00	0.17	0.59
60.00	0.15	0.52
90.00	0.15	0.52
120.00	0.08	0.28

Expt. No.: BHA12
Initial pH: 5
Probe cpd: BHA 0.3 mM
Rx: UV only

time (min)	Conc. (mM)	C/Co
0.00	0.29	1.00
1.50	0.26	0.90
3.00	0.25	0.85
5.00	0.23	0.77
8.00	0.22	0.75
10.00	0.21	0.72
20.00	0.21	0.73
30.00	0.19	0.66
40.00	0.17	0.57
60.00	0.13	0.44
90.00	0.13	0.44
120.00	0.10	0.34

Expt. No.: BHA13
Initial pH: 7
Probe cpd: BHA 0.3 mM
Rx: UV only

time (min)	Conc. (mM)	C/Co
0.00	0.31	1.00
1.50	0.28	0.91
3.00	0.26	0.85
5.00	0.25	0.82
8.00	0.23	0.76
10.00	0.23	0.74
20.00	0.20	0.64
30.00	0.19	0.62
40.00	0.15	0.50
60.00	0.13	0.42
90.00	0.07	0.23
120.00	0.02	0.08

Expt. No.: BHA14
Initial pH: 9
Probe cpd: BHA 0.3 mM
Rx: UV only

time (min)	Conc. (mM)	C/Co
0.00	0.28	1.00
1.50	0.24	0.88
3.00	0.23	0.83
5.00	0.22	0.81
8.00	0.21	0.77
10.00	0.21	0.75
20.00	0.18	0.63
30.00	0.14	0.49
40.00	0.12	0.43
60.00	0.09	0.34
90.00	0.07	0.27
120.00	0.00	0.00

Expt. No.: BHA15
Initial pH: 11
Probe cpd: BHA 0.3 mM
Rx: UV only

time (min)	Conc. (mM)	C/Co
0.00	0.28	1.00
1.50	0.24	0.88
3.00	0.24	0.87
5.00	0.24	0.85
8.00	0.22	0.80
10.00	0.22	0.79
20.00	0.19	0.69
30.00	0.18	0.64
40.00	0.15	0.55
60.00	0.14	0.52
90.00	0.10	0.34
120.00	0.08	0.28

Expt. No.: BHA16
Initial pH: 3
Probe cpd: BHA 0.1 mM
Rx: Ozone only

time (min)	Conc. (mM)	C/Co
0.00	0.10	1.00
0.50	0.06	0.55
1.50	0.04	0.38
3.00	0.02	0.18
5.00	0.00	0.03
8.00	0.00	0.00
10.00	0.00	0.00
20.00	0.00	0.00

Expt. No.: BHA17
Initial pH: 5
Probe cpd: BHA 0.1 mM
Rx: Ozone only

time (min)	Conc. (mM)	C/Co
0.00	0.09	1.00
0.50	0.05	0.55
1.50	0.04	0.39
3.00	0.02	0.21
5.00	0.00	0.04
8.00	0.00	0.00
10.00	0.00	0.00
20.00	0.00	0.00

Expt. No.: BHA18
Initial pH: 7
Probe cpd: BHA 0.1 mM
Rx: Ozone only

time (min)	Conc. (mM)	C/Co
0.00	0.10	1.00
0.50	0.08	0.83
1.50	0.07	0.67
3.00	0.04	0.43
5.00	0.02	0.18
8.00	0.00	0.00
10.00	0.00	0.00
20.00	0.00	0.00

Expt. No.: BHA19
Initial pH: 9
Probe cpd: BHA 0.1 mM
Rx: Ozone only

time (min)	Conc. (mM)	C/Co
0.00	0.09	1.00
0.50	0.08	0.85
1.50	0.06	0.68
3.00	0.04	0.48
5.00	0.02	0.24
8.00	0.00	0.02
10.00	0.00	0.00
20.00	0.00	0.00

Expt. No.: BHA20
Initial pH: 11
Probe cpd: BHA 0.1 mM
Rx: Ozone only

time (min)	Conc. (mM)	C/Co
0.00	0.10	1.00
0.50	0.06	0.60
1.50	0.04	0.41
3.00	0.02	0.23
5.00	0.01	0.08
8.00	0.00	0.00
10.00	0.00	0.00
20.00	0.00	0.00

Expt. No.: BHA21
Initial pH: 3
Probe cpd: BHA 0.2 mM
Rx: Ozone only

time (min)	Conc. (mM)	C/Co
0.00	0.24	1.00
0.50	0.15	0.63
1.50	0.13	0.53
3.00	0.09	0.36
5.00	0.05	0.22
8.00	0.02	0.07
10.00	0.01	0.02
20.00	0.00	0.00

Expt. No.: BHA22
Initial pH: 5
Probe cpd: BHA 0.2 mM
Rx: Ozone only

time (min)	Conc. (mM)	C/Co
0.00	0.22	1.00
1.50	0.13	0.58
3.00	0.09	0.41
5.00	0.06	0.26
8.00	0.03	0.11
10.00	0.01	0.06
20.00	0.00	0.00

Expt. No.: BHA23
Initial pH: 7
Probe cpd: BHA 0.2 mM
Rx: Ozone only

time (min)	Conc. (mM)	C/Co
0.00	0.22	1.00
0.50	0.14	0.63
1.50	0.11	0.52
3.00	0.10	0.44
5.00	0.07	0.31
8.00	0.04	0.18
10.00	0.03	0.12
20.00	0.00	0.02

Expt. No.: BHA24
Initial pH: 9
Probe cpd: BHA 0.2 mM
Rx: Ozone only

time (min)	Conc. (mM)	C/Co
0.00	0.18	1.00
0.50	0.15	0.86
1.50	0.13	0.71
3.00	0.09	0.52
5.00	0.05	0.28
8.00	0.04	0.20
10.00	0.01	0.08
20.00	0.00	0.00

Expt. No.: BHA25
Initial pH: 11
Probe cpd: BHA 0.2 mM
Rx: Ozone only

time (min)	Conc. (mM)	C/Co
0.00	0.20	1.00
0.50	0.13	0.66
1.50	0.11	0.56
3.00	0.09	0.43
5.00	0.06	0.29
8.00	0.02	0.10
10.00	0.01	0.05
20.00	0.00	0.02

Expt. No.: BHA26
Initial pH: 3
Probe cpd: BHA 0.3 mM
Rx: Ozone only

time (min)	Conc. (mM)	C/Co
0.00	0.26	1.00
0.50	0.22	0.82
1.50	0.18	0.68
3.00	0.13	0.48
5.00	0.07	0.27
8.00	0.02	0.09
10.00	0.00	0.00
20.00	0.00	0.00

Expt. No.: BHA27
Initial pH: 5
Probe cpd: BHA 0.3 mM
Rx: Ozone only

time (min)	Conc. (mM)	C/Co
0.00	0.29	1.00
0.50	0.20	0.67
1.50		0.00
3.00	0.15	0.51
5.00	0.07	0.26
8.00	0.04	0.14
10.00	0.02	0.07
20.00	0.00	0.00

Expt. No.: BHA28
Initial pH: 7
Probe cpd: BHA 0.3 mM
Rx: Ozone only

time (min)	Conc. (mM)	C/Co
0.00	0.30	1.00
0.50	0.27	0.89
1.50	0.22	0.73
3.00	0.18	0.59
5.00	0.13	0.43
8.00	0.07	0.22
10.00	0.04	0.13
20.00	0.00	0.01

Expt. No.: BHA29
Initial pH: 9
Probe cpd: BHA 0.3 mM
Rx: Ozone only

time (min)	Conc. (mM)	C/Co
0.00	0.29	1.00
0.50	0.25	0.84
1.50	0.22	0.74
3.00	0.17	0.57
5.00	0.12	0.42
8.00	0.07	0.23
10.00	0.04	0.15
20.00	0.00	0.00

Expt. No.: BHA30
Initial pH: 11
Probe cpd: BHA 0.3 mM
Rx: Ozone only

time (min)	Conc. (mM)	C/Co
0.00	0.29	1.00
0.50	0.24	0.83
1.50	0.14	0.49
3.00	0.10	0.35
5.00	0.06	0.21
8.00	0.02	0.08
10.00	0.01	0.04
20.00	0.00	0.00

Expt. No.: BHA31
Initial pH: 3
Probe cpd: BHA 0.1 mM
Rx: UV/O_3

time (min)	Conc. (mM)	C/Co
0.00	0.10	1.00
0.50	0.06	0.56
1.50	0.04	0.39
3.00	0.02	0.20
5.00	0.01	0.06
8.00	0.00	0.00
10.00	0.00	0.00
20.00	0.00	0.00

Expt. No.: BHA32
Initial pH: 5
Probe cpd: BHA 0.1 mM
Rx: UV/O_3

time (min)	Conc. (mM)	C/Co
0.00	0.09	1.00
0.50	0.06	0.60
1.50	0.03	0.34
3.00	0.02	0.16
5.00	0.00	0.05
8.00	0.00	0.00
10.00	0.00	0.00
20.00	0.00	0.00

Expt. No.: BHA33
Initial pH: 7
Probe cpd: BHA 0.1 mM
Rx: UV/O_3

time (min)	Conc. (mM)	C/Co
0.00	0.10	1.00
0.50	0.08	0.76
1.50	0.05	0.50
3.00	0.03	0.25
5.00	0.01	0.08
8.00	0.00	0.00
10.00	0.00	0.00
20.00	0.00	0.00

Expt. No.: BHA34
Initial pH: 9
Probe cpd: BHA 0.1 mM
Rx: UV/O_3

time (min)	Conc. (mM)	C/Co
0.00	0.09	1.00
0.50	0.07	0.74
1.50	0.05	0.57
3.00	0.03	0.31
5.00	0.01	0.11
8.00	0.00	0.00
10.00	0.00	0.00
20.00	0.00	0.00

Expt. No.: BHA35
Initial pH: 11
Probe cpd: BHA 0.1 mM
Rx: UV/O_3

time (min)	Conc. (mM)	C/Co
0.00	0.11	1.00
0.50	0.05	0.49
1.50	0.03	0.27
3.00	0.01	0.12
5.00	0.00	0.04
8.00	0.00	0.00
10.00	0.00	0.00
20.00	0.00	0.00

Expt. No.: BHA36
Initial pH: 3
Probe cpd: BHA 0.2 mM
Rx: UV/O_3

time (min)	Conc. (mM)	C/Co
0.00	0.24	1.00
0.50	0.16	0.67
1.50	0.13	0.54
3.00	0.00	0.00
5.00	0.05	0.21
8.00	0.02	0.07
10.00	0.01	0.02
20.00	0.00	0.00

Expt. No.: BHA37
Initial pH: 5
Probe cpd: BHA 0.2 mM
Rx: UV/O_3

time (min)	Conc. (mM)	C/Co
0.00	0.23	1.00
0.50	0.15	0.67
1.50	0.12	0.52
3.00	0.08	0.35
5.00	0.05	0.20
8.00	0.04	0.19
10.00	0.00	0.01
20.00	0.00	0.00

Expt. No.: BHA38
Initial pH: 7
Probe cpd: BHA 0.2 mM
Rx: UV/O_3

time (min)	Conc. (mM)	C/Co
0.00	0.24	1.00
0.50	0.14	0.58
1.50	0.11	0.47
3.00	0.08	0.33
5.00	0.05	0.20
8.00	0.02	0.08
10.00	0.01	0.03
20.00	0.00	0.00

Expt. No.: BHA39
Initial pH: 9
Probe cpd: BHA 0.2 mM
Rx: UV/O_3

time (min)	Conc. (mM)	C/Co
0.00	0.21	1.00
0.50	0.17	0.78
1.50	0.14	0.65
3.00	0.09	0.44
5.00	0.06	0.27
8.00	0.02	0.10
10.00	0.01	0.04
20.00	0.00	0.00

Expt. No.: BHA40
Initial pH: 11
Probe cpd: BHA 0.2 mM
Rx: UV/O_3

time (min)	Conc. (mM)	C/Co
0.00	0.19	1.00
0.50	0.14	0.71
1.50	0.11	0.55
3.00	0.06	0.34
5.00	0.04	0.19
8.00	0.01	0.04
10.00	0.00	0.01
20.00	0.00	0.00

Expt. No.: BHA41
Initial pH: 3
Probe cpd: BHA 0.3 mM
Rx: UV/O_3

time (min)	Conc. (mM)	C/Co
0.00	0.29	1.00
0.50	0.21	0.73
1.50	0.12	0.41
3.00	0.07	0.22
5.00	0.02	0.07
8.00	0.01	0.03
10.00	0.00	0.00
20.00	0.00	0.00

Expt. No.: BHA42
Initial pH: 5
Probe cpd: BHA 0.3 mM
Rx: UV/O_3

time (min)	Conc. (mM)	C/Co
0.00	0.29	1.00
0.50	0.21	0.74
1.50	0.17	0.58
3.00	0.12	0.43
5.00	0.08	0.29
8.00	0.04	0.14
10.00	0.02	0.07
20.00	0.00	0.00

Expt. No.: BHA43
Initial pH: 7
Probe cpd: BHA 0.3 mM
Rx: UV/O_3

time (min)	Conc. (mM)	C/Co
0.00	0.29	1.00
0.50	0.23	0.79
1.50	0.18	0.62
3.00	0.14	0.47
5.00	0.08	0.29
8.00	0.03	0.11
10.00	0.01	0.05
20.00	0.00	0.00

Expt. No.: BHA44
Initial pH: 9
Probe cpd: BHA 0.3 mM
Rx: UV/O_3

time (min)	Conc. (mM)	C/Co
0.00	0.29	1.00
0.50	0.21	0.70
1.50	0.19	0.64
3.00	0.13	0.44
5.00	0.08	0.27
8.00	0.03	0.11
10.00	0.01	0.05
20.00	0.00	0.00

Expt. No.: BHA45
Initial pH: 11
Probe cpd: BHA 0.3 mM
Rx: UV/O_3

time (min)	Conc. (mM)	C/Co
0.00	0.29	1.00
0.50	0.00	0.00
1.50	0.16	0.55
3.00	0.11	0.37
5.00	0.07	0.24
8.00	0.03	0.09
10.00	0.01	0.03
20.00	0.00	0.00

Expt. No.:	BHAS1		
Initial pH:	3		
Probe cpd:	BHA	0.1	mM
Rx:	UV only		
time (min)	Conc.	(mM)	C/Co
0.00	0.11		1.00
1.50	0.08		0.73
3.00	0.07		0.69
5.00	0.07		0.64
8.00	0.06		0.57
10.00	0.06		0.53
20.00	0.04		0.40

Expt. No.:	BHAS2		
Initial pH:	3		
Probe cpd:	BHA	0.3	mM
Rx:	UV only		
time (min)	Conc.	(mM)	C/Co
0.00	0.29		1.00
0.50	0.26		0.90
1.50	0.25		0.85
3.00	0.23		0.77
5.00	0.22		0.75
8.00	0.21		0.72
10.00	0.21		0.73
20.00	0.19		0.66
30.00	0.17		0.57

Expt. No.:	BHAS3		
Initial pH:	3		
Probe cpd:	BHA	0.5	mM
Rx:	UV only		
time (min)	Conc.	(mM)	C/Co
0.00	0.53		1.00
1.50	0.51		0.96
3.00	0.50		0.93
5.00	0.48		0.91
8.00	0.46		0.87
10.00	0.45		0.85
20.00	0.36		0.68
40.00	0.34		0.63
60.00	0.28		0.53

Expt. No.:	BHAS4		
Initial pH:	3		
Probe cpd:	BHA	0.1	mM
Rx:	UV/$S_2O_8^{2-}$		
Conc. :	$S_2O_8^{2-}$	2	mM
time (min)	Conc.	(mM)	C/Co
0.00	0.09		1.00
1.00	0.04		0.47
2.00	0.03		0.32
3.00	0.02		0.22
4.00	0.01		0.15
5.00	0.01		0.09
6.00	0.00		0.05
8.00	0.00		0.00
10.00	0.00		0.00

Expt. No.:	BHAS5		
Initial pH:	3		
Probe cpd:	BHA	0.2	mM
Rx:	UV/$S_2O_8^{2-}$		
Conc. :	$S_2O_8^{2-}$	2	mM
time (min)	Conc.	(mM)	C/Co
0.00	0.21		1.00
0.50	0.17		0.83
1.00	0.16		0.76
3.00	0.12		0.58
5.00	0.10		0.49
8.00	0.08		0.40
10.00	0.07		0.35
20.00	0.04		0.21
20.00	0.04		0.21
30.00	0.02		0.07

Expt. No.:	BHAS6		
Initial pH:	3		
Probe cpd:	BHA	0.3	mM
Rx:	UV/$S_2O_8^{2-}$		
Conc. :	$S_2O_8^{2-}$	2	mM
time (min)	Conc.	(mM)	C/Co
0.00	0.34		1.00
1.00	0.27		0.80
2.00	0.24		0.71
3.00	0.23		0.67
4.00	0.21		0.63
5.00	0.20		0.61
6.00	0.19		0.58
8.00	0.18		0.54
10.00	0.17		0.50
20.00	0.13		0.38
30.00	0.10		0.29
60	0.05		0.15

Expt. No.:	BHAS7		
Initial pH:	3		
Probe cpd:	BHA	0.5	mM
Rx:	UV/$S_2O_8^{2-}$		
Conc. :	$S_2O_8^{2-}$	2	mM
time (min)	Conc.	(mM)	C/Co
0.00	0.54		1.00
1.50	0.44		0.81
3.00	0.40		0.74
5.00	0.37		0.68
8.00	0.34		0.62
10.00	0.32		0.58
20.00	0.25		0.47
40.00	0.19		0.34
60.00	0.14		0.25
120.00	0.06		0.11

Expt. No.:	BHAS8		
Initial pH:	3		
Probe cpd:	BHA	0.3	mM
Rx:	UV/$S_2O_8^{2-}$		
Conc. :	$S_2O_8^{2-}$	0.1	mM
time (min)	Conc.	(mM)	C/Co
0.00	0.33		1.00
1.50	0.33		0.98
3.00	0.32		0.96
5.00	0.30		0.91
8.00	0.29		0.87
10.00	0.28		0.84
20.00	0.25		0.75
30.00	0.22		0.65
45.00	0.19		0.57
60.00	0.16		0.50

Expt. No.:	BHAS9		
Initial pH:	3		
Probe cpd:	BHA	0.3	mM
Rx:	UV/$S_2O_8^{2-}$		
Conc. :	$S_2O_8^{2-}$	0.5	mM
time (min)	Conc.	(mM)	C/Co
0.00	0.33		1.00
1.50	0.26		0.80
3.00	0.25		0.77
5.00	0.24		0.73
8.00	0.22		0.67
10.00	0.21		0.63
20.00	0.18		0.53
30.00	0.15		0.46
45.00	0.13		
60.00	0.11		

Expt. No.:	BHAS10		
Initial pH:	3		
Probe cpd:	BHA	0.3	mM
Rx:	UV/$S_2O_8^{2-}$		
Conc. :	$S_2O_8^{2-}$	1	mM

time (min)	Conc.	(mM)	C/Co
0.00	0.33		1.00
1.50	0.26		0.80
3.00	0.23		0.68
5.00	0.21		0.65
8.00	0.19		0.57
10.00	0.18		0.55
20.00	0.14		0.43
30.00	0.12		0.36
45.00	0.10		0.29
60.00	0.07		0.22

Expt. No.:	BHAS11		
Initial pH:	3		
Probe cpd:	BHA	0.3	mM
Rx:	UV/$S_2O_8^{2-}$		
Conc. :	$S_2O_8^{2-}$	5	mM

time (min)	Conc.	(mM)	C/Co
0.00	0.33		1.00
1.50	0.22		0.67
3.00	0.18		0.55
5.00	0.15		0.46
8.00	0.12		0.38
10.00	0.11		0.32
20.00	0.05		0.16
30.00	0.02		0.05
45.00	0.00		0.00
60.00	0.00		0.00

Expt. No.:	BHAS12		
Initial pH:	3		
Probe cpd:	BHA	0.3	mM
Rx:	UV/$S_2O_8^{2-}$		
Conc. :	$S_2O_8^{2-}$	10	mM

time (min)	Conc.	(mM)	C/Co
0.00	0.33		1.00
1.00	0.23		0.69
2.00	0.19		0.59
3.00	0.17		0.51
5.00	0.14		0.41
8.00	0.10		0.31
10.00	0.08		0.23
20.00	0.03		0.08
30.00	0.00		0.00
60.00	0.00		0.00

Expt. No.:	BHAS13		
Initial pH:	3		
Probe cpd:	BHA	0.5	mM
Rx:	UV/$S_2O_8^{2-}$		
Conc. :	$S_2O_8^{2-}$	1	mM

time (min)	Conc.	(mM)	C/Co
0.00	0.46		1.00
1.50	0.39		0.85
3.00	0.37		0.80
5.00	0.35		0.74
8.00	0.32		0.70
10.00	0.31		0.67
20.00	0.26		0.57
30.00	0.23		0.50
45.00	0.20		0.42
60.00	0.17		0.36

Expt. No.:	BHAS14		
Initial pH:	3		
Probe cpd:	BHA	0.5	mM
Rx:	UV/$S_2O_8^{2-}$		
Conc. :	$S_2O_8^{2-}$	5	mM

time (min)	Conc.	(mM)	C/Co
0.00	0.46		1.00
1.50	0.36		0.77
3.00	0.32		0.69
5.00	0.28		0.61
8.00	0.25		0.54
10.00	0.23		0.49
20.00	0.16		0.35
30.00	0.12		0.26
45.00	0.07		0.16
60.00	0.04		0.10

Expt. No.:	BHAS15		
Initial pH:	3		
Probe cpd:	BHA	0.5	mM
Rx:	UV/$S_2O_8^{2-}$		
Conc. :	$S_2O_8^{2-}$	10	mM

time (min)	Conc.	(mM)	C/Co
0.00	0.46		1.00
1.50	0.34		0.73
3.00	0.29		0.64
5.00	0.25		0.53
8.00	0.21		0.46
10.00	0.19		0.41
20.00	0.11		0.24
35.00	0.04		0.09
45.00	0.00		0.00
60.00	0.00		0.00

Expt. No.:	BHAS16	
Initial pH:	3	
Probe cpd:	BHA	0.1 mM
Rx:	UV/$S_2O_8^{2-}$	
Conc. :	$S_2O_8^{2-}$	0.1 mM

time (min)	Conc.	(mM)	C/Co
0.00	0.10		1.00
1.00	0.08		0.75
2.00	0.07		0.70
3.00	0.07		0.65
4.00	0.07		0.64
5.00	0.06		0.56
6.00	0.06		0.55
8.00	0.05		0.53
10.00	0.05		0.49
20.00	0.04		0.36

Expt. No.:	BHAS17	
Initial pH:	3	
Probe cpd:	BHA	0.1 mM
Rx:	UV/$S_2O_8^{2-}$	
Conc. :	$S_2O_8^{2-}$	0.25 mM

time (min)	Conc.	(mM)	C/Co
0.00	0.10		1.00
1.50	0.06		0.62
3.00	0.05		0.54
4.00	0.05		0.50
5.00	0.05		0.46
6.00	0.04		0.43
8.00	0.04		0.38
10.00	0.03		0.35
20.00	0.02		0.22
30.00	0.01		0.15

Expt. No.:	BHAS18	
Initial pH:	3	
Probe cpd:	BHA	0.1 mM
Rx:	UV/$S_2O_8^{2-}$	
Conc. :	$S_2O_8^{2-}$	0.5 mM

time (min)	Conc.	(mM)	C/Co
0.00	0.12		1.00
1.00	0.08		0.66
2.00	0.06		0.54
3.00	0.06		0.48
5.00	0.05		0.39
8.00	0.04		0.30
10.00	0.03		0.25
20.00	0.01		0.10

Expt. No.:	BHAS19	
Initial pH:	3	
Probe cpd:	BHA	0.1 mM
Rx:	UV/$S_2O_8^{2-}$	
Conc. :	$S_2O_8^{2-}$	1 mM

time (min)	Conc.	(mM)	C/Co
0.00	0.12		1.00
1.00	0.06		0.53
2.00	0.05		0.41
3.00	0.04		0.33
4.00	0.03		0.26
5.00	0.03		0.21
6.00	0.02		0.17
8.00	0.01		0.11
10.00	0.01		0.06

Expt. No.:	BHAS20	
Initial pH:	3	
Probe cpd:	BHA	0.1 mM
Rx:	UV/$S_2O_8^{2-}$	
Conc. :	$S_2O_8^{2-}$	5 mM

time (min)	Conc.	(mM)	C/Co
0.00	0.12		1.00
1.00	0.04		0.38
2.00	0.02		0.21
4.00	0.00		0.04
5.00	0.00		0.01
6.00	0.00		0.01
8.00	0.00		0.00
10.00	0.00		0.00

Expt. No.:	BHAS21	
Initial pH:	3	
Probe cpd:	BHA	0.1 mM
Rx:	UV/$S_2O_8^{2-}$	
Conc. :	$S_2O_8^{2-}$	10 mM

time (min)	Conc.	(mM)	C/Co
0.00	0.09		1.00
0.50	0.05		0.54
1.00	0.03		0.35
1.50	0.02		0.26
2.00	0.01		0.11
2.50	0.01		0.08
3.00	0.00		0.03
4.00	0.00		0.00

Expt. No.:	BHAS22	
Initial pH:	3	
Probe cpd:	BHA	0.1 mM
Rx:	UV/$S_2O_8^{2-}$	
Conc. :	$S_2O_8^{2-}$	15 mM

time (min)	Conc.	(mM)	C/Co
0.00	0.09		1.00
0.25	0.06		0.68
0.50	0.05		0.56
0.75	0.04		0.45
1.00	0.04		0.37
1.50	0.03		0.27
2.00	0.02		0.21
2.50	0.00		0.00

Expt. No.:	BHAS23	
Initial pH:	3	
Probe cpd:	BHA	0.1 mM
Rx:	UV/$S_2O_8^{2-}$	
Conc. :	$S_2O_8^{2-}$	20 mM

time (min)	Conc.	(mM)	C/Co
0.00	0.10		1.00
1.00	0.03		0.27
2.00	0.00		0.05
3.00	0.00		0.00
4.00	0.00		0.00
5.00	0.00		0.00

Expt. No.:	BHAS24	
Initial pH:	3	
Probe cpd:	BHA	0.1 mM
Rx:	UV/$S_2O_8^{2-}$	
Conc. :	$S_2O_8^{2-}$	40 mM

time (min)	Conc.	(mM)	C/Co
0.00	0.09		1.00
1.00	0.01		0.11
2.00	0.00		0.00
3.00	0.00		0.00
4.00	0.00		0.00
5.00	0.00		0.00

Expt. No.:	BHAS25		
Initial pH:	7		
Probe cpd:	BHA	0.1	mM
Rx:	UV/$S_2O_8^{2-}$		
Conc. :	$S_2O_8^{2-}$	0.1	mM

time (min)	Conc.	(mM)	C/Co
0.00	0.09		1.00
1.50	0.07		0.78
3.00	0.06		0.71
5.00	0.06		0.63
8.00	0.05		0.55
10.00	0.05		0.51
20.00	0.03		0.36
30.00	0.02		0.27
45.00	0.02		0.19
60.00	0.01		0.13

Expt. No.:	BHAS26		
Initial pH:	7		
Probe cpd:	BHA	0.1	mM
Rx:	UV/$S_2O_8^{2-}$		
Conc. :	$S_2O_8^{2-}$	0.25	mM

time (min)	Conc.	(mM)	C/Co
0.00	0.09		1.00
1.50	0.06		0.66
3.00	0.05		0.52
5.00	0.04		0.43
8.00	0.03		0.32
10.00	0.02		0.28
20.00	0.01		0.15
30.00	0.01		0.06
45.00	0.00		0.01
60.00	0.00		0.00

Expt. No.:	BHAS27		
Initial pH:	7		
Probe cpd:	BHA	0.1	mM
Rx:	UV/$S_2O_8^{2-}$		
Conc. :	$S_2O_8^{2-}$	0.5	mM

time (min)	Conc.	(mM)	C/Co
0.00	0.09		1.00
1.00	0.06		0.59
2.00	0.04		0.43
3.00	0.03		0.31
4.00	0.02		0.25
5.00	0.02		0.20
6.00	0.01		0.15
8.00	0.01		0.10
10.00	0.00		0.03
20.00	0.00		0.00

Expt. No.:	BHAS28		
Initial pH:	7		
Probe cpd:	BHA	0.1	mM
Rx:	UV/$S_2O_8^{2-}$		
Conc. :	$S_2O_8^{2-}$	2	mM

time (min)	Conc.	(mM)	C/Co
0.00	0.09		1.00
1.00	0.02		0.22
2.00	0.01		0.10
3.00	0.00		0.01
4.00	0.00		0.00

Expt. No.:	BHAS29		
Initial pH:	7		
Probe cpd:	BHA	0.1	mM
Rx:	UV/$S_2O_8^{2-}$		
Conc. :	$S_2O_8^{2-}$	1	mM

time (min)	Conc.	(mM)	C/Co
0.50	0.06		1.00
1.00	0.01		0.21
2.00	0.01		0.13
3.00	0.00		0.04
4.00	0.00		0.01
5.00	0.00		0.01
6.00	0.00		0.00

Expt. No.:	BHAS30		
Initial pH:	7		
Probe cpd:	BHA	0.1	mM
Rx:	UV/$S_2O_8^{2-}$		
Conc. :	$S_2O_8^{2-}$	5	mM

time (min)	Conc.	(mM)	C/Co
0.00	0.09		1.00
0.50	0.02		0.22
1.00	0.01		0.09
2.00	0.00		0.03
3.00	0.00		0.01
4.00	0.00		0.01
5.00	0.00		0.00
6.00	0.00		0.00

Expt. No.:	BHAS31		
Initial pH:	7		
Probe cpd:	BHA	0.1	mM
Rx:	UV/$S_2O_8^{2-}$		
Conc. :	$S_2O_8^{2-}$	10	mM

time (min)	Conc.	(mM)	C/Co
0.00	0.10		1.00
0.50	0.01		0.11
1.00	0.00		0.01
2.00	0.00		0.01

Expt. No.:	BHAS32		
Initial pH:	7		
Probe cpd:	BHA	0.1	mM
Rx:	UV/$S_2O_8^{2-}$		
Conc. :	$S_2O_8^{2-}$	15	mM

time (min)	Conc.	(mM)	C/Co
0.00	0.09		1.00
0.50	0.01		0.09
1.00	0.00		0.01
1.50	0.00		0.02
2.00	0.00		0.00
2.50	0.00		0.00
3.00	0.00		0.00
4.00	0.00		0.00

Expt. No.:	BHAS33		
Initial pH:	11		
Probe cpd:	BHA	0.1	mM
Rx:	UV/$S_2O_8^{2-}$		
Conc. :	$S_2O_8^{2-}$	0.1	mM

time (min)	Conc.	(mM)	C/Co
0.00	0.09		0.96
1.50	0.06		0.69
3.00	0.05		0.55
5.00	0.04		0.43
8.00	0.03		0.32
10.00	0.02		0.26
20.00	0.01		0.11
30.00	0.00		0.03
45.00	0.00		0.00
60.00	0.00		0.00

Expt. No.:	BHAS34		
Initial pH:	11		
Probe cpd:	BHA	0.1	mM
Rx:	UV/$S_2O_8^{2-}$		
Conc. :	$S_2O_8^{2-}$	0.25	mM

time (min)	Conc.	(mM)	C/Co
0.00	0.09		1.00
1.50	0.05		0.52
3.00	0.03		0.31
5.00	0.01		0.12
8.00	0.00		0.03
10.00	0.00		0.01
20.00	0.00		0.00
30.00	0.00		0.00

Expt. No.:	BHAS35		
Initial pH:	11		
Probe cpd:	BHA	0.1	mM
Rx:	UV/$S_2O_8^{2-}$		
Conc. :	$S_2O_8^{2-}$	0.5	mM

time (min)	Conc.	(mM)	C/Co
0.00	0.10		1.05
0.50	0.07		0.71
1.00	0.05		0.49
1.50	0.03		0.28
2.00	0.02		0.16
3.00	0.00		0.05
5.00	0.00		0.00

Expt. No.:	BHAS36		
Initial pH:	11		
Probe cpd:	BHA	0.1	mM
Rx:	UV/$S_2O_8^{2-}$		
Conc. :	$S_2O_8^{2-}$	1	mM

time (min)	Conc.	(mM)	C/Co
0.00	0.10		1.00
0.25	0.07		0.70
0.50	0.05		0.56
0.75	0.04		0.44
1.00	0.03		0.34
1.25	0.03		0.26
1.50	0.02		0.18
2.00	0.01		0.08

Expt. No.:	BHAS37		
Initial pH:	11		
Probe cpd:	BHA	0.1	mM
Rx:	UV/$S_2O_8^{2-}$		
Conc. :	$S_2O_8^{2-}$	2	mM

time (min)	Conc.	(mM)	C/Co
0.00	0.09		1.00
0.25	0.05		0.53
0.50	0.04		0.38
0.75	0.03		0.30
1.00	0.00		0.00
1.25	0.00		0.00
1.50	0.00		0.00
2.00	0.00		0.00

Expt. No.:	BHAS38		
Initial pH:	11		
Probe cpd:	BHA	0.1	mM
Rx:	UV/$S_2O_8^{2-}$		
Conc. :	$S_2O_8^{2-}$	5	mM

time (min)	Conc.	(mM)	C/Co
0.00	0.10		1.00
0.25	0.05		0.48
0.50	0.02		0.19
0.75	0.01		0.08
1.00	0.00		0.02
1.25	0.00		0.01
1.50	0.00		0.00

Expt. No.:	BHAS39		
Initial pH:	11		
Probe cpd:	BHA	0.1	mM
Rx:	UV/$S_2O_8^{2-}$		
Conc. :	$S_2O_8^{2-}$	10	mM

time (min)	Conc.	(mM)	C/Co
0.00	0.10		1.05
0.25	0.04		0.42
0.50	0.01		0.13
0.75	0.00		0.01
1.00	0.00		0.01
1.25	0.00		0.00
1.50	0.00		0.00
2.00	0.00		0.00

Expt. No.:	BHAS40		
Initial pH:	11		
Probe cpd:	BHA	0.1	mM
Rx:	UV/$S_2O_8^{2-}$		
Conc. :	$S_2O_8^{2-}$	15	mM

time (min)	Conc.	(mM)	C/Co
0.00	0.10		1.05
0.25	0.02		0.26
0.50	0.01		0.06
0.75	0.00		0.00

Expt. No.: BHAS41
Initial pH: 7
Probe cpd: BHA 0.1 mM
Rx: UV/$S_2O_8^{2-}$
Conc. : $(NH_4)_2S_2O_8$ 2 mM

time (min)	Conc. (mM)	C/Co
0.00	0.30	1.00
1.50	0.15	0.50
3.00	0.14	0.47
5.00	0.10	0.35
8.00	0.05	0.15
10.00	0.02	0.08
20.00	0.00	0.00

Expt. No.: BHAS42
Initial pH: 3
Probe cpd: BHA 0.1 mM
Rx: UV/$S_2O_8^{2-}$
Conc. : $S_2O_8^{2-}$ 2 mM
UV: 300 nm
Intensity: 6.72×10^{-4} Einsten L^{-1} min^{-1}

time (min)	Conc. (mM)	C/Co
0.00	0.09	1.00
1.00	0.04	0.43
2.00	0.02	0.25
3.00	0.01	0.15
4.00	0.01	0.09
5.00	0.00	0.04
6.00	0.00	0.02
8.00	0.00	0.00
10.00	0.00	0.00

Expt. No.: BHAS43
Initial pH: 3
Probe cpd: BHA 0.1 mM
Rx: UV/$S_2O_8^{2-}$
Conc. : $S_2O_8^{2-}$ 2 mM
UV: 350 nm
Intensity: $7.46 \times 10^{-}$ Einsten L^{-1} min^{-1}

time (min)	Conc. (mM)	C/Co
0.00	0.09	1.00
1.00	0.08	0.99
2.00	0.08	0.99
3.00	0.08	0.98
4.00	0.08	0.97
5.00	0.08	0.96
6.00	0.08	0.96
8.00	0.08	0.94
10.00	0.08	0.93
20.00	0.07	0.86
30.00	0.07	0.80
40.00	0.06	0.74

Expt. No.: BHAS44
Initial pH: 3
Probe cpd: BHA 0.1 mM
Rx: UV/$S_2O_8^{2-}$
Conc. : $S_2O_8^{2-}$ 2 mM
UV: 300 nm
Intensity: 3.36×10^{-4} Einsten L^{-1} min^{-1}

time (min)	Conc. (mM)	C/Co
0.00	0.08	1.00
1.00	0.06	0.78
2.00	0.05	0.61
3.00	0.04	0.50
5.00	0.03	0.33
6.00	0.03	0.32
8.00	0.02	0.19
10.00	0.01	0.10
20.00	0.00	0.01
30.00	0.00	0.00

Expt. No.: BHAS45
Initial pH: 3
Probe cpd: BHA 0.1 mM
Rx: UV/$S_2O_8^{2-}$
Conc. : $S_2O_8^{2-}$ 2 mM
UV: 350 nm
Intensity: 14.9×10^{-4} Einsten L^{-1} min^{-1}

time (min)	Conc. (mM)	C/Co
0.00	0.09	1.00
1.00	0.08	0.97
2.00	0.08	0.96
3.00	0.08	0.94
4.00	0.08	0.93
5.00	0.08	0.91
6.00	0.08	0.90
8.00	0.08	0.90
10.00	0.07	0.87
20.00	0.06	0.76
30.00	0.06	0.68
40.00	0.05	0.61
150.00	0.02	0.25

Expt. No.: BHAS46
Initial pH: 3
Probe cpd: BHA 0.1 mM
Rx: UV only
UV: 300 nm
Intensity: $6.72 \times 10^{-}$ Einsten L^{-1} min^{-1}

time (min)	Conc. (mM)	C/Co
0.00	0.09	1.00
1.00	0.08	0.88
2.00	0.07	0.83
3.00	0.07	0.77
4.00	0.06	0.73
5.00	0.06	0.69
6.00	0.06	0.66
8.00	0.05	0.62
10.00	0.05	0.55
20.00	0.03	0.38
30.00	0.00	0.00

Expt. No.: BHAS47
Initial pH: 3
Probe cpd: BHA 0.1 mM
Rx: UV only
UV: 350 nm
Intensity: 7.46×10^{-4} Einsten L^{-1} min^{-1}

time (min)	Conc. (mM)	C/Co
0.00	1.00	1.00
1.50	1.00	1.00
3.00	1.00	1.00
5.00	1.00	1.00
8.00	1.00	1.00
10.00	0.99	0.99
20.00	0.99	0.99
30.00	0.99	0.99
60.00	0.98	0.98
120.00	0.98	0.98

Expt. No.: BHAS48
Initial pH: 3
Probe cpd: BHA 0.1 mM
Rx: UV only
UV: 300 nm
Intensity: 3.36×10^{-4} Einsten L^{-1} min^{-1}

time (min)	Conc. (mM)	C/Co
0.00	0.08	1.00
1.00	0.08	0.96
2.00	0.08	0.95
3.00	0.08	0.93
4.00	0.07	0.90
5.00	0.07	0.88
6.00	0.07	0.86
8.00	0.07	0.82
10.00	0.06	0.78
20.00	0.05	0.65
30.00	0.04	0.46

Expt. No.: BHAS49
Initial pH: 3
Probe cpd: BHA 0.1 mM
Rx: UV only
UV: 350 nm
Intensity: $14.9 \times 10^{-}$ Einsten L^{-1} min^{-1}

time (min)	Conc. (mM)	C/Co
0.00	1.00	1.00
1.50	1.00	1.00
3.00	0.99	0.99
5.00	1.00	1.00
8.00	0.99	0.99
10.00	0.99	0.99
20.00	0.99	0.99
30.00	0.98	0.98
60.00	0.98	0.98
120.00	0.97	0.97

Expt. No.:	BHAAS1		
Initial pH:	3		
Probe cpd:	BHA	0.1	mM
Rx:	UV/Ag_2SO_4		
Conc. :	$S_2O_8^{2-}$	0	mM
Conc. :	Ag_2SO_4	1	mM
UV:		254	nm
time (min)	Conc.	(mM)	C/Co
0.00	0.11		1.00
1.50	0.10		0.89
3.00	0.09		0.80
5.00	0.08		0.76
8.00	0.07		0.69
10.00	0.07		0.66
20.00	0.05		0.51
30.00	0.04		0.39
45.00	0.03		0.28
60.00	0.02		0.20

Expt. No.:	BHAAS2		
Initial pH:	3		
Probe cpd:	BHA	0.1	mM
Rx:	$Ag_2SO_4/S_2O_8^{2-}$		
Conc. :	$S_2O_8^{2-}$	2	mM
Conc. :	Ag_2SO_4	1	mM
time (min)	Conc.	(mM)	C/Co
0.00	0.11		1.00
2.00	0.09		0.87
3.00	0.09		0.79
5.00	0.08		0.78
8.00	0.07		0.69
20.00	0.05		0.43
30.00	0.03		0.28
45.00	0.02		0.23
60.00	0.03		0.23

Expt. No.:	BHAAS3		
Initial pH:	3		
Probe cpd:	BHA	0.1	mM
Rx:	$UV/Ag_2SO_4/S_2O_8^{2-}$		
Conc. :	$S_2O_8^{2-}$	2	mM
Conc. :	Ag_2SO_4	1	mM
UV:		254	nm
time (min)	Conc.	(mM)	C/Co
0.00	0.10		1.00
1.50	0.04		0.37
3.00	0.02		0.22
5.00	0.01		0.12
8.00	0.00		0.03
10.00	0.00		0.00
20.00	0.00		0.00

Expt. No.:	BHAAS4		
Initial pH:	3		
Probe cpd:	BHA	0.1	mM
Rx:	$UV/AgNO_3/S_2O_8^{2-}$		
Conc. :	$S_2O_8^{2-}$	2	mM
Conc. :	$AgNO_3$	2	mM
A:S Ratio:		1:1	
UV:		254	nm
time (min)	Conc.	(mM)	C/Co
0.00	1.00		1.00
0.50	0.47		0.47
1.00	0.37		0.37
2.00	0.24		0.24
3.00	0.16		0.16
4.00	0.10		0.10
5.00	0.06		0.06
6.00	0.01		0.01
8.00	0.00		0.00
10.00	0.00		0.00

Expt. No.:	BHAAS5		
Initial pH:	3		
Probe cpd:	BHA	0.1	mM
Rx:	UV Only		
Conc. :	$S_2O_8^{2-}$	0	mM
Conc. :	$AgNO_3$	0	mM
UV:		350	nm
time (min)	Conc.	(mM)	C/Co
0.00	0.10		1.00
1.50	0.10		1.00
3.00	0.09		0.98
5.00	0.10		1.00
8.00	0.10		0.99
10.00	0.10		0.99
20.00	0.09		0.99
30.00	0.09		0.98

Expt. No.:	BHAAS6		
Initial pH:	3		
Probe cpd:	BHA	0.1	mM
Rx:	$UV/S_2O_8^{2-}$		
Conc. :	$S_2O_8^{2-}$	2	mM
Conc. :	$AgNO_3$	0	mM
UV:		350	nm
time (min)	Conc.	(mM)	C/Co
0.00	0.09		1.00
1.00	0.08		0.97
2.00	0.08		0.96
3.00	0.08		0.94
4.00	0.08		0.93
5.00	0.08		0.91
6.00	0.08		0.90
8.00	0.08		0.90
10.00	0.07		0.87
20.00	0.06		0.76

Expt. No.:	BHAAS7		
Initial pH:	3		
Probe cpd:	BHA	0.1	mM
Rx:	$UV/AgNO_3$		
Conc. :	$S_2O_8^{2-}$	0	mM
Conc. :	$AgNO_3$	2	mM
UV:		350	nm
time (min)	Conc.	(mM)	C/Co
0.00	0.10		1.00
1.50	0.05		0.51
3.00	0.07		0.64
5.00	0.06		0.62
10.00	0.08		0.73
20.00	0.08		0.75
30.00	0.07		0.70
45.00	0.08		0.76
60.00	0.08		0.75

Expt. No.:	BHAAS8		
Initial pH:	3		
Probe cpd:	BHA	0.1	mM
Rx:	$UV/AgNO_3/S_2O_8^{2-}$		
Conc. :	$S_2O_8^{2-}$	2	mM
Conc. :	$AgNO_3$	2	mM
A:S Ratio:		1:1	
UV:		350	nm
time (min)	Conc.	(mM)	C/Co
0.00	0.10		1.00
1.50	0.07		0.70
3.00	0.06		0.57
5.00	0.06		0.55
8.00	0.05		0.53
10.00	0.06		0.56
20.00	0.02		0.23
30.00	0.00		0.00

Expt. No.:	BHAAS9		
Initial pH:	3		
Probe cpd:	BHA	0.1	mM
Rx:	$UV/AgNO_3/S_2O_8^{2-}$		
Conc. :	$S_2O_8^{2-}$	2	mM
Conc. :	$AgNO_3$	0.1	mM
A:S Ratio:		0.05:1	
UV:		254	nm
time (min)	Conc.	(mM)	C/Co
0.00	0.11		1.00
1.50	0.04		0.41
3.00	0.03		0.30
5.00	0.01		0.10
8.00	0.00		0.00

Expt. No.:	BHAAS10		
Initial pH:	3		
Probe cpd:	BHA	0.1	mM
Rx:	$UV/AgNO_3/S_2O_8^{2-}$		
Conc. :	$S_2O_8^{2-}$	2	mM
Conc. :	$AgNO_3$	1	mM
A:S Ratio:		0.5:1	
UV:		254	nm

time (min)	Conc.	(mM)	C/Co
0.00	0.11		1.00
0.50	0.05		0.48
1.00	0.04		0.39
2.00	0.03		0.27
3.00	0.02		0.19
4.00	0.01		0.13
5.00	0.01		0.09
6.00	0.01		0.05
8.00	0.00		0.01
10.00	0.00		0.00

Expt. No.:	BHAAS11		
Initial pH:	3		
Probe cpd:	BHA	0.1	mM
Rx:	$UV/AgNO_3/S_2O_8^{2-}$		
Conc. :	$S_2O_8^{2-}$	2	mM
Conc. :	$AgNO_3$	1.5	mM
A:S Ratio:		0.75:1	
UV:		254	nm

time (min)	Conc.	(mM)	C/Co
0.00	0.11		1.00
0.50	0.06		0.52
1.00	0.05		0.42
2.00	0.03		0.28
3.00	0.02		0.18
4.00	0.01		0.12
5.00	0.01		0.07
6.00	0.00		0.00

Expt. No.:	BHAAS12		
Initial pH:	3		
Probe cpd:	BHA	0.1	mM
Rx:	$UV/AgNO_3/S_2O_8^{2-}$		
Conc. :	$S_2O_8^{2-}$	2	mM
Conc. :	$AgNO_3$	2.5	mM
A:S Ratio:		1.25:1	
UV:		254	nm

time (min)	Conc.	(mM)	C/Co
0.00	0.11		1.00
0.25	0.05		0.50
0.50	0.05		0.41
0.75	0.04		0.39
1.00	0.04		0.33
1.50	0.03		0.27
2.00	0.02		0.20
3.00	0.02		0.14
4.00	0.01		0.09
5.00	0.01		0.05
6.00	0.00		0.02

Expt. No.:	BHAAS13		
Initial pH:	3		
Probe cpd:	BHA	0.1	mM
Rx:	$UV/AgNO_3/S_2O_8^{2-}$		
Conc. :	$S_2O_8^{2-}$	2	mM
Conc. :	$AgNO_3$	5	mM
A:S Ratio:		2.5:1	
UV:		254	nm

time (min)	Conc.	(mM)	C/Co
0.00	0.11		1.00
0.50	0.05		0.48
0.75	0.04		0.38
1.00	0.04		0.32
1.50	0.03		0.28
2.00	0.03		0.23
3.00	0.02		0.15
4.00	0.01		0.08
6.00	0.00		0.01
8.00	0.00		0.00

Expt. No.:	BHAAS14		
Initial pH:	3		
Probe cpd:	BHA	0.1	mM
Rx:	$UV/AgNO_3/S_2O_8^{2-}$		
Conc. :	$S_2O_8^{2-}$	2	mM
Conc. :	$AgNO_3$	15	mM
A:S Ratio:		7.5:1	
UV:		254	nm

time (min)	Conc.	(mM)	C/Co
0.00	0.11		1.00
0.25	0.02		0.17
0.50	0.01		0.11
0.75	0.01		0.05
1.00	0.00		0.02
2.00	0.00		0.04
3.00	0.00		0.00
4.00	0.00		0.00
5.00	0.00		0.00

Expt. No.:	BHAAS15		
Initial pH:	3		
Probe cpd:	BHA	0.1	mM
Rx:	$UV/AgNO_3/S_2O_8^{2-}$		
Conc. :	$S_2O_8^{2-}$	2	mM
Conc. :	$AgNO_3$	20	mM
A:S Ratio:		10:1	
UV:		254	nm

time (min)	Conc.	(mM)	C/Co
0.00	0.11		1.00
0.25	0.02		0.15
0.50	0.01		0.07
0.75	0.01		0.07
1.00	0.00		0.04
2.00	0.00		0.00

Expt. No.:	BHAAS16		
Initial pH:	3		
Probe cpd:	BHA	0.1	mM
Rx:	$UV/AgNO_3/S_2O_8^{2-}$		
Conc. :	$S_2O_8^{2-}$	2	mM
Conc. :	$AgNO_3$	30	mM
A:S Ratio:		15:1	
UV:		254	nm

time (min)	Conc.	(mM)	C/Co
0.00	0.11		1.00
0.25	0.02		0.21
0.50	0.03		0.27
0.75	0.02		0.22
1.00	0.02		0.20
1.50	0.01		0.13
2.00	0.01		0.09
3.00	0.00		0.02
4.00	0.00		0.00
5.00	0.00		0.00

Expt. No.:	BHAAS17		
Initial pH:	3		
Probe cpd:	BHA	0.1	mM
Rx:	$UV/Ag_2O/S_2O_8^{2-}$		
Conc. :	$S_2O_8^{2-}$	2	mM
Conc. :	Ag_2O	1	mM
A:S Ratio:		1:1	
UV:		254	nm

time (min)	Conc.	(mM)	C/Co
0.00	0.11		1.00
0.50	0.06		0.52
1.00	0.04		0.37
2.00	0.02		0.22
3.00	0.02		0.15
4.00	0.01		0.10
5.00	0.01		0.06
6.00	0.00		0.04
8.00	0.00		0.00

Expt. No.:	BHAAS18		
Initial pH:	3		
Probe cpd:	BHA	0.1	mM
Rx:	$UV/Ag_2O/S_2O_8^{2-}$		
Conc. :	$S_2O_8^{2-}$	2	mM
Conc. :	Ag_2O	7.5	mM
A:S Ratio:		7.5:1	
UV:		254	nm

time (min)	Conc.	(mM)	C/Co
0.00	0.11		1.00
0.50	0.05		0.49
1.00	0.03		0.27
2.00	0.02		0.16
3.00	0.01		0.09
4.00	0.00		0.02
5.00	0.00		0.00
6.00	0.00		0.00

Sulfate and peroxydisulfate

Expt. No.:	BHAS28		
Initial pH:	7		
Probe cpd:	BHA	0.1	mM
Rx:	UV/$S_2O_8^{2-}$		
Conc. :	$S_2O_8^{2-}$	2	mM
	Concentration (mM)		
Time (min)	$S_2O_8^{2-}$	SO_4^{2-}	
0.00	2.04	0.00	
1.00	1.99	0.00	
2.00	1.99	0.00	
3.00	1.95	0.00	
4.00	1.90	0.85	
5.00	1.81	1.63	
6.00	1.81	1.76	
8.00	1.67	1.76	
10.00	1.67	2.40	
20.00	0.95	2.78	
30.00	0.59	3.00	
45.00	0.18	4.18	
60.00	0.09	4.22	

pH

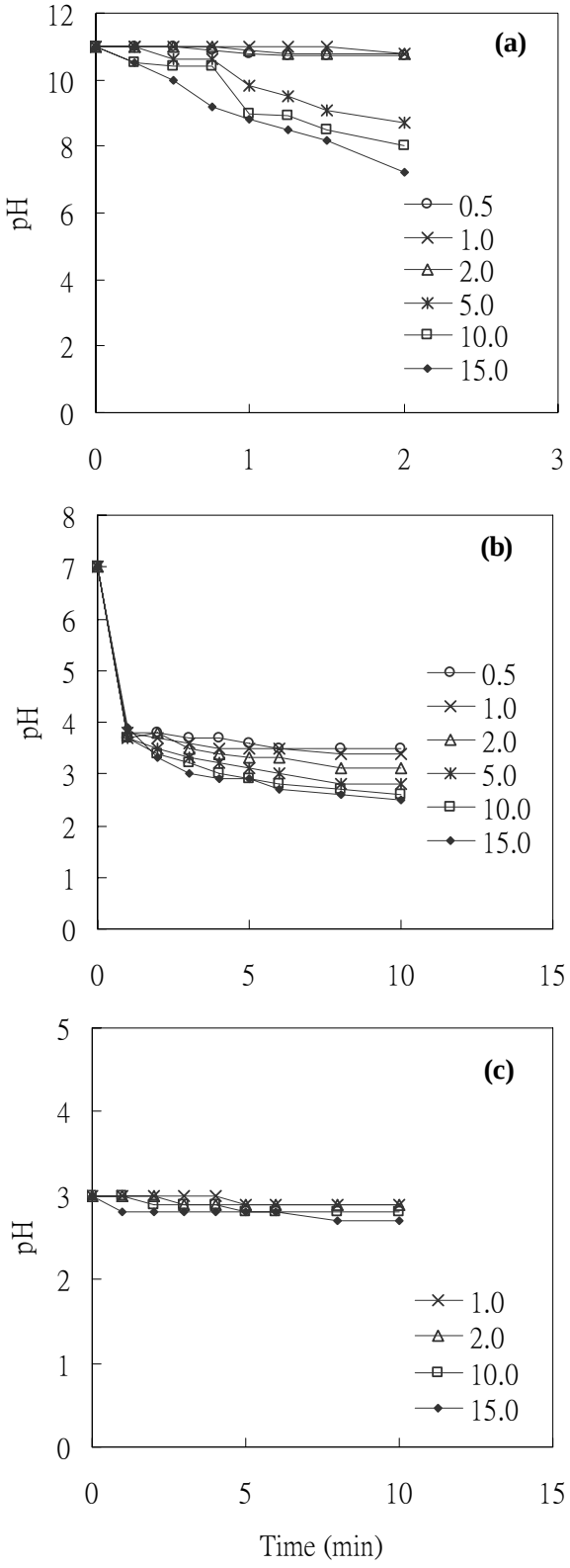

pH trend of UV/$S_2O_8^{2-}$ process in various $S_2O_8^{2-}$ concentration (mM) at pH (a) 11; (b) 7; and (c) 3.